

**COMPUTATIONAL DESIGN, SYNTHESIS,
CHARACTERIZATION AND
PHARMACOLOGICAL EVALUATION OF SOME
PIPERIDINE DERIVATIVES**

THESIS

Submitted to

**The Tamilnadu Dr. M.G.R. Medical University
Guindy, Chennai -600032, Tamilnadu, India.**

*As a partial fulfillment of the requirement for the
award of the degree of*

**DOCTOR OF PHILOSOPHY
(Faculty of Pharmacy)**

Submitted by

C.N.NALINI, M.Pharm

Under the supervision of

**Prof. Dr.G.SRINIVASA RAO, M.Pharm., Ph.D.,
Director, Research and Development,**



**VEL'S COLLEGE OF PHARMACY,
PALLAVARAM, CHENNAI,
TAMILNADU, INDIA.**

APRIL - 2009

**COMPUTATIONAL DESIGN, SYNTHESIS,
CHARACTERIZATION AND
PHARMACOLOGICAL EVALUATION OF SOME
PIPERIDINE DERIVATIVES**

THESIS

Submitted to

**The Tamilnadu Dr. M.G.R. Medical University
Guindy, Chennai -600032, Tamilnadu, India.**

*As a partial fulfillment of the requirement for the
award of the degree of*

**DOCTOR OF PHILOSOPHY
(Faculty of Pharmacy)**

Submitted by

C.N.NALINI, M.Pharm

Under the supervision of

**Prof. Dr.G.SRINIVASA RAO, M.Pharm., Ph.D.,
Director, Research and Development,**



**VEL'S COLLEGE OF PHARMACY,
PALLAVARAM, CHENNAI,
TAMILNADU, INDIA.**

APRIL - 2009

CERTIFICATE

This is to certify that the thesis entitled “**Computational Design, synthesis, characterization and pharmacological evaluation of some piperidine derivatives**” submitted by **NALINI C.N.**, in partial fulfillment of the requirements for the award of the degree of “**Doctor of philosophy**” (Faculty of Pharmacy) under **The Tamilnadu Dr. M.G.R. Medical University**, Chennai, was carried out at Vel’s College of pharmacy, Chennai under my guidance and supervision during the academic years 2005-2009.

Date:

Prof. Dr.G.SRINIVASA RAO, M.Pharm., Ph.D.,

Chennai-117

Director, Research and Development,

Vel’s College of pharmacy,

Pallavaram,

Chennai-117.

DECLARATION

I hereby declare that the thesis entitled “**COMPUTATIONAL DESIGN, SYNTHESIS, CHARACTERIZATION AND PHARMACOLOGICAL EVALUATION OF SOME PIPERIDINE DERIVATIVES**” submitted to The Tamilnadu Dr. M.G.R. Medical University, Chennai, as partial fulfillment of the requirements for the award of the degree of **DOCTOR OF PHILOSOPHY** (Faculty of Pharmacy) was completely carried out by me during the period 2005-2009 under the guidance of **Prof. (Dr.) G. SRINIVASA RAO**, M. Pharm., Ph.D., Director, Research and Development, Vels College of Pharmacy, Chennai, Tamilnadu, India. This work is original and has not formed the basis for the award of any diploma, degree, associateship, fellowship or other similar title.

Date:

(**C.N.NALINI**)

Chennai-117

ACKNOWLEDGEMENT

I express my heartfelt gratitude and most respectful regards to my revered supervisor **Prof.Dr.G.Srinivasa Rao, M.Pharm., Ph.D.**, Director, Research and development, Vel's college of pharmacy for his excellent guidance, encouragement, helpful criticism and inspiring suggestion throughout the course of this investigation.

I express my deep sense of gratitude to **Dr.Ravichandran, M.Pharm., Ph.D** Principal, Vel' college of Pharmacy, for providing me with necessary support to complete this project successfully.

I would like to thank **Shri Harish L. Metha, Secretary and Correspondent**, and **Shri Vinod Khanna, Chairman**, C.L.Baid Metha College of pharmacy for providing me the requisite facilities.

It is a great pleasure to acknowledge my indebtedness to **Dr.T.R.Radhakrishnan, M.Sc.,Ph.D.,F.I.C.S.,A.M.N.S.A.** (India), Principal, Prince Bavani college of Arts and Science,Chennai for his keen interest,inspiring guidance,constant encouragement and patience throughout the course of my research work.

I would like to express my deepest sense of indebtedness to **Prof.Grace Rathnam, M.Pharm., (Ph.D), Director and Prof .Dr. A. Shantha, M.Pharm., Ph.D Principal**, C.L.Baid Metha college of pharmacy for encouraging me over the years in a brighter direction.

I express my sincere thanks to **Dr.Vadivelan shankaran M.Pharm., Ph.D**, for guiding me throughout my in CADD studies.

I profoundly thank **Dr.Niranjali Devarajan M.Sc, Ph.D** HOD, Dept of Biochemistry,AC tech college of Engineering, Guindy for permitting me to work in her laboratory for yhe phosphatase inhibition activity.

I would like to convey my sincere thanks to **Mr.Murali, M.Pharm.** of CLBMCP for helping me in my anticancer screening. I am thankful to Deshpande laboratories, Bhopal for carrying out my screening studies.

I am thankful to **Dr. V. Suba, M.Pharm., Ph.D**, Vel's college and **Dr. Venkatraman**, Director, Research and Development, C.L. Baid Metha College of pharmacy for the advice rendered for the work.

I express my sincere thanks to **Mrs.K.Kavitha M.Pharm., (Ph.D)**, and **Dr.M.D.Dhanaraju M.Pharm., Ph.D** for their inspiration throughout my project.

My thanks are due to **IIT, Chennai, and IISc, Bangalore**, for the spectral studies. I would also like to thank **Mrs Dhanalakshmi, CEEAL Analytical Lab** for providing me the I.R. Spectral data and also to **Mr.Narayanan, Miss.Hema and Miss.Monica** for helping me during the research.

The acknowledgement would be incomplete if I don't mention the name of **Dr.Gunasekaran M.Pharm., Ph.D, Mr. Anbu M.Pharm., , Mr.Hari M.Pharm., Vel's college of Pharmacy, Mrs. Banumathi (Librarian), Mr.Srinivasan (Stores In charge), Mrs. R,Usha, Mrs. Kalpakam and Mrs.Valli(Office Staff)** who helped me in my work.

I would like to express my adoration and regards to **my parents** and all **my family members** for their patience, courage, consistent motivation and affection towards me to surpass the hurdles in my life.

I would like to express my humble thanks to the Almighty, who has given me the Strength, Confidence and Capacity to complete the work.

LIST OF ABBREVIATIONS

$^{13}\text{C-NMR}$	-	Carbon Nuclear magnetic resonance
$^1\text{H-NMR}$	-	Proton nuclear magnetic resonance
C f u mL^{-1}	-	Colony forming unit per milliliter
$^{\circ}\text{C}$	-	Degree Celsius
DMF	-	Dimethyl formamide
DMSO	-	Dimethyl sulfoxide
mcg	-	micrograms
g	-	Gram
g / L	-	Grams per liter
IR	-	Infrared
μg	-	Microgram
$\mu\text{g mL}^{-1}$	-	Microgram per millilitre
μl	-	Micro litres
ppm	-	Parts per million
MWI	-	Microwave Irradiation
M/z	-	Mass per Charge ratio
nM	-	nanomoles
mm	-	millimeter
MIC	-	Minimum inhibitory concentration
min	-	minutes
R_F	-	Retention factor
TLC	-	Thin layer chromatography
GLIDE	-	Grid-based ligand docking with energetics
NCI	-	National Cancer Institute
PDB	-	Protein Data Bank
RMSD	-	Root Mean Square Deviation
RTK	-	Receptor Tyrosine Kinases
STK	-	Serine threonine kinases
PP	-	Protein phosphatases

CONTENTS

CHAPTER NO	TITLE	PAGE NO
1	INTRODUCTION	
	1.0 Drug Design	1
	1.1 Enzyme Inhibitors	10
	1.2 Computational Drug Design	15
	A. Pharmacophore Modeling	15
	B. Docking Studies	28
	1.3 Synthesis	36
2.	REVIEW OF LITERATURE	45
3.	RATIONALE BEHIND THE RESEARCH	71
4.	PLAN OF WORK	73
5.	THE TARGET ENZYME - AURORA KINASE-A	75
6.	PHARMACOPHORE MODELING	
	6.1 Materials and Methods	83
	6.2 Results and Discussion	88
7.	DOCKING STUDIES	
	7.1 Materials and Methods	97
	7.2 Results and Discussion	99
8.	PASS PREDICTION STUDIES	
	8.1 Materials and Methods	109
	8.2 Results and Discussion	113

9.	DRUG LIKENESS SCREENING	
	9.1 OPTIMIZATION USING LIPINSKI RULE	
	Materials and Methods	116
	Results and Discussion	121
	9.2 TOXICITY ASSESSMENT	
	Materials and Methods	127
	Results and Discussion	129
10.	SYNTHESIS	
	10.1 Synthetic Scheme	132
	10.2 Experimental Procedure	135
11.	CHARACTERISATION	
	11.1 Physicochemical Characterization	142
	11.2 Spectral Studies-Discussion	162
12.	<i>IN VITRO</i> ANTICANCER SCREENING	170
	12.1 Materials and Methods	172
	12.2 Results and Discussion	177
13.	PHOSPHATASE INHIBITION ACTIVITY	
	13.1 Materials and Methods	181
	13.2 Results and Discussion	184
14.	SUMMARY AND CONCLUSION	191
15.	REFERENCES	195

1. INTRODUCTION

1.1 DRUG DESIGN

Drugs play an indispensable role in modern medicine. Medicinal chemistry is the branch of science that provides these drugs through discovery or through design. Contemporary medicinal chemistry draws upon many disciplines, so that the medicinal chemist must have a broad working knowledge about organic chemistry and in addition he must also be comfortable with significant elements of biochemistry, molecular biology, pharmacology, neurobiology, toxicology, genetics, cell biology, biophysics, quantum mechanics, anatomy physiology pathology clinical medicine, computer technology and the like. This is tall but manageable order. There is a lot to learn about pathophysiology also.

The central objective of each branch of chemistry is to possess such an understanding of the relationship between chemical structure and molecular properties to give a set of desired characteristics. Then the molecules can be proposed and prepared that come close to possessing the characteristics. A daunting feature is the no of properties that a candidate substance must possess in order to function therapeutically in the human body and so to become a drug. Despite all this a remarkable range of pharmaceuticals have been developed successfully and the pace of new entity introduction is gratifyingly rapid.

Several million compounds must be screened in order to find a thousand or so that have approximately correct characteristics and only few of these successfully advance through analoging and bio testing to produce only dozen agents suitable for clinical study. Only six of these on average progress in to clinical trials and just one reaches the market.

The pace of screening has accelerated dramatically in recent years. The applications of high throughput screening methods require rapid synthesis of large arrays of compounds suitable for screening. For targets that have structural information available, docking methods can be used to select compounds that are complementary to the binding site(s). Applications encompass both high throughput screening (HTS) ¹ and therapeutic area screening where only smaller numbers of compounds can be screened.

Molecules which attach themselves significantly to selected enzymes or receptor preparations are called 'hits'. These are screened for potentially toxic moieties, untoward reactivity or other undesirable features. Those surviving molecules that warrant the time, costs and effort of analog preparation to further enhance their desirable properties are called

‘leads’. When the leads have been refined further so that satisfactory potency, selectivity, freedom from toxicity, chemical novelty, suitable pharmacokinetic and pharmacodynamic properties etc., are present in animal models of diseases, the survivors are elevated to the status of ‘candidate drugs’ suitable for extensive biological evaluation up to and including clinical trials in humans².

CADD IN LEAD GENERATION

CADD STRATEGIES IN THE DRUG DISCOVERY PROCESS

Strategies for CADD (Computer Aided Drug Design) vary depending on the extent of structural and other information available regarding the target (enzyme/receptor) and the ligands. “Direct and indirect” designs are the two major modeling strategies currently used in the drug design process³. In the indirect approach the design is based on comparative analysis of the structural features of known active and inactive compounds. In the direct design the three-dimensional features of the target are directly considered Figure 1.1.

COMPOUNDS (inhibitor/ligand)	TARGET (enzyme/receptor)	
	Unknown	Known
Unknown	Similarity Searching Rational Screening	de novo design
Known	Analog-Based Drug Design	Structure-Based Drug Design

Figure 1.1 Four major cases in CADD also known as “direct” and “indirect design when the structure of the target is respectively known or unknown.

The rapid increase in relevant structural information, attributed to advances in molecular biology to generate the target proteins in adequate quantities for study, and the

equally impressive gains in NMR⁴⁻¹² and crystallography^{13,14} to provide three-dimensional structures as well as identify leads, have stimulated the need for design tools and the molecular modeling community is rapidly evolving useful approaches. A number of reviews¹⁵⁻²¹ of computer-aided drug design have relevant sections with different perspectives.

Structure of the Compound and Target Both Unknown (Similarity searching and rational screening)

In the early stage of a drug discovery process, researchers may be faced with little or no structure activity relationship (SAR) information. At this point, assay development and screening should be undertaken immediately by the high-throughput screening (HTS) group²²⁻²⁴. Investigations were done using two-dimensional fingerprints as a validated molecular descriptor and the performance of rational selection methods vs. random approach has been compared²⁵⁻²⁸.

If, however, a lead is known, then more focused approach can be adopted by searching for compounds with similar (two or three-dimensional) structures to the lead candidate or by substructure searching²⁹.

Once primary leads and their corresponding structural information are available the computational chemist can use these data to derive new lead classes. By comparison of the stereo electronic properties of primary leads, a pharmacophore is defined. A pharmacophore model is a spatial arrangement of atoms or functional groups believed to be responsible for biological activity³⁰. In this model the rest of the molecule acts as a skeleton to hold the groups in the right place. Typically, the derived Pharmacophores consist, generally, of 3-5 features, and the distances between them (angles and other geometric measures are sometimes used).

In the course of the pharmacophore identification process, two different steps have to be taken in succession. First a conformational analysis has to be carried out. Indeed, the biological activity of a drug is supposed to depend on one unique conformation hidden among all the low-energy conformations³¹⁻³⁵. During the second step, the bioactive conformations are used to calculate their stereo electronic properties. Based on this three-dimensional description of the stereo electronic properties of considered compounds, a pharmacophore can be obtained. Once the pharmacophore has been, at least, partially identified, the next step is to find compounds which contain the same pharmacophore

embedded in their structure by three dimension database searching⁴⁰. The classic database of three-dimensional molecular structures is the Cambridge Structural Database (CSD)⁴¹. The use of CADD in lead generation when no structural information about the target protein is available is summarized in Figure 1.2.

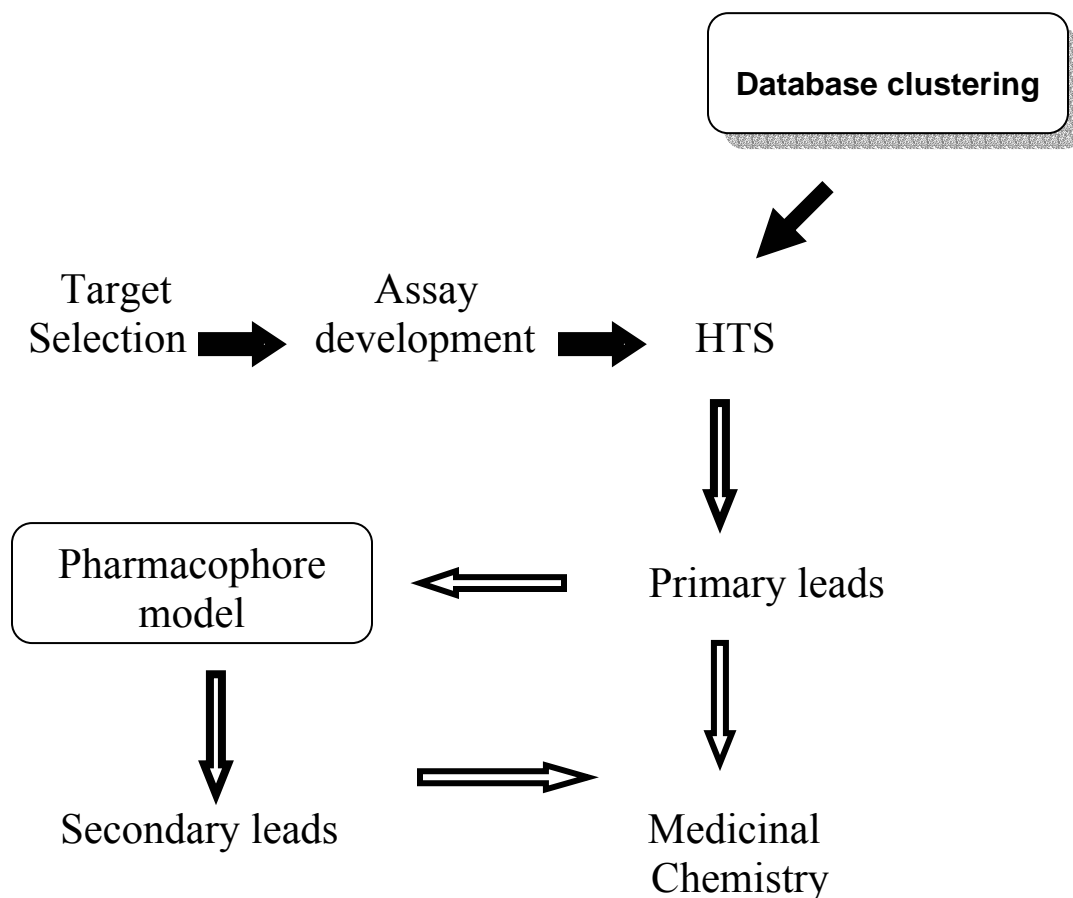


Figure 1.2 Summary of the use of CADD in focusing HTS process, designing secondary leads, and focusing medicinal chemistry.

3d Structure of the Protein Known but the Compound Unknown (De Novo design)

Advances in the molecular biology field had a dramatic impact on the drug discovery process^{42,43}. The ability to produce significant quantities of pure protein has led to the structural determination of many biologically relevant targets by X-ray crystallography⁴⁴ and nuclear magnetic resonance (NMR)^{44, 45}. Protein structures are available through the Protein Data Bank⁴⁶.

Homology modeling can also be used in cases where no experimental proteins structures are available. According to a recent evaluation of homology modeling methods,

accurate models, such as those preferred for drug design, can only be obtained in cases in which the two proteins have a high percentage of sequence identity⁴⁷⁻⁵². Given a high resolution structure of proteins, new ligands can be designed *de novo*. De Novo Design is the Designing of novel chemical structures that are capable of interacting with a receptor of known structure using methodology that is much more robust.

Unknown Targets and Known Compounds (Analog Based Drug Design)

Most drugs, because of inherent conformational freedom, are capable of presenting a multitude of three-dimensional patterns to a receptor. The pharmacophore, a concept introduced by Ehrlich at the turn of the 20th century, is the critical three-dimensional arrangement of molecular fragments (or distribution of electron density) that is recognized by the receptor and, in the case of agonists, that causes subsequent activation of the receptor upon binding. One corollary of the pharmacophoric concept is the ability to replace the chemical scaffold holding the pharmacophoric groups with retention of activity. The pharmacophore approach is the most appropriate one because of the lack of detailed information regarding the receptor as seen in the case of clinical success with tyrosine kinase inhibitors^{53,54} and other recent examples⁵⁵.

The concept of analog design¹ presupposes that a lead has been discovered; that is, a chemical compound has been identified which possesses some desirable pharmacological property. Analog design is most fruitful in the study of pharmacologically active molecules that are structurally specific: their biological activity depends on the nature and the details of their chemical structure (including stereochemistry). Hence, a seemingly minor modification of the molecule may result in a profound change in the pharmacological response.

The goal of analog design is twofold: (1) to modify the chemical structure of the lead compound to retain or to reinforce the desirable pharmacologic effect while minimizing unwanted pharmacological (e.g., toxicity, side effects, or undesired routes of and/or unacceptable rates of metabolism) and physical and chemical properties (e.g., poor solubility and solvent partition characteristics or chemical instability), which may result in a superior therapeutic agent; (2) to use target analogs as pharmacological probes to gain better insight into the pharmacology of the lead molecule and perhaps to reveal new knowledge of basic biology. Studies of analog structure-activity relationships may increase the medicinal

chemist's ability to predict optimum chemical structural parameters for a given pharmacological action.

In analog design, molecular modification of the lead compound can involve one or more of the strategies including Bio iso steric replacement, Design of rigid analogs, Homologation of alkyl chain(s) or alteration of chain branching, design of aromatic ring-position isomers, alteration of ring size, and substitution of an aromatic ring for a saturated one, or the converse, Alteration of stereochemistry or design of geometric isomers or stereo isomers, Design of fragments of the lead molecule that contain the pharmacophoric group (bond disconnection), Alteration of inter atomic distances within the pharmacophoric group or in other parts.

All of the strategies of analog design and the subsequent decisions concerning target compounds to be synthesized can be facilitated by the use of computational chemistry (computer-assisted molecular modeling) techniques.

3d Structure of the Target and the Compound Both Known (Structure-Based Drug Design)

A significant challenge is the design of novel ligands for therapeutic targets in which the three-dimensional structure has been determined by either X-ray crystallography or NMR⁵⁶. The search for the global minimum, or the complete set of low energy minima, on the free energy surface when two molecules come in contact is commonly referred to as the "docking".

When the structure of the target protein is available the process of lead optimization can be profoundly influenced and speeded, particularly when the three-dimensional structure of Protein-ligand complex is available. These can be obtained experimentally by X-ray crystallography or NMR^{44, 45} or computationally by using docking programs⁵⁷. Then this process can be iterated with further rounds of design, synthesis, testing, and so on to ultimately produce potent and specific compounds.⁵⁸⁻⁶⁰

Structure-based drug design by use of structural biology remains one of the most logical and aesthetically pleasing approaches in drug discovery paradigms. The first paper on the potential use of crystallography in medicinal chemistry was written in 1974 and was presented at Professor Alfred Burger's retirement symposium in 1972 by Abraham J. The concept of structure-based drug discovery combines information from several fields: X-ray

crystallography and/or NMR, molecular modeling, synthetic organic chemistry, qualitative structure-activity relationships (QSAR), and biological evaluation.

Figure 1.3 represents a general road map where a cyclic process refines each stage of discovery. Initial binding site information is gained from the three-dimensional solution of a complex of the target with a lead compound(s). Molecular modeling is usually next applied with the intent of designing a more specific ligand) with higher affinity. Synthesis and subsequent *in vitro* biological evaluation of the new agents produces more candidates for crystallographic or NMR analysis, with the hope of correlating the biological action with precise structural information. The most active derivative (~) from this cyclic process can be forwarded for *in vivo* evaluation in animals.

Several HIV-P inhibitors have been approved for human therapeutic use in the past 10 years, and the speed with which they were developed is attributed in part to the successful use of SBDD methods.

The different steps involved in the process of Structure Based Drug Design⁶¹ are as follows:

1. The selection of an enzyme which is important in a particular pathological condition is chosen
2. Determination of the three dimensional structure of the active site of the enzyme often by x-ray crystallography.
3. Preparation of a chemical to fit the active site of the enzyme which alters the properties of the enzyme .e.g. .the enzyme is inactivated.

The Advantages of SBDD are, useful results obtained faster than the traditional drug design methods. The process is less expensive than other drug design methods. The compounds are more specific for the active site and less toxic than compounds prepared by other approaches.

CADD IN LEAD OPTIMIZATION

When leads are available, the next step consists in their optimization. In medicinal chemistry the lead optimization process concerns many aspects such as the optimization of the affinity for the biological target, the toxicity, the oral bioavailability, the cell permeability, the plasma binding, the ease of metabolism. This process requires the synthesis of a series of analogues and testing their biological activities. The principle employed is that

any incremental change in the chemical structure produces incremental (positive or negative) changes in bio-activity.

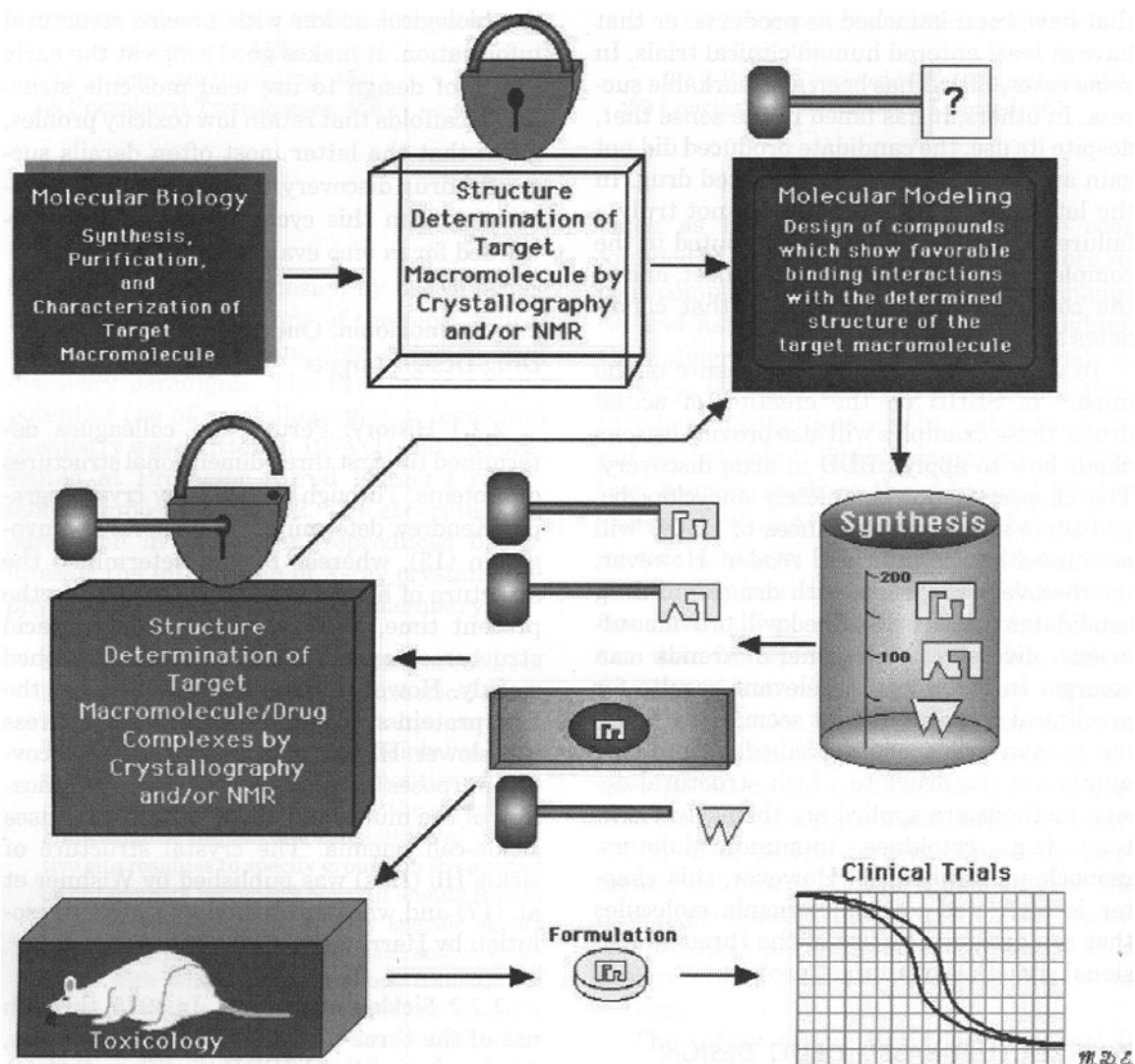


Figure 1.3. Schematic of the structure-based drug discovery/design process figure maps out the iterative steps that make use of X-ray crystallography molecular modeling, organic synthesis, and biological testing to identify and optimize ligand-protein interactions.

A systematic study of such cause and effect relationship is called structure activity relationship (SAR) study. The process is highly iterative and traditionally based on trial-and-error. Some strategies (Hansch and Leo method ⁶², Topliss tree ⁶³, Craig plot ⁶⁴) have also

been advocate to help in focusing on the most informative experiments. CADD can also be used in this process to make it more methodological.

When no structural data about the target (receptor/enzyme) is available, the lead optimization process can be made more methodological by using quantitative structure-activity relationship (QSAR) studies. QSAR methods are used to attempt to correlate the biological activities of compounds with their associated stereo electronic properties. The aim of such investigations is to produce a suitably robust model capable of reliable predictions for novel chemical species. All QSAR techniques assume that (1) all the compounds being studied bind non-covalently to the same biological target; (2) structurally similar compounds are similarly oriented at that common receptor site, and (3) the dynamics of the system can be neglected. Two different approaches can be used in QSAR depending on the available compounds. The 2D-QSAR and 3D-QSAR approaches can be used for optimization depending on the availability of compounds.

1.2 ENZYME INHIBITORS

Interestingly until the 1970's known drug targets were primarily neurotransmitter receptors on cell surfaces⁶⁵. Since that time, a wealth of information has been uncovered and many other choices are now available. In this context it is interesting to consider the molecular targets for which drugs are contemporarily crafted even though this is shifting rapidly. Cellular receptors (45%) enzymes (28%), Hormones & factors (11%), Ion channels (5%), DNA (2%), Unknown (7%). Clearly cellular receptors and enzymes make up the bulk of the targets favored at this time.

RATIONAL DESIGN OF ENZYME INHIBITORS

The design of Captopril was a landmark in the application of structural models for developing enzyme inhibitors^{66, 67}. There are numerous reviews of the early work on HIV-P inhibitors^{68- 71}. Protein kinases and phosphatases play vital roles in intracellular signaling pathways and in the integration and control of major cellular processes. Kinases and other phosphoryl group transferases are essential in the metabolism of lipids, nucleotides, and other small bio molecules. The use of SBDD⁶⁷ methods on such targets has expanded as more of their X-ray structures have been solved.

A selective inhibitor may block either a single enzyme or a group of enzymes, leading to the disruption of a metabolic pathway(s). This will result in either a decrease in the concentration of enzymatic products or an increase in the concentration of enzymatic substrates⁷². The effectiveness of an enzyme inhibitor as a therapeutic agent will depend on (1) the potency of the inhibitor, (2) its specificity toward its target enzyme, (3) the choice of metabolic pathway targeted for disruption, and (4) the inhibitor or a derivative possessing appropriate pharmacokinetic characteristics.

The abolition of aberrant enzyme activity through the administration of small molecule enzyme inhibitors is a common strategy for pharmaceutical intervention in human diseases. In fact, a recent survey demonstrates that nearly 30% of all drugs in current clinical use elicit their pharmacological effects by inhibition of specific enzyme targets. As new targets are identified through the recent advances in genomic and proteomic sciences, the proportion of the drugs that act through enzyme inhibition is likely to increase further. Hence a significant effort is target key enzymes for inhibition by small molecular wt., orally bio available drugs⁷¹.

Diseases such as cancers, and inflammatory diseases, involve aberrant hyper proliferation of specific cell types. The metabolic pathways that fuel cell proliferation all involve enzyme catalysis, making the enzyme of these pathways attractive targets for chemotherapeutic intervention.

Even though it has proved possible to selectively inhibit the enzymes of a number of pathogens, the enzymes of cancer cells have proved to be a far more elusive target. Indeed, the majority of the currently employed anti tumor agents can be described as anti proliferative agents. These take advantage of the fact that many, but not all, tumor cells grow and divide more rapidly than normal cells. Table (1.1). They can also be described as anti metabolites because they inhibit a metabolic pathway involved in DNA biosynthesis, which is important for cell survival or replication. 5-Fluorouracil the pro drug form of an inactivator of thymidylate synthase⁷³, and methotrexate, an inhibitor of dihydrofolate reductase^{74, 75}, both fit into this category. Unfortunately, rapidly dividing normal cells, such as hair follicles, the cells lining the gastrointestinal tract, and the bone marrow cells involved in the immune system are also significantly affected. The resultant hair loss, nausea, and susceptibility to infection means that this type of chemotherapy is seldom employed as a first-line defense against cancer.

The inhibition of enzymes involved in metabolic pathways is not restricted to anticancer agents. A variety of diseases have been correlated with either the dysfunction of an enzyme or an imbalance of metabolites.

In basic research, enzyme inhibitors have found a multitude of uses. They serve as useful tools for the elucidation of structure and function of enzymes, as probes for chemical and kinetic processes, and in the detection of short-lived reaction intermediates⁷⁶. Product inhibition patterns provide information about an enzyme's kinetic mechanism and the order of substrate binding⁷⁷. Covalently binding enzyme inhibitors have been used to identify active-site amino acid residues that could potentially be involved in substrate binding and catalysis of the enzyme^{78, 79}.

Reversible enzyme inhibitors are routinely used to facilitate enzyme purification by using the inhibitor as a ligand for affinity chromatography^{80, 81} or as eluants in affinity-elution chromatography⁸². Immobilized enzyme inhibitors can also be used to identify their

intracellular targets ⁸³, whereas irreversible inhibitors can be used to localize and quantify enzymes *in vivo* ⁸⁴.

TABLE 1.1 ENZYME INHIBITORS USED IN THE TREATMENT OF CANCER

TYPE OF CANCER	ENZYME INHIBITED	INHIBITOR
Benign prostatic hyperplasia	Steroid 5 α -reductase	Finasteride
Estrogen-mediated Breastcancer	Aromatase	arinoglutethimide, fadrozole
Leukemia, Osteosarcoma Head, neck & breast cancer	Dihydrofolate reductase	Methotrexate
Colorectal cancer	Thymidylate synthase	5-Fluorouracil
Leukemia	Glutamine-PRPP amido transferase	6-Mercaptopurine, azathioprine
Small-cell lung cancer, non-Hodgkin's lymphoma	Topoisomerase	Etoposide
Hairy-cell leukemia	Adenosine deaminase	Pentostatin

The Table 1.2 provides the classification of the various types of enzyme inhibitors. The classification may appear somewhat arbitrary, in that some inhibitors may fit into more than one category. This can arise because these categories are attempting to bring together some non related properties such as structure, mechanism of action, and kinetic behavior of that type of inhibitor, as well as indicating how it may be evaluated. There are many reviews of enzyme inhibitors available in the literature ^{76, 85}

NON-COVALENTLY BINDING ENZYME INHIBITORS

As their name indicates, this class of inhibitors binds to the enzyme's active site without forming a covalent bond. Therefore the affinity and specificity of the inhibitor for the active site will depend on a combination of the electrostatic and dispersive forces, and hydrophobic and hydrogen-bonding interactions. Traditionally, non covalently binding enzyme inhibitors were analogs of substrates, products, or reaction intermediates.

Forces Involved in Forming the Enzyme- Inhibitor Complex

The forces involved in a substrate or an inhibitor binding to an enzyme's active site are, as with a drug binding to a receptor, the same forces that are experienced by all interacting organic molecules. These include ionic (electrostatic) interactions, ion-dipole and dipole-dipole interactions, hydrogen bonding, hydrophobic interactions, and van der Waals interactions.

TABLE 1. 2 CLASSIFICATIONS OF ENZYME INHIBITORS

NON-COVALENT INHIBITORS	COVALENT INHIBITORS
Rapid reversible inhibitors (ground-state analogs)	Chemical modifiers
Tight, slow, slow-tight binding inhibitors	Affinity labels
Multi substrate analogs	Mechanism-based inhibitors
Transition-state analogs	Pseudo irreversible inhibitors

Hydrogen bonds are readily formed between water and biologically important atoms such as the hydrogen bond acceptors N and O and, to a lesser extent, S. The conjugate acids NH and OH may act as hydrogen bond donors. What may be strong hydrogen bonds in the gas phase, or in organic media, are often considerably weaker in aqueous media. However, collectively, hydrophobic forces are thought to transcend other types of forces, particularly in the folding of proteins, in all biological systems.

Electrostatic Forces

The strength of an ion-ion interaction is inversely related to the square of distance between the ions, whereas ion-dipole and dipole dipole interactions have $1/r^4$ and $1/r^6$ relationships, respectively. Because the strength of the interaction decreases more slowly with distance, ion-pair interactions can be thought of as long-range interactions. Conversely, interactions involving dipoles are effective over only a short range, although, because they are much more prevalent, dipole interactions may be more significant to the overall binding process. Clearly, the dependency of the strength of interaction on the distance between atoms is an important consideration when designing potential enzyme inhibitors.

Van der Waals Forces

These are the universal attractive interactions that occur between atoms. There will be an attractive force between the two molecules, with the magnitude of the force depending on

the polarizability of the particular atoms involved and the distance between each other. The optimal distance between the atoms is the sum of each of their van der Waals radii, so these forces come into play only when there is good complementarities between enzyme and inhibitor. Although van der Waals forces are quite weak, usually around 0.5-1.0 kcal/mol for an individual atom-atom interaction, they are additive and can make an important contribution to inhibitor binding.

Hydrophobic Interactions

Hydrophobic interactions may be described as entropy based forces. When a non polar inhibitor binds to a non polar region of an enzyme, all the ordered water molecules become less ordered as they associate with bulk solvent, leading to an increase in entropy. Any increase in entropy will lead to a decrease in free energy and, stabilization of the enzyme-inhibitor complex. Enzymes and inhibitors usually have large regions of hydrophobic surface and this type of bonding play a significant role in inhibitor binding.

Hydrogen Bonds

A hydrogen bond is a special type of dipole-dipole interaction. For a hydrogen bond to form between an enzyme and an inhibitor, any hydrogen bonds between the inhibitor and water, as well as those between the enzyme and water, must be broken. Formation of the enzyme-inhibitor complex usually leads to an overall 'increase of entropy because the inhibitor remains bound to the enzyme and the formerly bound water molecules are released.

Enzyme inhibitors have long played an important role in medicine, pharmacology, and basic research. The advances in DNA technology have enabled cloning and over expression of large numbers of enzymes have already led to the development of novel therapeutic agents. The evolution of algorithms that can predict enzyme function and mechanism will ensure that the rational design of enzyme inhibitors not only complements structure-based approaches but continues to play a stand-alone role in the discovery of novel therapeutics. The various steps involved in the design of enzyme inhibitors are

1. Determination of the structure of the protein using X-ray crystallography.
2. The active sites in the protein should be determined. Valuable information can be obtained using known inhibitors of the enzyme which suggests the shape of the active site.
3. The inhibitors can then be constructed by altering the binding sites of the molecules for improved activity.

1.3 COMPUTATIONAL DRUG DESIGN

Computational drug design is a fast growing field due to several factors. Significant advances in the development of computational tools have been made over the last ten years. Deployment of efficient computational methods can greatly reduce the cost and the time of drug development. Second, a large number of protein structures are being determined and deposited in the PDB⁸⁶ (Protein Data Bank) due to the proteomics project. In addition, the number of bioactive molecules as an outcome of structure based computer aided drug design is constantly growing. Nevertheless, computational tools can vastly contribute to rational drug design, to develop target-specific drugs.

There are two main approaches in computational drug design. If the structure of the target receptor is not available, only a pharmacophoric approach can be applied. If the receptor structure is known, docking methods can be used in addition to pharmacophore techniques⁸⁷. Although presented separately, the two approaches can combine to improve the results of computational procedures. If the target structure is available, the pharmacophore model can be used to restrict the docking algorithm⁸⁸. A database can be searched using a receptor based pharmacophore Docking can be applied afterwards, only to the potential candidates found, thereby reducing the amount of ligands to be screened. Alternatively, if we do not have the structure of the receptor, pharmacophore information can be used in the modeling of the active site⁸⁹.

A. PHARMACOPHORE MODELING

The term pharmacophore was first defined by Paul Ehrlich⁹⁰ in 1909 as "a molecular framework that carries (*phoros*) the essential features responsible for a drug's (=pharmac*on's*) biological activity". In 1977, this definition was updated by Peter Gund to "a set of structural features in a molecule that is recognized at a receptor site and is responsible for that molecule's biological activity" The IUPAC definition of a pharmacophore is "an ensemble of steric and electronic features that is necessary to ensure the optimal supra molecular interactions with a specific biological target and to trigger (or block) its biological response".

In modern computational chemistry, pharmacophores⁹¹ are used to define the essential features of one or more molecules with the same biological activity. A database of

diverse chemical compounds can then be searched for more molecules which share the same features located a similar distance apart from each other.

The utility of an approach where the detailed information about the three dimensional nature of the receptor is not available has been demonstrated by Bures et al ⁹² who used the pharmacophoric pattern derived for the plant hormone auxin, to find four novel classes of active compounds by searching a corporate three-dimensional database of structures. It is often useful to assume that the receptor site is rigid and that structurally different drugs bind in conformations that present a similar steric and electronic pattern, the pharmacophore.

One corollary of the pharmacophoric concept is the ability to replace the chemical scaffold holding the pharmacophoric groups with retention of activity. In the pharmacophoric hypothesis, physical overlap of similar functional groups is assumed. Despite its limitations, the pharmacophore approach is often the most appropriate because of lack of detailed information regarding the receptor and can yield useful insights, as seen in the case of clinical success with tyrosine kinase inhibitors ^{53, 54} and other recent examples ⁵⁵.

Thus we can postulate the following conditions for activity:

1. The compound must be metabolically stable and capable of transportation to the site for receptor interaction.
2. The compound must be capable of assuming a conformation that will present the pharmacophoric or binding-site pattern complementary to that of the receptor.
3. The compound must not compete with the receptor for space while presenting the pharmacophoric or binding-site pattern.

PHARMACOPHORE FEATURES

Typical pharmacophore features ⁹³ define, where a molecule is Hydrogen bond acceptor, Hydrogen bond donor, Hydrophobic, Hydrophobic aliphatic, Hydrophobic aromatic, Positive ionizable, Negative ionizable, Ring aromatic. The features need to match different chemical groups with similar properties, in order to identify novel ligands. Ligand

receptor interactions are typically “polar positive”, “polar negative” or “hydrophobic”. A well-defined pharmacophore model includes both hydrophobic volumes and hydrogen bond vectors.

A pharmacophore model or hypothesis consists of a three-dimensional configuration of chemical functions surrounded by tolerance spheres. A tolerance sphere defines that area in space that should be occupied by a specific type of chemical functionality. Each chemical function is assigned a weight, which describes its relative importance within the hypothesis. A larger weight indicates that the feature is more important in conferring activity than other composite parts of the hypothesis. Pharmacophore models are routinely used in lead identification and optimization in the areas of library focusing, evaluation and prioritization of virtual high throughput screening (v HTS) results, *de novo* design, and scaffold hopping.

Pharmacophore models can be constructed using analog-based (using known active ligands) or receptor-based techniques (using receptor active site information). In the absence of crystallographic structure data of a protein for which the active site for receptor binding is clearly identified, a chemist must rely on the structure activity data for a given set of ligands. If these ligands are known to bind to the same receptor, then one can attempt to define the commonality between them.. In the presence of protein crystal structure data, active site pharmacophore models can be used as a pre-filter for docking large libraries. Generation of a pharmacophore model using the active site residue information is the key to the success of any pharmacophore-based docking algorithm.

MANUAL PHARMACOPHORE GENERATION: VISUAL PATTERN RECOGNITION

The various steps involved in the development of Pharmacophore⁹¹ model are

1. Visual identification of common structural and chemical features among the active molecules and those features missing in the inactive ones.
2. Measurement of the 3D aspects of the common features with each other
3. Development of a draft Pharmacophore and validation of the model so that the Pharmacophore fits the active compounds and fails to fit the inactive ones
4. Refinement of the Pharmacophore model by applying it to a database of compounds with known activity, until the desired result is obtained.

Particular compound can be inactive because

- I. It does not contain groups in the geometry required for recognition by the biomolecular target, that is, it does not match the required Pharmacophore.
- II. Although it contains the Pharmacophore, it also contains groups that interfere with recognition and that can be detected by a subsequent QSAR.
- III It is less soluble than its bioactive conformation.
- IV. It contains groups that sterically prevent interaction with the target bio molecule, another potency-decreasing property that can be detected by QSAR.

ACCELRYS' CATALYST

Catalyst⁹⁴ can generate two types of automated pharmacophore models, Hypo Gen and HipHop, depending on whether or not activity data is used. If activity data is included, then Catalyst – Hypo Gen is used. Feature based models derived by Hypo Gen have been successfully used to suggest new directions in lead generation – lead discovery and for searching a database to identify new structural classes of potential lead candidates. When no activity is considered during hypothesis building, and only common chemical features are requested, the Catalyst – HipHop can be used for this purpose.

HIPHOP

Hip-Hop provides feature-based alignment of a collection of compounds without considering activity. HipHop matches the chemical features of a molecule, against drug candidate molecules or searches of 3D databases. The resulting hypotheses can be used to iteratively search chemical databases to find new lead candidates. When the ligand set is small (less than 15 compounds), and sufficient biological data is absent, one can build a model based on common feature alignments using Catalyst/HipHop.⁹⁴⁻⁹⁶ Hip-Hop has been used to align a set of molecules based on their common chemical features.

Hip-Hop identifies configurations or three-dimensional spatial arrangements of chemical features that are common to molecules in training set. The configurations are identified by pruned exhaustive search, starting with small sets of molecules and extending them until no longer configuration is found. The user defines the number of molecules that must map completely or partially to the hypothesis. This user-defined option allows broader and more diverse hypotheses to be generated. If a pharmacophore model is less likely to map the active compound, then it will be given higher rank; the reverse is also true.

HYPOGEN

It creates SAR hypothesis models⁹⁴⁻⁹⁶ from a set of molecules for which activity values are known. Given only available experimental information such as 2D structures and biological activities of a set of molecules, Catalyst can be used to generate general interaction hypotheses that explain variations in activity across a set of molecules.

Hypo Gen selects pharmacophore that are common among the active compounds but not among the inactive compounds and then optimizes the pharmacophores using simulated annealing. The top pharmacophores can be used to predict the activity of unknown compounds or to search for new possible leads contained in 3D chemical databases. Hypo Gen generates hypotheses that are set of features in 3D space, each containing a certain tolerance and weight that fit to the features of the training set, and that correlate to the activity data.

The hypotheses are created in three phases Constructive, subtractive and optimization phase. The constructive phase identifies hypotheses that are common among active compounds, the subtractive phase removes hypotheses that are common among the inactive compounds, and the optimization phase attempts to improve the initial hypotheses. The resulting hypotheses models consist of set of generalized chemical features in three-dimensional space as well as regression information. Therefore, the hypotheses models can be used as search queries to mine for potential leads (Figure 1.4) from a three-dimensional database or in the form of an equation to predict the activity of a potential lead.

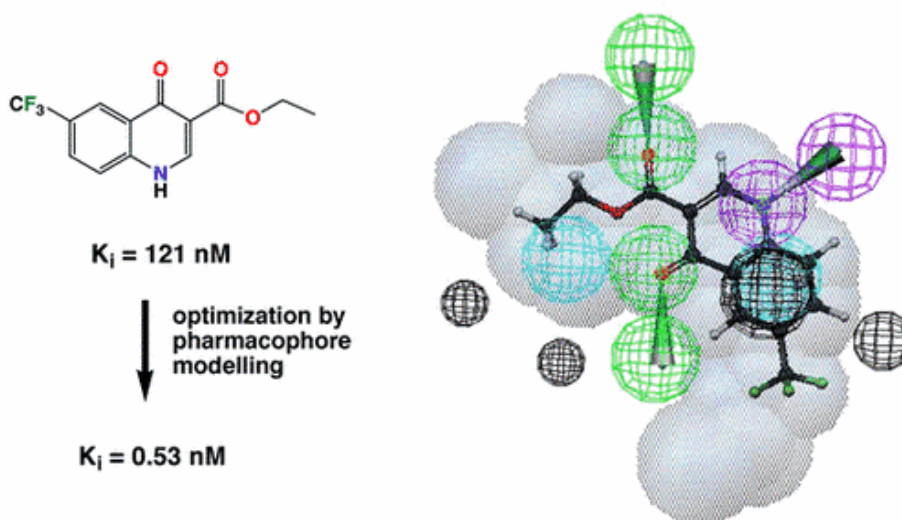


Figure 1.4 Lead optimization using Pharmacophores

Running Hypothesis

The requirements of Ideal Training Set are

1. At least 16 compounds are necessary to assure statistical power.
2. Activities should span 4 orders of magnitude.
3. Each order of magnitude should be represented by at least 3 compounds.
4. No redundant information.
5. No excluded volume problems.

Each of these points is explained one by one below.

Any analysis procedure that employs statistics requires a sample size large enough to distinguish between trivial and real correlations. With Catalyst, the odds of computing a chance correlation begin to increase as the dataset falls below 16 compounds. This doesn't mean training sets of 14 compounds will be useless, just that the probability of finding a useful model is less than optimal.

Catalyst favors models where each feature has a weight of 2, representing the number of orders of magnitude in activity that can be explained by a given feature. For example, consider a carbonyl group which participates in a critical hydrogen bond between a ligand and its receptor. Catalyst considers compounds that do not have this carbonyl group to be 100 times less active than compounds that do and can align this group perfectly within the tolerance sphere. Compounds that have the carbonyl group but place it off-center within the tolerance sphere get partial credit according to the Fit equation. With the five features limit, up to 10 orders of magnitude of activity are theoretically explainable. However, a minimum of 2 features are required just to align molecules relative to each other. Furthermore, Catalyst considers any molecule-hypothesis mapping where more than two features are missed to be a complete miss. Thus, for a 5 featured model, the most inactive compounds in the training set must map at least 3 features while the most active will map all 5. Therefore, the entire range of activity in the set must be explained by the presence or absence of 2 features, hence the 4 orders of magnitude.

Catalyst also favors models where estimated and measured activities correlate well. A regression procedure is used to establish this correlation and such procedures have inherent limitations. For example groups of data points that correlate tend to overwhelm the effect of outliers. If a data set consists of many compounds whose IC_{50} s are close to 100 nMol and

only 1 with an IC_{50} of 1 n Mol, there is a real possibility that the most active compound will be ignored; clearly not a desirable situation. This sort of imbalance can be prevented by assuring that each order of magnitude of activity in the training set is equally represented.

Catalyst pays particular attention to the most active compounds in the training set when it generates the chemical feature space relevant to the experiment. This space is the subset of possible chemical feature-based models among all models in the universe that is likely to contain the model that provides the best explanation of the training set data. Catalyst assumes this subset can be constructed from the features present in the most active compounds in the training set. It determines these compounds by performing a simple calculation based on the activity and uncertainty values. The most active compound (smallest activity value) activity is multiplied by the uncertainty (defaulted to 3) to establish a comparison number A. The next most active compound activity is divided by the uncertainty and this result B compared to A. If B is smaller than A, the compound is included in the "most active" set, if not, the procedure stops. Therefore, in the example above, the 1 n Mol compound would be the only compound used to determine chemical feature space for the experiment and that may not be the desired result. This situation can be avoided by making sure the top order of magnitude of activity is well represented in the training set. Note that changing the uncertainty value from the default to a smaller number will also influence how Catalyst determines the relevant chemical feature space. Therefore, values less than 3 for this parameter are not generally a good idea.

Catalyst derives information from the training set in two ways, from the activity data and from the structures themselves. In order to maximize the probability of finding a good model, it is important to maximize the information content of the training set. Think of Catalyst as a signal analyzer. The stronger the signal, the easier it will be to find. The information content of activity data is maximized by providing compounds that cover 4 orders of magnitude wherein each order is well represented. Structure information content is more subtle. Catalyst looks at molecules as collections of chemical features, not as assemblies of atoms and bonds. Thus, one should provide examples that maximize the kinds, and relative positions, of chemical features recognized by Catalyst. A good way to pick training set members that avoids redundancy is to consider the compounds the same way Catalyst does and apply the following rules of thumb.

Rules for Picking Training Sets

1. The most active compounds should be included.
2. Each compound must possess something new to teach Catalyst.
3. If two compounds have similar structures (collections of features), they must differ in activity by an order of magnitude to be included, otherwise, pick only the more active of the two.
4. If two compounds have similar activities (within one order of magnitude), they must be structurally distinct (from a chemical feature point of view) in order to both be included, otherwise, pick only the most active of the two.

HypoGen is done in three phases, a constructive, subtractive and optimization phase as shown in figure 1.5.

Constructive phase

This is done in several steps:

- 1) All active compounds are identified
- 2) All hypotheses (maximum 5 features) among the two most active compounds are identified and stored
- 3) Those that fit the remaining active compounds are kept separately.

Subtractive phase

In this phase, the program removes hypotheses from the data structure that are not likely to be useful. The hypotheses that were created in the constructive phase are inspected and if they are common to most of the inactive compounds then they are removed from consideration.

Optimization phase

The optimization is done using the well-known algorithm simulated annealing. The algorithm applies small perturbations to the hypotheses created in the constructive and subtractive phases in an attempt to improve the score.

HYPOREFINE

The Hypo Refine algorithm is an extension of the Catalyst HypoGen algorithm for generating SAR-based pharmacophore models which can be used to estimate activities of new compounds. Hypo Refine helps to improve the predictive models generated from a

dataset by a better correlating hypothesis with the steric properties that contribute to biological activity. In addition, Hypo Refine can help overcome over-prediction of inactive compounds with pharmacophore features in common with other active compounds in the dataset, where inactivity is due to steric clashes with the target.

HypoGen - Generate Hypothesis

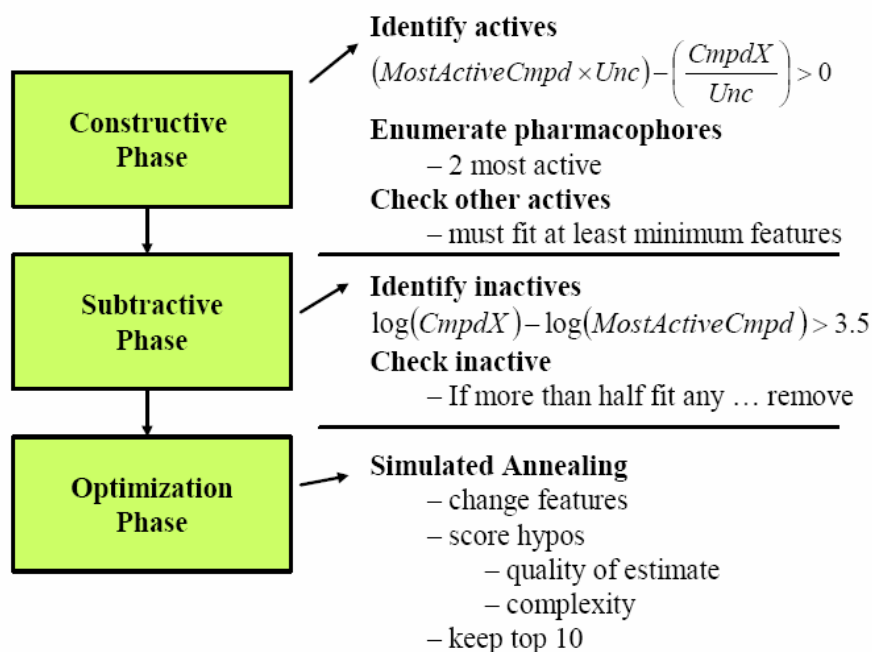


Figure 1.5: Hypotheses generation in Catalyst

INTERPRETING THE COST PARAMETERS IN THE OUTPUT FILES

During an automated hypothesis generation run, Catalyst considers and discards many thousands of models. It distinguishes between alternatives by applying a cost analysis. Catalyst uses bits for language, so the program assigns costs to hypotheses in terms of the number of bits required to describe them fully.

HypoGen calculates the cost of two theoretical hypotheses, one in which the cost is minimal (Fixed cost), and one where the cost is high (Null cost). Each optimized hypothesis cost should have a value between these two values and should be closer to the Fixed than the Null cost.

Randomized studies have found that if a returned hypothesis has a cost that differs from the Null hypothesis by 40-60 bits, it has 75-90% chance of representing a true correlation in the data.

Another useful number is the Entropy of hypothesis space. If this is less than 17, a thorough analysis of all the models will be carried out. The overall assumption is based on Occam's razor; that is between equivalent alternatives, the simplest model is best. In general, if this difference is greater than 60 bits, there is an excellent chance of the model to represent a true correlation. Since most returned hypotheses are higher in cost than the fixed cost model, a difference between fixed cost and null cost of 70 or more is necessary to achieve the 60 bits difference.⁹⁴⁻⁹⁶

Fixed Cost

This is the cost of the simplest possible hypothesis (initial)

Null Cost

This is the cost when each molecule estimated as mean activity, acts like a hypothesis with no features

Weight Cost

A value that increases in a Gaussian form as the feature weight in a model deviates from an idealized value of 2.0. This cost factor favors hypotheses in which the feature weights are close to 2. The standard deviation of this parameter is given by the weight variation parameter.

Error Cost

A value that increases as the rms difference between estimated and measured activities for the training set molecules increases. This cost factor is designed to favor models for which the correlation between estimated and measured activities is better. The standard deviation of this parameter is given by the uncertainty parameter.

Configuration Cost

A fixed cost depends on the complexity of the hypothesis space being optimized. It is equal to the entropy of the hypothesis space. This parameter is constant among all the hypotheses. The main assumption made by HypoGen is that an active molecule should map more features than an inactive molecule. In other words, the molecule is inactive because a) it misses important feature or b) the feature is present but cannot be oriented in correct space. Based

on this assumption, the most active molecule in the dataset should map to all features of the generated hypotheses.

METRIC FOR ANALYZING HIT LISTS AND PHARMACOPHORES

Validity of the pharmacophore model is determined by its ability to retrieve known active molecules from the various known databases Figure 1.6.⁹¹

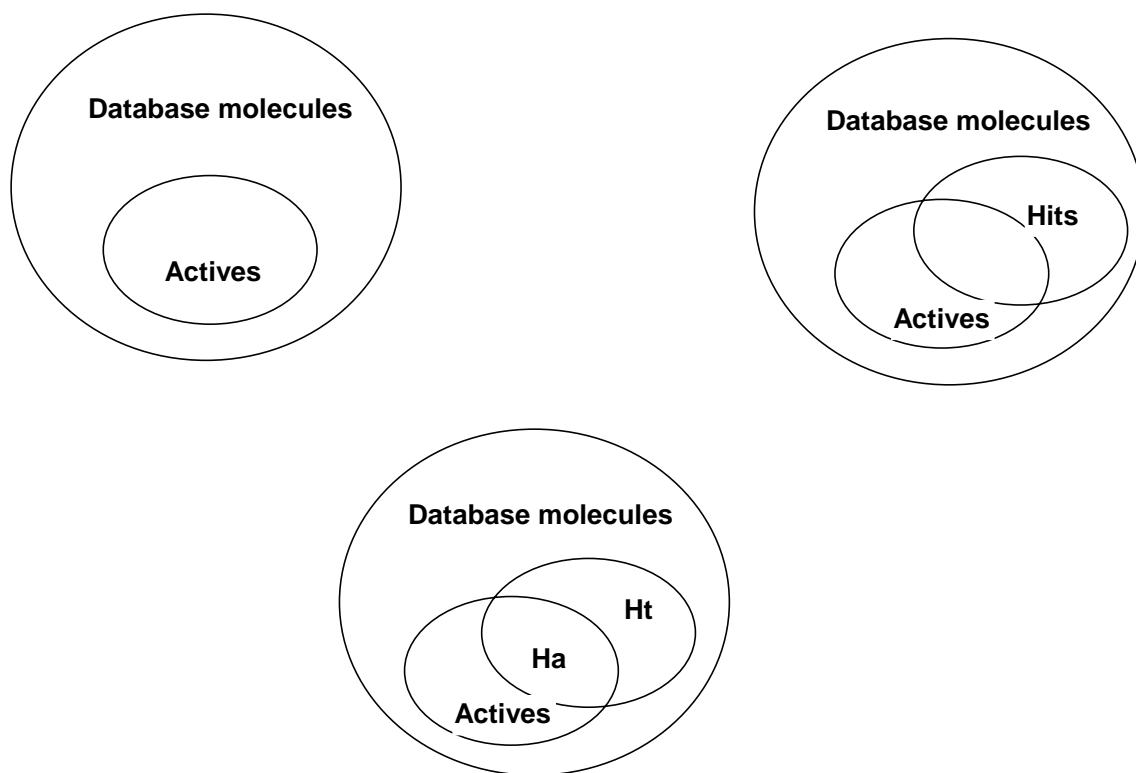


Figure 1.6: Database searching using pharmacophore models

D = Total number of compounds in database, A = Number of active compounds in database,

H_t = Number of compounds in search hit list, H_a = Number of active compounds in hit list.

PHARMACOPHORE VALIDATION

Percent yield of actives:

$$\% Y = H_a / H_t \times 100$$

Percent ratio of the activities in the hit list:

$$\% A = H_a / A \times 100$$

Enrichment (enhancement)

$$E = \frac{H_a / H_t}{A / D} = \frac{H_a \times D}{H_t \times A}$$

False negatives: $A - H_a$

False positives: $H_t - H_a$

$$\text{Goodness of fit} = \left(\frac{H_a (3A + H_t)}{4 H_t A} \right) \times \left(\frac{1 - H_t - H_a}{D - A} \right)$$

The best hit list is obtained when there is perfect overlap of the hit list to the known active compounds in the database. This occurs when both conditions $H_a = H_t$ and $H_a = A$, hence $H_a = H_t = A$, are satisfied, which is a nearly impossible case to achieve in a real-life situation.

In reality, there may be many compounds in the database that may be active but either have not been listed as active, or have not been tested for specific activity. In either case, these compounds end up in the “False positives” list. Hence we consider the list of false positives as opportunities for potential leads. The objective is to improve the hit list in such a manner that the false positives can contain a large number of potential leads.

“False negatives” list is nothing but missing the retrieval of active molecules from database.

The best hit list is the one that retrieves all the actives and nothing else (i.e., $H_t = H_a = A$); False negatives = 0, false positives = 0.

The worst list is the one that retrieves everything else but the known actives in the database (i.e., $H_a = 0$, $H_t = D - A$) False negatives = A, false positives = D - A.

The GH score gives a good indication of how good the hit list is with respect to a compromise between maximum yield and maximum percent of activities retrieved. The Table 1.3 provides an acceptable sorting of the hit lists, from best to worst, via the GH score.

The Goodness of Hit formula is a convenient way to quantify hit lists obtained from searches with various queries.

TABLE 1.3 GOODNESS OF FIT SCORE VALUES

CASE	% Y	% A	ENRICHMENT	FALSE NEGATIVES	FALSE POSITIVES	GH
Best	100	100	500	0	0	1
Typical Good	40	80	200	20	120	0.60
Extreme Y	100	1	500	99	0	0.50
Extreme A	0.2	100	1	0	49,900	0.50
Typical Bad	5	50	25	50	950	0.26
Worst	0	0	0	100	49,900	0

The applications of Pharmacophore model are

- Testing ideas (find new candidate molecule)
- Prioritizing leads
- Designing compound libraries
- Predicting activity
- Using the resulting alignments for additional studies
- Search queries for database mining

B. DOCKING STUDIES

Structure-based drug design methods utilize knowledge of the three-dimensional structure of a receptor complexed with a lead molecule in an attempt to optimize the bound ligand or a series of congeneric molecules. Computational method that predicts the 3D structure of a protein-ligand complex is often referred to as molecular docking approaches. Docking plays an important role in this process by placing a molecule into the active site of the target macromolecule in a non covalent fashion. In that light, docking can be viewed as a search or optimization⁴⁶ method which, given the degree of conformational flexibility at the macromolecular level, can be a very challenging problem.⁹⁷⁻¹⁰¹

Docking is frequently used to predict the binding orientation of small molecule drug candidates to their protein targets in order to predict the affinity and activity of the small molecule. The number of proteins with a known three-dimensional structure is increasing rapidly, and structures produced by structural genomics initiatives are beginning to become publicly available.^{102,103} The increase in the number of structural targets is in part due to improvements in techniques for structure determination, such as high throughput X-ray crystallography.¹⁰⁴ With large-scale structure-determination projects driven by genomics consortia, many target proteins have been selected for their therapeutic potential.¹⁰⁵⁻¹⁰⁷

The docking process involves the prediction of ligand conformation and orientation (or posing) within a targeted binding site. In general, there are two aims of docking studies: accurate structural modeling and correct prediction of activity. However, the identification of molecular features that are responsible for specific biological recognition, or the prediction of compound modifications that improve potency, are complex issues that are often difficult to understand and even more so to simulate on a computer.¹⁰⁸

POSING, SCORING AND RANKING

POSING

The process of determining whether a given conformation and orientation of a ligand fits the active site is called posing. This is usually a fuzzy procedure that returns many alternative results.

SCORING

Both posing and ranking involve scoring. The pose score is often a rough measure of the fit of a ligand into the active site. The rank score is generally more complex and might attempt to estimate binding energies.

RANKING

A more advanced process than pose scoring that typically takes several results from an initial scoring phase and re-evaluates them. This process usually attempts to estimate the free energy of binding as accurately as possible.

Although the posing phase might use simple energy calculations (electrostatic and van der Waals), ranking procedures typically involve more elaborate calculations (perhaps including properties such as entropy or explicit solvation).

SEARCH METHODS AND MOLECULAR FLEXIBILITY

Algorithms use both ligand flexibility and to some extent protein flexibility. Treatment of ligand flexibility can be divided into three basic categories: systematic methods (incremental construction, conformational search, databases); random or stochastic methods (Monte Carlo, genetic algorithms, tabu search); and simulation methods (molecular dynamics, energy minimization). Some of the soft wares used in flexible ligand docking methods¹⁰⁸ are given in Table 1.4

SCORING FUNCTIONS

Scoring functions estimate interaction energies between small ligands and proteins to rank docking results, according to the relative binding affinities of different ligands.¹⁰⁹ The evaluation and ranking of predicted ligand conformations is a crucial aspect of structure-based virtual screening. Even when binding conformations are correctly predicted, the calculations ultimately do not succeed if they do not differentiate correct poses from incorrect ones and if ‘true’ ligands cannot be identified¹⁰⁸.

Scoring functions implemented in docking programs make various assumptions and simplifications in the evaluation of modeled complexes and do not fully account for a

number of physical phenomena that determine molecular recognition — for example, entropic effects. The different types of scoring functions are presented in Table 1.5.

TABLE 1. 4 FLEXIBLE LIGAND DOCKING SOFTWARES

RANDOM/STOCHASTIC	SYSTEMATIC	SIMULATION
Auto Dock (MC)	DOCK (incremental)	DOCK
MOE-Dock (MC, TS)	Flex X (incremental)	Glide
GOLD (GA)	Glide (incremental)	MOE-Dock
PRO_LEADS (TS)	Hammerhead (incremental)	Auto Dock
	FLOG (database)	Hammerhead

The three types or classes ¹⁰⁸of scoring functions that currently applied are Empirical, Force-Field based and Knowledge-based scoring functions.

TYPES OF SCORING FUNCTIONS

1) Force-Field-Based

Non-bonded energy terms of molecular mechanics force fields were first used to score protein–ligand complexes. The binding affinity is estimated by summing up the electrostatic and Vander Waals interaction energies

2) Empirical

A second class of scoring functions has become known as empirical scoring functions. Binding energy is essentially expressed as a weighted sum of explicit hydrogen bonding and hydrophobic contact terms.

3) Knowledge-Based

The third class of scoring functions owes its existence to the massive increase of structures in the Protein Database⁸⁶. The so-called knowledge-based scoring functions¹¹⁰ are exclusively built from statistical analyses of experimentally determined complex structures, based on the assumption that inter atomic distances occurring more often than some average value should represent favorable contacts and vice versa.

TABLE 1. 5 TYPES OF SCORING FUNCTIONS AND ITS CORRESPONDING SOFT WARES

FORCE-FIELD-BASED	EMPIRICAL	SIMULATION
D-Score	LUDI	PMF
G-Score	F-Score	Drug Score
GOLD	Chem Score	SMoG
Auto Dock	SCORE	
DOCK	Fresno	

The different docking programs¹⁰⁷ and their searching and scoring techniques is shown in Table 1.6. The examples of recent successful structure-based virtual screening studies¹⁰⁸ are shown in Table 1.7.

TABLE 1. 6 DIFFERENT DOCKING PROGRAMS AND THEIR SEARCHING AND SCORING TECHNIQUES

PROGRAM	SEARCHING ALGORITHM	SCORING FUNCTION	LIGAND FLEXIBILITY	PROTEIN FLEXIBILITY
Mining Minima	Combination of GA/ Tabu Search and other methods	Empirical free energy	yes	Side chain
Dock It	Distance Geometry	MM/Pmf/PLP	yes	no
Darwin	Genetic Algorithm	CHARMM	yes	no
Divali	Genetic Algorithm	Amber	yes	no
Gambler	Genetic Algorithm	PLP	yes	no
GOLD 3.0	Genetic Algorithm	MM +Fragmental/ Chem Score	yes	Partial
Adam	Incremental construction	Amber	yes	no
Flex E	Incremental construction plus computability search	Fragmental empirical free energy	yes	Partial
Flex X	Incremental construction	Fragmental empirical free energy	yes	no

PROGRAM	SEARCHING ALGORITHM	SCORING FUNCTION	LIGAND FLEXIBILITY	PROTEIN FLEXIBILITY
Hammerhead	Incremental construction	Empirical free energy	yes	no
Ludi	Incremental construction	Fragmental empirical free energy	yes	No
DOCK 4.0	Incremental construction /Graph matching	Shape complementary/mm/empirical free energy	yes	no
Auto dock 3.0	MC/SA - GA - LGA	Modified Amber	yes	no
Amber	Molecular Dynamics	MM	yes	yes
CHARMM	Molecular Dynamics	MM	yes	yes
Dock vision	Monte Carlo	Shape Complementary	yes	no
Glide	Monte Carlo	Modified ChemScore	yes	no
ICM	Monte Carlo	ECEPP	yes	Partial
MCDOCK	Monte Carlo	MM	yes	no
MCM	Monte Carlo	CHARMM + Solvation term	yes	Active Site
Pro dock	Monte Carlo	MM (Amber/ECEPP)	yes	Partial
QXP	Monte Carlo	Amber	yes	no
Affinity	MonteCarlo/Simulated Annealing	MM	yes	Side chain
FLOG	Point Complementary	Empirical free energy	no	no
FTDOCK	Point Complementary	Shape Complementary +Electrostatic	no	no
Sandock	Point Complementary	Shape Complementary	no	no
Slide	Point Complementary	Shape Complementary	no	no
Eudoc	Systematic	Amber	no	no
Tree dock	Systematic tree search	Leonard Jones function	no	no
PRO_LEADS	Tabu Search	ChemScore	yes	no

TABLE 1. 7EXAMPLES OF RECENT SUCCESSFUL STRUCTURE-BASED VIRTUAL SCREENS

S. NO.	METHOD	STUDY	TARGET
1	DOCK	Crystal structure; 200,000 compounds; 1,000 top-scoring clustered; rule-of-five; 15 compounds tested; 3 hits (0.4 μ M)	BCR-ABL tyrosine kinase
2	DOCK	Homology model; 250,000 NCI compounds; rigid docking (50,000 orientations per ligand); 444 ligands flexibly docked; 13 tested; 3 hits (<100 μ M)	Thymidine phosphorylase
3	FlexX	800,000 ACD compounds reduced to 856; 9 hits; (0.25–256 μ M)	t RNA-guanine transglycosylase
4	DOCK	1,700-fold enrichment over actual HTS; 1.7 μ M inhibitor through VS	Phosphatase-1B
5	FlexX	ACD search, 1 hit (43 μ M)	IGF1/IGF-BP-5
6	DOCK	Homology model; 400,000 compounds; 12 test; one hit (80 nM)	Protein kinase CK2
7	Catalyst/DOCK	4,000 ACD compounds; pharmacophore search; 24 tested; 12 in μ M range across 6 mutants	Plasmodium falciparum DHFR
8	DOCK	Homology model; 200,000 NCI compounds; 35 tested; 7 hits (1.6–14 μ M)	BCL2/BCL-XL

GLIDE

The Docking algorithm used in the study is glide¹¹¹ (Grid-based ligand docking with energetics- GLIDE) calculations are performed with Impact version v3.5 (L. Schrödinger). The grid generation step requires Maestro input files of both ligand and active site, including hydrogen atoms. The protein charged groups that were neither located in the ligand-binding pocket nor involved in salt bridges were neutralized using the Schrödinger pprep script. The center of the grid enclosing box was defined by the center of the bound ligand as described in the original PDB entry. The enclosing box dimensions, which are automatically deduced

from the ligand size, fit the entire active site. For the docking step, the size of bounding box for placing the ligand center was set to 12 Å. A scaling factor of 0.9 was applied to Van der Waals radii of ligand atoms.

SCORING FUNCTIONS OF GLIDE

GLIDE 3.5 employs two forms of Glide Score:

- (i) GLIDE Score 3.5 SP, used by Standard-Precision Glide;
- (ii) GLIDE Score 3.5 XP, used by Extra-Precision Glide.

These functions use similar terms but are formulated with different objectives in mind. Specifically, GLIDE^{112,113} score 3.5 SP is a “softer”, more forgiving function that is adept at identifying ligands that have a reasonable propensity to bind, even in cases in which the GLIDE pose has significant imperfections. This version seeks to minimize false negatives and is appropriate for many database screening applications. In contrast, GLIDE score 3.5 XP is a harder function that exacts severe penalties for poses that violate established physical chemistry principles such as that charged and strongly polar groups be adequately exposed to solvent. This version of GLIDE score is more adept at minimizing false positives and can be especially useful in lead optimization or other studies in which only a limited number of compounds will be considered experimentally and each computationally identified compound needs to be as high in quality as possible.

GLIDE score 3.5 modify and extend the ChemScore function as follows:

$$\begin{aligned} \Delta G_{\text{bind}} = & C_{\text{lipo-lipo}} \sum f(r_{lr}) + \\ & C_{\text{hbond-neut-neut}} \sum g(\Delta r) h(\Delta \alpha) + \\ & C_{\text{hbond-neut-charged}} \sum g(\Delta r) h(\Delta \alpha) + \\ & C_{\text{hbond-charged-charged}} \sum g(\Delta r) h(\Delta \alpha) + \\ & C_{\text{max-metal-ion}} \sum f(r_{lm}) + C_{\text{rotb}} H_{\text{rotb}} + \\ & C_{\text{polar-phob}} V_{\text{polar-phob}} + C_{\text{coul}} E_{\text{coul}} + \\ & C_{\text{vdW}} E_{\text{vdW}} + \text{solvation terms} \end{aligned}$$

The lipophilic-lipophilic term is defined as in Chem-Score. The hydrogen-bonding term also uses the Chem-Score form but is separated into differently weighted components that depend on whether the donor and acceptor are both neutral, one is neutral and the other is charged, or both are charged. In the optimized scoring function,

the first of these contributions is found to be the most stabilizing and the last, the charged-charged term, is the least important.

The metal-ligand interaction term (the fifth term) uses the same functional form as it is employed in ChemScore but varies in three principal ways. First, this term considers only interactions with anionic acceptor atoms (such as either of the two oxygen of a carboxylate group). This modification allows GLIDE to recognize the strong preference for coordination of anionic ligand functionality to metal centers in metalloproteases. The seventh term, from Schrodinger's active site mapping facility, rewards instances in which a polar but non-hydrogen-bonding atom (as classified by ChemScore) is found in a hydrophobic region. The second major component is the incorporation of contributions from the Coulomb and vdW interaction energies between the ligand and the receptor. The third major component is the introduction of a solvation model. To include solvation effects, GLIDE 3.5 docks explicit waters into the binding site for each energetically competitive ligand pose and employs empirical scoring terms that measure the exposure of various groups to the explicit waters.

DOCKING METHODOLOGY

The method is an interactive procedure in which random ligand conformations are generated for specified number of times, number of maximum trials. The procedure maintains a 'Save List' in which the best-docked structures found by the algorithm is stored. One specifies the number of structures, N save, to be saved into the Save List. The shape of each candidate ligand conformation is compared with that of the active site. If the Save List is full (i.e. it contains N save docked ligand structures), and if the shape similarity of the candidate is worse than that of any saved structure (in the Save List), the candidate conformation is rejected. Otherwise, the candidate conformation is selected for docking. Initially when the save list is empty, the candidate is selected for docking regardless of its shape similarity. When the Save List is full, the shape similarity comes into play. As the algorithm proceeds, the save list evolves towards better-docked structures as these replace the worse ones.

DOCKING OF THE LIGAND (CALCULATION OF DOCK ENERGY)

There are two energy terms in the expression for the dock energy, internal energy of the ligand and the interaction energy of the ligand with the protein. The interaction energy is taken as the sum of the Vander-Waals energy and electrostatic energy. The internal energy of the ligand is taken as the sum of the internal van der Waals and electrostatic energy.

1.4 SYNTHESIS

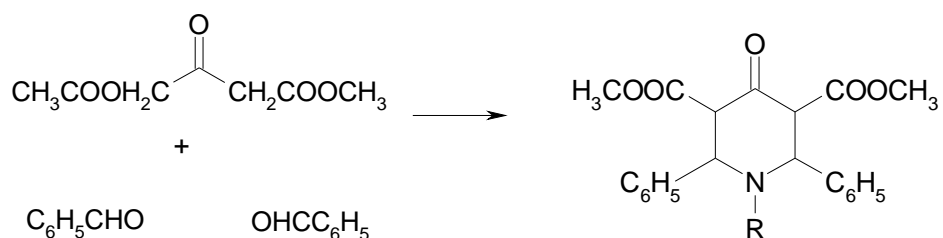
PIPERIDINE-4-ONES

Among the family of heterocyclic compounds, nitrogen containing heterocycles especially piperidine-4-ones presumably gaining considerable importance owing to their varied biological properties such as, Anti-viral, anti-cancer, analgesic anti-tumour, local anaesthetic, anti-microbial, bactericidal, fungicidal, anti-histaminic, anti-inflammatory, CNS stimulant and depressant activities.

The synthesis of piperidin 4-ones involves two ¹¹⁴ processes. The methods include inter molecular and intramolecular reactions. The intermolecular reactions involve the preparation of piperidine-4-ones from 1-acylpyridinium salts. The imino Diels-Alder reaction used for the preparation of piperidine-4ones are also classic example of intermolecular processes.

The intra molecular processes involve Mannich reactions, Cyclo additions and the preparation from β -amino carboxylates. The Mannich condensation is the most commonly used route for the synthesis of piperidine-4-ones.

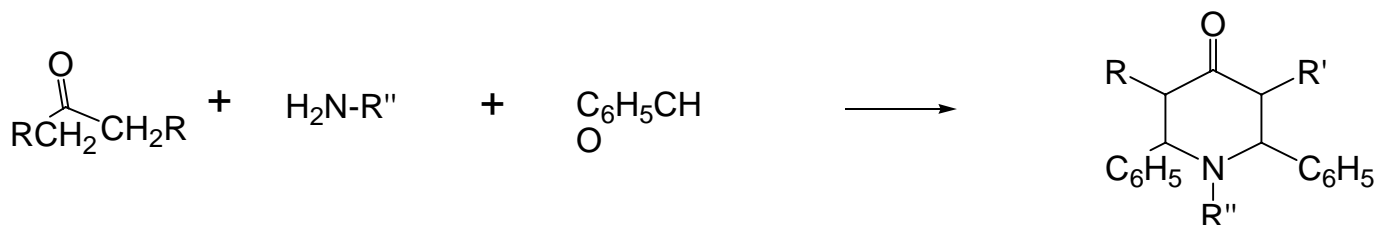
The synthesis of piperidone compounds developed by Petrenko-krit schenko involves the condensation of two molecules of benzaldehyde with ammonia (or a primary aromatic or aliphatic amine) and an ester of acetone dicarboxylic acid is given below.



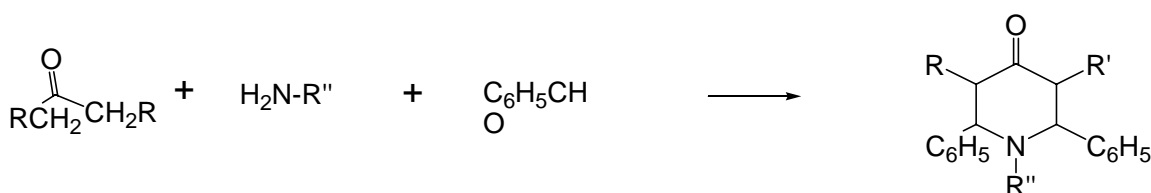
The reaction proceeds successfully when acetaldehyde was substituted for benzaldehyde (46% yield), although the reaction has been reported to fail with formaldehyde.

Ethyl α , α' diethyl acetone carboxylate reacts with formaldehyde and methylamine, to give a piperidone. Only two active hydrogen atoms are available on the substituted ethyl acetone dicarboxylate in the 1 & 3 positions. Accordingly the formation of the many possible byproducts by further condensation of formaldehyde is eliminated and the yield of piperidone is fairly good. When R in the equation is further condensed

with formaldehyde and methylamine the reaction can proceed to give bicyclic pyridone known as bispidin.



Attempts to conduct the same reaction on simple ketones instead of acetone dicarboxylic ester were unsatisfactory until Baliah et al found that this reaction proceeds with experimental ease when acetic acid is the solvent.



The yields were highest with ammonia (R''=H) and were poorer as the size of the R group increased, on the other hand, benzaldehyde can be readily replaced with other aromatic aldehydes such as Anisaldehyde, Piperonal and Veratraldehyde without substantially altering the yields.

MICROWAVE ASSISTED ORGANIC SYNTHESIS

Microwave activation as a non-conventional energy source has become a very popular and useful technology in organic chemistry. In the electromagnetic spectrum, the microwave radiation region is located between infrared radiation and radio waves. Microwaves¹¹⁵ have wavelengths of 1mm-1m, corresponding to frequencies between 0.3 and 300GHz. The short reaction times and expanded reaction range that is offered by microwave assisted organic synthesis are suited to the increased demands in industry.

The combination of solvent-free reaction conditions and microwave irradiation leads to large reductions in reaction times, enhancements in conversions and, sometimes, in selectivity with several advantages of the eco-friendly approach, termed Green chemistry.

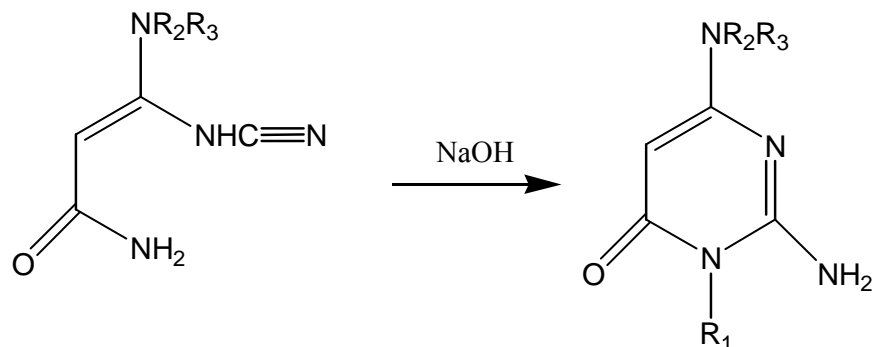
Green chemistry is defined as "environmentally benign chemical synthesis". It is a science-based non-regulatory and economically driven approach to achieving the goals of environmental protection. The ultimate value of green chemistry lies in its applicability for the new millennium¹¹⁶.

AMINOPYRIMIDINES

Pyrimidines are six-membered heterocyclic diazine group of compounds similar to benzene and pyridine containing two nitrogen atoms^{117,118} in positions 1 and 3. Pyrimidines are the basic nucleus of nucleic acids. Pyrimidines have been isolated from the nucleic acid hydrolysate. Three nucleobases found in nucleic acids, namely cytosine, thymine, and uracil, are pyrimidine derivatives.

In 1818, Gaspare Brungnatelli isolated the first pyrimidine derivative alloxan by the oxidation of uric acid with nitric acid¹¹⁹. The first example of principal pyrimidine synthesis was the synthesis of barbituric acid, in 1878 from malonic acid and urea¹²⁰.

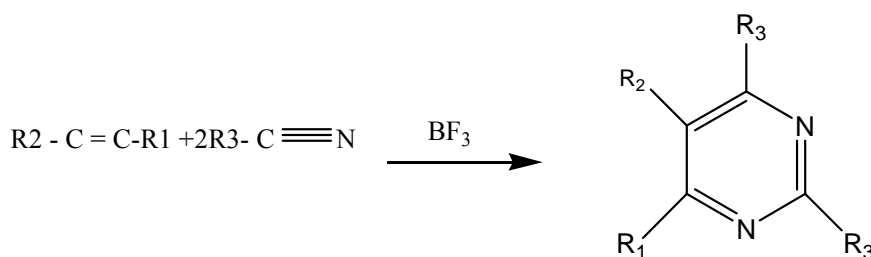
The synthetic methods for pyrimidines are classified on the basis of number of components employed in the pyrimidine ring construction and also based on the type of the starting material used. One of the examples of one-component synthesis is the base-catalyzed cyclization of the N-cyanoamine¹²¹ derivatives to the 2-aminopyrimidines.



Another reaction is the two-component synthesis^{122,123} the most versatile and widely used methods for pyrimidine and pyridine synthesis. It involves the condensation of two reactants. One of the components used may contribute 3, 4 or 5 atoms of pyrimidine ring system, while the other contributes 3, 2 or 1 atom respectively.

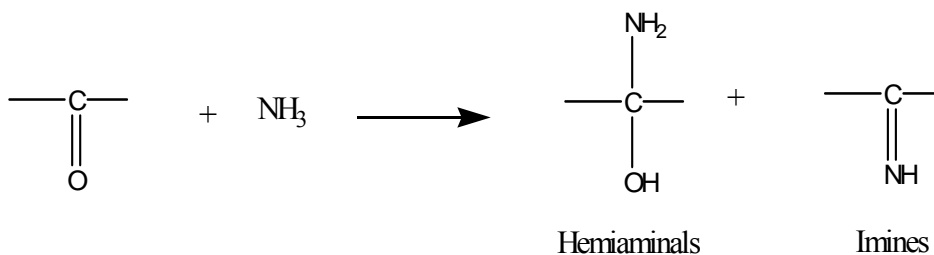
One of the important reactions for efficient synthesis of pyrimidine is principal component method ¹²⁴. This reaction involves condensation of three-carbon fragment with compound capable of donating N-C-N fragment and is generally referred to as principal synthetic method for pyrimidine. A variety of dicarbonyl compounds such as β -aldehyde esters, β -keto-nitriles have been condensed with 1, 3 bi nucleophile. Various N-C-N fragments used are NH_2CONH_2 (urea), $\text{NH}_2\text{C}=\text{NHNH}_2$ (guanidine), NH_2CSNH_2 (thiourea)

An example of three-component synthesis is the reaction of acetylene with two molecules of nitriles in the presence of boron trifluoride to yield pyrimidine¹²⁵.

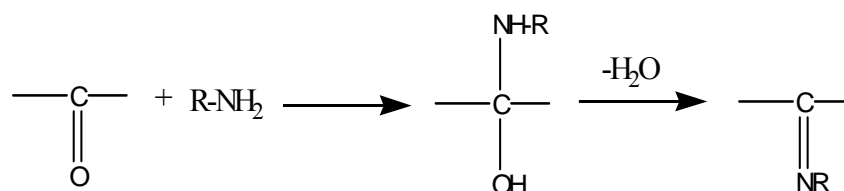


SCHIFF BASES

Schiff bases are a class of compounds that undergoes hydrolysis readily under mild acidic conditions to liberate the active aldehydes. Schiff bases are other wise called as aldimines, azomethines. The addition of ammonia to aldehydes or ketones does not generally give useful products. According to the pattern followed by analogous nucleophiles, the initial products would be expected to be hemiaminals (aldehyde ammonia) and/or imines. However these compounds are generally unstable. Most imines with hydrogen on the nitrogen spontaneously polymerize. Stable hemiaminals can be prepared from poly halogenated aldehydes and ketones do give stable imines ($\text{Ar}_2\text{C}=\text{NH}$).



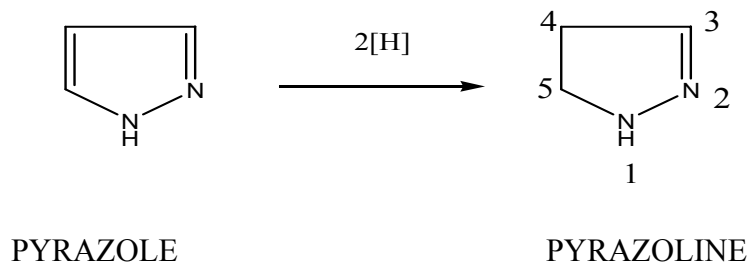
Aldehyde or ketone reacts with primary amines gives imines. These imines are stable enough for isolation. However, in some cases, especially with simple R groups, they rapidly decompose or polymerize unless there is at least one aryl group on nitrogen or carbon. When there is an aryl group, the compounds are quite stable. They are usually called Schiff bases, and this reaction is the best way to prepare them. The reaction is straightforward and proceeds in high yields. The initial N-substituted hemiaminals lose water to give the stable Schiff bases.

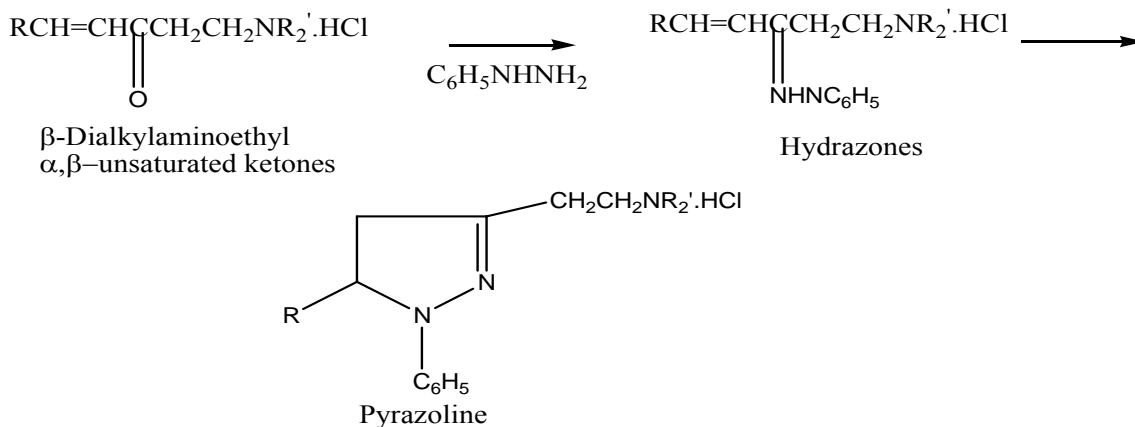


In general, ketones react more slowly than aldehydes, and higher temperature and longer reaction times are often required. In addition, the equilibrium must often be shifted, usually by removal of the water, either azeotropically by distillation, or with a drying agent such as TiCl_4 or with a molecular sieve.

PYRAZOLINES

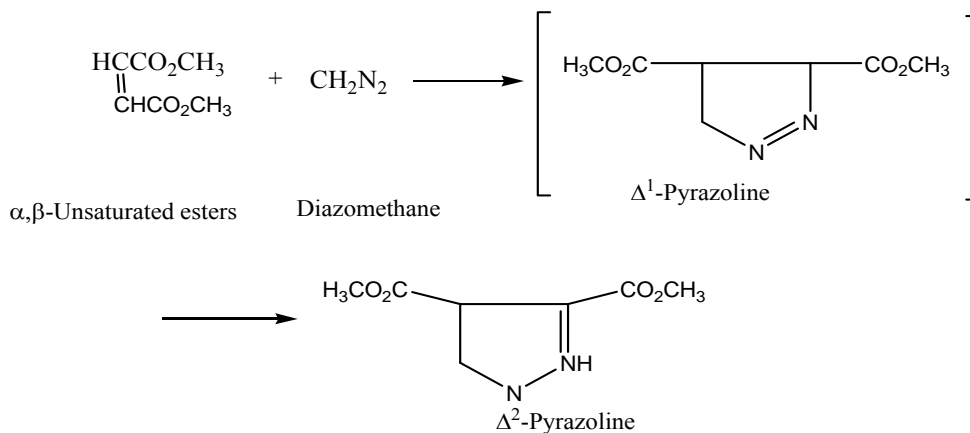
Electron-rich nitrogen heterocyclics play an important role in diverse biological activities. Pyrazolines are the important nitrogen-containing five-membered heterocyclic compounds with noteworthy applications. Pyrazoline is the reduced form of pyrazole nucleus.





- **From Diazo Compounds And Olefins:**

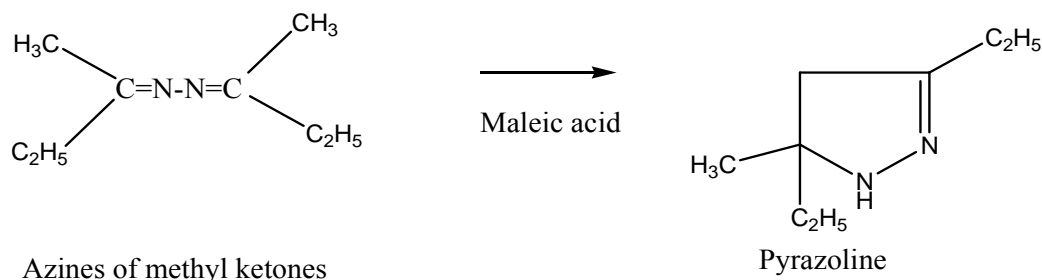
Pyrazolines are readily obtained from α , β -unsaturated esters and diazole compounds. The Δ^1 -pyrazolines that are formed first as a rule rearrange spontaneously to Δ^2 -pyrazolines



Compounds containing double bonds not ordinarily subject to nucleophilic attack often fail to react with diazo compounds or react only under more vigorous conditions or in the presence of catalysts. Ethylene reacts slowly with diazomethane in cold ether to give pyrazoline.

- **From Azines:**

The last method of synthesizing the pyrazoline nucleus is from the azines. The azines of methyl ketones cyclize by reaction with maleic acid or other organic acids.



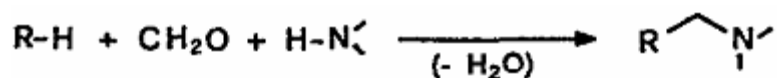
Of the four methods discussed above, most commonly used method for synthesizing pyrazoline nucleus is from α , β -unsaturated carbonyl compounds (Chalcones) is one of the best examples for α , β -unsaturated carbonyl compounds.

MANNICH REACTION

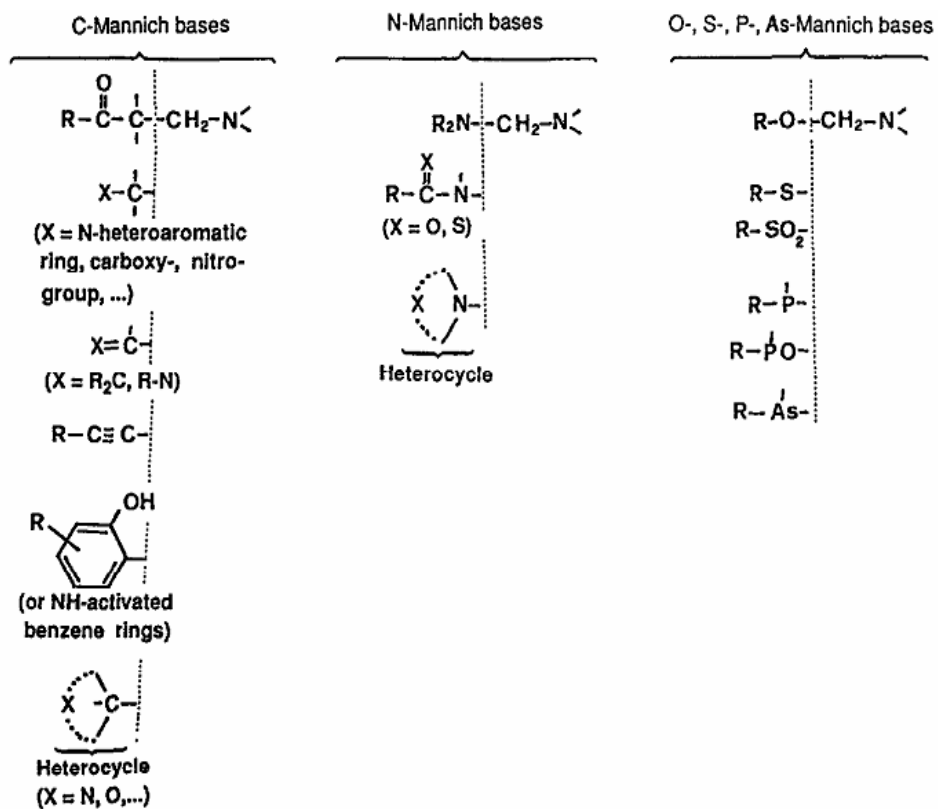
Compounds having active hydrogen react with non-enolizable aldehydes and ammonia (or primary or secondary amines) to give amino methylated products which are known as Mannich bases.

The Mannich reaction is one of the most basic and useful method for the preparation of β -amino carbonyl compounds and it has been one of the most important reactions in organic chemistry for its use in synthesis of various pharmaceuticals, natural products, and versatile synthetic intermediates.

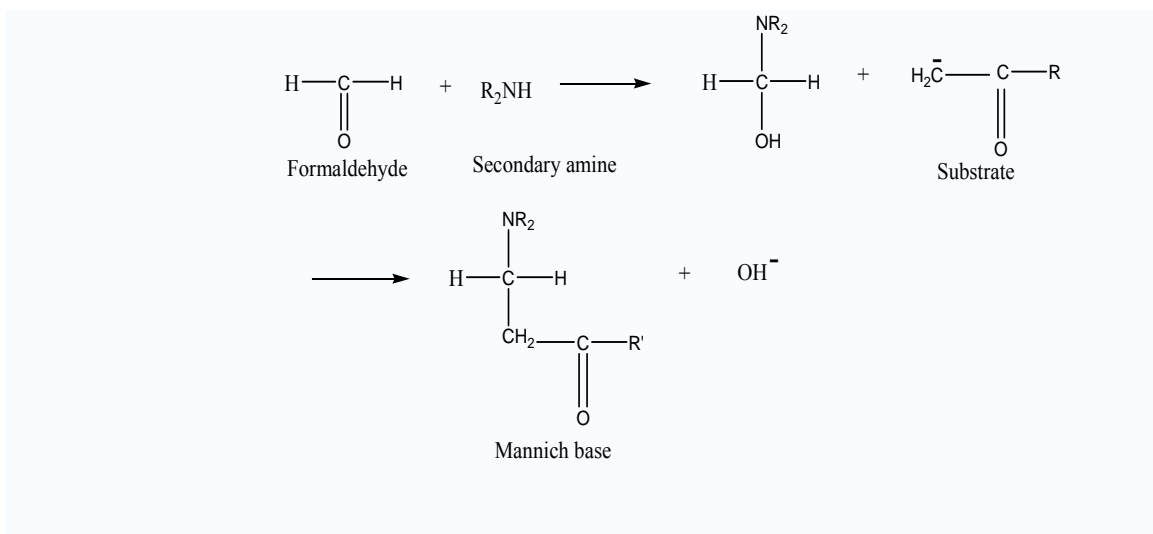
The Mannich reaction¹²⁶ is the condensation of a compound having active hydrogen atoms (the substrate) with formaldehyde and an amine.



The structures of the products depend on the nature of the substrate, as the amine moieties of Mannich bases are frequently derived from quite common primary or secondary alkyl- and aryl-amines. A general classification of the substrates employed in Mannich reactions is as follows:



C-aminomethylation is favored by acidic conditions whereas N-Mannich bases are produced when free amine and formaldehyde or O, N-acetals in anhydrous solvents are employed as amino methylating agents. The Mechanism for base catalyzed Mannich reaction:



2. REVIEW OF LITERATURE

Ooms. F.⁶⁰ has outlined the technological advances in the field of Medicinal Chemistry and he has emphasized more on lead generation and optimization.

Gerhard Klebe¹²⁷ has discussed in detail about the target selection, analysis, preparation, the tools, strategies of a virtual screening campaign, the accuracy of scoring and ranking of results.

Juswinder Singh *et al.*¹²⁸, applied a combination of SBDD methods and Structural genomics to the design of inhibitor complexes from protein kinase family.

William.L.Jorgensen¹²⁹ presented an overview emphasizing more on virtual screening, denovo design, evaluation of drug likeness and advanced methods for determining protein-ligand binding,

Giovanna Scapin¹³⁰ explored the recent examples to illustrate the evolution of macromolecular crystallography and the usage of structural information in different stages of drug discovery process.

Mitchell A.Miller¹³¹ looked at the generation and types of databases that are becoming powerful tools in drug discovery. He also discussed how to formulate and run the queries & how the results of the searches are processed.

Ricardo M. Biondi and Angel R.Nebrada¹³² reviewed the recent studies that illuminate the mechanisms used by three families of Ser/Thr protein kinases to achieve substrate specificity.

Albert C.Pierce *et al.*¹³³ presented evidence for the hydrogen bonding interactions in the heterocyclic CH groups in kinase ligands while other aromatic CH groups do not exhibit these characteristics. Thus they showed that heterocycles are preferred in kinetic inhibitors showing favorable interactions.

Janet Dancey and Edward A.Sausville¹³⁴ considered the crucial issues in the development of kinase inhibitors for cancer and discussed strategies to address the challenges raised by these issues in the light of preclinical and clinical experiences.

Adrian Gill¹³⁵ discussed the novel strategies for kinase inhibitor generation and associated technologies for target identification and validation including RNAi applications.

Dongyu sun¹³⁶ designed a kinase focused compound collection and generated promising hits and leads using a ligand shape based virtual screening and a receptor based approach.

Gerhard Muller¹³⁷ gave an overview of potentially interesting transmembrane proteins which serve as targets for biomedical research which includes Ser/Thr-kinase receptors.

Martin E.M.Noble *et al.*¹³⁸ have reviewed many serine/threonine kinases which have been targeted with productive results for inflammation and cancer.

Adeel Malik *et al.*¹³⁹ made a survey of bioinformatics databases and QSAR for cancer research and reported the cancer related databases along with some case studies.

A detailed review on the role of Aurora-A inhibitors in cancer therapy was given by Agnese V, *et al.*¹⁴⁰.

The first crystal structure of Aurora 2 kinase in complex with adenosine was reported by Cheetam GM, *et al.*¹⁴¹



Lee Ec, *et al.*¹⁴² reported that Aurora-A and Aurora-B are highly expressed in primary human and mouse prostate cancers and prostate cancer cell lines and their findings support a functional relationship between Aurora kinase expression and prostate cancer and the application of small-molecule inhibitors in therapeutic modalities.

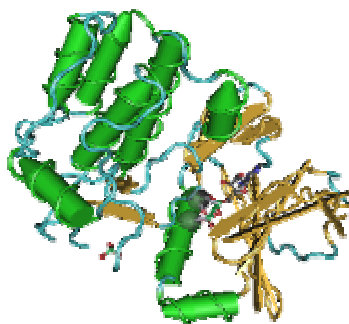
Warner SL, *et al.*¹⁴³ observed that there is no advantage in targeting both kinases simultaneously and felt that an Aurora A targeted therapy may have some beneficial

consequences over an Aurora B targeted therapy such as mitotic arrest and the rapid induction of apoptosis

Meraldi P.Honda and Nigg EA.¹⁴⁴ discussed the regulation and deregulation of Aurora kinases and showed their strong link between mitotic errors and carcinogenesis.

Mahadevan D, *et al.*¹⁴⁵, validated human Ark1 as a drugable target in pancreatic cancer by undertaking a structure based approach to design specific inhibitors utilizing homology modeling, affinity docking and an invitro kinase assay in an iterative process.

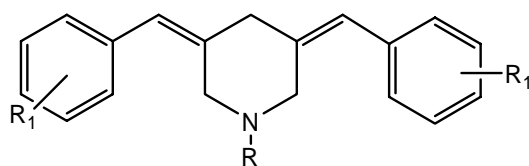
The crystal structure of Aurora A along with two other kinases was determined by Nowakowski J, *et al.*¹⁴⁶, and all the three structures provide new sights into kinase regulation and the design of selective inhibitors.



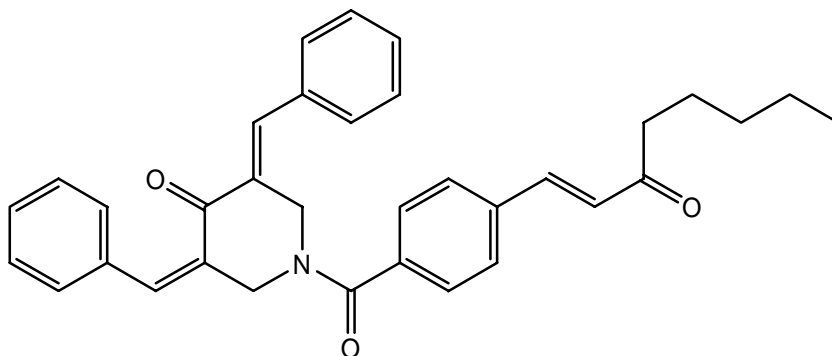
Soncini C, *et al.*¹⁴⁷ identified PHA-680632 as the first representation of a new class of Aurora inhibitors with a high potential for further development as an anticancer therapeutic.

The antitumor activity of MLN 8054, an orally active small-molecule inhibitor of Aurora-A kinase that has entered phase I clinical trials was described by Manfredi. M.G. *et al.*¹⁴⁸.

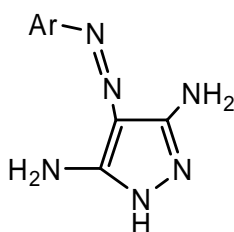
Hari N.Pati, *et al.*¹⁴⁹, demonstrated the cytotoxic properties and preferential toxicity to tumour cells displayed by some 2, 4-bis (benzylidene) 8-methyl-8-azabicyclo [3.2.1] octane-3-ones and 3, 5-bis (benzylidene)-1-methyl 4-piperidones.



A Novel series of N (4-(3-aryl-3-oxo-1-propenyl) phenyl carbonyl)-3, 5-bis (phenyl methylene)-4-piperidones were synthesized and tested for their cytotoxicity by Jonathan R.Dimmock¹⁵⁰.

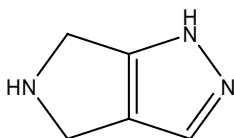


Pyrazole derivatives were identified as a novel group of ATP antagonists with moderate potency against CDK₂-cyclinE (anticancer) by Vladimir krystof *et al.*¹⁵¹

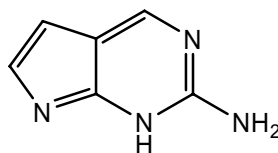


Nicholas Keen and Stephen tailor¹⁵² discussed about the various inhibitors of Aurora A, B and C, the complete biology, evolution and their association with cancer.

Fancelli.D.*et al.*¹⁵³ identified 1,4,5,6 tetrahydropyrrolo (3, 4-c) pyrazoles as potent Aurora kinase inhibitor with a favorable antitumor kinase inhibition profile.

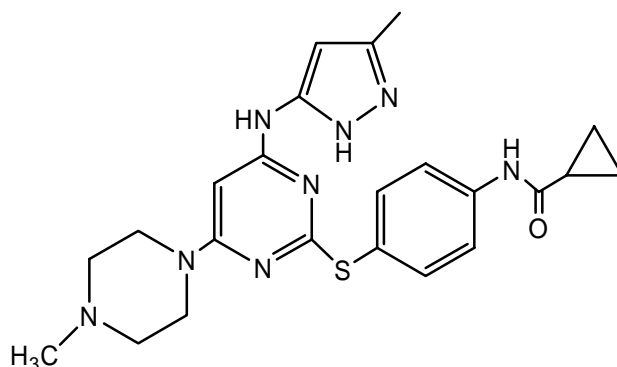


Moriarty KJ, *et al.*¹⁵⁴ identified 2-amino-pyrrolo (2, 3-d) pyrimidine scaffold as a new class of Aurora-A inhibitors and described the SAR of the novel series.

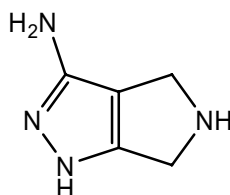


From the combinatorial expansion of the 1,4,5,6-tetrahydropyrrolo(3,1-c) pyrazole bi-cycle, a novel and versatile scaffold designed to target the ATP pocket of protein kinases, Fancelli D, *et al.*¹⁵⁵, discovered potent and selective Aurora kinase inhibitors.

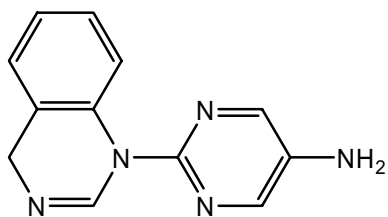
Harrington EA *et al.*¹⁵⁶ reported the discovery of a highly potent and selective small molecule inhibitor of Aurora kinases, VX-680 that blocks cell cycle progression and induces apoptosis in a diverse range of human tumor types.



Pevarello P, *et al.*¹⁵⁷ reported 3-amino-1,4,5,6-tetrahydropyrrolo [3,4-c]pyrazoles as a new class of CDK2 inhibitors.

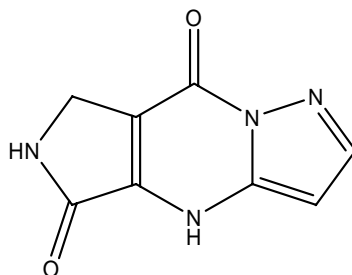


Heron NM *et al.*¹⁵⁸ developed a novel series of 5-aminopyrimidinyl quinazolines from aniline-quinazoline as potent and specific Aurora kinase inhibitors.



Carpinelli *et al.*¹⁵⁹, worked on PHA-739358 a 3-amino pyrazoles derivative which inhibited all Aurora kinase family members.

Tricyclic 6,7-dihydro-4-H-pyrazolo(1,5-a) pyrrolo[3,4-d] pyrimidines 5,8-dione was identified as a novel scaffold for Aurora kinase A inhibition through virtual screening by Coumar MS et al.¹⁶⁰.



Venkataraman Mohan *et al.*¹⁶¹ discussed the fundamental issues and challenges involved in comparing various docking methods.

A genetic algorithm that explores the full conformational flexibility of the ligand with partial flexibility of the protein was designed by Gareth Jones *et al.*¹⁶².

Thomas Lengaver *et al.*¹⁶³ focused on virtual screening methods that are based on analyzing ligand similarity on a structural level. They concentrated on methods that exploit structural properties of complete ligand molecules instead of pharmacophores.

An evaluation of ten docking programs and thirty seven scoring functions against eight proteins of seven protein types for three tasks: binding mode prediction, virtual screening for lead identification and rank-ordering by affinity for lead optimization was conducted by Gregory L. Warren *et al.*¹⁶⁴.

Richard A. Friesner *et al.*¹⁶⁵ developed a novel scoring function to estimate protein-ligand binding affinities and implemented as the GLIDE 4.0 XP scoring function and docking protocol.

The key concepts and specific features of small molecule-protein docking methods were reviewed by Douglas B. Kitchen¹⁰⁸ and he also highlighted the selected applications.

Natasja Brooijmans and Irwin D. Kuntz¹⁶⁶ summarized several critical methodological issues including molecular recognition, molecular docking and Database methods.

Glen RC and Allen SC,¹⁰⁷ described some of the more common methods and algorithms used to solve the docking problem including GLIDE and they reviewed the recent applications in cancer research.

The Basics and Characteristics of five key commercial docking tools including GLIDE were discussed by Tanja Schulz-Gasch and Martin Stahl¹⁶⁷.

Hougming chen *et al.*¹⁶⁸ examined four commercially available docking programs, FLEX X, GOLD, GLIDE and ICM for their ligand docking and virtual screening capabilities. They concluded that ICM and GLIDE appear to be the primary choices for everyday molecular docking.

Kontoyianni *et al.*¹⁶⁹ carried out an extensive computational study in which five docking programs FLEX X, DOCK, GOLD, LIGAND FIT, GLIDE were investigated against 14 protein families(69 targets).They observed a higher success rate with GLIDE's ability to identify binding modes as its top-scoring poses.

A new docking methodology that has been implemented in the First Discovery Software package GLIDE (Grid-based LIgand Docking with Energetics) was described by Richard A. Friesner, *et al.*¹¹² and they reported that GLIDE is nearly twice as accurate as GOLD and FLEX X for ligands having up to 20 rotatable bonds.

The ability of GLIDE 2.5 to identify the known binders seeded into database screens for a wide variety of pharmaceutically relevant receptors and their comparison study investigated by Thomas A.Halgren, *et al.*¹¹³, showed that GLIDE 2.5 performs better than GOLD1.1, FLEX X 1.8 or DOCK 4.01.

Eight docking programs were compared by Esther Kellenberger, *et al.*¹⁷⁰ and the study showed that GLIDE, GOLD and SURFLEX are the most successful in ranking known inhibitors in a virtual screening experiment.

Perola, *et al.*¹⁷¹ gave a detailed comparison of current docking and scoring methods on systems of pharmaceutical relevance.

Krovat EM, *et al.*¹⁷² reviewed the recent advances in docking and scoring.

Camille G. Wermuth¹⁷³ reveals that majority of small molecule therapeutics result from analogue design. The analogue of an existing drug molecule has structural and pharmacological similarities with the original compound.

The structure based approach to design novel enzyme inhibitors and the combination of molecular structure determination with computation was explained by Irwin D. Kuntz¹⁶ with examples.

Gilbert M. Rishton¹⁷⁴ has discussed simple chemistry guidelines for the evaluation of ‘positives’ in biochemical screens with the aim of selecting stable, non-covalent binders (ligands) and eliminating protein-reactive compounds (reagents) from consideration as drug leads at an early stage.

Deng XQ *et al.*¹⁷⁵ performed the pharmacophore modeling and the hit molecules obtained were subjected to filtration by Lipinski rule, docking study. He identified two compounds showing inhibition of Aurora –A kinase in micro molar levels.

A 3D chemical feature-based pharmacophore model was developed by Roberto Di santo *et al.*¹⁷⁶ using catalyst software which produced 10 pharmacophore hypothesis. These results demonstrated that the hypothesis derived is a useful tool in designing new leads.

A three dimensional pharmacophore model for 5-Hydroxytryptamine₆ (5-HT₆) receptor antagonists with the catalyst software was developed by Maria L, *et al.*¹⁷⁷.

Gisbert Schneider and Uli Fechner¹⁷⁸ outlined the various design concepts and highlighted current development in computer-based denovo design. According to them the denovo design supports drug discovery projects by generating novel pharmaceutically active agents with desired properties in a most and time efficient manner.

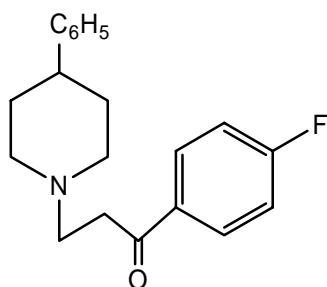
Mark Rogers-Evans *et al.*¹⁷⁹, identified a rapid entry to novel and patentable cannabinoid receptor (CB-1) ligands using computer based denovo design in combination with parallel synthesis.

Theodora steindl and Thierry Langer¹⁸⁰ compared the two virtual screening methods (i.e) docking and pharmacophore modeling and summarized their benefits and disadvantages. They also developed a Virtual library.

A comparative performance assessment of the conformational model generators Omega and catalyst was carried out by Johannes Kirchmair *et al.*¹⁸¹ It was confirmed that

catalyst proves to be the best choice for the most exhaustive conformational search and it also shows better performance in high throughput screening.

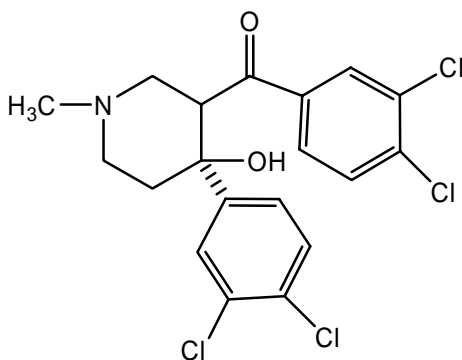
Pharmacophore-based discovery, Synthesis and Biological evaluation of 4-phenyl 1-arylalkyl piperidines as dopamine transporter inhibitors were disclosed by Sukumar Sakamuri *et al.*¹⁸² They found that the lead compound has significant DAT inhibitory activity.



Istvan J.Enyedy *et al.*¹⁸³ discovered substituted pyridines as novel Dopamine Transporter inhibitors using pharmacophore based methods.

Min-Yong Li *et al.*¹⁸⁴ developed a chemical feature based pharmacophore model for α_1 A-adrenoreceptor antagonists. The results of their study provided a valuable tool in designing new leads with desired biological activity by virtual screening.

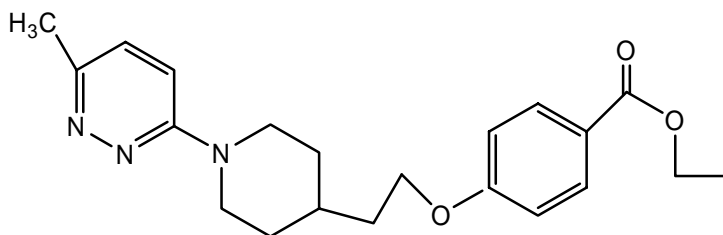
3, 4-disubstituted pyrrolidines were discovered as a novel class of MAO-transporter inhibitors using pharmacophore-based discovery by Istvan J.Enyedy *et al.*¹⁸⁵



Krisztina Boda and A. Peter Johnson¹⁸⁶ described a novel method for complexity analysis of the de novo designed ligands.

Theodora M. Steindl *et al.*¹⁸⁷ screened a large commercially available database of compounds using a highly selective structure based pharmacophore model generated with

the program catalyst. They also performed a docking study and a principal component analysis within the software package cerius². The combined efforts led to the selection of six candidate structures for which invitro anti rhino viral activity was carried out.



Stepanchikova AV, *et al.*¹⁸⁸ evaluated the PASS prediction ability by activity spectra prediction for 63 substances which were presented in the molecule of the month section of prous science, from different chemical classes and having various types of biological activity. They found that mean accuracy of prediction was about 90% and concluded that it is reasonable to use PASS for finding and optimizing new lead compounds.

Poroikov VV and Filimonov DA¹⁸⁹ proved that PASS can be effectively used for selection of compounds with the required actions and without the unwanted effects by, PASS applications to the 880 compounds from Prestwick chemical library.

The application of the program PASS (Prediction of Activity Spectra for Substances) to about 250,000 compounds of the NCI open database and the incorporation of over 64 million PASS predictions in the enhanced NCI database browser were described by Vladimir.V. Poroikov. *et al.*¹⁹⁰. It is also shown that how the user can conduct complex searches by combining ranges of PASS-predicted probabilities of compounds to be active or to be inactive.

Alka Marwaha *et al.*¹⁹¹ virtually designed 400 imidazoline N-oxides, out of which five cyclic nitrones were selected on the basis of PASS prediction as potent nootropics and were evaluated for their biological activities in albino mice.

Athina Geronikaki *et al.*¹⁹² discovered new anxiolytics by prediction of biological activity with computer programs PASS and DEREK for a heterogeneous set of 5494 highly chemically diverse heterocyclic compounds. The majority of tested compounds exhibited the predicted anxiolytic effect. They found that the application of the computer

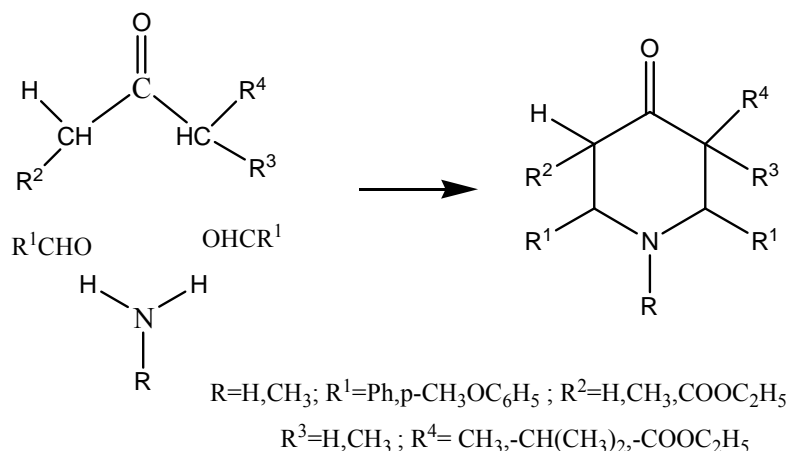
assisted approach significantly reduced the number of synthesized and tested compounds and increased the chance of finding new chemical entities.

Hugo Kubinyi¹⁹³ described neural nets in addition to drug likeness for the definition of drug like character and he also described some other filtering techniques to eliminate undesirable atom or groups and compounds with potential to be cytotoxic.

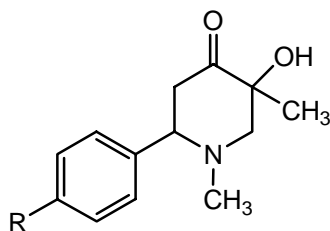
The latest protocols employed in rational drug design including druglikeness and computational ADME was outlined by Nouri Neamati and Joseph J. Barchi, Jr¹⁹⁴.

Tobias Wunberg *et al.*¹⁹⁵ described drug like and lead like hits derived from HTS campaigns provide good starting points for lead optimization.

Noller and Baliah¹⁹⁶ prepared piperidine-4-one derivatives by heating a mixture of ketone, aldehyde and ammonium acetate in acetic acid in the ratio of 1:2:1.

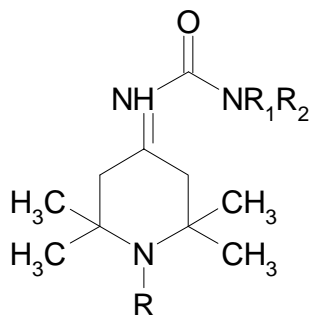


Andreeva *et al.*¹⁹⁷ has discussed the antiviral activity of 3-hydroxy-1,3-dimethyl-6-phenyl-4-piperidone, 3-hydroxy-1,3-dimethyl-6-(4-fluoro phenyl)-4-piperidone and 3-hydroxy-1,3-dimethyl-6-(4-methoxyphenyl)-piperidine-4-thiosemicarbazone against adenovirus.

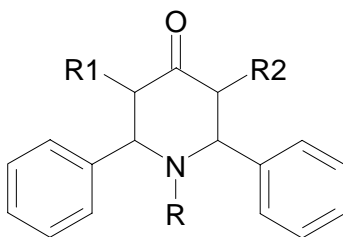


Bagley and Spencer ¹⁹⁸ prepared 4-(hetero cyclyl acylamino) piperidines. They were found to be useful as narcotic antagonists and analgesics.

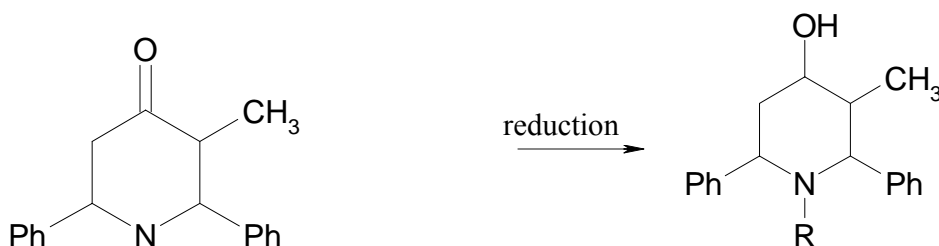
Baracu *et al.* ¹⁹⁹ reported that coupling of 2, 2, 6, 6-tetramethyl-4-amino piperidine with RNCO gave piperidyl ureas which under went nitrosation to yield nitroso ureas. They studied the anticancer treatment of these compounds against L 1210 Cells.



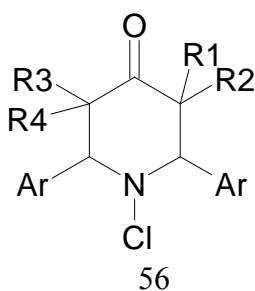
Balasubramaniam M and Padma N ²⁰⁰ were prepared and studied the stereochemistry of some 4-Piperidinols



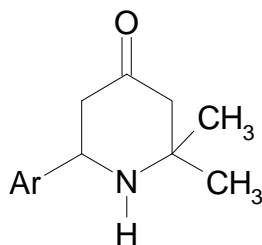
Edersberg and Haller ²⁰¹ synthesized various substituted cis-2, 6-phenyl-3-methyl-4-piperidinols by the reduction of the corresponding 4-Piperidones.



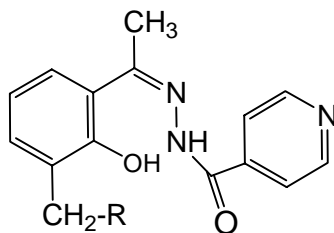
Ganapathy and Vijayan B. ²⁰² synthesized various substituted N-Chloro piperidine-4-ones based on Noller and Balliah method.



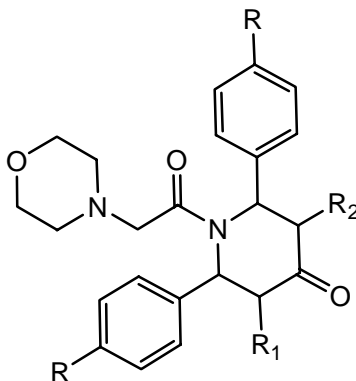
Ganellin and Spickett ²⁰³ prepared 2, 2-dimethyl-6-aryl-4-piperidones. They found to possess a combination of stimulant and depressant effects on the central nervous system.



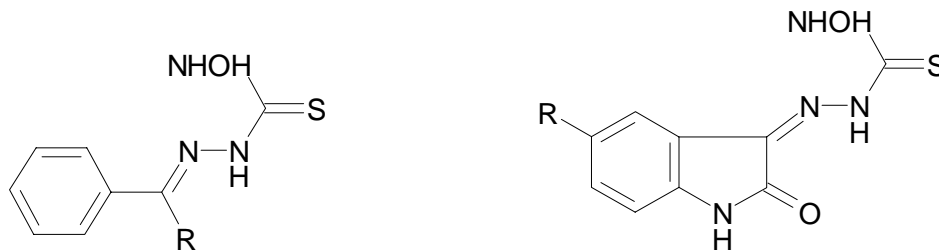
Sriram D, *et al.* ²⁰⁴ reported the synthesis, *in vitro* and *in vivo* anti mycobacterial activity of isonicotinyl hydrazones.



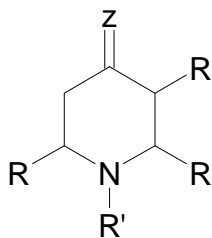
Synthesis, Stereochemistry and Antimicrobial evaluation of some N-morpholinoacetyl-2, 6-diarylpiperidin-4-ones were studied by S.Kabilan *et al.* ²⁰⁵



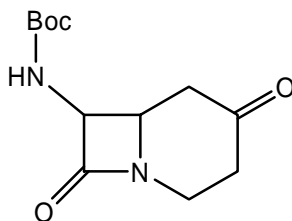
Sriram D, *et al.* ²⁰⁶ synthesized N-Hydroxythio semicarbazones and reported their *in vitro* antitubercular activity.



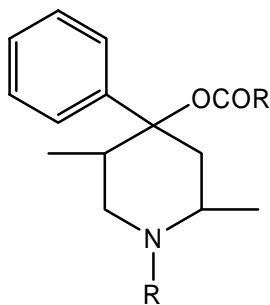
Mobio *et al.*²⁰⁷ studied the physiological activities of 2, 3, 6-triacyl-4-oxopiperidines. They showed bactericidal, fungicidal and herbicidal activity.



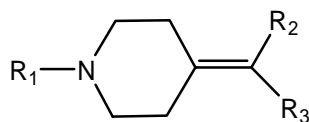
Achille Barco *et al.*²⁰⁸ prepared 2-substituted Piperidin-4-ones as precursors of carbacephams.



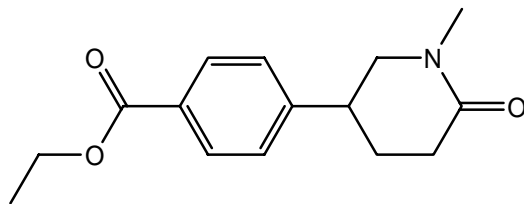
Hassan MMA and Casy AF.²⁰⁹ reported the PMR details of N-substituted -2,5-dimethyl -4-piperidones.



A two step synthesis for N-aryl- and N-aryl substituted 4-piperidones was reported by Scherer.T, *et al.*²¹⁰. They studied the influence of the N-aryl donor on the electronic absorption and fluorescence spectra.



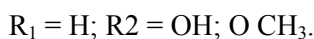
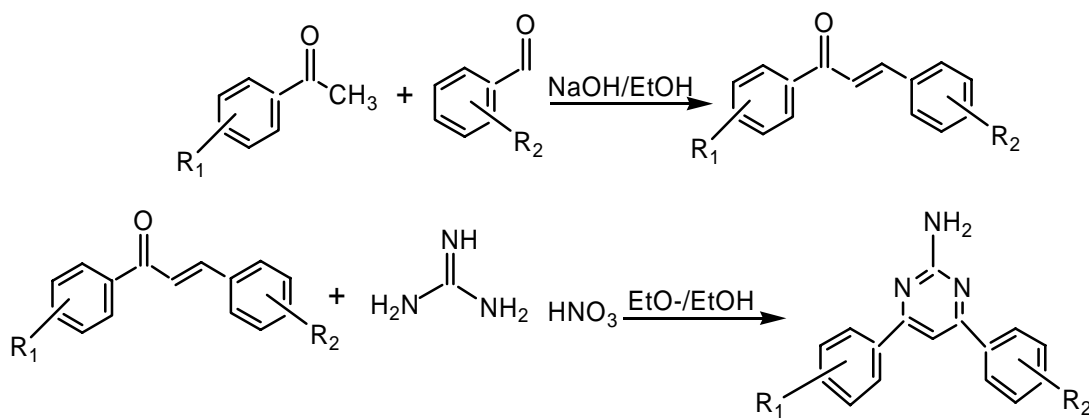
In search for the non steroidal inhibitors of 5α -reductase, Rolf W. Hartmann and Martin Reichert ²¹¹ synthesized and studied the structure-Activity relationships of carboxamide phenyl alkyl-substituted Pyridones and piperidones.



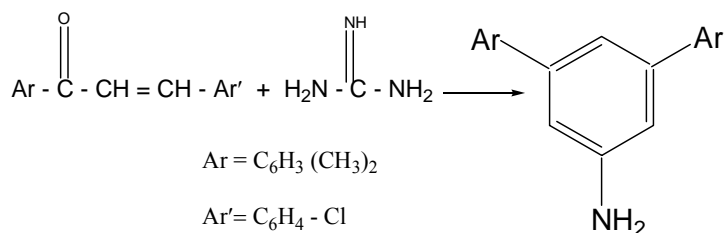
Philip M. Weintraub, *et al* ²¹² highlighted the recent methodologies that have been used to synthesize piperidones and piperidones with a focus on literature from mid1999 to late-2002.

A Series of 2, 6-diaryl-4-piperidones were prepared and the infrared spectra of substituted piperidones in carbon tetrachloride were recorded in the range of 4000–400 cm^{-1} . by Sampathkumar R, *et al* ²¹³.

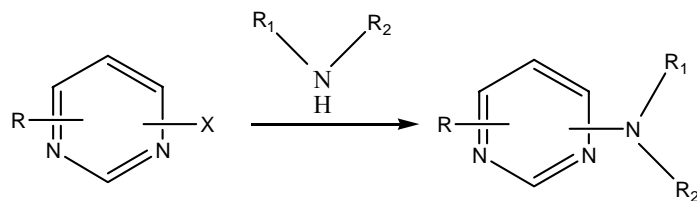
Venkatesan J, *et al.* ²¹⁴, synthesized different substituted derivatives of chalcones and amino- pyrimidines and reported their biological activities.



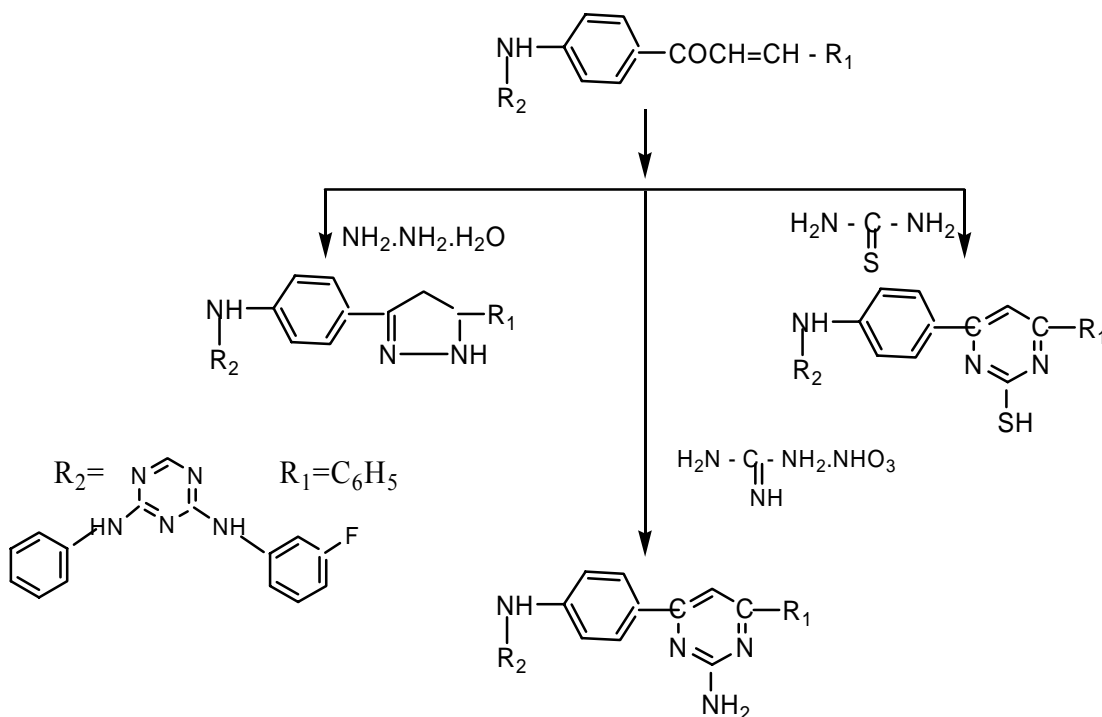
El-Hashash *et al.* ²¹⁵ studied synthesis of pyrimidine derivatives and their anti-microbial, anti-fungal activities.



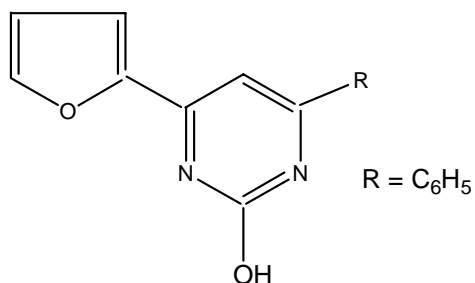
Guanglin Luo *et al.*²¹⁶ studied Microwave Assisted Synthesis of Amino - Pyrimidines by Suzuki coupling reactions.



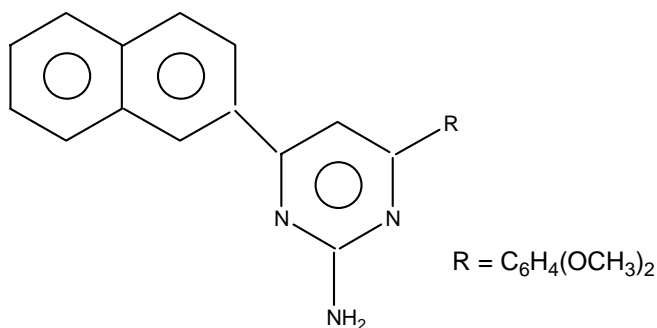
Anjani Solankee, Jayesh Patel²¹⁷ synthesized Chalcones, Pyrazolines, Aminopyrimidines, Pyrimidinethiones by the condensation of 2-phenyl amino-4-(3'-fluorophenylamino)-6-(4'-acetylphenyl amino)-S-triazine on treatment with aromatic aldehydes yields chalcones, which on cyclization with hydrazine hydrate, guanidine nitrate and thiourea.



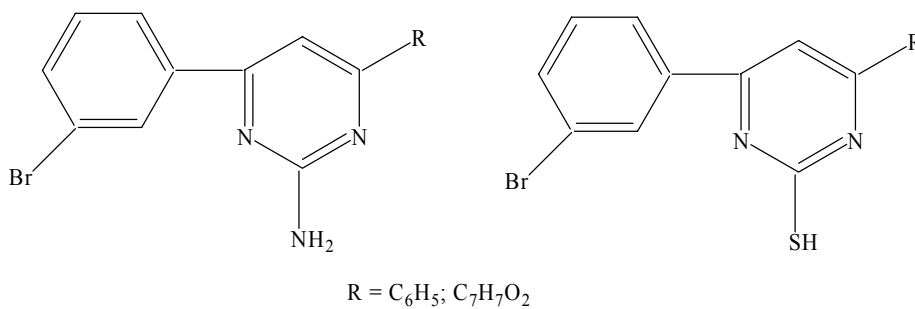
Amol Bhendkar *et al.*²¹⁸ synthesized Amino-pyrimidine and Pyrimidione derivatives and reported their anti-microbial activities.



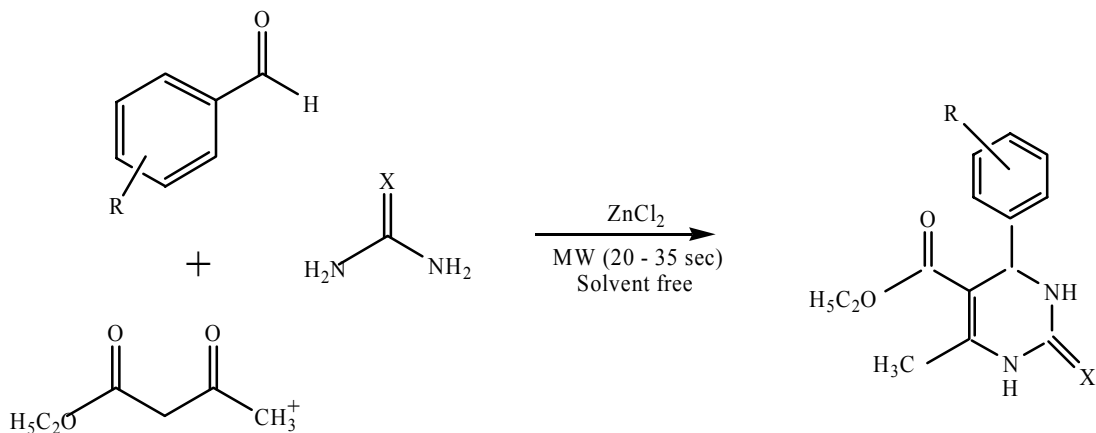
Patel *et al.*²¹⁹ synthesized substituted Amino-pyrimidines by condensation of chalcones with Guanidine Nitrate and reported their anti-microbial activities.



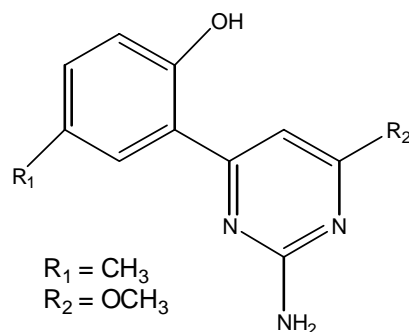
Kiran S. Nimavat *et al.*²²⁰ reported synthesis, anti-cancer, anti-tubercular, anti-microbial activities of some new pyrimidine derivatives.



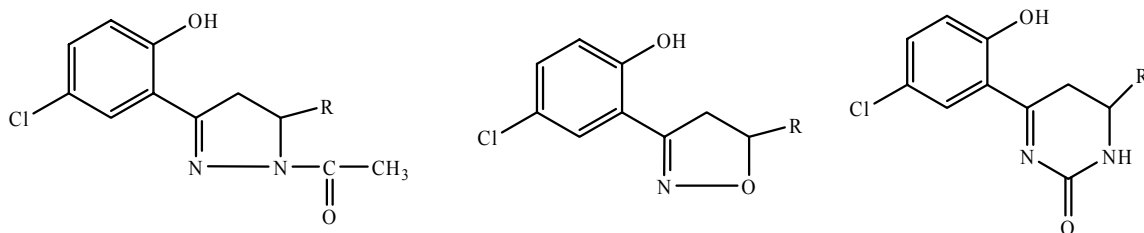
Pasha *et al.*²²¹ synthesized 3,4-dihydro-Pyrimidin 2-(1H)-ones-thiones in the presence of Zinc chloride catalysis by Microwave Assisted Organic synthesis.



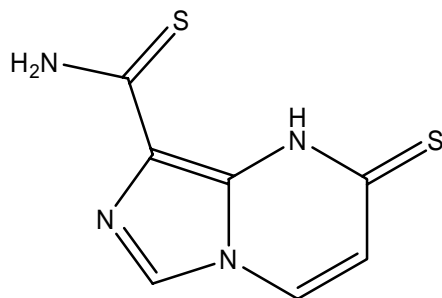
Mandhare *et al.*²²² synthesized some substituted amino- pyrimidine derivatives.



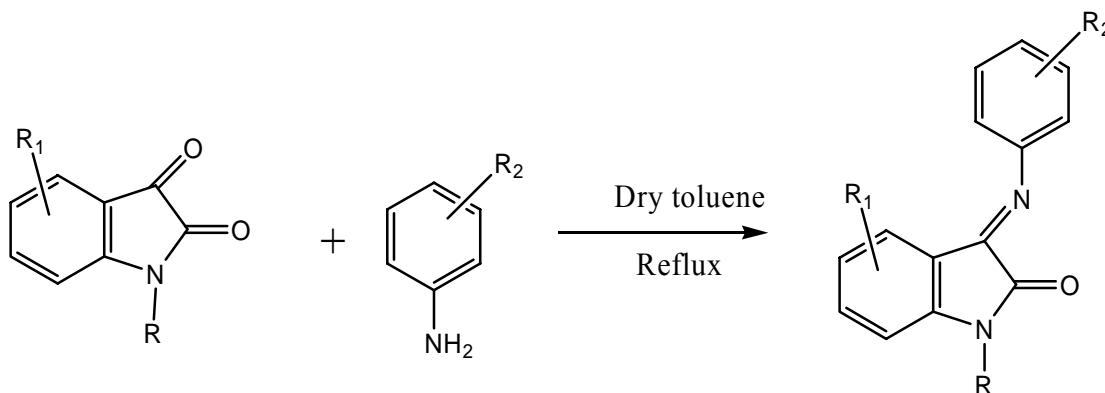
Raga Basawaraj *et al.*²²³ carried out the Claisen-Schmidt reaction of substituted acetophenones with aromatic aldehydes to give substituted propen-1-ones which upon cyclisation with hydrazine hydrate, hydroxylamine hydrochloride, urea and thiourea furnished the corresponding pyrazolines, isoxazoles and the pyrimidines. The compounds were screened for antibacterial and antifungal activity.



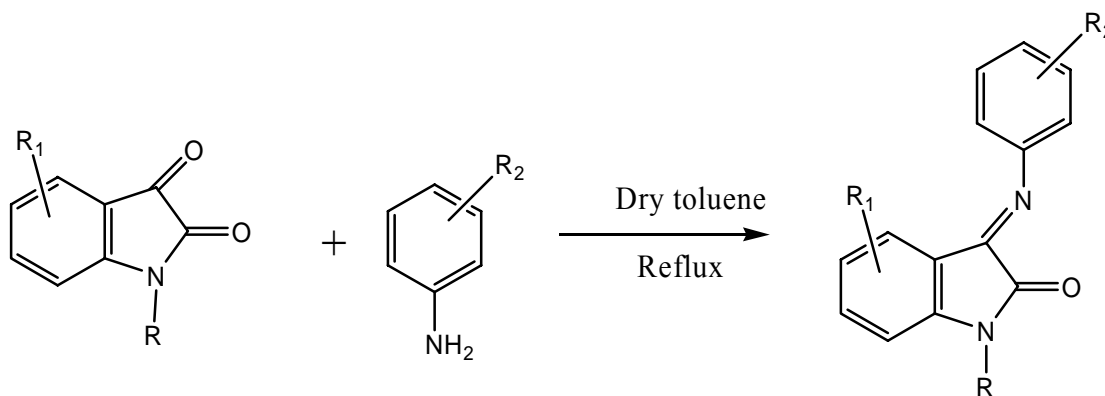
Seventeen 1,2,3,4-tetrahydroimidazo[1,5-*a*]pyrimidine derivatives bearing electron- withdrawing substituents were designed and synthesized by novel ring closure as potential antitumor agents by Hiroatsu Matsumoto *et al.*²²⁴



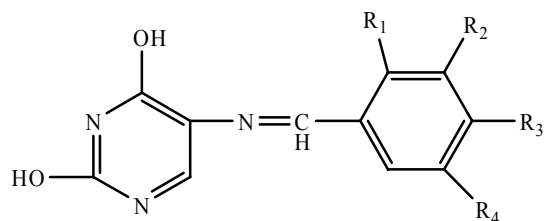
Substituted 4-amino-4,5-dihydro-1*H*- 1,2,4-triazole-5-ones were prepared and treated with Isatin and 5-chloroisatin to form Schiff bases and *N*-Mannich bases of these compounds were synthesized by reacting with formaldehyde and piperidine by Olcay Bekircan and Hakan Bektas²²⁵ Their chemical structures were confirmed by means of IR, ¹H- and ¹³C-NMR data and by elemental analysis.



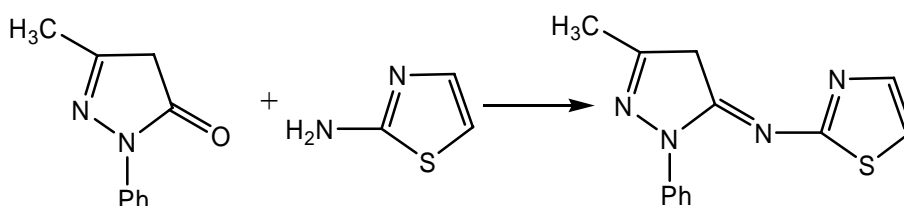
Krishna C Joshi *et al.*²²⁶ synthesized Schiff bases by the condensation of appropriate indole-2, 3-diones with fluorinated anilines in dry toluene under reflux.



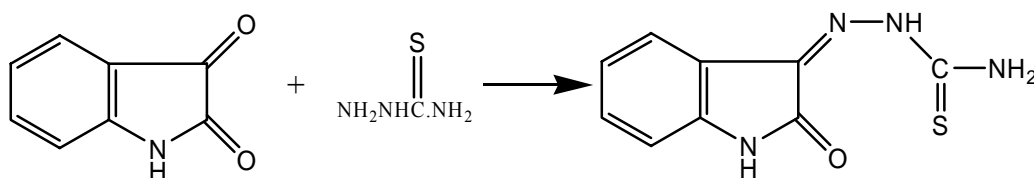
.Chakraborti SK and Barun Kumar DE,²²⁷ has discussed the importance of azomethine linkage for the anticancer activity and synthesized pyrimidine Schiff bases as potential anticancer agents,



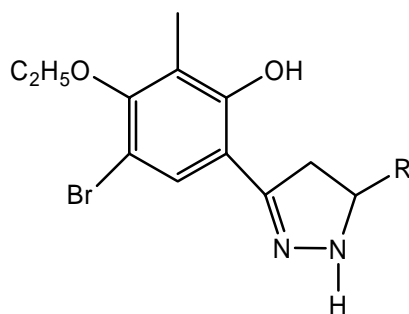
The Spiro Schiff base was prepared by Khalafallah, AK,*et al.*²²⁸ through the condensation reaction of 3-methyl-1-phenyl-5-pyrazolone with 2-aminothiazole in presence of a base catalyst. This was further converted to β -lactam derivative by treatment with chloroacetyl chloride.



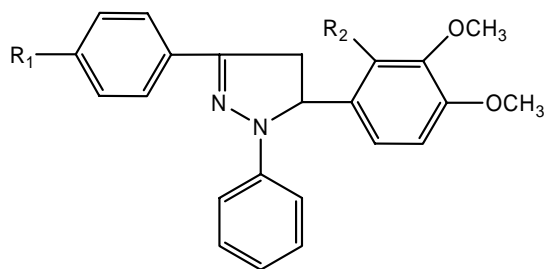
Hemant panwar *et al.*²²⁹ synthesized substituted azetidinylyl and thiazolidinylyl-1,3,4- thiadiazino {6,5-b}indoles as prospective antimicrobial agents through Schiff base formation.



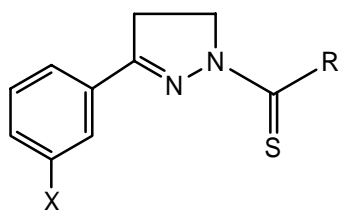
Upadhyay TM and Barot VM²³⁰ carried out the synthesis and biological evaluation of some new pyrazolines. Their structures were established by elemental and Spectral study.



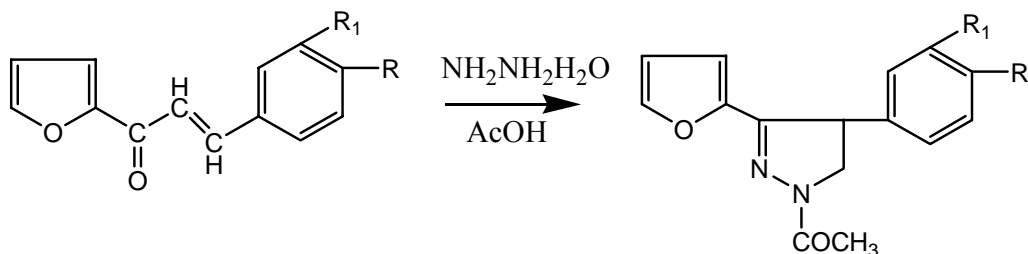
Synthesis and antidepressant activities of some 1, 3, 5-triphenyl -2-pyrazolines were performed by E. Palaska *et al.*²³¹



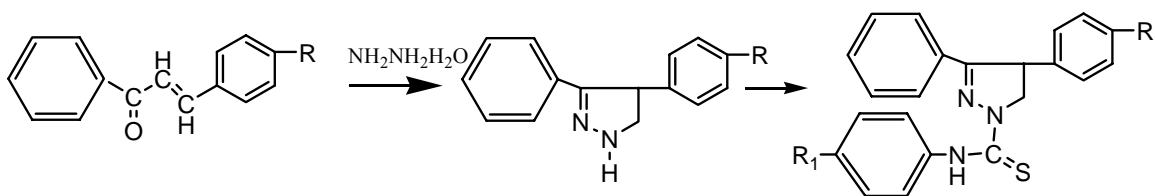
Mohammad Abid *et al.*²³² synthesized thirty new pyrazoline derivatives by the cyclisation of Mannich bases with substituted thio semicarbazides and they were found to be good leads for antiamebic activity.



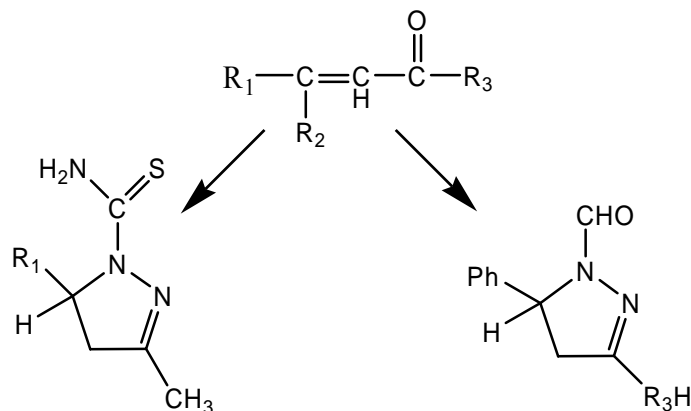
Amol H. Bhendkar *et al.*²³³ reported the formation of 1-acetyl-pyrazoline by the action of hydrazine hydrate and acetic acid on 1-Furyl-3-(substituted phenyl)-propene-1-one. They were found to be active against both Gram+ve and Gram-ve bacteria.



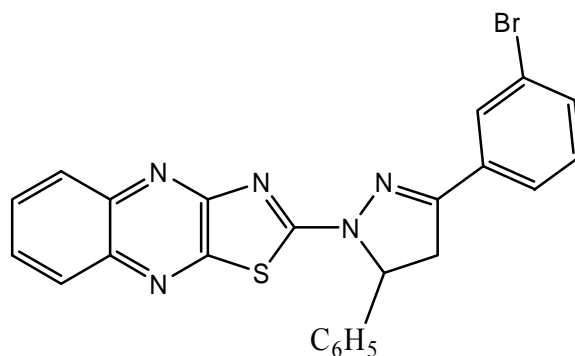
The cyclisation of 1, 3-diphenyl-2-propene-1-ones with Hydrazine hydrate followed by condensation with aryl isothiocyanates was done by Vineet Malhotra *et al.*²³⁴. The 1-N-substituted thiocarbamoyl -3, 5-diphenyl-2- pyrazolines were evaluated for their cardiovascular activity and toxicity.



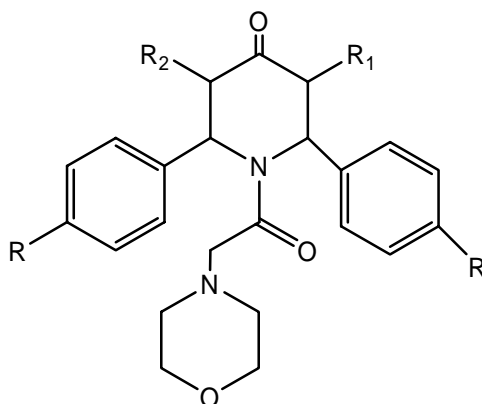
Werner Seebacher *et al.*²³⁵ reported the reaction of α,β -unsaturated ketones with hydrazinediium dithiocyanate giving 1-thiocarbamoyl or 1-formyl-2-pyrazolines depending on the nature of the ketone.



Asha budakoti *et al.*²³⁶ synthesized and evaluated a variety of 3-(3-bromo phenyl)-5-phenyl-1-(thiazolo[4,5-b]quinoxaline-2-yl)-2-pyrazoline derivatives.

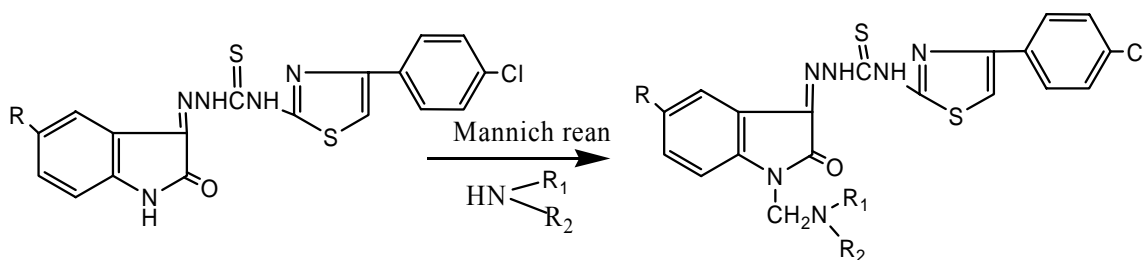


Aridoss G, *et al.*²³⁷ discussed the gaining importance of piperidine-4-ones owing to their varied biological properties including antitumour and anticancer activities. They synthesized an array of novel N-morpholinoacetyl-2,6-diarylpiperidine-4-ones (Mannich bases) and their in-vitro antibacterial activity was tested against a variety of organisms.

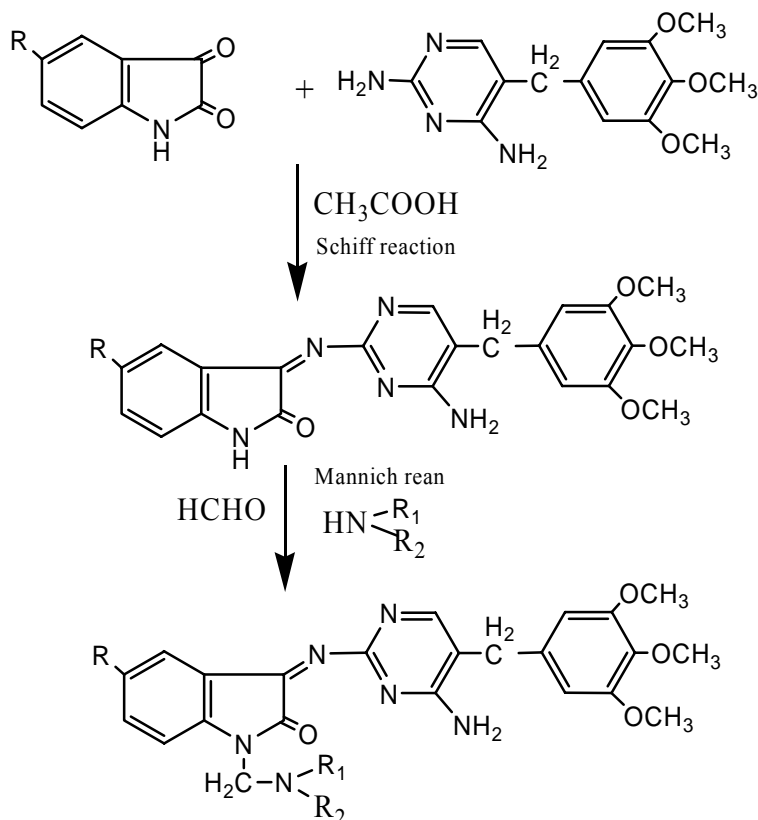


Novel sulfone linked bis heterocycles pyrazolines in combination with thiadiazoles, oxadiazoles and triazoles were prepared and screened for their antimicrobial activity by Padmavathi V, *et al.*²³⁸

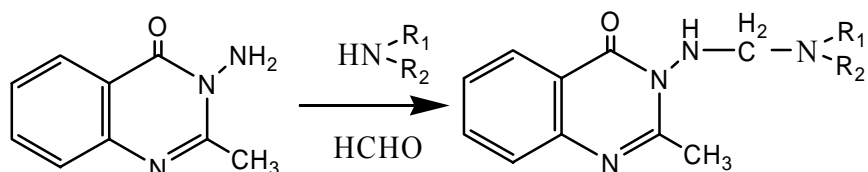
Pandeya SN *et al.*²³⁹, synthesized the Schiff bases and N-Mannich bases of N-[4-(4'-chlorophenyl) thiazol-2-yl] thiosemicarbazide by making them to react with Isatin and its derivatives. The compounds were investigated for their antimicrobial properties.



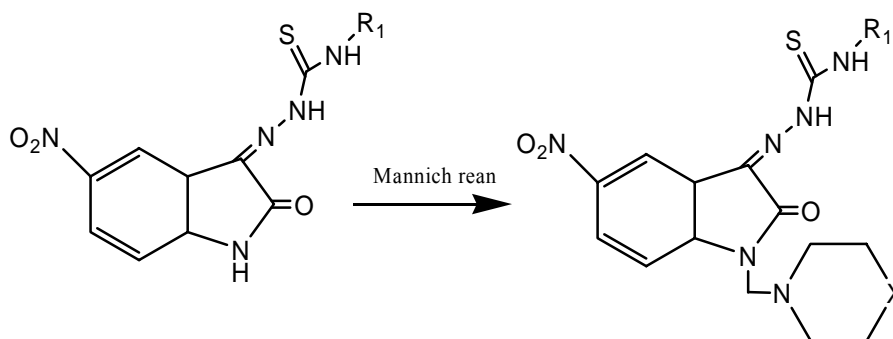
Dharmarajan Sriram *et al.*²⁴⁰ designed and synthesized aminopyrimidino Isatin analogues as novel non-nucleoside HIV-1 reverse transcriptase inhibitors through Schiff reaction between Isatin and Aminopyrimidines followed by Mannich condensation with different piperazines.



Alagarsamy V, *et al.*²⁴¹ synthesized 2-methyl-3-(substituted methylamino)-(3H)-quinazolin-4-ones by condensing the active hydrogen atom of the amino group of the quinoxalines with formaldehyde and appropriate amines. The compounds were screened for their anti HIV, antibacterial and antifungal activities.



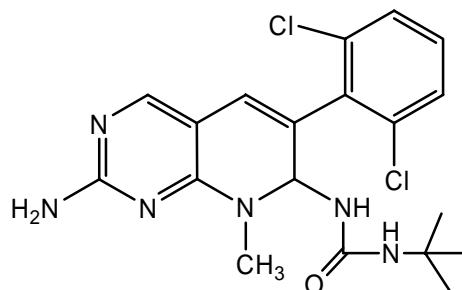
The reported compounds 1-morpholino/piperidinomethyl-5-nitroindole-2,3-dione-3-thiosemicarbazones were evaluated against some pathogenic viruses by Nalan Terzioglu *et al.*²⁴²



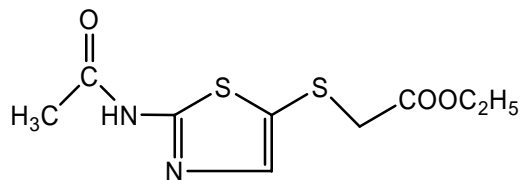
Werner Scheithaner *et al.*²⁴³ described the application of a in-vitro screening system for cancer of the large bowel using cancer cell lines.

The in-vitro studies of Sclareol induced apoptosis in human HCT116 colon cancer cell lines and suppression of HCT 116 tumor growth in immunodeficient mice was carried out by Konstantinos Dimas *et al.*²⁴⁴

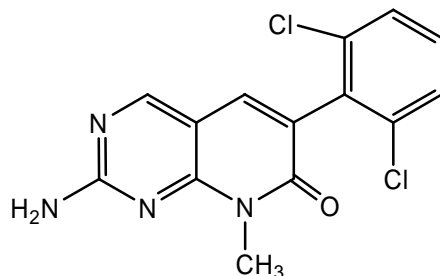
Mel C.Schroeder *et al.*²⁴⁵ synthesized soluble 2-substituted Aminopyrido[2,3-d] pyrimidines-7-yl ureas and studied the SAR of these compounds against selected tyrosine kinases. They also carried out the in-vitro anticancer activity in three colon cell lines, rat vascular smooth muscle cell line, platelet derived growth factor and in-vivo studies against a panel of five human tumor xenografts.



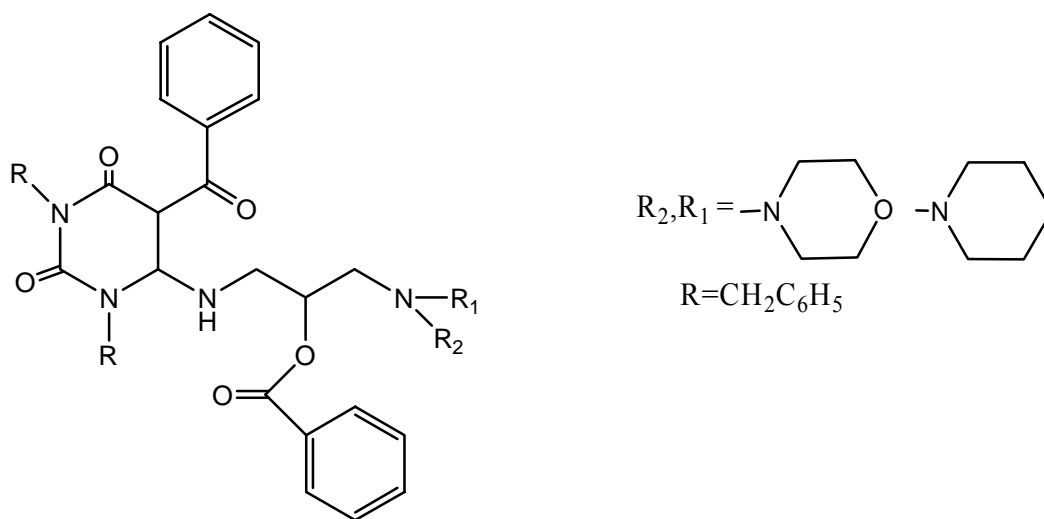
Synthesis, X-ray crystallographic analysis and biological activities of Aminothiazoles as inhibitors of cyclin dependent kinase -2 was carried out by Kyoung Soon kim *et al.*²⁴⁶. Many of these analogues displayed potent and broad spectrum anti proliferative activity in-vitro, across a panel of tumor cell lines.



Sylvester. R. Klutchko *et al.*²⁴⁷ studied the synthesis SAR of 2-substituted Aminopyrido[2,3-d] pyrimidin-7(8H)ones as a novel class of potent, broadly active TK inhibitors. They also carried out in-vitro and in-vivo anticancer activity of these compounds against different kinds of cancers



Palwinder Singh and Kamaldeep Paul²⁴⁸ investigated nine 1, 3 dialkylated-pyrimidine-2,4-diones against 59 human tumor cell lines. Their SAR studies indicate the presence of piperidine/pyrrolidines at the end of C-6 chain, Benzoyl group at C-5, Benzyl groups at N₁ and N₃ of pyrimidines ring increases the anticancer activity.



Ohashi.S. *et al.*²⁴⁹ found that human activated Aurora –A forms complexes with the negative regulator protein Serine/Threonine phosphatase type 1(PP₁) that was negatively phosphorylated on Thr.320. they also reported the in-vitro restrain of Aurora-A kinase activity by Phospho-specific Aurora-A monoclonal antibodies which provided further therapeutic arenas to explore.

US Patent 7005445. Hangauer Jr. *et al.*²⁵⁰ designed protein kinase and phosphatase inhibitors which can be used to treat number of diseases including cancer.

3. RATIONALE BEHIND THE RESEARCH

The main objective of the study is to identify a potent anticancer lead using computational drug designing methods. Many natural compounds and drugs contain the Piperidine ring system as a structural element²⁵¹. The 2, 6-disubstituted piperidine-4-one derivatives are the constituents of a number of alkaloids which possess broad spectrum of biological activities.

Among the family of heterocyclic compounds, nitrogen containing heterocycles, especially piperidine-4-ones presumably gaining considerable importance owing to their variable biological properties including antiviral, antitumour^{252,253} activities. Lijinsky and Taylor²⁵⁴ reported that blocking of α -positions to that of nitrogen in piperidine-4-ones by alkyl groups has good advantages over unblocked one in improving the biological activity. Furthermore, significance of piperidones as intermediates in the synthesis of a variety of physiologically active compounds has been reviewed by Prostakov and Galvoronskaya²⁵⁵.

Similarly the 2-Aminopyrimidines and 2-Pyrazolines were also reported to possess an array of biological activities including the anticancer activity^{227, 256}.

With this background it was decided to construct a pharmacophore model, based on common chemical features of molecules with inhibitory activity towards Aurora kinase A whose level is elevated in cancerous conditions, using HypoGen /Hypo Refine modules implemented in the Catalyst software package. The validated pharmacophore model was used to retrieve molecules from the constructed virtual library and the retrieved hits/leads were further refined using the docking studies with the crystalline structure of aurora A kinase using the software glide to reduce the number of false positives and false Negatives. This virtual screening approach was used to identify and design inhibitors with greater selectivity.

These molecules were further subjected to optimization using Lipinski rule. Based on the synthetic feasibility and the chemical and toxicity filters, the hits obtained were subjected to PASS prediction studies and the activity was decided based on these predictions.

The above observations prompted the synthesis of the title compounds as a continuation of our earlier work on piperidine-4-ones. So it was decided to synthesize the Schiff and Mannich bases of Piperidine-4-ones substituted with Aminopyrimidines and pyrazolines. Some of the designed molecules, with good predicted capability to inhibit the Aurora A kinase, were synthesized and screened for their anti-cancer activity.

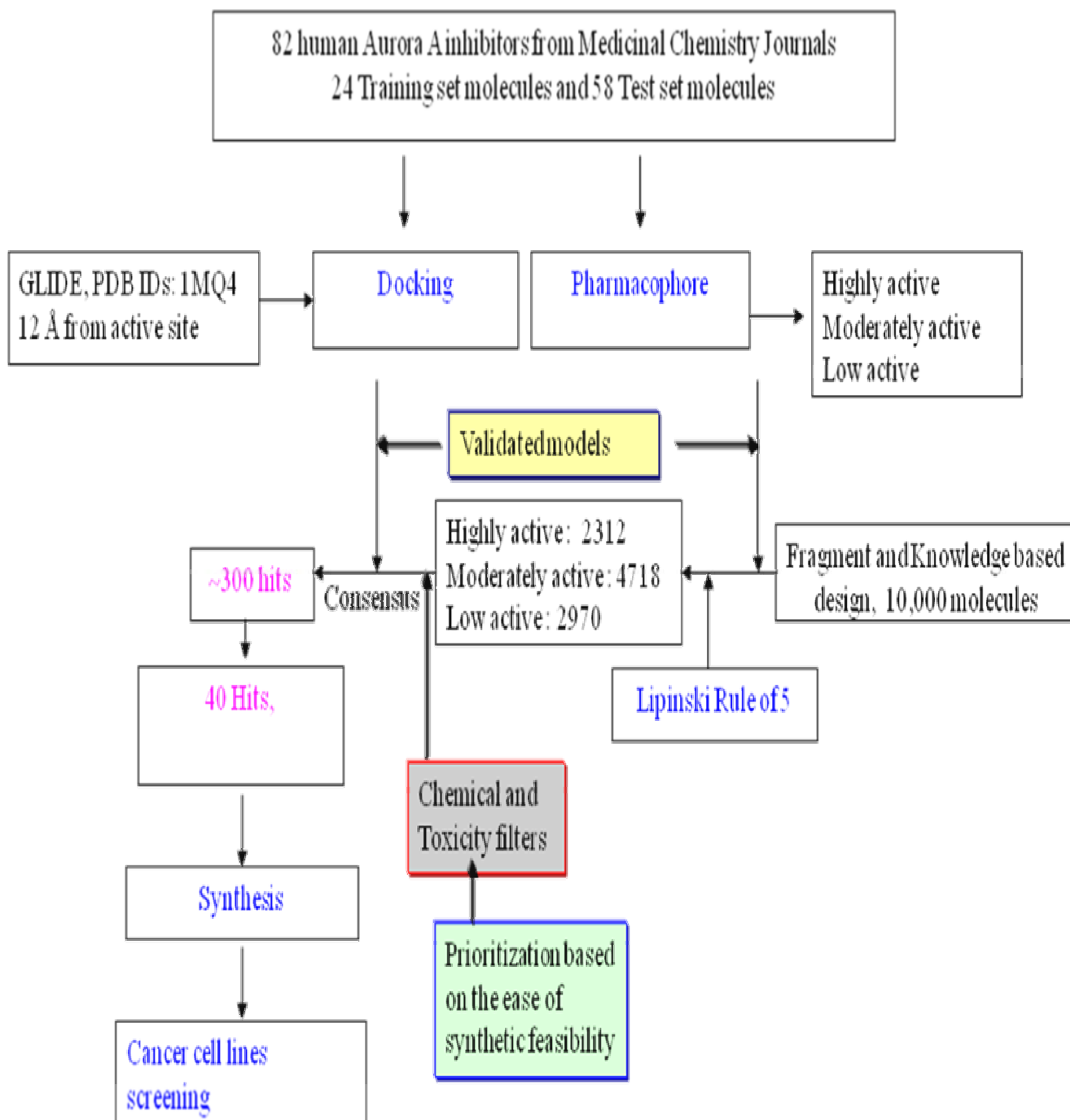
4. PLAN OF WORK

In the present study, some new biologically active lead compounds were designed using computational tools. Initial analog and structure based design studies were performed using Catalyst and Glide respectively to develop a comparative model. Then fragment and knowledge based approaches are employed to design molecules of selective Aurora A kinase inhibitors and the activities of those molecules are predicted using the comparative model. The selected molecules were further subjected to Drug likeness screening. The obtained hits were synthesized, characterized and subjected to in-vitro anticancer screening. The plan of work includes the following steps and the work flow chart is shown in the next page.

- Construction of a validated pharmacophore Model.
- Construction of a virtual compound library using the Fragment and knowledge based drug design.
- Carrying out the pharmacophore studies using catalyst with the pharmacophore model.
- Docking of the selected molecules using GLIDE with Aurora A Kinase(PDB ID:IMq4)
- Prediction studies using PASS.
- Drug likeness screening including the application of LIPINSKI rule and toxicity assessment using OSIRIS property explorer.
- Synthesis of the obtained hits based on the synthetic feasibility.
- Characterization by elemental analysis, UV, IR, NMR (^1H and ^{13}C), Cosy NMR and Mass spectral analysis.

- Cytotoxic activity-By tissue culture using human cancer cell lines - evaluation with MTT assay.

Virtual screening work flow for design of Aurora A inhibitors



5. THE TARGET ENZYME - AURORA KINASE-A

Kinase enzymes that catalyze the reversible addition of phosphate groups to proteins are involved in many critical biological signaling pathways. The protein kinases²⁵⁷ responsible for the phosphorylation of tyrosine, threonine and serine residues in other proteins, are among the most extensively studied gene families^{258,259}.

Aurora is the name given to a family of highly conserved protein kinases (Serine/Threonine) with essential roles in many aspects of cell division.²⁶⁰ In mammalian cells, Aurora has evolved into three related kinases known as Aurora-A, Aurora-B, and Aurora-C. These kinases are over expressed in a number of human cancers, and transfection studies have established Aurora-A as a bonafide oncogene²⁶¹⁻²⁶³. The bonafied oncogene activity and the amplification of Aurora-A in tumors^{264,265} were also observed and it has been highlighted as a drug target²⁶⁶.

Discovery

The aurora kinases were first identified in 1990 during a cDNA screen of *Xenopus* eggs.²⁶⁷ The kinase discovered, Eg2, is now referred to as Aurora A²⁶⁸. It was not until 1998, however, that Aurora A's meiotic and mitotic importance was realized.

Aurora Kinase Families

The human genome contains three members the Aurora kinase family: Aurora A, Aurora B and Aurora C. The *Xenopus*, *Drosophila*, and *Caenorhabditis elegans* genomes, on the other hand, contain orthologues only to Aurora A and Aurora B.²⁶⁷

In all studied species, the three Aurora mitotic kinases localize to the centrosome during different phases of mitosis. The family members have highly conserved C-terminal catalytic domains. Their N-terminal domains, however, exhibit a large degree of variance in the size and sequence.²⁶⁷

Aurora A and Aurora B kinases play important roles in mitosis. Aurora-A is a serine–threonine kinase which requires phosphorylation in order to become activated. The Aurora A kinase is associated with centrosome maturation and separation and thereby regulates spindle assembly and stability. Repression of Aurora-A expression by RNA interference (RNAi) delays mitotic entry in human cells²⁶⁹ and over expression of the wild type kinase can compromise spindle- checkpoint function²⁷⁰ as well as inhibit

cytokinesis²⁷¹. The Aurora B kinase is a chromosome passenger protein and regulates chromosome segregation and cytokinesis.

Although there is evidence to suggest that Aurora C might be a chromosomal passenger protein, the cellular function of it is less clear. Aurora A is a member of a family of mitotic serine/threonine kinases. It is implicated with important processes during mitosis and meiosis whose proper function is integral for healthy cell proliferation. Aurora A is activated by one or more phosphorylations¹¹ and its activity peaks during G2 phase to M phase transition in the cell cycle²⁷².

Localization

Aurora A associates with the centrosomes²⁶⁰ that are separating during late S/early G2. Low levels of Aurora A have also been reported on the spindle midzone and midbody late in mitosis.^{273,274} Human Aurora-A is located at chromosome 20q13.2, which is commonly amplified in several tumoural tissues^{275,276}.

During the late-G 2 to M phase, the Aurora-A levels and kinase activity increases in order to be able to perform the role of 'guardian of the poles'. As the cell cycle progresses, concentrations of Aurora A increase and the kinase associates with the mitotic poles and the adjacent spindle microtubules.(Figure 5.1) Aurora A remains associated with the spindles through telophase.²⁶⁷ Right before mitotic exit, Aurora A relocates to the mid-zone of the spindle²⁷⁷.By means of the phosphorylation of different substrates, in fact, Aurora-A regulates the correct development of the various phases of mitosis, including centrosome maturation and separation, mitotic entry, bipolar spindle assembly, chromosome alignment on the metaphase plate and cytokinesis²⁷⁸.In human cell lines, Aurora-A depletion results in the inhibition of both centrosome maturation and centriole pairs separation²⁷⁹.

Aurora A and Cancer

A perfect timing of Aurora-A activation and destruction is necessary for a proper cytokinesis. Both Aurora-A over expression and inhibition, in fact, lead to multinucleated cell formation²⁸⁰. Aurora A dys regulation has been associated with a high occurrence of cancer. For example, one study showed that 94% of the invasive tissue growth in breast cancer over expresses Aurora A. Meanwhile, the surrounding normal tissues, however, had normal levels of Aurora A expression²⁶⁷.

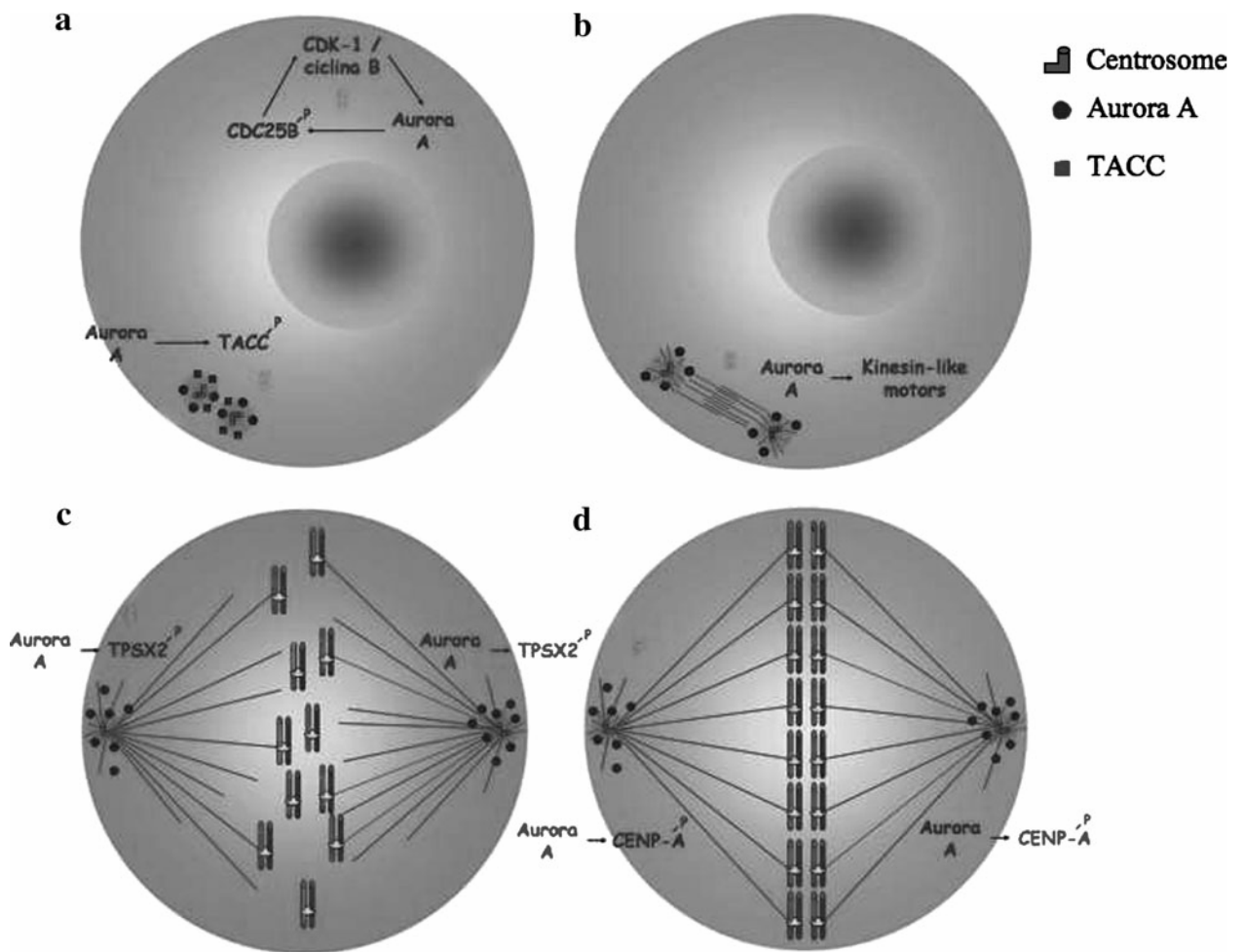


Figure 5.1 (a) Aurora-A is first detected in late G2 phase at the centrosome, where it is involved in the commitment to mitosis (1) and in maturation of centrosome through the phosphorylation of TACC (2). (b) Aurora-A is required for the separation of centrosomes in pro metaphase through the activation of the kinesin-like motors (3). (c) For the bipolar spindle assembly (4). (d) Aurora-A cooperates with Aurora-B in the activation and maintenance of CENP-A (5), allowing a correct chromosome alignment on the metaphase plate.

Loss-of-function studies established some time ago that Aurora-A is required for multiple steps during mitosis. Perturbing Aurora-A leads to defective Centrosome separation and maturation in a wide variety of experimental model systems^{281,282}. Cell cycle progression, mitotic spindle pole organization and MT stability are also often compromised in the absence of Aurora-A²⁸³⁻²⁸⁵. Regulation of Aurora A is complex and

involves both phosphorylation /dephosphorylation and degradation²⁸⁶⁻²⁸⁸. Phosphorylation stimulates kinase activity.

Dys regulation of Aurora A may lead to cancer because Aurora A is required for the completion of cytokinesis. If the cell begins mitosis, duplicates its DNA, but is then not able to divide into two separate cells it becomes an aneuploid, it contains more chromosomes than normal. Aneuploidy is a trait of many cancerous tumors²⁷⁷. Ordinarily, however, Aurora A expression levels are kept in check by the tumor suppressor protein p 53. Mutations of the chromosome region that contains Aurora A, 20q13, are generally considered to have a poor prognosis²⁶⁷.

Aurora Crystal Structure

Structure and active site of Aurora-2-adenosine complex has been determined²⁸⁹ and reported. The hinge (yellow), glycine-rich loop (blue), and activation loop (red) are key features of the protein kinase fold involved in binding adenosine. The protein backbone atoms of residues Glu-211, Ala-213 in the hinge region of Aurora-2, and the side chain of residue Trp-277, located in the activation loop, bind adenosine through specific hydrogen bonds. There are no hydrogen bonds between the 2'-OH or 3'-OH groups of the ribose moiety and Aurora-2. Residues Lys-162 and Asp-274 are essential for Aurora-2 kinase activity but do not hydrogen bond to each other as seen in crystal structures of several other protein kinases.

AURORA A KINASE INHIBITORS

Because Aurora over expression is associated with malignancy, these kinases have been targeted for cancer therapy. The levels of Aurora-A kinases are usually regulated during the cell cycle phases by means of two different processes. They are ubiquitin dependent proteolysis^{290,291} and phosphorylation/dephosphorylation events²⁹². The mechanism of feedback regulation through phosphorylation/dephosphorylation events during the cell cycle is, instead, mediated by the action of kinase and protein phosphatases¹²⁹³.

In the last few years, several drugs with an inhibition action towards Aurora-A kinase have been developed and several protein kinase inhibitors, already present in other preclinical studies, have been tested to assess the specificity to Aurora-A. The identification of Aurora-A inhibitors may require the choice of two different

approaches—blocking the protein–protein interaction between Aurora-A and co-factor or substrates or blocking the ATP-binding site of the serine threonine kinase. Most of the small molecules with Aurora-A inhibitor function identified so far show good specificity for the ATP-binding site but less for the target protein.

The various heterocyclic skeletons^{294,264} such as pyrazolines, Aminopyrimidines, Aminoquinazolins, Triazole 2,3diamines, indolinones and quinazoline derivatives have been developed as ATP competitive Aurora kinase inhibitors.

Aurora Kinase Inhibitors in Preclinical Studies

A new approach to inhibit cancer growth that shows great promise for structure-based drug development is targeting enzymes which are central to cellular mitosis²⁹⁵. Aurora kinases, so named because the scattered mitotic spindles generated by mutant forms resemble the Aurora Borealis, have gained a great deal of attention as possible anticancer drug targets^{152, 264}. The Aurora enzymes are particularly exciting because they are involved in a direct path to the nucleosome by phosphorylating histone H3^{296,297}. Furthermore, Aurora kinases are known to be oncogenic and over expressed in various forms of cancerous growth, including leukemia, colon cancer, prostate cancer²⁹⁸ and breast cancer,²⁹⁹ tumors.³⁰⁰ So far three Aurora-kinase inhibitors have been described: ZM447439,³⁰¹ Hesperadin^{302,303} and VX-680.

The last is in advanced stages (Phase II clinical trial) of a joint drug development by Vertex Pharmaceutical's VX-680 (Sausville, 234, last posted on 12/18/06) and Merck & Co.,³⁰⁴ although the Phase II clinical trial was suspended in November, 2007 due to QT prolongation observed in one patient in Phase I trial (Figure 5.2).

MK0457, initially developed by Vertex and now being developed clinically by Merck & Co., Inc., is a 4, 6 diamino pyrimidine that targets the ATP-binding site common to all Aurora kinases.

AZD1152 is an inhibitor developed by AstraZeneca. It is a highly soluble acetanilide-substituted pyrazole-amino quinazoline pro-drug that is cleaved completely in human plasma to yield the active drug substance hydroxy-QPA. It inhibits Aurora-A, Aurora B-INCENP, and Aurora C-INCENP with respective inhibitory coefficients of 687, 3.7, and 17.0 nmol/L, indicating a 100-fold selectivity for Aurora-B over Aurora-A.

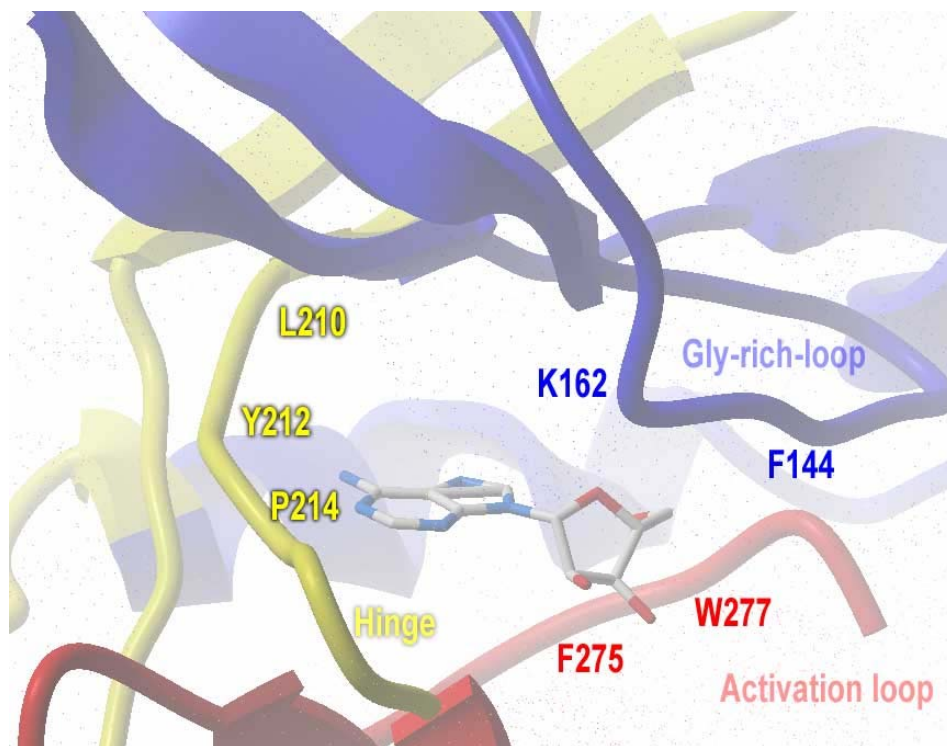


Figure 5.2 Aurora's active center

The JNJ-7706621 molecule is a [1, 2, 4] triazole-3, 5-diamine with a dual inhibitor effect on cyclin-dependent kinases and Aurora kinase family members but with a unique inhibitor profile [42].

Hesperadin is a novel indolinone that inhibits immuno precipitated Aurora-B with an inhibitory concentration 50% (IC_{50}) of 250 n mol/L

ZM447439 is a quinazoline derivative developed by Astra Zeneca that is an ATP competitor of Aurora.

The summary of the Aurora kinase Inhibitors and their site of action under development are shown in Figure 5.3.

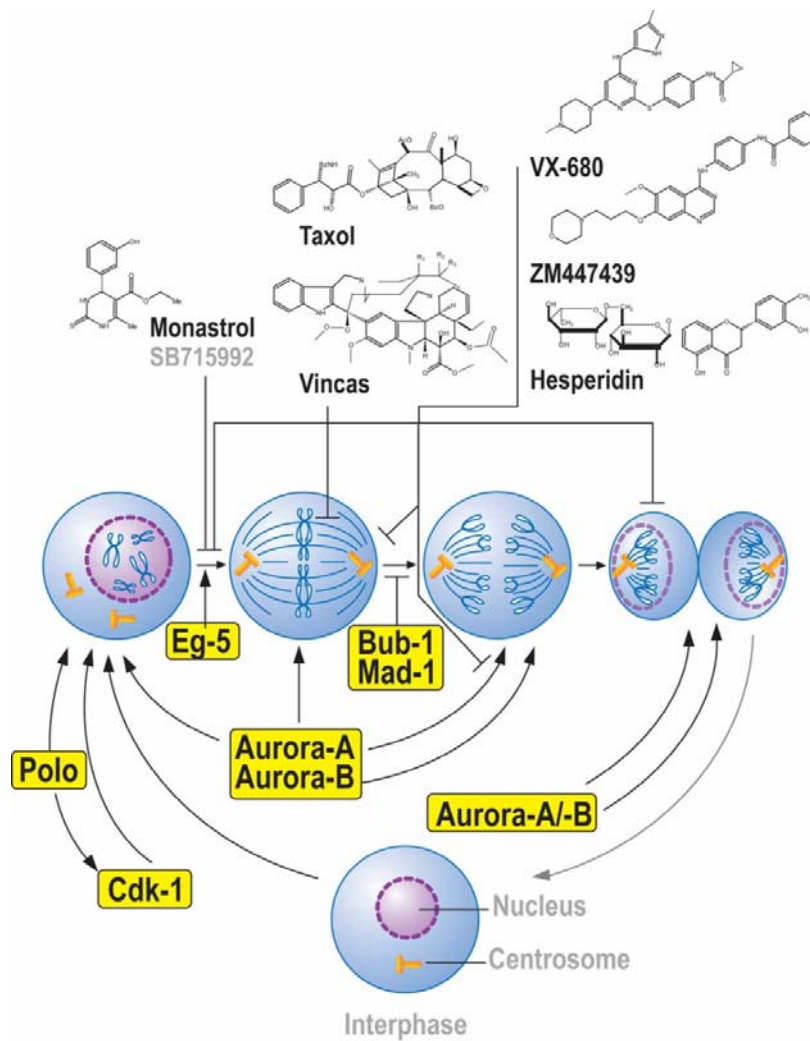


Figure 5.3 Aurora case study - six inhibitors and their action during cytokinesis

Table 5.1 shows the main Aurora kinase inhibitors which have already undergone pre clinical or phase I/II clinical trials. Unfortunately, very few data are available since a great many of these molecules are in still in the experimental phase of each study.

TABLE 5.1 MAIN AURORA KINASE INHIBITORS WHICH HAVE ALREADY UNDERGONE PRECLINICAL OR PHASE I/II CLINICAL TRIALS

PRECLINICAL	PHASE I	PHASE II
CHR-3520	PHA-739358	VX-680
CTK-110	AT-9283	
CYC-116	MLN-8054	
ENMD-981693	R-763	
JNJ-7706621	SU6668	
PHA-680632	Hesperadin	
SNS-314	ZM447439	
MP-529		
MP-235		

6. PHARMACOPHORE MODELING

6.1 MATERIALS AND METHODS

Fragment-based drug design has become an important and powerful tool for the discovery and optimization of potent drug leads.³⁰⁵⁻³⁰⁷ Thus, the design and optimization of the ultimate “lead” compound is carried out by identifying and optimizing the individual fragments, followed by synthetic linking or merging to produce the required high affinity for the target protein with appropriate lead-like properties.^{308,309} The main attractions of fragment-based techniques lie in the synthesis and testing of fewer significant compounds, compared to HTS methods, structurally characterized binding modes and the potential high success rate of generating new chemical series with attractive lead-like properties.³¹⁰ Another key advantage of using molecular fragments for lead discovery is the sampling of significant amount of chemical space using a relatively small library of compounds.³¹⁰ Hence, different sets of molecular fragments are used to target a particular protein, based upon diversity or focused pharmacophore models. For example, family-specific fragment libraries can be assembled, such as focused kinase fragment library. This diverse collection of synthetically tractable chemo types is based on known ATP-site binders with acceptable lead-like properties. It is generally accepted that fragment leads need to be smaller (MW \sim 250 Da) and less lipophilic (cLogP \sim 3) than conventional HTS leads that possess good physiochemical properties.²⁶⁶ Knowledge based approach is based on another popular technique applied in the drug discovery, known as ‘Scaffold hopping’^{311,312} where the goal is to ‘jump’ in chemistry space, i.e., to discover a new structure starting from a known active compound via the modification of the central core of this molecule.³¹³

All molecular modeling works were performed on a Silicon Graphics Octane R12000 computer running Irix 6.5.12 (SGI, 1600 Amphitheatre Parkway, Mountain View, CA 94043) Catalyst³¹⁴ 4.11 software was used to generate pharmacophore models.

DATABASE MINING AND TRAINING SET

Eighty two Aurora A Kinase inhibitors from Medicinal chemistry journals were selected for modeling studies based on chemical and biological diversity. The most critical aspect of pharmacophore hypothesis generation is the selection of the training set. There should not be any redundancy in information content in terms of both structural

features and activity ranges. The 82 molecules are arranged in the decreasing order of their activities and were clustered into 20 bins. Based on atom-atom pair distance descriptors, similarity between most active molecules to all other molecules in 20 bins has been performed based on ISIS 960 keys and tanimoto analysis. All these 82 molecules contain IC₅₀ values either in nM or μM only and have similar Aurora A kinase inhibitory assay. The molecules with Ki, ED₅₀, EC₅₀ and other activity type values were ignored for modeling studies. The most diverse molecules from 5 bins have been selected as the training set and are given in Figure 6.1 and the Figure 6.2 depicts some test set molecules. Aurora A kinase activities for the training set of 21 molecules, covers 5 orders of magnitude ($0.00014 \mu\text{M} \leq \text{IC}_{50} \leq 420 \mu\text{M}$). These training set molecules were used for HypoGen to generate pharmacophore models.³¹⁴ The mol files of all molecules from the database were exported and minimized using modified CHARMM force field in Catalyst package, installed on a SGI Octane 275 MHz MIPS R12000 processor, and conformational analysis was carried out using best method in Confirm module. Poling algorithm of Confirm module reduces considerably the probability of reappearance of nearly similar conformers by usage of penalty function. For each molecule, a maximum of 250 conformers that lie within 10 Kcal/mol from the observed global minimum was considered for the model generation. This method ensures an exhaustive conformational mapping even for most complex molecules.

HYPOGEN MODEL DEVELOPMENT

The training set of 21 molecules defined earlier has been used in HypoGen to generate pharmacophore models, which could be used for quantitative estimation of activities while screening large virtual compound libraries.¹⁶ While generating HypoGen model, a minimum of 0 to a maximum of 5 features involving hydrogen bond acceptor, hydrogen bond donor and hydrophobic systems have been specified based on the common features and Aurora A Kinase inhibitory activities. The molecules in the training set are broadly classified into three categories namely highly active (<0.02 μM), moderately active (>0.02-0.2 μM) and Low active (>0.2 μM), uncertainty value of 3 was used. The quality of HypoGen models are best described in terms of fixed cost, null cost and total cost and these terms are well defined by Debnath.⁹⁵ The cost for each hypothesis is the summation of the three cost components (error (*E*), weight (*W*), and configuration

(C) multiplied by a coefficient (default coefficient is 1.0 for each). The fixed cost represents the simplest model that fits the data perfectly. The null cost represents the cost of a hypothesis with no features that estimates every activity to be the average activity.¹⁶ In simple terms there should be a large difference between fixed cost and null cost with a value of 40-60 bits for the unit of cost, which would imply a 75-90% probability for correlating the experimental and predicted activity data. For a good model, the total cost of any hypothesis should be close to the fixed cost.

The best pharmacophore hypothesis was used initially to screen 61 Aurora A Kinase inhibitors from the Kinase Inhibitor Database. All queries were performed using Best Flexible Search databases/ Spreadsheet method .To validate the model,⁹¹ enrichment factors and goodness of hit has been calculated.

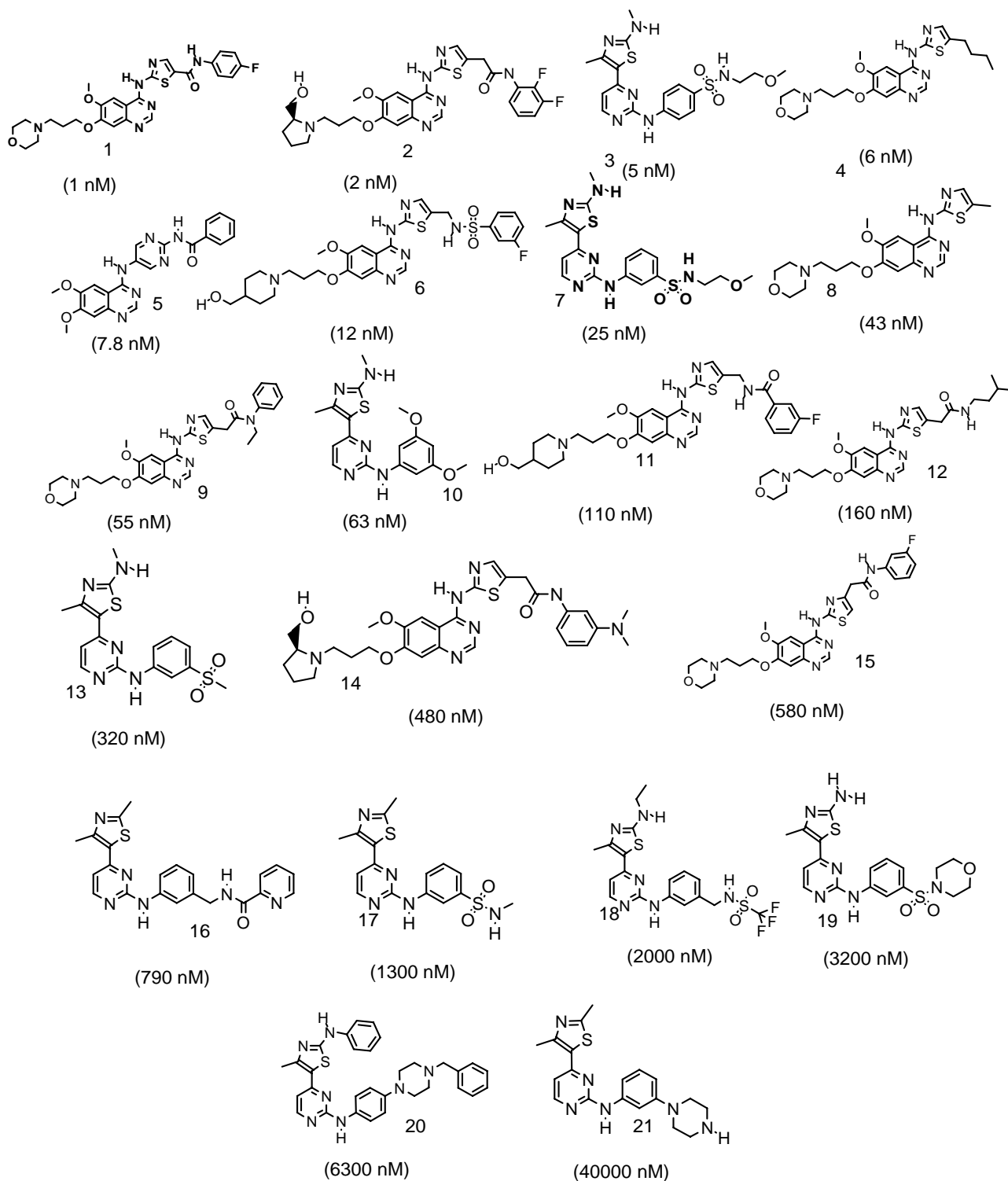
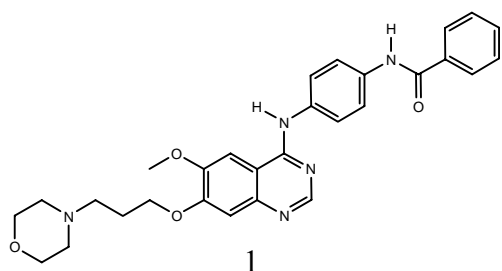
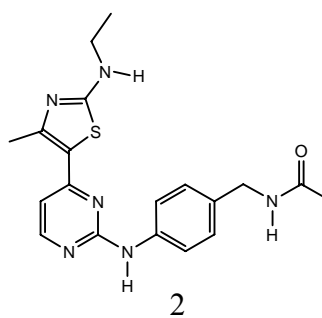


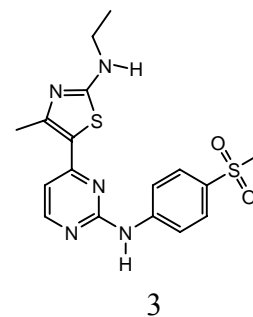
Figure 6.1 Structures of training set molecules of aurora kinase A inhibitors with their experimental IC_{50} values.



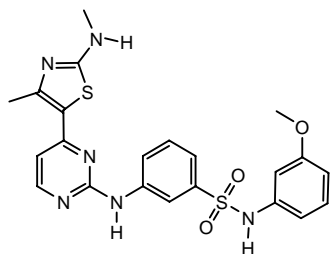
Exp IC50 10 nM
Pred IC50 580nM



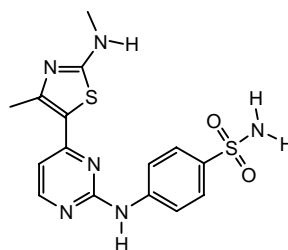
Exp IC50 15.84 nM
Pred IC50 75nM



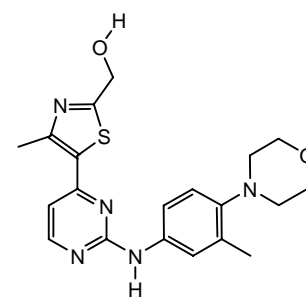
Exp IC50 39.81 nM
Pred IC50 1900nM



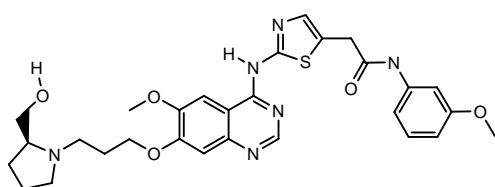
Exp IC50 12.58 nM
Pred IC50 27nM



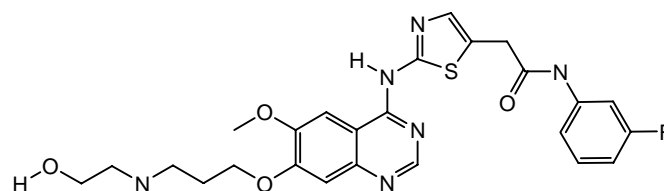
Exp IC50 31.62 nM
Pred IC50 1100



Exp IC50 50.11 nM
Pred IC50 420



Exp IC50 106 nM
Pred IC50 5.2nM



Exp IC50 5 nM
Pred IC50 200nM

Figure 6.2 some test set molecules

6.2 RESULTS AND DISCUSSION

HYPOGEN STUDIES

In the HypoGen studies, a couple of sets of 10 hypotheses were generated using the most diverse 21 molecules in the training set molecules. As evident from the data summarized in Table 6.1, good cost values, correlation and low RMSD were observed for the generated hypotheses.

TABLE 6.1 PHARMACOPHORE MODELS GENERATED BY THE HYPOGEN ALGORITHM

HYPO NO.	TOTAL COST	COST DIFFERENCE[§]	ERROR COST	RMS DEVIATION	TRAINING SET (R)	TEST SET (R) CORRELATION	FEATURES[#]
1	102.967	57.87	86.6856	1.30687	0.945	0.64	AHRR
2	107.518	57.46	92.342	1.49959	0.9266	0.62	AHRR
3	116.039	56.11	93.8365	1.66812	0.9095	0.6	AHRR
4	122.646	55.26	94.4513	1.91845	0.8762	0.62	AHRR
5	125.396	48.43	96.4804	1.9761	0.8683	0.49	AHRR
6	129.196	47.17	97.4972	2.05478	0.8569	0.51	AHRR
7	132.269	46.74	97.5607	2.12046	0.8468	0.61	AHRR
8	134.108	46.12	99.1785	2.24908	0.8236	0.54	AHRR
9	134.371	45.73	99.0087	2.20355	0.8323	0.59	AHRR
10	136.689	45.62	100.905	2.27422	0.8197	0.61	AHRR

[§](Null cost-Total cost), Null cost = 160.84, Fixed cost = 89.35, For the Hypo-1 Weight = 5.80, Configuration = 18.26, All cost units are in bits. [#]A- Hydrogen Bond Acceptor, H- Hydrophobic aliphatic, R - Ring aromatic

The best 10 hypotheses consist of 1) one hydrogen bond acceptor, 2) one hydrophobic aliphatic and 3) two Ring aromatic. The best hypothesis Hypo-1 is characterized by the highest cost difference (58 bits), lowest RMS deviation (1.30) with a correlation of 0.94. The fixed cost, pharmacophore (total) cost and null cost for hypo-1 are 89, 103 and 161 bits respectively. It is evident that as error, weight and configuration

component are very low and not deterministic to the model; the total pharmacophore cost is also low and close to the fixed cost. Also, as total cost is less than the null cost, this model appears to possess all the pharmacophore features and has a good predictability power. The pharmacophore features of Hypo-1 with their geometric parameters are shown in Figure 6.3.

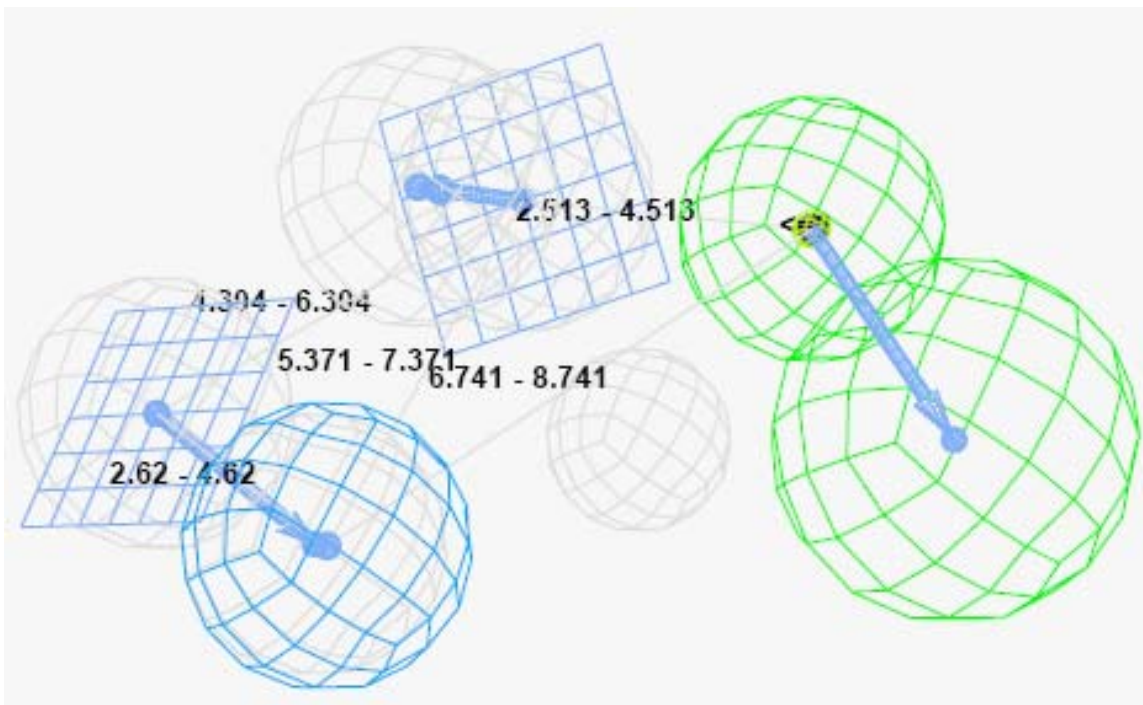


Figure 6.3 HypoGen Model with its distance constraints

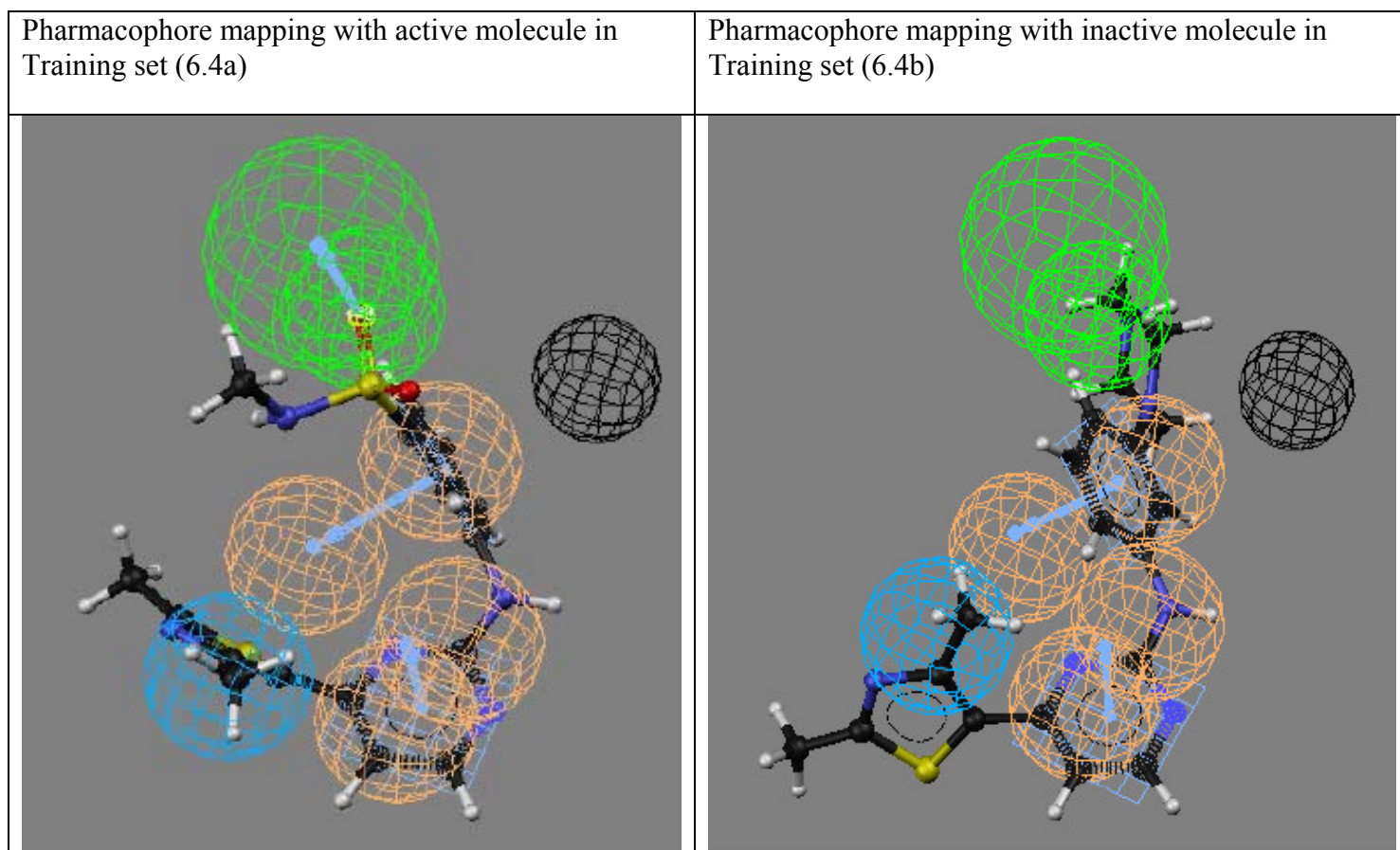


Figure 6.4: Hypo-1 mapped to the most active molecule **1** ($IC_{50} = 0.089$ nM, Figure 6.4a) and also mapped to low active molecule **26** ($IC_{50} = 34000$ nM, Figure 6.4 b) in the training set. Pharmacophore features are color coded with green: Hydrogen bond acceptor lipid, light blue: Hydrophobic aliphatic, Orange: Aromatic rings.

Figure 6.4a and 6.4 b represents the Hypo-1 aligned with the most active and inactive molecules (**1** and **21**; IC_{50} values are 1nM and 40,000 nM respectively) and shows a nice fit with all the features of Hypo-1. In this case of **1**, the one hydrogen bond acceptor lipids seem to be mapped to the thiazolidinyl nitrogen and methoxy oxygen and the hydrophobic group fit well with the fluorine while the pyrimidine and the benzene moiety matches with the ring aromatic features. On the other hand, for molecule **21**, the Hydrogen bond acceptor lipid group and the ring aromatics could not fit well (Figure 6.4 b)

The difference between experimental and predicted IC_{50} values for 25 training set molecules, based on the Hypo-1 model, along with other details such as, error values and fitness scores is shown in Table 6.2

TABLE 6.2 EXPERIMENTAL AND PREDICTED IC₅₀ DATA OF 20 TRAINING SET MOLECULES.

S.NO	MOLECULE	FIT VALUE ^B	EXPERIMENTAL IC ₅₀ , nM	PREDICTED	ERROR ^A	EXPERIMENTAL ACTIVITY SCALE ^C	PREDICTED ACTIVITY SCALE ^C
				IC ₅₀ , nM			
1	Sdmol 70	10.97	1	1.7	1.7	+++	+++
2	Sdmol 77	10.43	2	6.1	3	+++	+++
3	Sdmol 32	10.63	5.01	3.9	-1.3	+++	+++
4	Sdmol 69	9.59	6	42	7	+++	+++
5	Sdmol 2	10.32	7.85	7.8	-1	+++	+++
6	Sdmol 76	10.58	12	4.3	-2.8	+++	+++
7	Sdmol 38	9.22	25.12	98	3.9	++	++
8	Sdmol 68	9.55	43	46	1.1	++	++
9	Sdmol 73	8.93	55	190	3.5	++	++
10	Sdmol 61	9.03	63.1	150	2.4	++	++
11	Sdmol 75	8.83	111	240	2.1	++	++
12	Sdmol 74	9.38	158	67	-2.3	++	++
13	Sdmol 22	8.88	316.23	210	-1.5	++	++
14	Sdmol 79	8.64	483	370	-1.3	++	++
15	Sdmol 71	8.89	578	210	-2.8	++	++
16	Sdmol 51	8.47	794.33	560	-1.4	++	++
17	Sdmol 26	8.9	1258.93	200	-6.2	+	++
18	Sdmol 10	8.16	1995.26	1100	-1.8	+	+
19	Sdmol 47	7.9	3162.28	2000	-1.6	+	+
20	Sdmol 8	7.54	6309.57	4700	-1.4	+	+
21	Sdmol 63	6.54	39810.7	47000	1.2	+	+

^A + Indicates that the Predicted IC₅₀ is higher than the Experimental IC₅₀; - indicates that the Predicted IC₅₀ is lower than the Experimental IC₅₀; a value of 1 indicates that the predicted IC₅₀ is equal to the Experimental IC₅₀

^B Fit value¹² indicates how well the features in the Pharmacophore overlap the chemical features in the molecule. Fit = weight*[max(0,1-SSE)] where SSE = (D/T)², D = displacement of the feature from the center of the location constraint and T = the radius of the location constraint sphere for the feature (tolerance)

^C Activity scale - IC₅₀ < 20 nm = +++ (Highly active) - IC₅₀ 20 - 200 nm = ++ (Moderately active) - IC₅₀ > 200 nm = + (Low active).

In the training set, six highly active molecules and the ten medium active molecules were correctly predicted as highly active and moderately active, while one molecule predicted as moderately active was found to be less active and all four low active molecules were also predicted as low active. This shows that the model retrieved high, medium and low active molecules from database and it can be seen that the

difference between the experimental and predicted activities were also found to be minimal.

PHARMACOPHORE MODEL VALIDATION USING KNOWN AURORA KINASE A INHIBITORS

The validity of the pharmacophore model was ascertained by screening some known inhibitors (test set) that are retrieved from the Kinase Inhibitor Databases in order to check how many active molecules are picked in the screening process, how their predicted activities are correlated with the experimental activities and the efficiency in reducing the false positives or negatives.

Hypo-1 was used to screen 61 Aurora kinase A inhibitors of known high, medium and low active inhibitors of the test set the data are presented in Table 6.3. Database mining was performed in Catalyst software using the BEST flexible searching technique. A number of parameters⁹¹ such as hit list (Ht), number of active percent of yields (%Y), percent ratio of actives in the hit list (%A), enrichment factor of 2.13 (E), False negatives, False positives and Goodness of hit score of 0.85 (GH) are calculated (Table 6.4) while carrying out the pharmacophore model and virtual screening of test set molecules. While the False positives and negatives, 2 and 1 respectively, are minimal, enrichment factor of 1.154 against a maximum value of 2.25 is a very good indication on the high efficiency of the screening. In 69 molecules predicted to be active, 68 molecules were correctly picked, thus missing only 1 false negatives with 2 false positives overall. GH score assessment of hit lists was used to optimize the working pharmacophore model as databases with known biological activities. The Goodness of hit score was found to be 0.65 indicating that the model developed is a good model. (GH Score of 0.6 – 0.7 indicates a very good model).

It is to be noted that the technique can also be used to focus a list of active molecules as a post-HTS processing, or to prioritize a virtual library as a pre-HTS screening.

TABLE 6.3 EXPERIMENTAL IC₅₀ DATA AND PREDICTED IC₅₀ DATA OF TEST SET**MOLECULES BASED ON TOP RANKED HYPOTHESIS (HYPO 1)**

S.NO.	MOLECULE	EXP. IC ₅₀ (nM)	PREDICTED IC ₅₀ (nM)	ERROR	ACTIVITY SCALE	ESTIMATED ACTIVITY SCALE
1	sdmol 1	10	580	58	+++	++
2	sdmol 3	19.95	1300	63	+++	+
3	sdmol 4	251.19	1600	6.2	++	+
4	sdmol 5	31.62	1100	34	++	+
5	sdmol 7	125.89	710	5.6	++	++
6	sdmol 6	199.53	4800	24	++	+
7	sdmol 9	158.49	1100	7.3	++	+
8	sdmol 11	199.53	800	4	++	++
9	sdmol 12	251.19	980	3.9	++	++
10	sdmol 13	15.85	75	4.7	+++	++
11	sdmol 14	39.81	1000	26	++	+
12	sdmol 15	79.43	1300	17	++	+
13	sdmol 17	39	40	1	++	++
14	sdmol 16	79.43	100	1.3	++	++
15	sdmol 18	81	190	2.4	++	++
16	sdmol 20	3.98	620	160	+++	++
17	sdmol 21	2.51	160	63	+++	++
18	sdmol 23	19.95	150	7.4	+++	++
19	sdmol 24	50.12	420	8.3	++	++
20	sdmol 25	15.85	770	48	+++	++
21	sdmol 33	12.59	27	2.1	+++	++
22	sdmol 34	31.62	15	-2	++	+++
23	sdmol 35	12.59	1400	110	+++	+
24	sdmol 36	1000	510	-1.9	+	++
25	sdmol 37	501.19	1700	3.3	++	+
26	sdmol 39	125.89	25	-5	++	++
27	sdmol 40	25.12	1100	45	++	+
28	sdmol 41	5.01	200	39	+++	++
29	sdmol 42	100	19	-5.3	++	+++
30	sdmol 43	100	4.3	-23	++	+++
31	sdmol 44	158.49	450	2.8	++	++
32	sdmol 45	1584.89	230	-6.8	+	++
33	sdmol 46	316.23	14	-22	++	+++

34	sdmol 48	63.1	170	2.7	++	++
35	sdmol 49	1000	460	-2.2	+	++
36	sdmol 50	2511.89	200	-12	+	++
37	sdmol 52	100	380	3.8	++	++
38	sdmol 53	630.96	140	-4.6	++	++
39	sdmol 54	398.11	310	-1.3	++	++
40	sdmol 55	3162.28	670	-4.7	+	++
41	sdmol 56	398.11	250000	630	++	+
42	sdmol 57	1584.89	240000	150	+	+
43	sdmol 58	2511.89	2200	-1.2	+	+
44	sdmol 59	630.96	1400	2.2	++	+
45	sdmol 60	5011.87	1200	-4.2	+	+
46	sdmol 62	501.19	3300	6.6	++	+
47	sdmol 64	1258.93	6700	5.3	+	+
48	sdmol 65	50.12	610	12	++	++
49	sdmol 67	3981.07	700	-5.7	+	++
50	sdmol 72	316.23	7700	24	++	+
51	sdmol 78	794.33	670	-1.2	++	++
52	sdmol 80	100	3000	30	++	+
53	sdmol 81	63.1	170	2.8	++	++
54	sdmol 82	39.81	1900	48	++	+
55	sdmol 28	50.12	9.2	-5.5	++	+++
56	sdmol 29	50.12	1200	25	++	+
57	sdmol 30	472	140	-3.5	++	++
58	sdmol 31	106	5.2	-20	++	+++
59	sdmol 19	452	430	-1	++	++
60	sdmol 66	1	15	15	+++	+++
61	sdmol 27	5	5	1	+++	+++

+ Indicates that the Predicted IC₅₀ is higher than the Experimental IC₅₀; - indicates that the Predicted IC₅₀ is lower than the Experimental IC₅₀; a value of 1 indicates that the predicted IC₅₀ is equal to the Experimental IC₅₀

Activity scale - IC₅₀ < 20 nm = +++ (Highly active) - IC₅₀ 20 – 200 nm = ++ (Moderately active) - IC₅₀ > 200 nm = + (Low active).

TABLE 6.4 STATISTICAL PARAMETERS FROM SCREENING TEST SET MOLECULES.

S. NO	PARAMETER	MOLECULES
1	Total molecules in database (D)	82
2	Total Number of actives in database (A)	69
3	Total Hits (H_t)	70
4	Active Hits (H_a)	68
5	% Yield of actives $[(H_a/H_t)*100]$	97.14
6	% Ratio of actives $[(H_a/A)*100]$	98.55
7	Enrichment factor (E) $[(H_a*D)/(H_t*A)]$	1.154
8	False Negatives $[A - H_a]$	1
9	False Positives $[H_t - H_a]$	2
10	Goodness of Hit Score ^{\$}	0.65

$\$ [(H_a/4H_tA) (3A+H_t)]*(1-((H_t-H_a) / (D-A)))$; GH Score of 0.6 – 0.7 indicates a very good model

The correlation between experimental and predicted activities for the 61 test set molecules against Hypo-1 model along with 21 training set molecules are depicted graphically in figure 6.5.

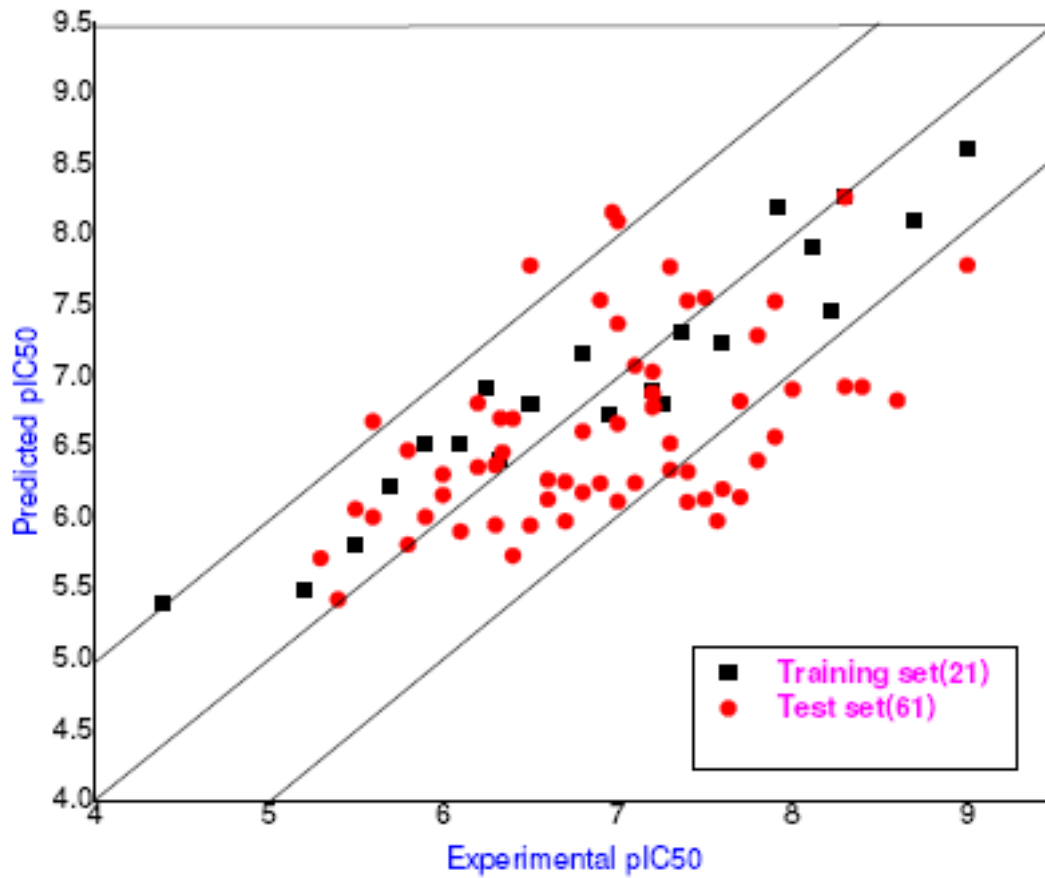


Figure 6.5: Chemo type-wise Correlation between experimental and predicted activities for the 61 test set molecules against Hypo-1 model along with 21 training set molecules

7. DOCKING STUDIES

7.1 MATERIALS AND METHODS

LIGAND AND PROTEIN PREPARATION

GLIDE (Grid-based ligand docking with energetics, Schrodinger, L.L.C., New York)¹¹¹, is the docking program used for the structure based studies. Crystal structure of Aurora Kinase A (PDB code: IMq4)¹⁴⁶ was employed for the docking studies. The 3D structure of protein was downloaded from the protein databank (PDB) and loaded to the Maestro³¹⁵ workbench. Hydrogen adjust was made to calculate the bond orders for the protein and ligand. Protein preparation and refinement were done in GLIDE and then used for all the three docking studies. Structure based docking studies were carried out using Glide^{111,112} on Aurora kinase A inhibitors to the 3D structure of Aurora Kinase A and generated 50 best docking poses. The best poses were selected based on the scoring functions and poses orientation with the active site amino acids.

In the Aurora A protein, the binding site coordinates ($X = 24.0$, $Y = 22.8$ and $Z = 8.9$) were taken from the centroid of the ligand to define the active site region. Active site radius was taken as 12.0 \AA so that the active site residues namely Glu-211, Ala-213 in the hinge region and the side chain residue Trp-277 located in the activation loop, bind adenosine through specific hydrogen bonds. The residues Lys-162 and Asp-274 which are essential for Aurora kinase activity is also an active site. The 82 Aurora A inhibitors taken for the pharmacophore studies were considered for docking studies to develop the comparative model. All ligand structures were built in Cerius² and minimized by OFF methods³¹⁶ using the steepest descent algorithm with a gradient convergence value of 0.001 kcal/mol . Open force field is an environment designed to maximize the effectiveness, flexibility, and ease-of use of force field based atomistic simulation methods.

COMPARATIVE MODEL DEVELOPMENT

The comparative model was generated with structure-based, pharmacophore studies like GLIDE, and Catalyst using multiple linear regression analysis in Cerius2. This type of comparative model is used to reduce the number of false positives and false negatives.

CONSTRUCTION OF A LARGE VIRTUAL SCAFFOLD LIBRARY

The fragments were generated from kinase inhibitor databases using simple iterative disconnection algorithm (Fragment descriptors) developed Inhouse.³¹⁷ The fragmentation rules were coded using Java and applied on SDF file formats. Substituents are defined as group connected to single ring systems. In general, the fragments in these sets have MW between 100 and 250 & cLogP P of <~3 and relatively simple with few functional groups, making them chemically tractable and suitable for rapid optimization.

7.2 RESULTS AND DISCUSSIONS

The initial Fragment docking studies and Aurora A kinase inhibitors docking were conducted using GLIDE.

The performance of the different scoring functions in docking of 82 molecules in the active site is analyzed in terms of correlation with GLIDE Standard precision, correlation value = 0.55

. Most of the potent Aurora A inhibitors form H-bond formation with Aurora A when binding in its ATP-binding site. The first two H-bonds are with Glu-211, Ala-213 in the Hinge region and also third H-bond with Trp-277 in some of the molecules. In some of the molecules it also forms H-bonds with Lys-162 and Asp-274 which are essential for Aurora kinase activity.

Comparative Model

The results obtained this far are mixed in nature but have several favorable features. To get a better VS model, a multiple linear regression analysis was carried out using Pharmacophore model and the docking scoring function (Comparative model).^{318, 319} Out of the 82 ligands, 21 were used in the training set and 61 in the test set.

A combination of Pharmacophore model, GLIDE SP score gave a good model (Figure 7.1). The MLR equation is given as:

$$\text{Activity} = 0.7541 + 0.3594 * \text{Pharmacophore_Predicted_pIC}_{50} + 0.231128 * \text{GLIDE_SP}$$

Figure 7.1 represents the Correlation of Glide SP score with Experimental pIC₅₀ and the Figure 7.2 gives the Consensus graph of Pred p IC₅₀ Vs Experimental p IC₅₀. The data showing the glide scores, Exp IC₅₀, pharmacophore predicted and experimental IC₅₀ and the consensus PIC₅₀ are given in table-7.1 and 7.2 for the training set and the test set respectively.

The coefficient of each term is a measure of the contribution of each scoring function towards the final model. The final linear regression model $r^2 = 0.843$, $r^2_{cv} = 0.812$, PRESS = 11.92, $r^2_{bs} = 0.844$, was validated by the test set of 61 molecules. The model was able to correctly predict the activity of 94% of 21 molecules in training set and 78% in case of 61 test set molecules within an order of magnitude.

TABLE 7.1 DATA OF THE TRAINING SET:

S. NO.	MODEL	EXP. IC ₅₀ (μ M OR nM)	GLIDE_SP	PHARMACOPHORE IC ₅₀ (NM OR MM)	PHARMACO PHORE PIC ₅₀	CONSENSUS PIC ₅₀
			Delta G	IC50 (nM)		
1	Sdmol 70	1.00	-9.30314	1.7	8.77	8.61734694
2	Sdmol 77	2.00	-8.18361	5.8	8.24	8.0996886
3	Sdmol 32	5.01	-8.05503	3.7	8.43	8.28011367
4	Sdmol 69	6.00	-7.66084	41	7.39	7.46657255
5	Sdmol 2	7.85	-7.11163	7.5	8.12	7.91033247
6	Sdmol 76	12.00	-8.52055	4.1	8.39	8.203949
7	Sdmol 38	25.12	-10.334	94	7.03	7.24078474
8	Sdmol 68	43.00	-7.70433	45	7.35	7.32433465
9	Sdmol 73	55.00	-7.62121	180	6.74	6.81252992
10	Sdmol 61	63.10	-7.28437	150	6.82	6.89819351
11	Sdmol 75	111.00	-7.32501	230	6.64	6.72964641
12	Sdmol 74	158.00	-6.36237	65	7.19	7.1721715
13	Sdmol 22	316.23	-8.33847	210	6.68	6.80619677
14	Sdmol 79	483.00	-6.49804	360	6.44	6.41619768
15	Sdmol 71	578.00	-7.13884	200	6.70	6.91451923
16	Sdmol 51	794.33	-6.59957	540	6.27	6.52561783
17	Sdmol 26	1258.93	-7.01738	300	6.52	6.52199164
18	Sdmol 10	1995.26	-7.50715	1100	5.96	6.22090205
19	Sdmol 47	3162.28	-6.12661	2000	5.70	5.81357696
20	Sdmol 8	3981.00	-5.74017	4430	5.35	5.40448801
21	Sdmol 63	6309.57	-7.04862	5500	5.26	5.49699392

TABLE 7.2 DATA OF THE TEST SET

S. NO.	MODEL	EXP. IC ₅₀ (μM OR nM)	GLIDE_SP	PHARMACOPHORE IC ₅₀ (μM OR nM)	PHARMACOPHORE PIC ₅₀	CONSENSUS PIC ₅₀
			Delta G	IC ₅₀ (nM)		
1	Sdmol 1	10.00	-9.08587	180	6.74	6.91135756
2	Sdmol 3	19.95	-7.8257	1100	5.96	6.14789603
3	Sdmol 4	251.19	-8.02718	1240	5.91	6.13328846
4	Sdmol 5	31.62	-9.30194	1110	5.95	6.13400741
5	Sdmol 6	125.89	-8.54097	710	6.15	6.24581899
6	Sdmol 7	199.53	-6.68842	1470	5.83	5.97803631
7	Sdmol 9	158.49	-6.21968	1100	5.96	6.18165476
8	Sdmol 11	199.53	-6.90169	800	6.10	6.25708871
9	Sdmol 12	251.19	-8.59176	980	6.01	6.27089595
10	Sdmol 13	15.85	-8.61638	75	7.12	7.29155061
11	Sdmol 14	39.81	-8.25801	1000	6.00	6.3282282
12	Sdmol 15	79.43	-8.51104	1300	5.89	6.24866591
13	Sdmol 16	39.81	-9.56957	40	7.40	7.53733234
14	Sdmol 17	79.43	-8.59963	100	7.00	7.07853772
15	Sdmol 18	63.10	-8.58386	190	6.72	6.87938067
16	Sdmol 19	3.98	-6.97502	120	6.92	6.92817394
17	Sdmol 20	2.51	-7.421	160	6.80	6.83283659
18	Sdmol 21	19.95	-6.87798	150	6.82	6.82614794
19	Sdmol 23	50.12	-7.38262	420	6.38	6.52934243
20	Sdmol 24	15.85	-8.59724	770	6.11	6.4064933
21	Sdmol 25	12.59	-7.92573	27	7.57	7.5329781
22	Sdmol 27	31.62	-9.1065	15	7.82	7.55847844
23	Sdmol 28	12.59	-7.67205	350	6.46	6.57368998
24	Sdmol 29	1000.00	-6.71561	910	6.04	6.16343221
25	Sdmol 30	501.19	-6.52181	1700	5.77	5.95143277
26	Sdmol 31	125.89	-9.45569	45	7.35	7.54069583
27	Sdmol 33	25.12	-7.48206	1100	5.96	6.20584241
28	Sdmol 34	5.01	-9.91804	200	6.70	6.93062568
29	Sdmol 35	100.00	-7.10673	39	7.41	7.37525368
30	Sdmol 36	100.00	-7.03499	4.3	8.37	8.0998074

31	Sdmol 37	158.49	-9.52743	450	6.35	6.61349716
32	Sdmol 39	1584.89	-7.60134	380	6.42	6.47874191
33	Sdmol 40	316.23	-7.64932	14	7.85	7.78718471
34	Sdmol 41	63.10	-9.752	170	6.77	7.03512184
35	Sdmol 42	1000.00	-7.35907	760	6.12	6.30849844
36	Sdmol 43	2511.89	-8.43517	400	6.40	6.6840598
37	Sdmol 44	100.00	-10.2076	380	6.42	6.66751235
38	Sdmol 45	630.96	-9.67005	240	6.62	6.81275987
39	Sdmol 46	398.11	-7.05152	310	6.51	6.70304011
40	Sdmol 48	3162.28	-6.12073	970	6.01	6.06406409
41	Sdmol 49	398.11	-6.04186	2100	5.68	5.73383476
42	Sdmol 50	1584.89	-5.39742	1400	5.85	5.81311308
43	Sdmol 52	2511.89	-8.3236	2200	5.66	6.00744348
44	Sdmol 53	630.96	-8.04808	900	6.05	6.36002923
45	Sdmol 54	5011.87	-5.70058	2200	5.66	5.71577054
46	Sdmol 55	501.19	-8.91895	1300	5.89	6.37436179
47	Sdmol 56	1258.93	-6.50085	1200	5.92	6.00880611
48	Sdmol 57	50.12	-8.04086	610	6.21	6.34087773
49	Sdmol 58	3981.07	-6.33535	2000	5.70	5.42477819
50	Sdmol 59	316.23	-6.35312	1500	5.82	5.94837365
51	Sdmol 60	794.33	-6.93373	670	6.17	5.90539831
52	Sdmol 62	100.00	-7.60677	1200	5.92	6.11644246
53	Sdmol 64	63.10	-6.76257	170	6.77	6.78431343
54	Sdmol 65	39.81	-6.84221	1200	5.92	6.11293355
55	Sdmol 66	50.12	-7.16602	9.2	8.04	7.77742463
56	Sdmol 67	27.00	-5.8841	1200	5.92	5.98041611
57	Sdmol 72	472.00	-7.86096	280	6.55	6.70601179
58	Sdmol 78	106.00	-7.68859	5.2	8.28	8.16448916
59	Sdmol 80	452.00	-6.46706	430	6.37	6.46493529
60	Sdmol 81	1.00	-7.5558	15	7.82	7.78903925
61	Sdmol 82	5.00	-9.74714	5.1	8.29	8.27002014

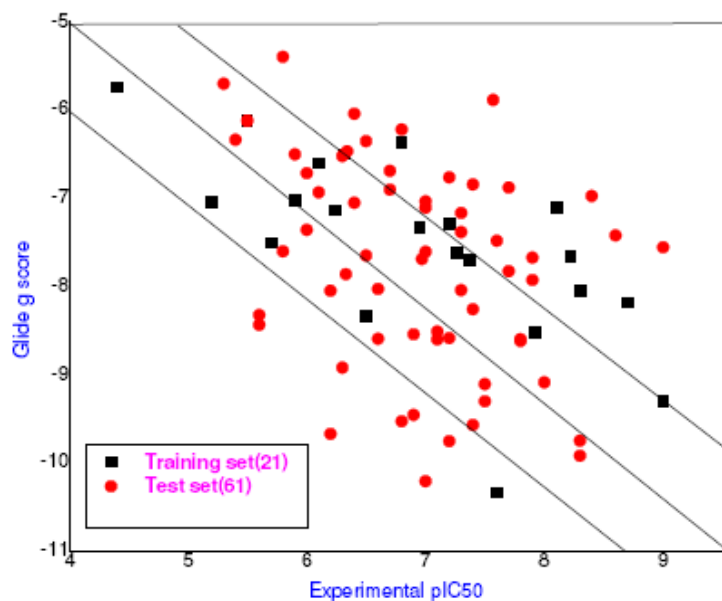


Figure 7.1 Correlation graph of Glide SP score Vs Experimental pic50

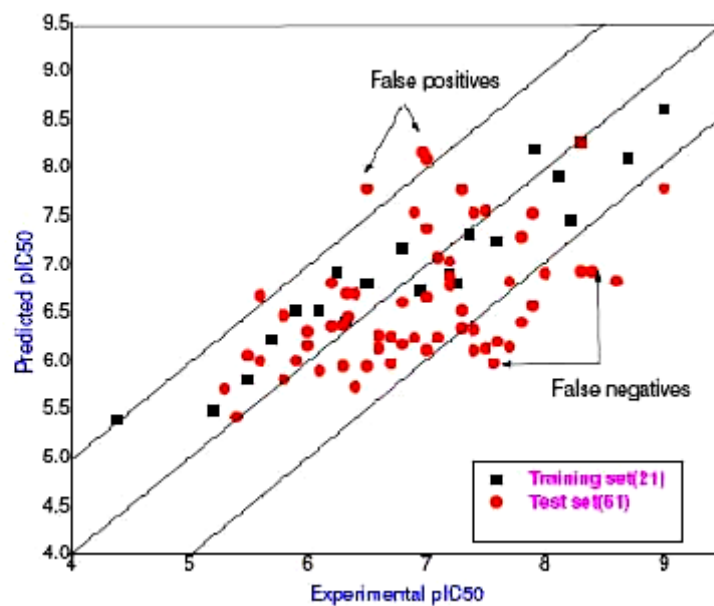


Figure 7.2 Consensus graph Pred pic50 Vs Experimental ic50

Figure 7.2 Correlation between experimental and predicted activities for the 82 Aurora A inhibitors (21 molecules in training set and 61 Molecules in test set) against comparative model (Multiple linear regression analysis).

Fragment and Knowledge based Virtual Screening

820 unique fragments were generated from Kinase Inhibitor Database of 113,868 molecules using the GVK in-house developed program fragment descriptors.³¹⁹ The structures of some of the fragments, substituents used for the incremental construction of molecules^{320, 321} have been shown in Figure 7.3 and 7.4. A total of 10,000 molecules were generated based on the knowledge of binding interaction of Ligand with the protein and also the common features necessary for the biological activity of molecule.

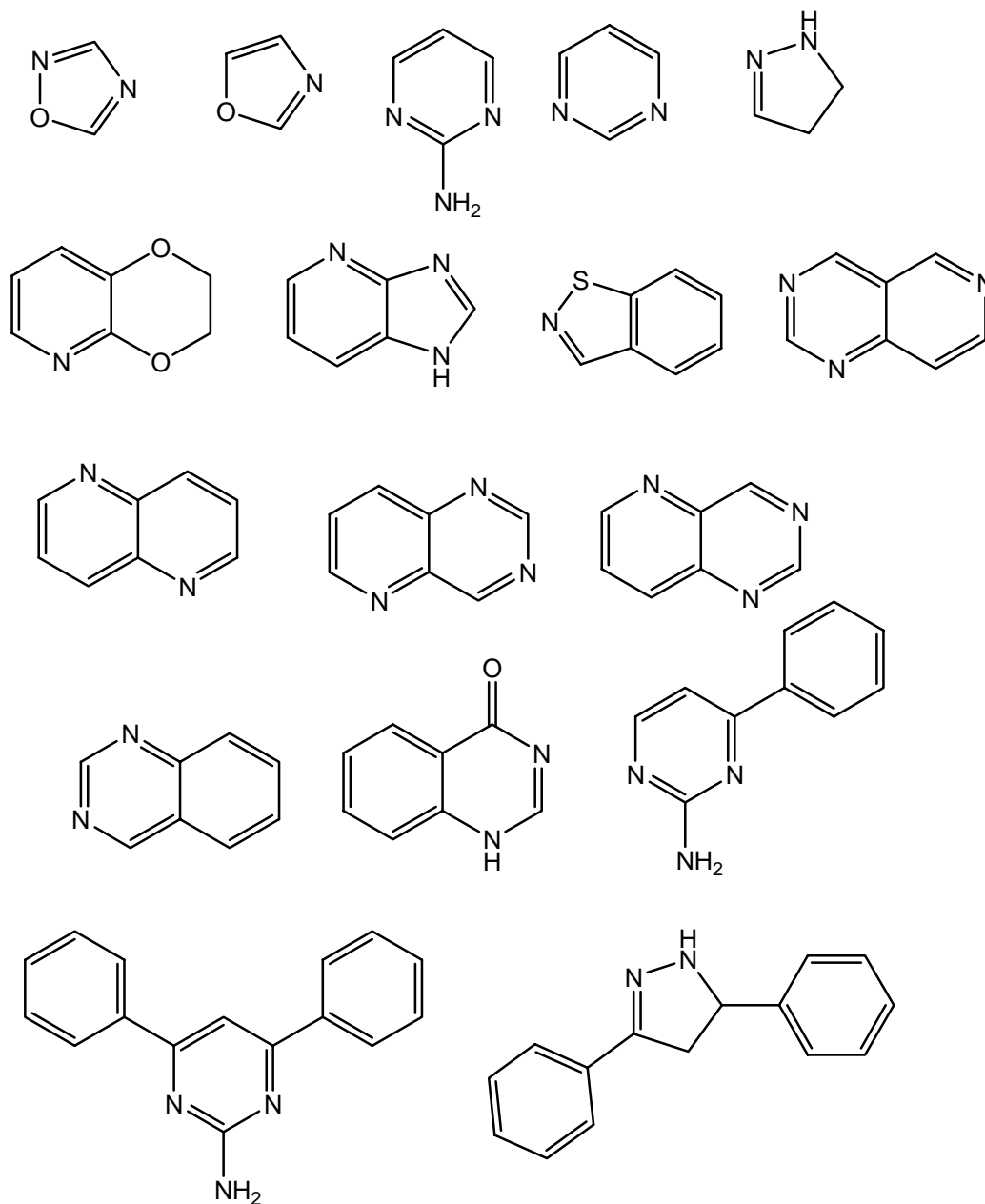


Figure 7.3 some of the fragments used for the construction of the molecules.

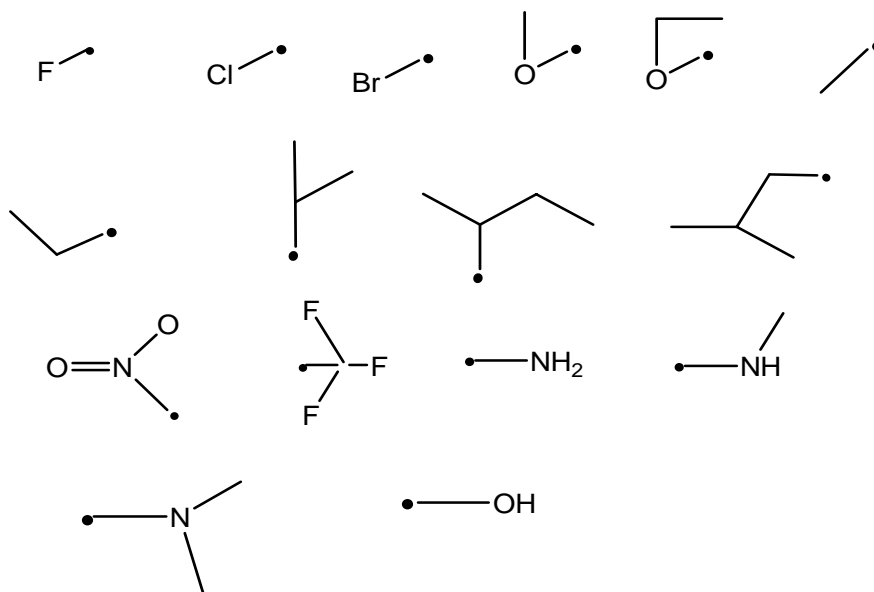
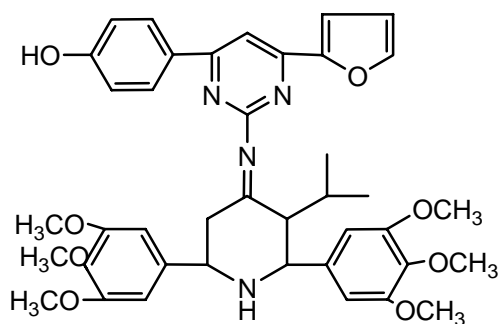


Figure 7.4 some of the substituents used in the ring systems.

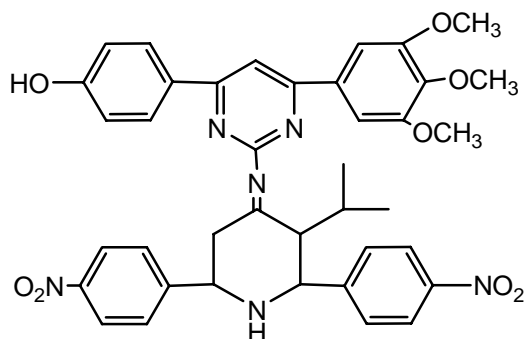
• - indicates point of attachment.

The comparative model developed using Pharmacophore and GLIDE, was used to screen the virtual library consisting of 10,000 molecules, which yielded hits comprising 2312 high, 4718 medium and 2970 low active molecules. The molecules were then broadly classified into three categories namely highly active ($<0.02 \mu\text{M}$), moderately active ($>0.02\text{-}0.2 \mu\text{M}$) and low active ($>0.2 \mu\text{M}$). Some of the potent lead molecules with its comparative predicted IC_{50} have been shown in Figure 7.5.

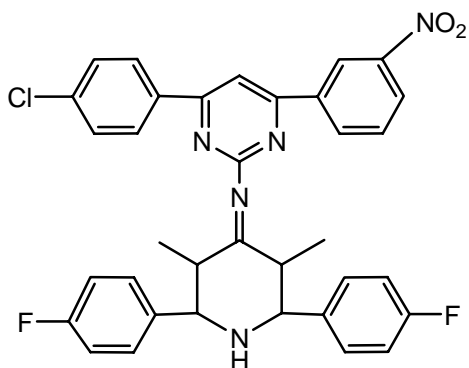
In an attempt to rationalize the high selectivity of the designed molecules molecular docking studies were conducted for the entire designed active molecules against the X-ray structure of Aurora A kinase. The binding mode derived from the docking pose of compound 21A and 25A in the ATP binding site of Aurora a kinase is illustrated in figure 7.6.



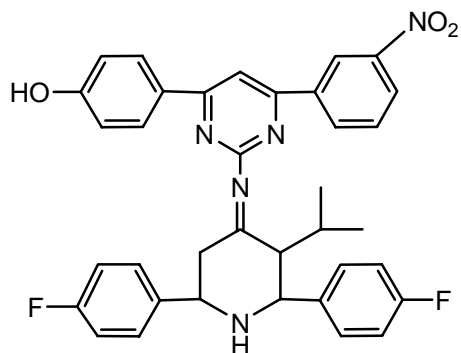
P IC₅₀ = 27 nM - Compound 28A



P IC₅₀ = 32 nM - Compound 7



P IC₅₀ = 13 nM - Compound-21A



P IC₅₀ = 18 nM - Compound-25A

Figure 7.5 some of the identified lead molecules as Aurora A kinase inhibitors through virtual library screening.

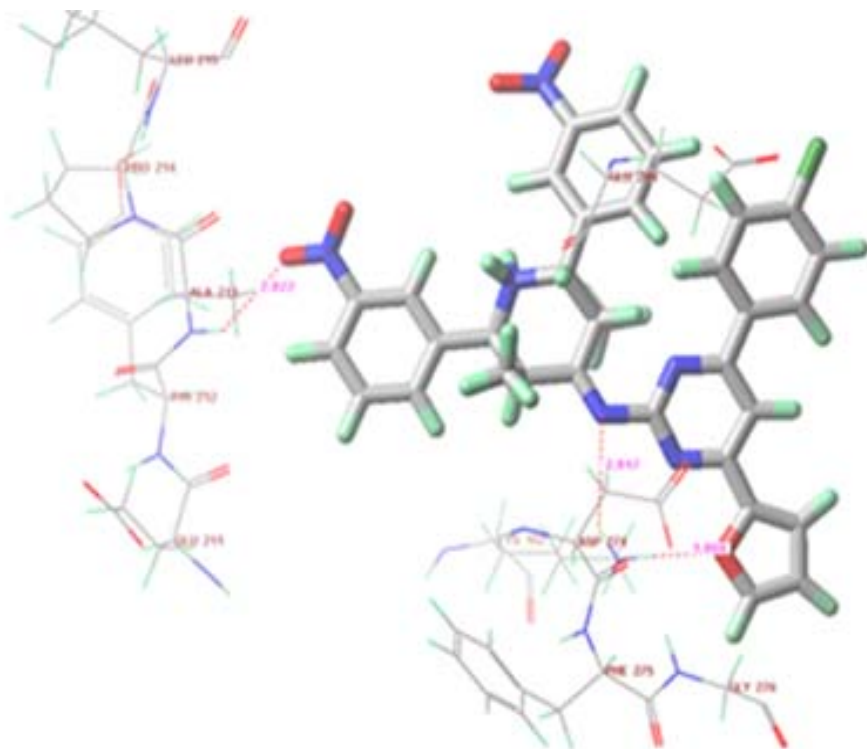


Figure 7.6 Stereo view of the binding mode of Aminopyrimidine substituted piperidine-4-ones.

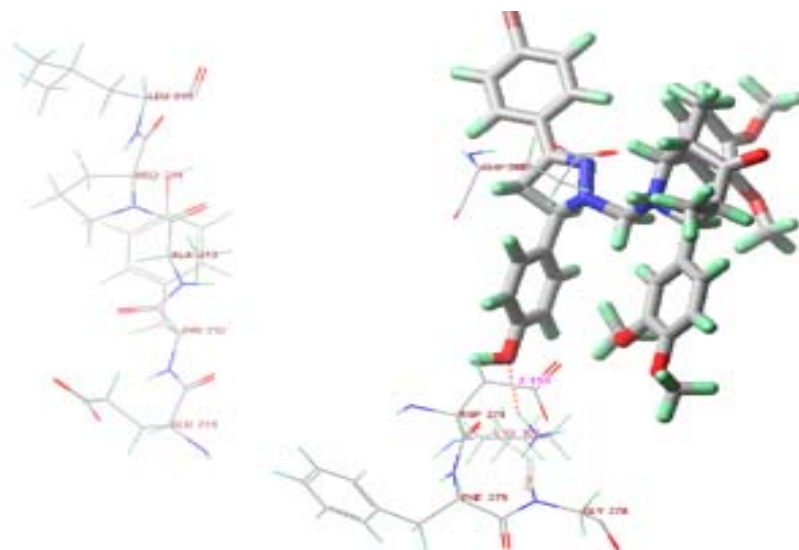


Figure 7.7 Stereo view of the binding mode of pyrazoline substituted piperidine-4-ones.

According to this docking model the Aminopyrimidine substituted piperidine-4-ones form hydrogen bonds with Aurora A kinase in its ATP binding site. The first hydrogen bond is formed with the ALA 213 of the enzyme and the other two hydrogen bonds are formed with ASP-274.

In the docking model of pyrazoline substituted piperidine-4-ones only one hydrogen bonding is observed with ALA 213. This accounts for the poor binding mode of the compounds P1-P11.

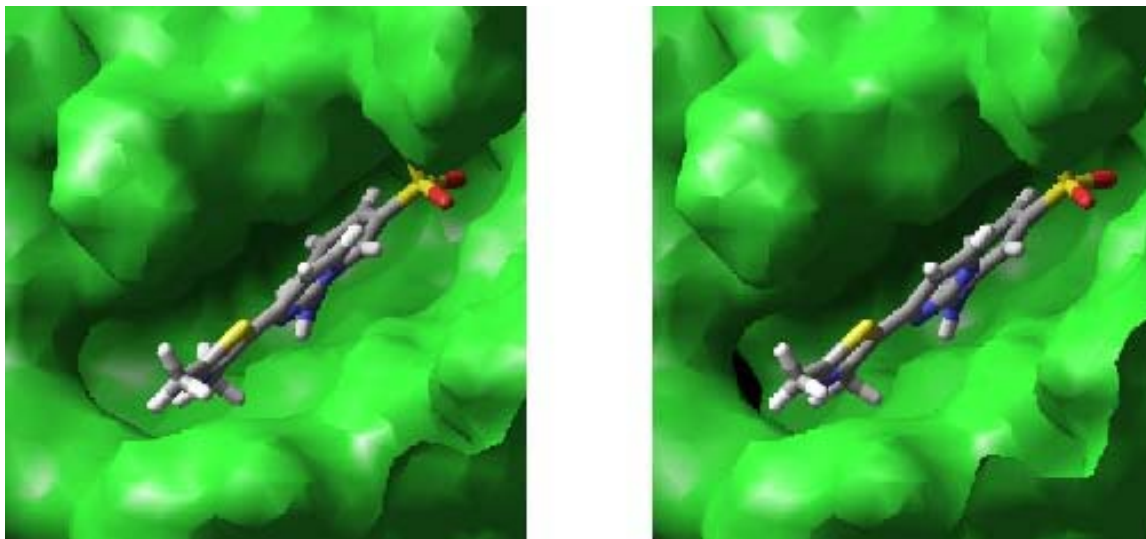


Figure 7.8 stereo surface view of molecule docked to aurora-A protein

Virtual screening produced some false positives and a few false negatives. It is believed that concurrent use of Docking and Multiple Linear Regression Analysis, which readily minimizes these errors, could be an added tool for Pharmacophore model based virtual screening in order to produce reliable true positives and negatives.

The pharmacophore model correlates well with the docking model, one hydrogen bond acceptor is for H-bond interaction with ALA213 and the hydrophobic feature is for H-bond interactions with ASP274. The first two H-bonds with ALA 213 and ASP 274 are identical to those observed in Hinge region and the third H-bond with Asp 274 appears to explain the high Aurora kinase selectivity observed for Pyrazolines, Pyrimidines, 1H Quinazolin-4-ones.

8. PASS PREDICTION STUDIES

8.1 MATERIALS AND METHODS

PASS: PREDICTION OF ACTIVITY SPECTRA FOR BIOLOGICALLY ACTIVE SUBSTANCES

Computer program PASS (Prediction of Activity Spectra for Substances) was developed as a tool for evaluation of general biological potential in a molecule under study³²². There have been several attempts to develop such a kind of computer system even earlier³²³⁻³²⁶. In particular, the feasibility for computer-aided prediction of biological activity of chemical compounds on the basis of their structural formulae was studied within the State System for Registration of New Chemical Compounds synthesized in the USSR in 1972–1990³²⁷.

The latest version of PASS (1.911) predicts about 1000 kinds of biological activity³²⁸ with the mean prediction accuracy of about 85%. The default list PASS of predictable biological activities includes main and side pharmacological effects (e.g., anti hypertensive, hepato protective, sedative, etc.), mechanisms of action (5-hydroxytryptamine agonist, acetyl cholinesterase inhibitor, adenosine uptake inhibitor, etc.), and specific toxicities (mutagenicity, carcinogenicity, teratogenicity, etc.).

The PASS estimations of biological activity spectra of new compounds are based on the structure–activity relationships knowledgebase (SAR Base), which accumulates the results of the training set analysis. The in-house developed PASS training set includes about 50,000 known biologically active substances (drugs, drug-candidates, leads, and toxic compounds). Since new information about biologically active compounds is discovered regularly, the special informational search and analysis of the new information is performed and further used for updating and correcting the PASS training set.

The PASS approach is based on the suggestion, $Activity = Function(Structure)$ ¹⁹². Thus, "comparing" structure of a new substance with that of well-known biologically active substances, it is possible to find out whether a new substance has a particular effect. PASS operates with many thousands of substances from the training set, so provides more objective estimate whether the compound is active or not for any kind of activity. The process of PASS development and use is shown in figure 8.1

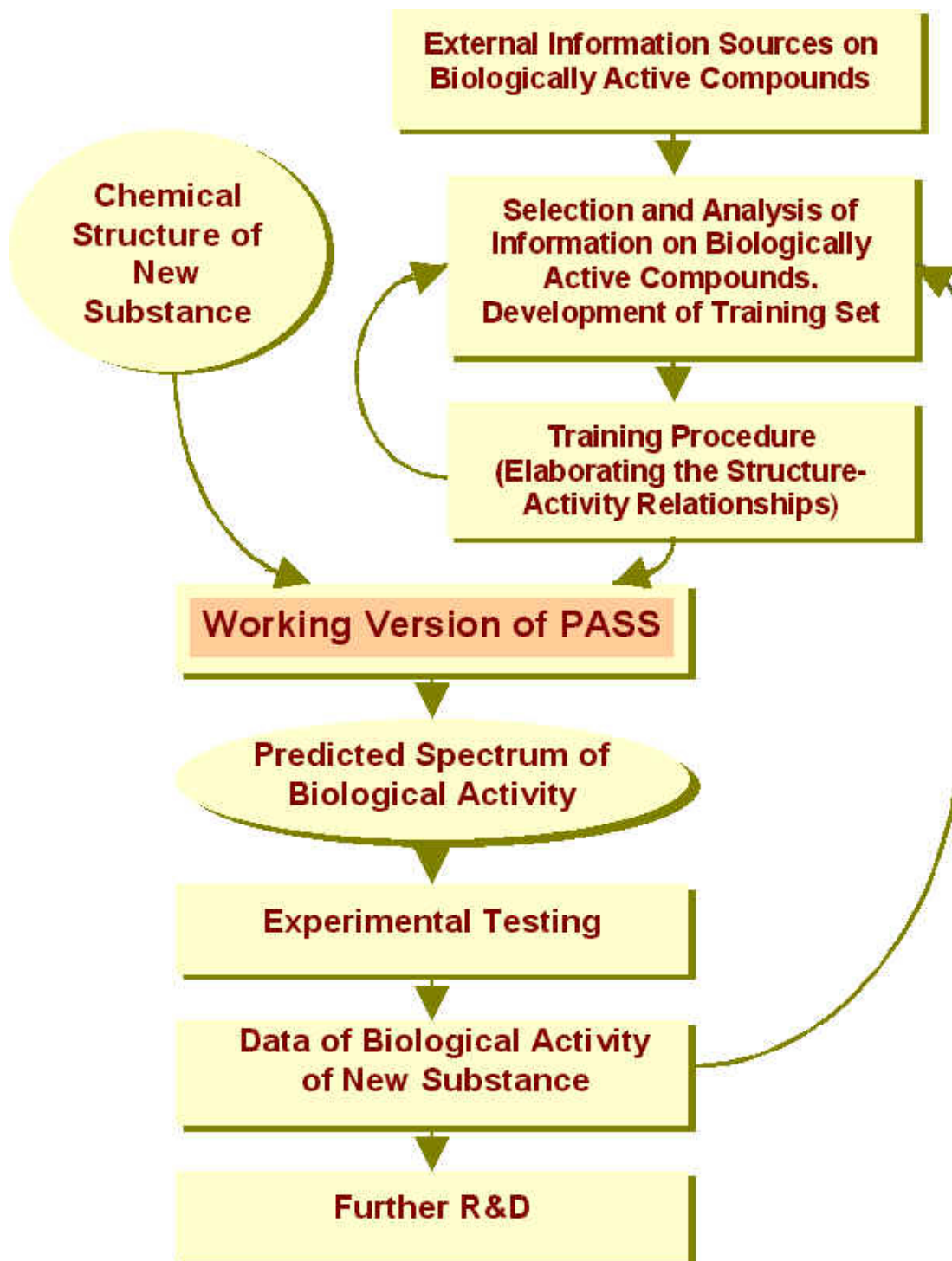


Figure 8.1 The process of PASS development and use

Input and Output of PASS

PASS uses as input data a MOL- or SD-file³²⁹ representing the structural information about the molecules under study. On the basis of these data, MNA descriptors (Multilevel Neighborhood Atoms) are generated automatically. It is important to note that the program is open: New MNA descriptors are generated if a new structural feature, never found before in any of the compounds in the training set, appears in the compound being read in. Based on the statistics of MNA descriptors for active and inactive compounds from the training set, two probabilities are calculated for each activity: P_a - the probability of the compound being active and P_i - the probability of being inactive. Being probabilities, the P_a and P_i values vary from 0.000 to 1.000 (with three relevant decimals being calculated), and in general $P_a + P_i < 1$, since these probabilities are calculated independently. P_a and P_i can be considered to be measures of the compound under study belonging to the classes of active and inactive compounds, respectively, or can be seen as estimates for the first and second kinds of errors in the prediction.

Interpretation of Predictions

The PASS predictions can be interpreted, and used, in a flexible manner. The most probable activities, for a given compound, are characterized by P_a values close to 1, and P_i values close to 0. Let us first consider cases where the P_a value is high and is much larger than P_i . If a statistically significant set of samples with predictions obtained with the threshold $P_a > 0.9$ is selected from a much larger database and assayed, one has to expect to lose 90% of the active compounds, but the fraction of false-positives will be very small. For a cut off of $P_a > 0.8$, only 80% of the actives will be lost, but the fraction of false positives will be a little bit higher. Finally, if one goes down to the criteria $P_a > P_i$, the probability of the first kind of error equals the probability of the second kind of error, i.e., one is just as likely to miss true actives as to find false positives. However, maximizing P_a values for the desired activity is not the only criteria for selection of the most promising compounds. Another aspect might be the novelty of a compound. If P_a is very high, the compound might be a close analogue of known pharmaceutical agents. Thus, if one is interested in finding new leads, especially New Chemical Entities (NCE), one may want to choose compounds for which the specified activity is predicted with

lower probability, say, $0.5 < Pa < 0.7$. In this case, the probability of false positives is likely to be higher, but if the activity is confirmed in the experiment, one has a higher chance of obtaining an NCE¹⁹².

Pass Predictions Via Internet.

Recently, an Internet version of PASS has been made available at the PASS developers' Web site.³³⁰ The users can submit a MOL-file of the molecule under study and obtain the predicted biological activity spectrum displayed on their computer immediately. This new Internet version of PASS provides access to the prediction of all 783 kinds of biological activity, in contrast to an earlier version that predicted 319 activities.³³¹ At this Web site,³³⁰ one can also find a detailed description of the algorithm and chemical descriptors used in PASS, the list of predicted activities, some examples of PASS applications to the discovery of new lead compounds with antiulcer, hepato protective, anti amnesic, antihypertensive, and other actions as well as references of current publications.

8.2 RESULTS AND DISCUSSION

In an effort to optimize their biological profile, a wide structural diversity of piperidine-4-ones possessing Aminopyrimidine and Pyrazolines as a silent feature of their chemical structure, have been virtually designed, synthesized and investigated for the pharmacological activity. The anticancer activity of the compounds were chosen on the basis of their best prediction values from the virtually screened compounds as well as ease of their synthesis. In order to accelerate search for potent New Chemical Entities (NCEs), the assistance of Computer aided drug discovery program PASS (Prediction of Biological Activity Spectra) was used to predict the activity of the designed molecule.

Out of the 300 hits obtained after the pharmacophore modeling and docking studies, 170 hits were selected on the basis of best docking scores. All these compounds were further subjected to PASS prediction studies. Out of these 170 hits the molecules which showed good prediction values ($P_a > 0.5$) against cancer were selected. At the same time care was taken to include the molecules showing high docking scores (> -7). The compounds having high docking values but poor prediction values were rejected. Thus a consensus was obtained between the docking values and the PASS prediction values.

The specificity of PASS prediction was so good that it was able to predict the type of the cancer against which the chemical entity is active. The compounds 1A-29A were predicted to be highly active against colorectal cancer and moderately active against Brain cancer. The increased levels of Aurora A kinase in colorectal cancer is already discussed by Hiroshi katayama *et al*³³². The compounds P1-P11 were predicted to have Phosphatase inhibition activity. The phosphatase inhibitory activity leads to apoptosis which is a programmed cell death of the cancer cell lines.

The details of the PASS prediction values of the selected compounds along with their respective docking scores are given in table 8.1 and 8.2.

From the analysis of the data presented in table 8.1, it is seen that the molecules predicted to show activity against colorectal cancer have one thing in common. That is they all possess substituted Aminopyrimidines in their structure along with piperidin-4-ones. The amino pyrimidines are already shown to be Aurora Kinase A inhibitors.²⁶⁴

TABLE 8.1 THE PASS PREDICTION VALUES OF THE SELECTED COMPOUNDS ALONG WITH THEIR DOCKING SCORES

COMPOUND NO	CODE NO	COLORECTAL CANCER Pa VALUES	DOCKING SCORES
26	1 A	0.619	-7.515232
214	2A	0.668	-8.369694
145	3 A	0.645	-7.236734
244	4A	0.671	-7.422266
556	5A	0.551	-9.834773
435	6A	0.566	-9.811307
683	7A	0.633	-10.38227
339	8A	0.645	-8.200636
442	9A	0.591	-9.678598
186	10 A	0.612	-10.181061
233	11A	0.664	-8.533238
253	12A	0.640	-8.20334
626	13A	0.595	-8.278845
726	14A	0.602	-8.333371
152	15A	0.664	-7.011087
624	16A	0.646	-9.400973
603	17A	0.642	-7.860743
724	18A	0.670	-9.191638
241	19 A	0.571	-9.453096
121	20 A	0.627	-7.986002
237	21A	0.551	-8.44307
575	22A	0.666	-8.233077
268	23A	0.625	-8.75339
360	24A	0.739	-10.0318
721	25A	0.559	-8.7115
700	26A	0.565	-8.193158
716	27A	0.575	-8.110679
690	28A	0.595	-10.477839
656	29A	0.606	-7.464531

From the table 8.2 it is evident that the compounds P1- P11 show a very good phosphatase inhibitory activity. It can also be seen that the docking scores as aurora A kinase inhibitors are not very significant when compared with the Aminopyrimidine molecules.

Phosphatases are essential for the phosphorylation of the Aurora A kinase which is necessary for the activation of the Aurora kinase³³³. If the phosphorylation is blocked by inhibiting the phosphatase the Aurora A Kinase will not be activated and this is an

indirect way of inhibiting Aurora A kinase which is an oncogene. The predicted activity data given in table 8.2 indicates that the compounds showing phosphatase inhibition have substituted 2-pyrazoline moiety as substitutions in piperidin-4-ones.

TABLE 8.2 THE PASS PREDICTION VALUES OF THE SELECTED COMPOUNDS ALONG WITH THEIR DOCKING SCORES

COMPOUND NO	CODE NO	PHOSPHATASE INHIBITION Pa VALUES	DOCKING SCORES
15	P1	0.723	-6.606088
53	P2	0.737	-4.81688
129	P3	0.738	-6.567164
149	P4	0.732	-7.849663
184	P5	0.713	-6.467198
405	P6	0.729	-6.471931
428	P7	0.765	-7.059283
668	P8	0.727	-7.193496
678	P9	0.731	-7.962651
685	P10	0.729	-6.382674
709	P11	0.771	-6.99039

Thus the compounds IA-29A were predicted to possess anticancer activity against colorectal cell lines and compounds P1-P11 were predicted to have phosphatase inhibition activity. After prediction, the selected compounds were (40 Nos) screened for druglikeness which includes optimization using Lipinski rule and toxicity assessment.

The prediction values were found to be in consensus with the experimental values. The Compound P11 with the highest prediction value corresponds to the highest phosphatase inhibitory activity. The next ranking compounds in the prediction also showed the activity spectrum in the same order. As expected from the prediction values all the other compounds showed moderate activity.

9. DRUG LIKENESS SCREENING

9.1 OPTIMIZATION USING LIPINSKI RULE

MATERIALS AND METHODS

Approaches for the experimental determination of protein–ligand molecular interactions are reliant on the quality of the compounds being tested. The application of large, randomly designed combinatorial libraries has given way to the creation of more-focused ‘drug-like’ libraries. Prior to synthesis, it is useful to screen the potential compounds to remove undesired chemical moieties and to get compounds within a required range of physiochemical properties. The successful application of the processes of virtual and physical screening for active ligands is totally reliant on the quality of the molecules being screened.

Druglikeness may be defined as a complex balance of various molecular properties and structural features which determine whether particular molecule is similar to the known drugs. These properties, mainly hydrophobicity, electronic distribution, hydrogen bonding characteristics, molecule size and flexibility and presence of various pharmacophoric features influence the behavior of molecule in a living organism, including bioavailability, transport properties, affinity to proteins, reactivity, toxicity, metabolic stability and many others.

Virtual Screening

A major impetus for a successful drug design strategies is to invest in *in silico* techniques with effective and reliable algorithms to predict oral bioavailability and avoid compounds that do not meet safety requirements³³⁴. Therefore, *in silico* algorithms are based on “drug like” properties of known drugs such as a required molecular weight range, optimum H-bond donor and acceptor numbers and desirable log P values. As the information on the structure and function of numerous transporters are becoming available and combination of this with the computational methods being developed to predict the drug-likeness of compounds shows that drug discovery is already on the road towards electronic R&D³³⁵.

Another approach of classifying drug-like from non-drug like entities is to use neural network methods. For example, the Bayesian neural network strategy could correctly predict over 90% of the Comprehensive Medicinal Chemistry (CMC) database and about 10% of the molecules in the Available Chemical Directory (ACD) as drug-like³³⁶. There are other equally important techniques with similar degrees of success in predicting drug-likeness features of a database³³⁷⁻³⁴⁰.

The recent computational approaches are taking into account numerous factors to predict bioavailability. For example, it has been suggested that lipophilicity, molecular size, molecular shape, polar surface area, hydrogen bonding capacity, and similar parameters correlate to absorption or permeability³⁴¹. Furthermore, prediction of specific binding to protein active sites and interaction with solvent systems are important features in ADME³⁴². The role of partition coefficient, molecular weight, carrier-mediated transport, conformational flexibility for designing orally bio available drugs³⁴³ and their physicochemical and delivery considerations were previously reviewed³⁴⁴. A numerical molecular representation called the molecular hashkey was developed to predict log P and intestinal absorption of a set of drugs³⁴².

An *in silico* or virtual screening (VS) approach helps to converge on possible active molecules from large molecular libraries and focus physical assaying on a smaller subset of compounds³⁴⁵. A developing area in VS is the use of computational methods that filter a molecular library before docking towards compounds with favorable pharmacokinetics, optimum oral bioavailability, compatibility with some types of metabolisms and consequently low toxicity³⁴⁶. As with all human endeavors, the urge to impose rules and structures on process is firmly engrained in the early phase of drug discovery. Framing rational discovery are a set of guiding rules that describe cheminformatic properties desirable in lead- or drug-like chemical scaffolds.

The ‘Rule of Five’ (Lipinski Rule)

Based on a study of the properties of orally available drugs, Lipinski’s analysis of the reasons why compounds fail in progression highlighted the necessity to consider pharmacokinetic properties in compound library design³⁴⁷. This work furnished drug designers with the ‘rule of five’ (RO5), which essentially directed library creation and our

consideration of screening collection diversity towards orally available drug-like space. Application of the RO5 would enforce the following properties on a screening collection:

- (i) Molecular weight (MW) ≤ 500 Da;
- (ii) Hydrophobicity ($\log P$) ≤ 5 ;
- (iii) Number of H-bond donors ≤ 5 and acceptors ≤ 10 .

Molecules violating more than one of these rules may have problems with bioavailability. The rule is called "Rule of 5", because the border values are 5, 500, 2*5, and 5.

The 'rule of three'

This rule set was proposed by Congreve *et al.*³⁴⁸ and is designed for compliance in fragment-based drug discovery³⁴⁹. Application of the rule of three would enforce the following properties on a screening collection:

- (i) MW < 300 Da;
- (ii) $\log P < 3$; (iii) number of H-bond donors and acceptors < 3 ;
- (iv) Flexible bonds < 3 .

Molinspiration

Molinspiration is an independent research organization focused on development and application of modern cheminformatics techniques, especially in connection with the internet. Molinspiration supports internet chemistry community by offering free on-line cheminformatics services for calculation of important molecular properties (for example $\log P$, polar surface area, number of hydrogen bond donors and acceptors).

Molinspiration offers broad range of cheminformatics software tools supporting molecule manipulation and processing, including SMILES and SDfile conversion, normalization of molecules, generation of tautomers, molecule fragmentation, calculation of various molecular properties needed in QSAR, Molecular modeling and drug design, high quality molecule depiction, molecular database tools supporting substructure search or similarity and pharmacophore similarity search.

It also supports fragment-based virtual screening, bioactivity prediction and data visualization. Molinspiration tools are written in Java, therefore are available practically on any computer platform. It contains a database of 21 thousand substituents and 49 thousand linkers extracted from bioactive molecules including calculated physicochemical properties. Possible application area of the database includes virtual

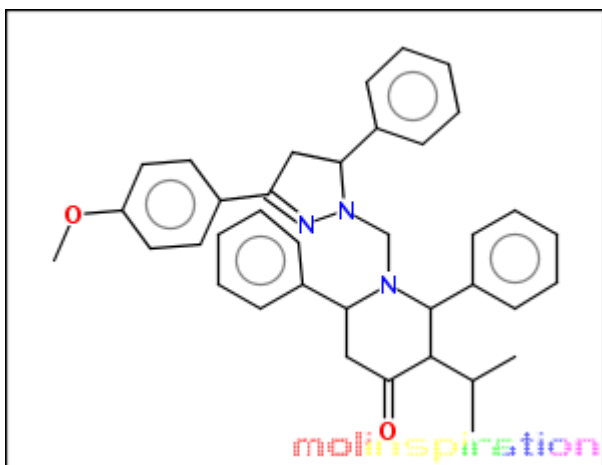
combinatorial chemistry, generation of bioactive molecules with desired properties by combining spacers and substituents, or bioisosteric design by replacing selected substructures in target molecules by their analogs identified by property similarity search. Molinspiration offers a molecular processing and property calculation tool kit. A model of the Molinspiration property calculator³⁵⁰ is shown (Figure 9.1). Once the structure is drawn in the calculator and by pressing the predict properties button, the data is displayed as shown below.

molinspiration

Calculation of Molecular Properties

SMILES

COc6ccc(C5=NN(CN2C(c1cccc1)CC(=O)C(C(C)C)C2c3ccccc3)C(c4ccccc4)C5)cc6



[Molinspiration property engine](#)
v2007.04

miLogP	8.299
TPSA	45.145
natoms	42
MW	557.738
nON	5
nOHNH	0
nviolations	2
nrotb	8
volume	537.609

[Get data as text](#) (for copy / paste).

[Get 3D geometry](#) BETA

Figure 9.1 mipc - Molinspiration property calculator

LogP (Octanol/water partition coefficient)

LogP is calculated by the methodology developed by Molinspiration as a sum of fragment-based contributions and correction factors. Method is very robust and is able to process practically all organic and most organometallic molecules

Molecular Polar Surface Area TPSA

TPSA is calculated based on the methodology published by Ertl *et al.* as a sum of fragment contributions. O- and N- centered polar fragments are considered. PSA has been shown to be a very good descriptor characterizing drug absorption, including intestinal absorption, bioavailability, Caco-2 permeability and blood-brain barrier penetration.

Molecular Volume

Method for calculation of molecule volume developed at Molinspiration is based on group contributions. These have been obtained by fitting sum of fragment contributions to "real" 3D volume for a training set of about twelve thousand, mostly drug-like molecules. 3D molecular geometries for a training set were fully optimized by the semi empirical AM1 method.

"Rule of 5" Properties

These are simple molecular descriptors used by Lipinski in formulating his "Rule of 5". The rule states, that most "drug-like" molecules have $\log P \leq 5$, molecular weight ≤ 500 , number of hydrogen bond acceptors ≤ 10 , and number of hydrogen bond donors ≤ 5 .

Number of Rotatable Bonds - Nrotb

This simple topological parameter is a measure of molecular flexibility. It has been shown to be a very good descriptor of oral bioavailability of drugs. Rotatable bond is defined as any single non-ring bond, bounded to non terminal heavy (i.e., non-hydrogen) atom. Amine C-N bonds are not considered because of their high rotational energy barrier.

RESULTS AND DISCUSSION

OPTIMISATION USING LIPINSKI RULE

The majority of effective oral drugs obey the Lipinski rule of five. The data upon which this rule rests is drawn from 2500 entries extracted from the U.S. adapted names, the world drug lists and the internal Pfizer compound collections. There are four criteria

1. The substance should have a molecular wt of 500 or less
2. It should have fewer than five hydrogen bond donating functions.
3. It should have fewer than ten hydrogen bond accepting functions.
4. The substance should have a calculated Log P (C Log P) between approximately -1 to +5.

In short the compound should have a comparatively low molecular weight, be relatively non-polar and partition between an aqueous and a particular lipid phase in favor of the lipid phase but, at the same time possess perceptible water solubility. There are many biologically active compounds that satisfy these criteria that fail to become drugs but there are comparatively a few successfully orally active drugs that fail to fit³⁵¹.

This shows the significance of the Lipinski rule and so all the synthesized compounds were screened for optimization with Lipinski rule using the Molinspiration property calculator. The results are summarized in Table 4.8 for 1A to 29A and in Table 4.9 for P1 to P11.

As we can see from the table 9.1 the No of violations is found to be 2 or 3 for all the compounds. The molecular weight and the Log P values are found to be the main reasons for the violations. Actually these violations are not considered for the cancer target drugs. The reason is explained below.

The annotation and visualization of medicinally relevant kinase space revealed that kinase inhibitors in the clinic are, on average of higher molecular weight and more Lipophilic than all other clinically investigated drugs³⁵². Only the discontinued and Phase I kinase compounds have similar molecular weight to other orally targeted compounds in the same development phase³⁵³.

TABLE 9.1 LIPINSKI RULE PROPERTIES OF THE DESIGNED MOLECULES

COMPOUND NO	LOGP	M.WT.	HYDROGEN BOND ACCEPTOR	HYDROGEN BOND DONOR	ROTATABLE BONDS	TPSA	MOL. VOLUME	NO OF VIOLATIONS
1A	8.228	613.71	9	1	8	114.46	476.83	2
2A	8.619	697.66	8	1	9	87.111	615.87	2
3a	9.033	682.06	6	1	7	68.64	569.13	2
4A	7.842	584.72	7	2	7	88.87	545.72	2
5A	8.685	677.16	11	1	9	151.05	589.17	3
6A	8.267	642.71	11	1	9	151.05	575.63	3
7A	7.401	718.76	14	2	11	189.75	634.74	3
8A	6.98	689.77	12	2	10	153.16	620.15	3
9A	7.896	672.74	12	1	10	160.29	601.18	3
10A	7.894	623.06	11	1	7	154.96	528.39	3
11A	8.82	609.12	5	1	6	59.409	535.56	2
12A	8.054	560.64	5	2	5	70.403	504.50	2
13A	8.016	556.68	5	2	6	70.403	516.37	2
14A	8.295	592.66	5	2	6	70.403	526.23	2
15A	7.46	621.18	5	1	7	58.224	563.42	2
16A	7.499	598.75	7	2	8	88.871	562.53	2
17A	8.685	653.17	6	1	8	68.643	577.91	2

COMPOUND NO	LOGP	M.WT.	HYDROGEN BOND ACCEPTOR	HYDROGEN BOND DONOR	ROTATABLE BONDS	TPSA	MOL. VOLUME	NO OF VIOLATIONS
18A	7.826	634.72	7	2	8	88.87	572.39	2
19A	8.84	622.16	5	1	6	53.413	555.12	2
20A	8.53	562.63	4	1	5	50.175	501.41	2
21A	8.764	624.09	7	1	6	95.999	533.35	2
22A	8.362	755.28	10	1	12	105.57	675.16	2
23A	7.777	629.71	10	2	8	134.69	569.06	2
24A	7.69	650.73	8	2	8	98.10	581.13	2
25A	8.108	619.67	8	2	7	116.227	544.63	2
26A	6.287	648.76	10	2	10	120.47	595.18	2
27A	8.199	642.82	7	2	8	76.87	608.18	2
28A	6.257	708.81	12	2	12	138.94	646.28	3
29A	8.969	714.47	5	2	6	70.403	552.14	2

TABLE 9.1 LIPINSKI RULE PROPERTIES OF THE DESIGNED MOLECULES

COMPOUND NO	LOGP	M.WT.	HYDROGEN BOND ACCEPTOR	HYDROGEN BOND DONOR	ROTATABLE BONDS	TPSA	MOL. VOLUME	NO OF VIOLATIONS
P1	6.523	503.64	5	0	6	49.051	476.829	2
P2	6.459	528.05	6	0	6	62.191	471.933	2
P3	7.24	609.71	6	0	8	54.379	556.215	2
P4	7.575	638.20	7	0	9	63.613	585.434	2
P5	7.137	562.50	6	0	6	62.191	485.469	2
P6	8.299	557.73	5	0	8	45.145	537.609	2
P7	8.645	586.56	5	0	7	49.051	520.763	2
P8	7.87	573.73	6	1	8	65.373	545.627	2
P9	7.983	633.78	8	1	10	83.841	596.718	2
P10	7.573	663.815	9	1	11	93.075	622.264	2
P11	7.006	558.078	7	1	7	82.419	496.753	2

David G.Lloyd *et al*³⁵⁴ have used a principal component analysis (PCA), computational approach to analyze the 3D descriptor space of active and non-active (hit like) cancer medicinal chemistry compounds. Cancer active compounds exist in a much greater volume of space than generic hit like space and most of them fail the commonly applied filter for orally bioavailable drugs. This is of great significance when designing orally bioavailable cancer target drugs.

In their analysis, the vast majority of compound failures stemmed from a lack of MW, LogP and H-bond acceptor compliance with regard RO5. While the examination of the cancer kinome (Figure 9.2) shows a view of the distribution of anticancer kinase targeting compounds in medicinal chemistry space. From a total of 915 active compounds examined (blue spheres) only 156(15%) lie within the defined hit like space (yellow cloud), where as 759(83%) lie outside (red cloud) and do not pass application of filter incorporating RO5 compliance.

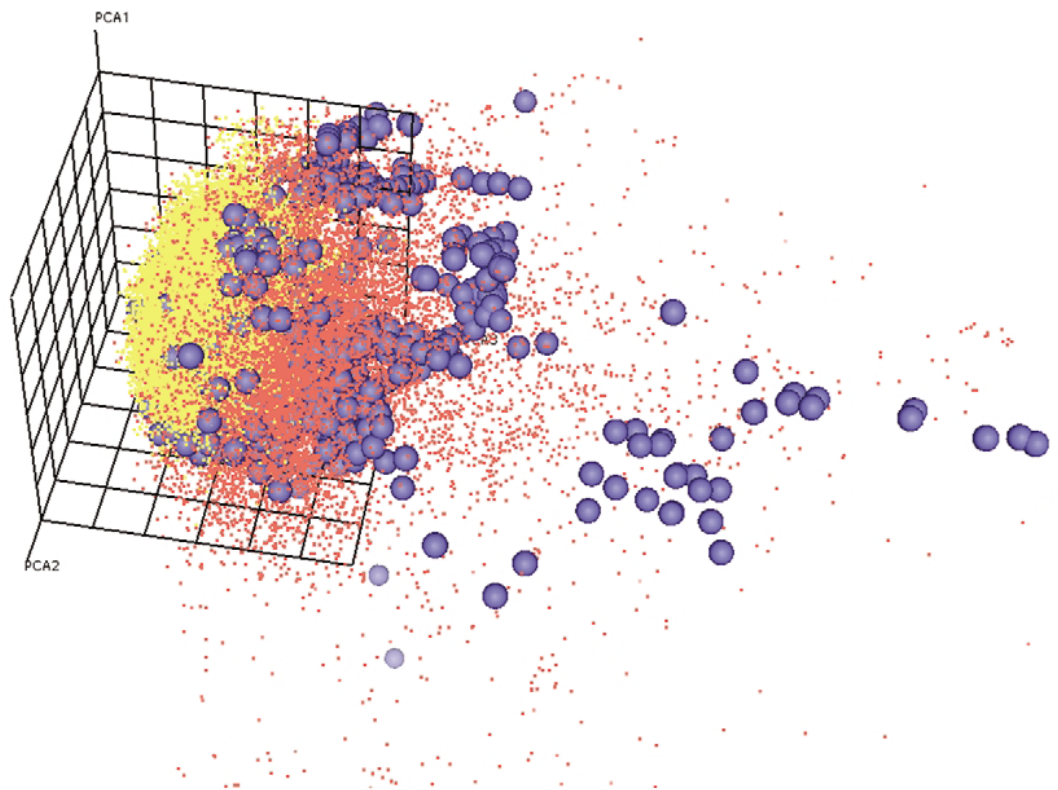


Figure 9.2 Anticancer kinase-targeted space. When a specific cancer target is studied, it is obvious that the majority of its active ligands populate non-generic drug like Space. Thus, care needs to be exercised when applying general drug-like filtering criteria to cancer ligand selection procedures. Key: blue spheres, active ligands; Yellow cloud, generic hit space; red cloud, non-kinase targeted medicinal chemistry space.

It was proved in their study that these rules need not be applied always. They have shown that application of the most commonly used Cheminformatic filters to bestow hit-likeness on a screening collection results in spatial partitions that are not generally occupied by oncology therapeutics. The parameters MW, Log P and Hydrogen bond acceptor should be given particular attention because these are primarily responsible for the removal of potential clinical candidate compound in such filtering process.

Since the current study is also a targeted anticancer study, the violations of RO5 can be accepted.

9.2 TOXICITY ASSESSMENT

MATERIALS AND METHODS

Lead-like versus drug-like compounds

Broadly speaking, compounds sought after in the drug discovery process can be split into two categories, drug-like and lead-like. The concept of lead-likeness implies a physicochemical profile in chemical libraries where the members have reduced complexity (e.g. MW <400) and other more-restricted properties than those deemed drug-like. This leaves room for chemical modification in lead optimization rounds, which subsequently modify the properties towards drug-likeness³⁵⁵. Various authors have proposed different concepts of what constitutes drug-like compounds. These models refer to having molecular similarities to known drugs³⁵⁶ or acceptable absorption, distribution, metabolism, excretion and toxicology (ADME-Tox) properties³⁵⁷. Drug-likeness is often entirely dependent on the mode of administration. The loose description of ‘hit-likeness’ is conferred to those small molecule compounds that pass the unmodified OpenEye FILTER (which uses XLOGP³⁵⁸ as a measure of the hydrophobicity partition coefficient with a maximum cut-off value of six) cheminformatic criteria including a strict application of the RO5. These criteria are now widely adopted in database filtering applied in the early stages of VS.

Cheminformatic filters

Cheminformatic treatment of computational representations of screening collections allows the filtering of the collections according to the criteria of the designer, using calculable properties of the compounds to prescribe discriminating parameters for grouping, excluding or considering those subsets of the dataset that can be advanced to *in silico* or *in vitro* HTS studies. Much effort has been expended in the database creation to ensure that maximum chemical structural diversity is in-built, while adhering to the guiding rules of drug- and lead-like chemical properties^{359,360}. Popular software utilities, such as FILTER (OpenEye), MOE (Chemical Computing Group) and the Daylight Toolkit (Daylight Chemical Information Systems) readily enable users to apply rapid partitioning of compound databases using tunable cheminformatics parameters based on

the 'classical' rules, often enhanced with functionality to recognize and remove compounds with toxic properties³⁶¹. These utilities are frequently employed in internal discovery efforts³⁶², as well as in the presentation and marketing of focused commercial screening libraries and non-targeted HTS collections.

Osiris Property Explorer

The OSIRIS Property Explorer lets us to draw chemical structures and calculates on-the-fly various drug-relevant properties whenever a structure is valid. Prediction results are valued and color coded. Properties with high risks of undesired effects like mutagenicity or a poor intestinal absorption are shown in red. Whereas a green color indicates drug-conform behavior.

While drawing a structure the toxicity risk predictor will start looking for potential toxicity risks as long as the currently drawn structure is a valid chemical entity. Toxicity risk alerts are an indication that the drawn structure may be harmful concerning the risk category specified. However, risk alerts are by no means meant to be a fully reliable toxicity prediction. In the same way it should not be concluded from the absence of risk alerts that a particular substance is completely free of any toxic effect.

The prediction process relies on a pre computed set of structural fragment that give rise to toxicity alerts in case they are encountered in the structure currently drawn. These fragment lists were created by rigorously shredding all compounds of the RTECS (Registry of Toxic Effects of Chemical Substances) database known to be active in a certain toxicity class (e.g. mutagenicity). During the shredding any molecule was first cut at every rotatable bonds leading to a set of core fragments. These in turn were used to reconstruct all possible bigger fragments being a substructure of the original molecule. Afterwards, a substructure search process determined the occurrence frequency of any fragment (core and constructed fragments) within all compounds of that toxicity class. It also determined these fragment's frequencies within the structures of more than 3000 traded drugs. Based on the assumption that traded drugs are largely free of toxic effects, any fragment was considered a risk factor if it occurred often as substructure of harmful compounds but never or rarely in traded drugs.

RESULTS AND DISCUSSION

Adverse safety or toxicity profiles for compounds of therapeutic interest can be indicated by a range of *insilico* methods. Individual compounds may have the originating factors for a potential toxicology or safety outcome but a difference in dose size, route of administration, pharmacokinetic profile, genetic risk factors, tissue distribution or metabolic pathway may result in different observed outcomes³⁶³. The fundamental origins of adverse safety or toxicity findings can be considered as deriving from four parameters.

- Primary mechanism of action of the therapeutic agent.
- Secondary pharmacology of the therapeutic agent(including interaction with DNA)
- The presence of a well defined structural fragment in the molecule with evidence that associates the fragment with adverse outcomes henceforth referred to as a toxicophore.
- The overall physicochemical properties of the molecule which may predispose it to adverse outcomes.

Screening of Drug candidates for mutagenicity is a regulatory requirement for drug approval³⁶⁴ since mutagenic compounds pose a risk to humans. So after screening the forty virtually designed compounds for Lipinski molecular properties all were subjected to preliminary toxicity assessment using OSIRIS property explorer. The data of the toxicity assessments are presented in table 9.2. Prediction results are valued and color coded. Properties with high risks of undesired effects like mutagenicity or a poor intestinal absorption are shown in red. Whereas a green color indicates drug-conform behavior.

A correlation was done between the data given in the table 4.10 with the structures of the virtual molecules. The molecules which showed Mutagenic and tumorigenic toxicities(5A,6A,7A,8A,9A,21A,23A,25A) were found to have aromatic nitro group which is identified as a toxicophore. It is a toxicophore which do not require metabolic activation and associated with direct effects on DNA³⁶⁵.

TABLE 9.2 TOXICITY RISK ASSESSMENTS OF THE DESIGNED MOLECULES

COMPOUND NO	MUTAGENICITY	TUMORIGENICITY	IRRITANTANCY	REPRODUCTIVE EFFECT
1A	Green	Green	Green	Green
2A	Green	Green	Green	Green
3A	Green	Green	Green	Green
4A	Green	Green	Green	Green
5A	RED	RED	Green	Green
6A	RED	RED	Green	Green
7A	RED	RED	Green	Green
8A	RED	RED	Green	Green
9A	RED	RED	Green	Green
10A	Green	Green	Green	Green
11A	Green	Green	Green	Green
12A	Green	Green	Green	Green
13A	Green	Green	Green	Green
14A	Green	Green	Green	Green
15A	Green	Green	Green	Green
16A	Green	Green	Green	Green
17A	Green	Green	Green	Green
18A	Green	Green	Green	Green
19A	Green	RED	Green	Green
20A	Green	Green	Green	Green
21A	RED	RED	Green	Green
22A	Green	Green	Green	Green
23A	RED	RED	Green	Green
24A	Green	Green	Green	Green
25A	RED	RED	Green	Green
26A	Green	Green	Green	Green
27A	Green	RED	Green	Green

COMPOUND NO	MUTAGENICITY	TUMORIGENICITY	IRRITANTANCY	REPRODUCTIVE EFFECT
28A	Green	Green	Green	Green
29A	Green	Green	Green	Green
P1	Green	Green	Green	Green
P2	Green	Green	Green	Green
P3	Green	Green	Green	Green
P4	Green	Green	Green	Green
P5	Green	Green	Green	Green
P6	Green	Green	Green	Green
P7	Green	Green	Green	Green
P8	Green	Green	Green	Green
P9	Green	Green	Green	Green
P10	Green	Green	Green	Green
P11	Green	Green	Green	Green

The other compounds showing tumorigenic toxicity are 27A and 19A. This may be due to the substituted aromatic amino groups present in the molecules. The aromatic nitro and amino groups are well recognized toxicophores³⁶⁶. Both the toxicophores maintain their high accuracy through out many compound classes and therefore has a high predictive capability. The accuracy of these groups can be increased by incorporating detoxifying substructures like trifluoromethyl, sulfonamide, sulfonic acid and aryl sulfonyl derivatives in the ortho, para and/or meta positions with respect to the Toxicophore³⁶⁷. Compounds with a bulky tert-butyl substituent, ortho to the aromatic nitro group showed strongly diminishing mutagenicity³⁶⁸.

Though some of the compounds exhibited mutagenicity and tumorigenicity no changes were made in the structure of the molecules because they were predicted to have good activity by PASS and the Docking results also showed good docking scores. The structures were used as such for synthesis and screening. Based on the activities shown by the compounds, lead obtained will be further refined in the future studies.

10. SYNTHESIS

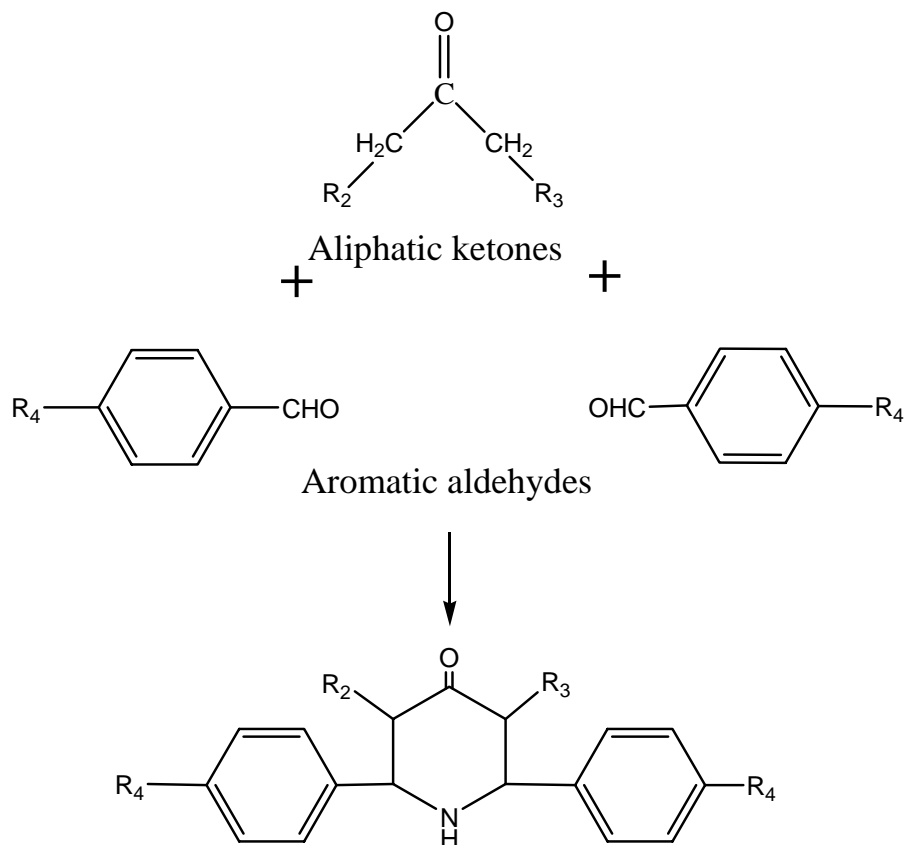
10.1 SYNTHETIC SCHEME

The synthesis of the designed compounds involves three schemes. The scheme-I involves the synthesis of Piperidine-4-ones by the condensation of aliphatic ketones and aromatic aldehydes in presence of ammonium acetate and ethanol.

The Schiff bases of Piperidine-4-ones (Scheme-II) were prepared by treatment with various 2-Aminopyrimidines which in turn were prepared by cyclizing the chalcones using Guanidine nitrate. The chalcones were prepared by Claisen-Schmidt condensation of aromatic aldehydes with aliphatic ketones.

The Mannich bases of piperidine-4-ones (Scheme-III) were prepared by the condensation of piperidine-4-ones with 2-pyrazolines. The pyrazolines were prepared by treating the synthesized chalcones with hydrazine hydrate.

SCHEME-I

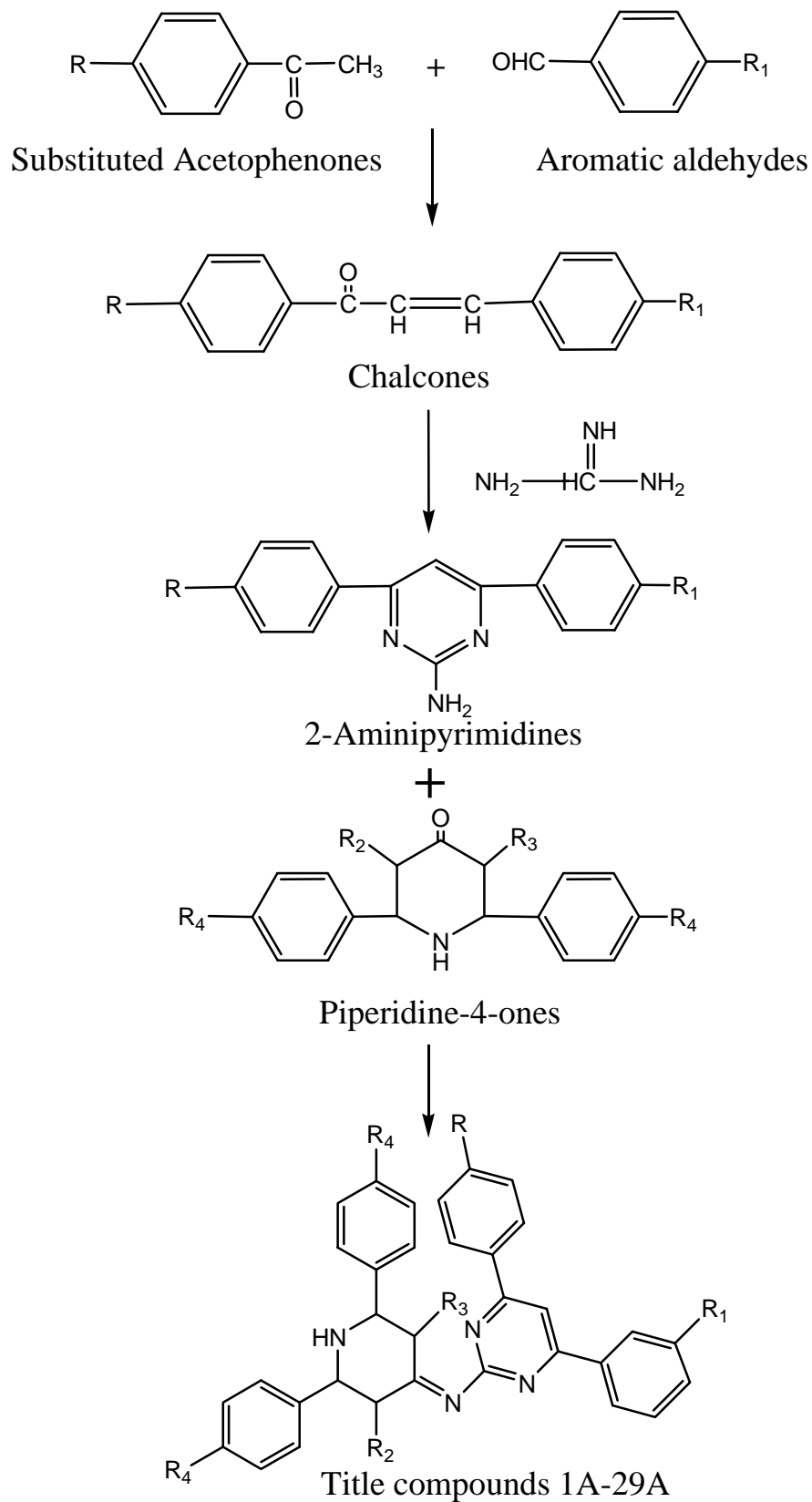


R₂ = H, CH₃

R₃ = Isopropyl, CH₃

R₄ = H, Cl, OMe, -3,4-dimethoxy, -3,4,5-trimethoxy, p-Br, p-F, p-NO₂, m-NO₂, diethylamino, furyl.

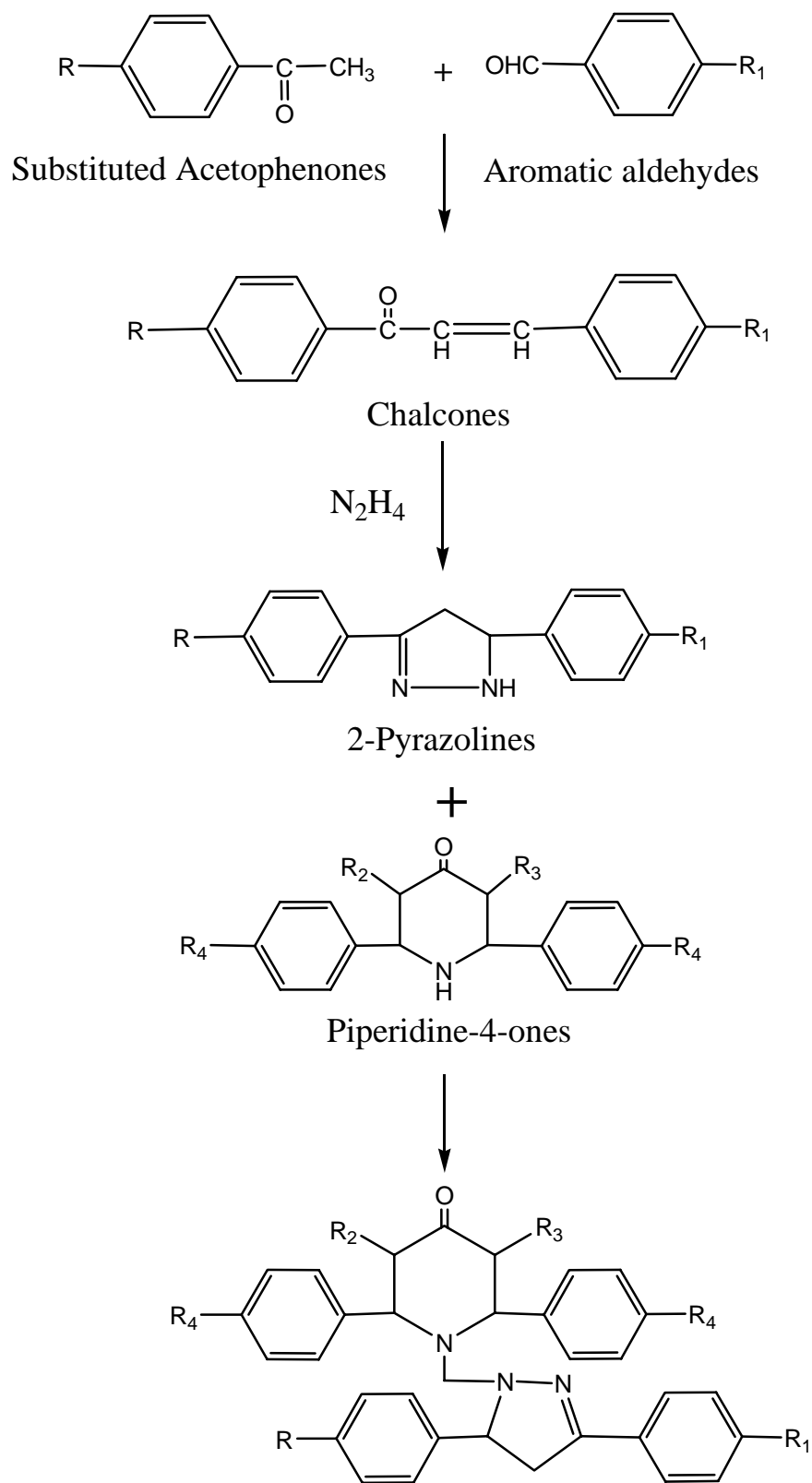
SCHEME II



R=H, OH, Cl; R₂=H, CH₃; R₃= Isopropyl, CH₃.

R₄=R₁=H, Cl, OMe, -3, 4-dimethoxy, -3, 4, 5-trimethoxy, p-Br, p-F, p-NO₂, m-NO₂, dimethyl amino, furyl.

Scheme-III



Title compounds P1-P11

R=H, OH, Cl; R₂=H, CH₃; R₃= Isopropyl, CH₃.

R₄=R₁=H, Cl, OMe, -3, 4-dimethoxy, -3, 4, 5-trimethoxy, p-Br, p-F, p-NO₂, m-NO₂, diethyl amino, furyl

10.2 EXPERIMENTAL PROCEDURE

Microwave Assisted Synthesis was carried out in whirlpool domestic MICROWAVE Oven ICE 705

The melting points were taken in open capillary tube and are uncorrected.

The IR spectra of the compounds were recorded on ABB Boomem FT-IR spectrometer MB 104 with potassium bromide pellets.

The ^1H -NMR spectra of the synthesized compounds were recorded on a BRUKER AV -III 400 NMR spectrometer in CDCl_3 .

The ^{13}C -NMR spectra of the synthesized compounds were recorded on a BRUKER AV-III 400 NMR spectrometer in CDCl_3 .

The COSY NMR spectrum was recorded on a BRUKER AV-III 400 NMR spectrometer in DMSO.

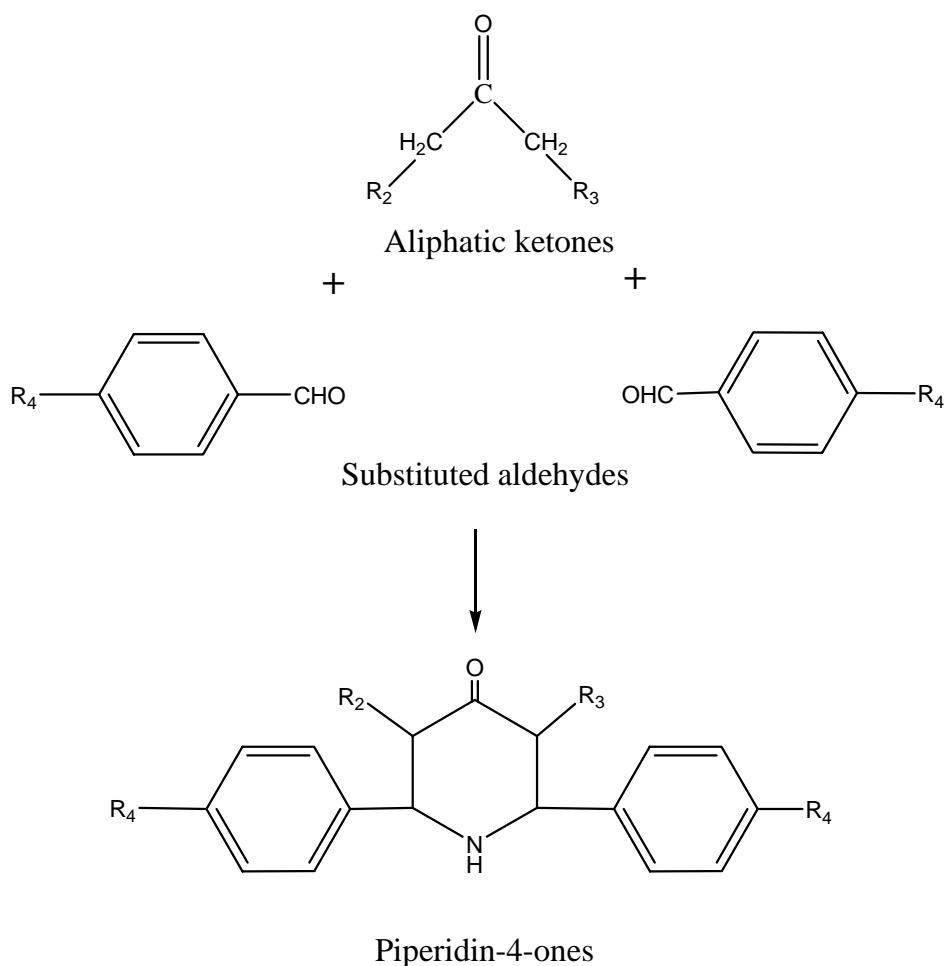
Mass spectra were recorded on Shimadzu GCMS QP 5000.

Elemental Analysis was recorded on a CHNS-O Perkin Elmer 2004 apparatus.

Thin Layer Chromatography was performed using Aluminum plates precoated with Silica gel 60F 254 [E-MERCK] Single Spots were visualized in the ultraviolet light chamber & Iodine chamber.

EXPERIMENTAL PROCEDURE FOR PIPERIDINE-4-ONES.

A mixture of aromatic aldehyde (0.2mole), aliphatic ketone (0.1mole) and dry ammonium acetate (0.1 mole) were taken in a beaker and mixed with ethanol (30 ml). The mixture was heated to simmering¹⁹⁶. It was kept aside overnight. Dry ether (50ml) was added followed by concentrated hydrochloric acid. (30ml). The precipitated hydrochloride was transferred to a one litre beaker and suspended in acetone. It was basified with strong ammonia solution. On dilution with water the base liberates out. The product was filtered, washed repeatedly with water and dried. The crude product was recrystallised from ethanol.



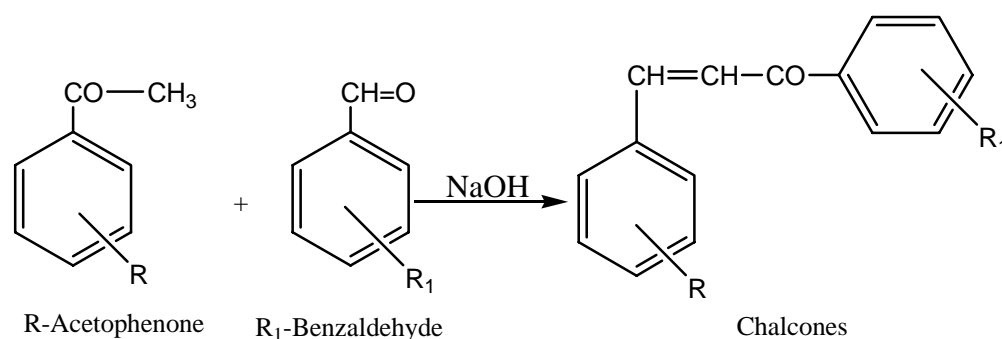
$\text{R}_2 = \text{H}, \text{CH}_3$; $\text{R}_3 = \text{Isopropyl}, \text{CH}_3$.

$\text{R}_4 = \text{R}_1 = \text{H}, \text{Cl}, \text{OMe}, -3, 4\text{-dimethoxy}, -3, 4, 5\text{-trimethoxy}, \text{p-Br}, \text{p-F}, \text{p-NO}_2, \text{m-NO}_2, \text{diethyl amino}, \text{furyl}.$

EXPERIMENTAL PROCEDURE FOR CHALCONES

Substituted acetophenones (0.01 mol) in anhydrous ethanol (7.5ml) were treated with aromatic aldehydes²²³ (0.01mol). The reaction mixture was cooled to 0-5°. Aqueous solution of sodium hydroxide (70%, 5ml) was added slowly while stirring. Stirring was continued for 3 hr and the contents were allowed to stand over night. The reaction mixture was decomposed in ice cold water, neutralized with dilute hydrochloric acid. The solids thus separated were collected, dried and recrystallized from ethanol. The completion of the reaction was monitored by TLC using Benzene and chloroform as solvent system in the ratio of 1:1.

The chalcones were prepared using the above procedure.



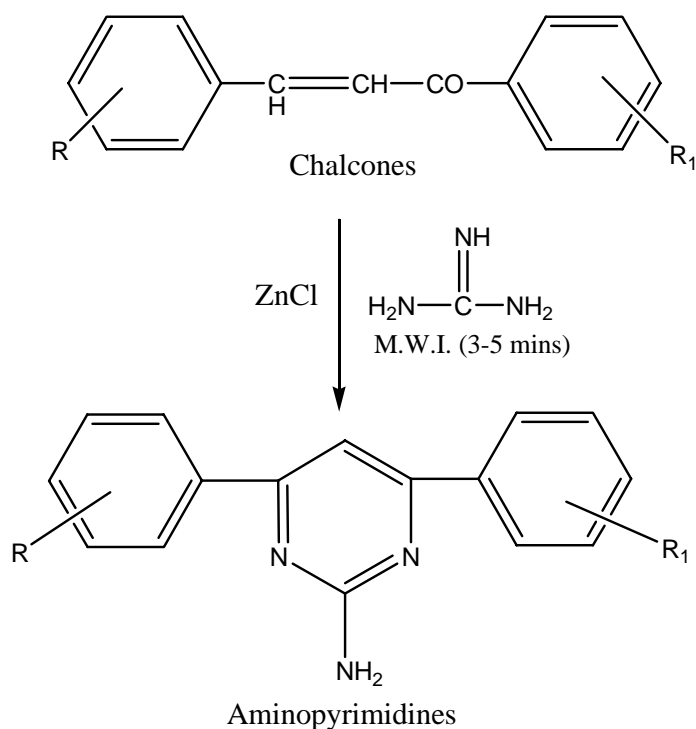
R =H, OH, Cl

R₁=H,Cl,OMe,-3,4-dimethoxy,-3,4,5-trimethoxy,p-Br,p-F,p-NO₂,m-NO₂,diethylamino, furyl.

MICROWAVE ASSISTED SYNTHESIS OF AMINO-PYRIMIDINES

The prepared chalcones (10 m. mole), (10 m. mole) of Guanidine nitrate and (5m.mole) of Zinc Chloride were mixed well in a 100 ml Erlenmeyer flask. The flask was placed in a microwave oven irradiated at 160 watts for up to 3-5 minutes. The reaction mixture was cooled to room temperature and poured over crushed ice. The separated solids were filtered ²¹⁶, dried and recrystallized from ethanol. The completion of the reaction was monitored by TLC using Benzene and chloroform as a solvent system.

The 2-Aminopyrimidines were prepared from the above procedure.



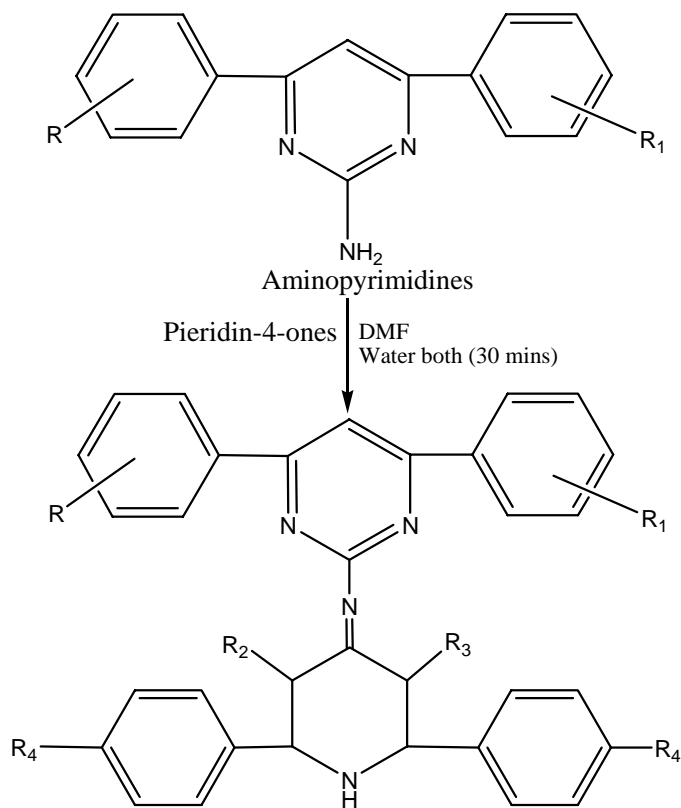
R =H, OH, Cl

R₁=H,Cl,OMe,-3,4-dimethoxy,-3,4,5-trimethoxy,p-Br,p-F,p-NO₂,m-NO₂,diethylamino, furyl.

SYNTHESIS OF SCHIFF BASES (1A-29A)

The 2-Aminopyrimidines (0.01mole) and the synthesized piperidine-4-ones (0.01mol) in DMF (10 ml) were mixed and heated on a water-bath for 30 min, cooled and poured into ice-cold water. Precipitates thus obtained were filtered ³⁶⁹, washed with water and recrystallized from ethanol. The completion of the reaction was monitored by TLC using Benzene and chloroform as a solvent system.

Title Compounds 1A-29A are prepared similarly from the above procedure.



Title Compounds 1A-29A

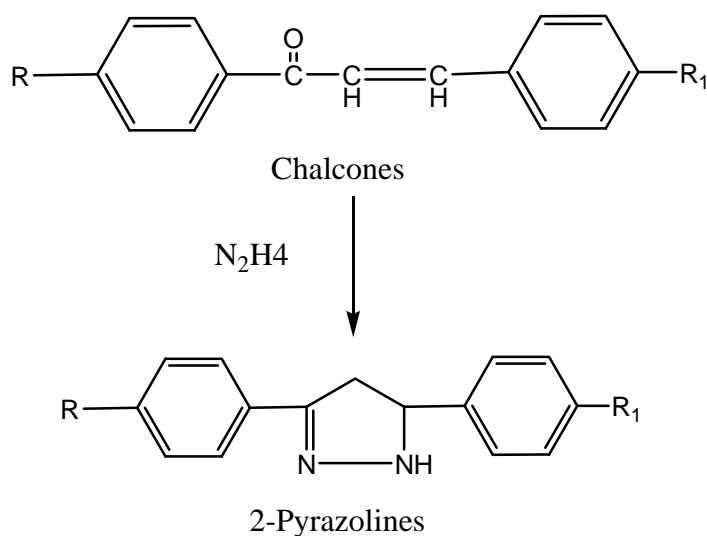
R=H, OH, Cl; R₂=H, CH₃; R₃= Isopropyl, CH₃.

R₄=R₁=H, Cl, OMe, -3, 4-dimethoxy, -3, 4, 5-trimethoxy, p-Br, p-F, p-NO₂, m-NO₂, dimethyl amino, furyl.

EXPERIMENTAL PROCEDURE FOR PYRAZOLINES

The chalcones (0.02 mole) were dissolved in ethanol (25ml) and to this 0.04 mole of (99%) hydrazine hydrate was added and refluxed for 4 hours. Then the reaction mixture was concentrated and allowed to cool. The separated solid ³⁷⁰ was filtered and dried. The separated solids were recrystallized from absolute alcohol. The completion of the reaction was monitored by TLC using benzene and acetone as a solvent system.

The pyrazolines were prepared similarly from the above procedure.

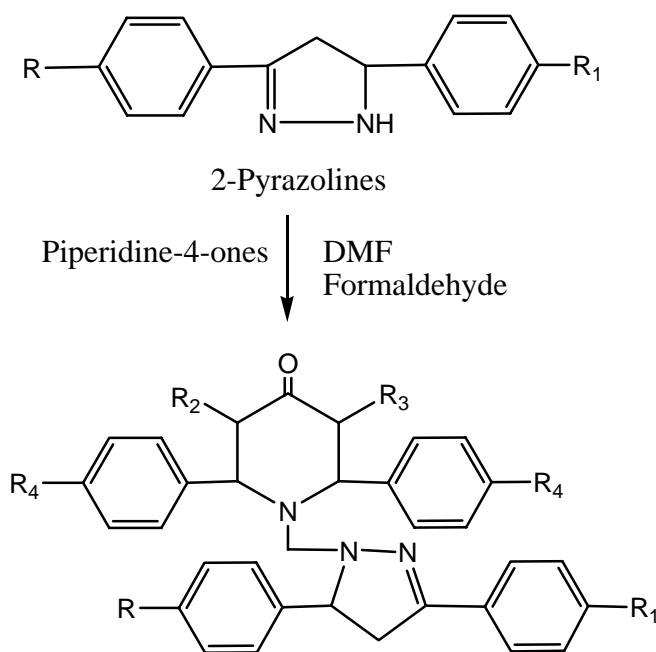


R=H, OH, Cl;

R₁=H, Cl, OMe, -3, 4-dimethoxy, -3, 4, 5-trimethoxy, p-Br, p-F, p-NO₂, m-NO₂, dimethyl amino, furyl.

SYNTHESIS OF MANNICH BASES (P1-P11)

The pyrazolines (0.01mole) were suspended in a minimum quantity (10 ml) of dimethyl formamide. To this slightly more than (0.01mole) of formaldehyde and piperidine-4-ones were added with vigorous stirring. The reaction mixture was heated on a water bath for 20 minutes and left overnight. The resultant compounds ²³⁹ were recrystallized using chloroform.



R=H, OH, Cl; R₂=H, CH₃; R₃= Isopropyl, CH₃.

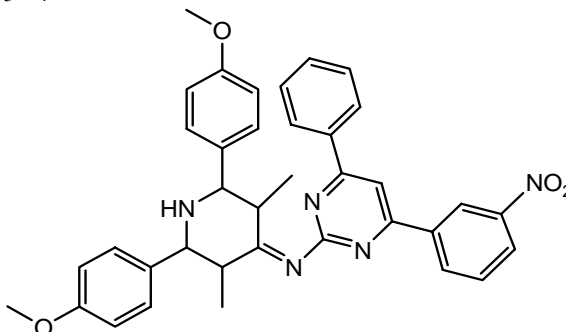
R₄=R₁=H, Cl, OMe, -3, 4-dimethoxy, -3, 4, 5-trimethoxy, dimethyl amino, furyl. p-Br, p-F, p-NO₂, m-NO₂.

11. CHARACTERISATION

11.1 PHYSICO CHEMICAL CHARACTERIZATION

COMPOUND NO: 1A

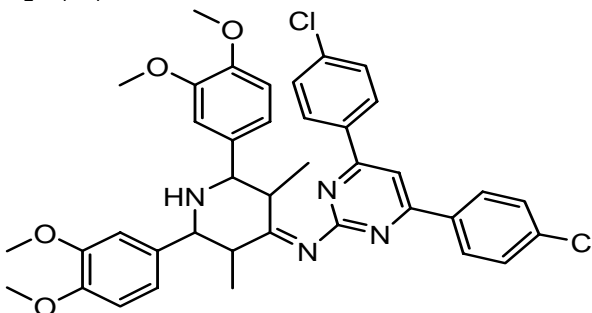
Molecular formula : C₃₇H₃₅N₅O₄



Molecular weight : 614 **R_F Value** : 0.96
Melting point : 148-154 °C **Yield** : 64%.
Solubility : Soluble in chloroform, DMSO, Ethanol, DMF, Benzene
Elemental Analysis : C-72.6(72.41); H- 5.43(5.75); N-11.61(11.41); O-10.91(10.43).
IUPAC Name : N-(2, 6-bis (4-methoxyphenyl)-3, 5-dimethylpiperidine
-4-ylidene)-4-(3-nitrophenyl)-6-phenylpyrimidine -2-amine.

COMPOUND NO: 2A

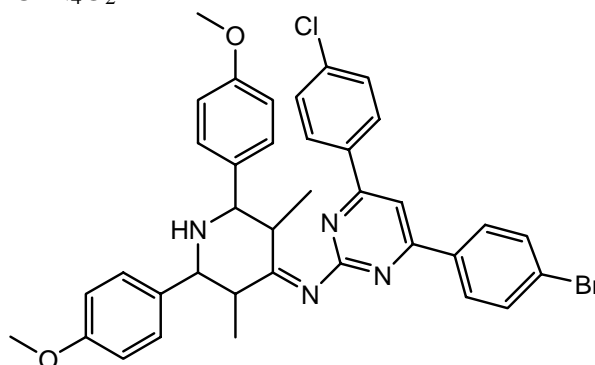
Molecular formula : C₃₉H₃₈Cl₂N₄O₄



Molecular weight : 698 **R_F Value** : 0.92
Melting point : 100-104 °C **Yield** : 67%.
Solubility : Soluble in chloroform, DMSO, Ethanol, DMF, Benzene
Elemental Analysis : C-67.46(67.14); H-5.13(5.49); Cl-10.24(10.16); N-8.73(8.03); O-9.09(9.17)
IUPAC Name : N-(2, 6-bis (3, 4-dimethoxyphenyl)-3, 5-dimethylpiperidine-4-ylidene)-4, 6-bis-(4-chlorophenyl)-6-phenylpyrimidine -2-amine.

COMPOUND NO: 3A

Molecular formula : C₃₇H₃₄BrClN₄O₂



Molecular weight : 682 **R_F Value** : 0.89

Melting point : 210-214 °C **Yield** : 72%.

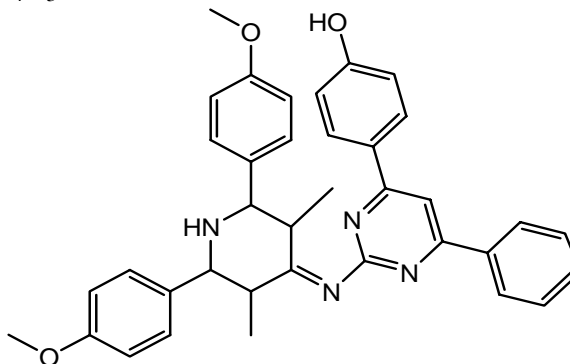
Solubility : Soluble in chloroform, DMSO, Ethanol, DMF, Benzene

Elemental Analysis : C-65.28(65.16); H- 5.57(5.02); N-8.42(8.21); O-4.19(4.69),
Cl-5.21(5.20); Br-11.76(11.72)

IUPAC Name : N-(2,6-bis (4-methoxyphenyl)-3, 5-dimethylpiperidine-4-ylidene)
-4-(4-bromophenyl)-6-(4-chlorophenyl) pyrimidine-2-amine

COMPOUND NO: 4A

Molecular formula : C₃₇H₃₆N₄O₃



Molecular weight : 585 **R_F Value** : 0.99

Melting point : 208-212 °C **Yield** : 68%.

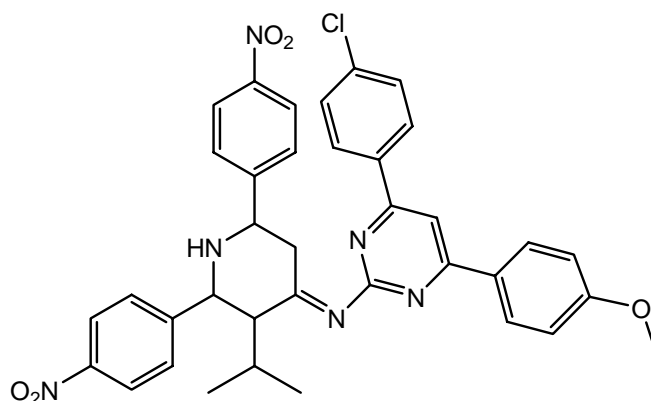
Solubility : Soluble in chloroform, DMSO, Ethanol, DMF, Benzene

Elemental Analysis : C-76.14(76); H- 6.32(6.21); N-9.48(9.58); O-8.25(8.21).

IUPAC Name : 4(2-(2, 6-bis (4-methoxyphenyl)-3, 5-dimethylpiperidine-4-ylidene
amino) 6-phenylpyrimidine-4-yl) phenol.

COMPOUND NO: 5A

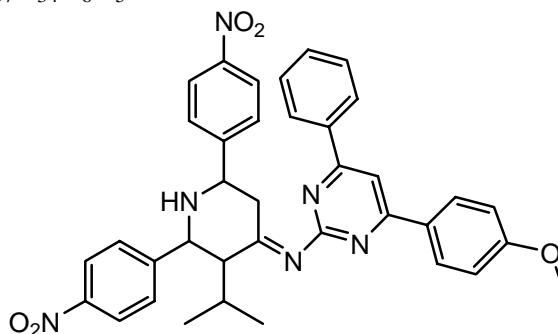
Molecular formula : C₃₇H₃₃ClN₆O₅



Molecular weight	: 677	R_F Value	: 0.96
Melting point	: 64-70 °C	Yield	: 64%.
Solubility	: Soluble in chloroform, DMSO, Ethanol, DMF, Benzene		
Elemental Analysis	: C-65.72(65.63); H- 4.95(4.91); Cl-5.67(5.24); N-12.32(12.41); O-11.43 (11.81).		
IUPAC Name	: 4-(4-chlorophenyl)-N-(3-isopropyl-2,6-bis(4-nitrophenyl)piperidine-4-ylidene)-6-(4-methoxyphenyl)pyrimidine-2-amine		

COMPOUND NO: 6A

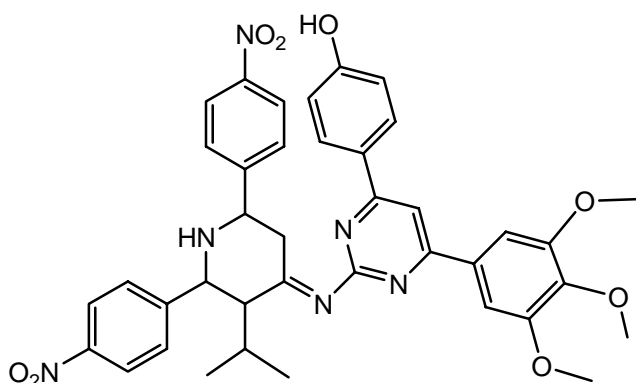
Molecular formula : C₃₇H₃₄N₆O₅



Molecular weight	: 643	R_F Value	: 0.92
Melting point	: 78-86 °C	Yield	: 76%.
Solubility	: Soluble in chloroform, DMSO, Ethanol, DMF, Benzene		
Elemental Analysis	: C-69.56(69.14); H-5.76(5.33); N-13.87(13.08); O-12.43(12.45).		
IUPAC Name	: N-(3-isopropyl-2,6-bis(4-nitrophenyl)piperidine-4-ylidene)-6-(4-methoxyphenyl)-4-ylidene-6-phenylpyrimidine-2-amine		

COMPOUND NO: 7A

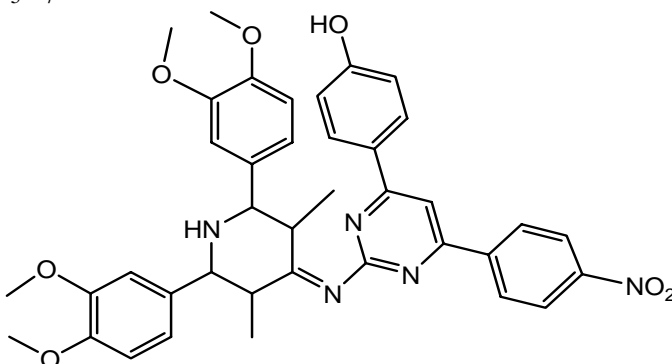
Molecular formula : C₃₉H₃₈N₆O₈



Molecular weight : 719 **R_F Value** : 0.98
Melting point : 96-102 °C **Yield** : 64%.
Solubility : Soluble in chloroform, DMSO, Ethanol, DMF, Benzene
Elemental Analysis : C-65.13(65.17); H-5.43(5.33); N-11.73(11.63); O-17.65(17.81)
IUPAC Name : 4-(2-(3-isopropyl-2,6-bis(4-nitrophenyl)piperidine-4-ylideneamino)-6-(3,4,5-trimethoxyphenyl)pyrimidine-4-yl)phenol.

COMPOUND NO: 8A

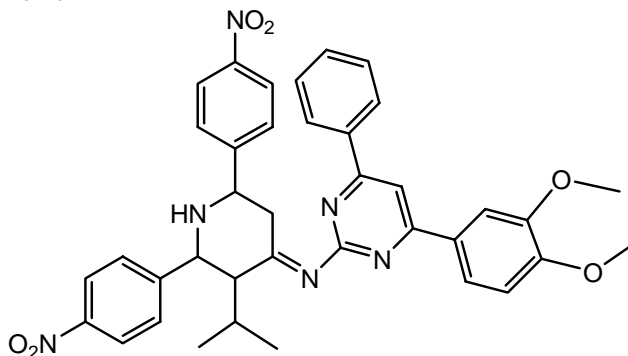
Molecular formula : C₃₉H₃₉N₅O₇



Molecular weight : 690 **R_F Value** : 0.89
Melting point : 152-156 °C **Yield** : 70%.
Solubility : Soluble in chloroform, DMSO, Ethanol, DMF, Benzene
Elemental Analysis : C-67.54(67.91); H-5.75(5.70); N-10.67(10.15); O-16.65(16.24)
IUPAC Name : 4-(2-(2,6-bis(3,4-dimethoxyphenyl)-3,5-dimethylpiperidine-4-ylideneamino)-6-(4-nitrophenyl)pyrimidine-4-yl)phenol

COMPOUND NO: 9A

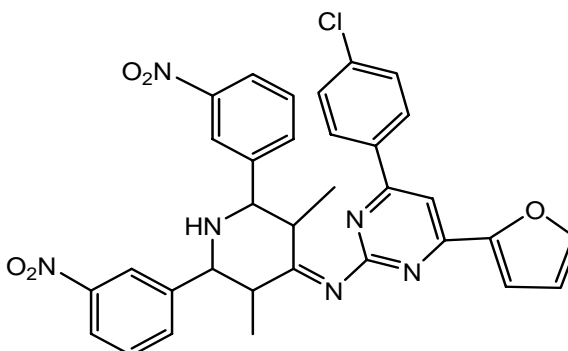
Molecular formula : C₃₈H₃₆N₆O₆



Molecular weight : 673 **R_F Value** : 0.92
Melting point : 92-100 °c **Yield** : 67%.
Solubility : Soluble in chloroform, DMSO, Ethanol, DMF, Benzene
Elemental Analysis : C-67.56(67.84); H-5.56(5.39); N-12.47(12.49); O-14.56(14.27).
IUPAC Name : N-(3-isopropyl-2,6-bis(4-nitrophenyl)piperidine-4-ylidene)-4-(3,4-dimethoxyphenyl)pyrimidine-2-amine.

COMPOUND NO: 10A

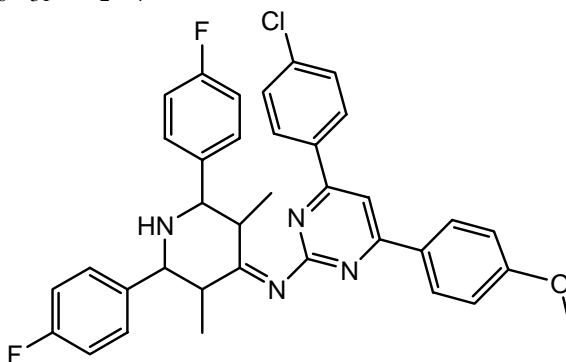
Molecular formula : C₃₃H₂₇ClN₆O₅



Molecular weight : 623 **R_F Value** : 0.96
Melting point : 116-120 °c **Yield** : 62%.
Solubility : Soluble in chloroform, DMSO, Ethanol, DMF, Benzene
Elemental Analysis: C-63.63(63.61); H-4.67(4.37); Cl-5.68(5.69); N-13.56(13.49); O-12.67(12.84).
IUPAC Name : 4-(4-chlorophenyl)-6-(furan-2-yl)-N-(3,5-dimethyl-2,6-bis(3-nitrophenyl)piperidine-4-ylidene)pyrimidine-2-amine

COMPOUND NO: 11A

Molecular formula : C₃₆H₃₁ClF₂N₄O



Molecular weight : 609 **R_F Value** : 0.99

Melting point : 114-118 °C **Yield** : 74%.

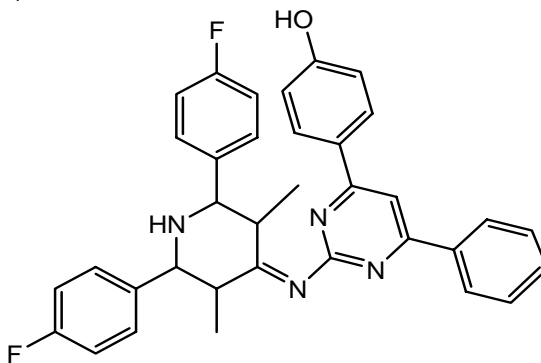
Solubility : Soluble in chloroform, DMSO, Ethanol, DMF, Benzene

Elemental Analysis : C-70.95(70.99); H-5.15(5.13); Cl-5.54(5.82), F-6.28(6.24),
N-9.42(9.20), O-2.64(2.63)

IUPAC Name :N-(2,6-bis(4-fluorophenyl)-3,5-dimethylpiperidin-4-ylidene)-4-(4-chlorophenyl)-6-(4-methoxyphenyl)pyrimidin-2-amine

COMPOUND NO: 12A

Molecular formula : C₃₅H₃₀N₄O



Molecular weight : 561 **R_F Value** : 0.92

Melting point : 72-76 °C **Yield** : 65%.

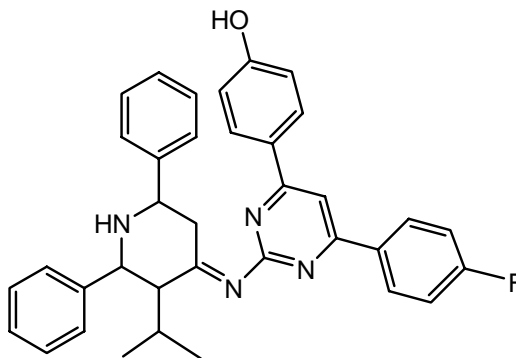
Solubility : Soluble in chloroform, DMSO, Ethanol, DMF, Benzene

Elemental Analysis : C-74.41(74.98); H- 5.75(5.39); N-9.45(9.99); O-2.78(2.85);
F-6.65(6.78)

IUPAC Name : 4 - (2 - (2,6-bis(4-fluorophenyl)-3,5-dimethylpiperidin-4-ylidene amino)-6-phenylpyrimidin -4-yl) phenol

COMPOUND NO: 13A

Molecular formula : C₃₆H₃₃FN₄O



Molecular weight : 557 **R_F Value** : 0.98

Melting point : 90-96 °C **Yield** : 63%.

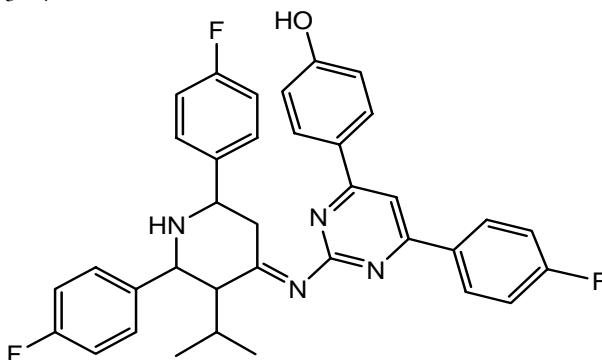
Solubility : Soluble in chloroform, DMSO, Ethanol, DMF, Benzene

Elemental Analysis : C-77.45(77.67); H- 5.96(5.98); N-10.41(10.06); O-2.78(2.87);
F-3.54(3.41)

IUPAC Name : 4-2-(3-isopropyl-2,6-diphenyl piperidine-4-ylideneamino)-6-(4-fluoro phenyl) pyrimidine-4-yl phenol

COMPOUND NO: 14A

Molecular formula : C₃₆H₃₁F₃N₄O



Molecular weight : 593 **R_F Value** : 0.96

Melting point : 70-76 °C **Yield** : 74%.

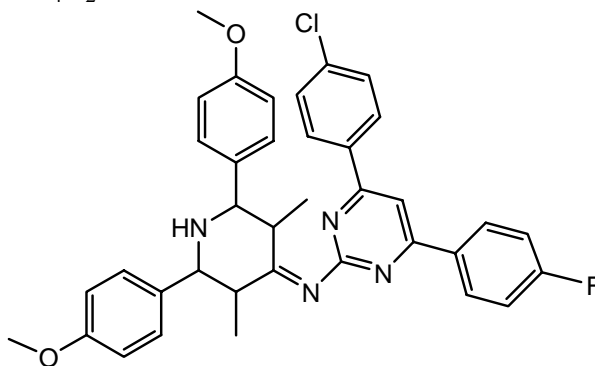
Solubility : Soluble in chloroform, DMSO, Ethanol, DMF, Benzene

Elemental Analysis :C-72.41(72.96); H- 5.75(5.27); N-9.34(9.45); O-2.76(2.70)
F-9.65(9.62)

IUPAC Name : 4-(2-(2,6-bis(4-fluorophenyl)-3-isopropyl piperidin-4-ylideneamino)-6-(4-fluorophenyl) pyrimidin-4-yl) phenol

COMPOUND NO: 15A

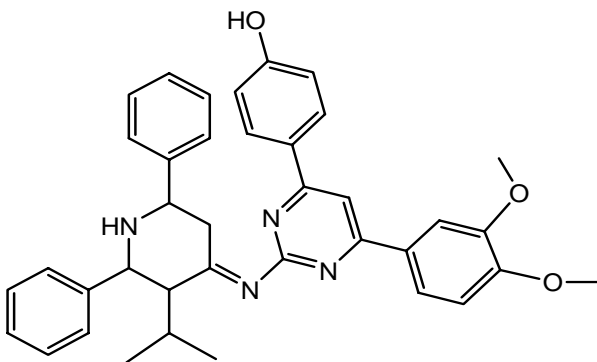
Molecular formula : $C_{37}H_{34}ClFN_4O_2$



Molecular weight : 621 **R_F Value** : 0.95
Melting point : 188-192 °C **Yield** : 56%.
Solubility : Soluble in chloroform, DMSO, Ethanol, DMF, Benzene
Elemental Analysis : C-71.41(71.54); H- 5.75(5.52); N-9.10(9.02); O-5.25(5.15)
Cl-5.69(5.71); F-3.13(3.06).
IUPAC Name : N-(2,6-bis(4-methoxyphenyl)-3,5-dimethylpiperidin-4-ylidene)
4-(4-chlorophenyl)-6-(4-fluorophenyl)pyrimidine-2-amine

COMPOUND NO: 16A

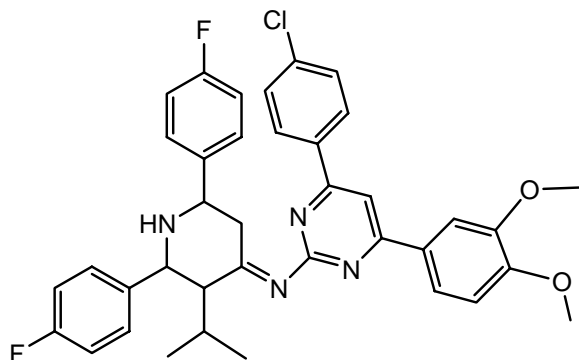
Molecular formula : $C_{38}H_{38}N_4O_3$



Molecular weight : 599 **R_F Value** : 0.96
Melting point : 78-82 °C **Yield** : 67%.
Solubility : Soluble in chloroform, DMSO, Ethanol, DMF, Benzene
Elemental Analysis : C-76.98(76.23); H- 6.54(6.40); N-9.46(9.36); O-8.42(8.02).
IUPAC Name : 4-2-(3-isopropyl-2,6-diphenyl piperidine-4-ylideneamino)-6-(3,4-dimethoxyphenyl)pyrimidine-4-yl phenol

COMPOUND NO: 17A

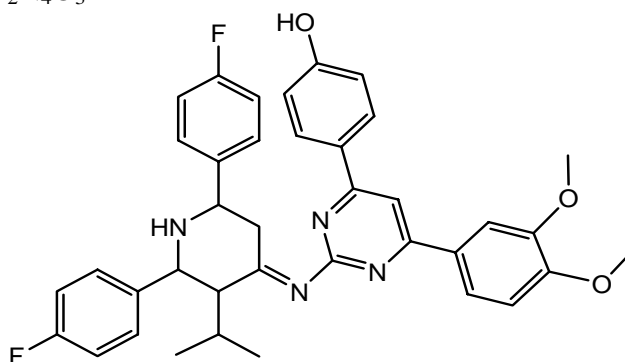
Molecular formula : C₃₈H₃₅ClF₂N₄O₂



Molecular weight : 653 **R_F Value** : 0.99
Melting point : 70-74 °C **Yield** : 64%.
Solubility : Soluble in chloroform, DMSO, Ethanol, DMF, Benzene
Elemental Analysis : C-69.56(69.88); H- 5.75(5.40); N-8.67(8.58); O-4.87(4.90)
F-5.79(5.8); Cl-5.41(5.82)
IUPAC Name : N-(2, 6-bis (4-fluorophenyl)-3-isopropylpiperidine-4-ylidene
-4-(4-chlorophenyl)-6-(3,4-dimethoxyphenyl)pyrimidine 2-amine

COMPOUND NO: 18A

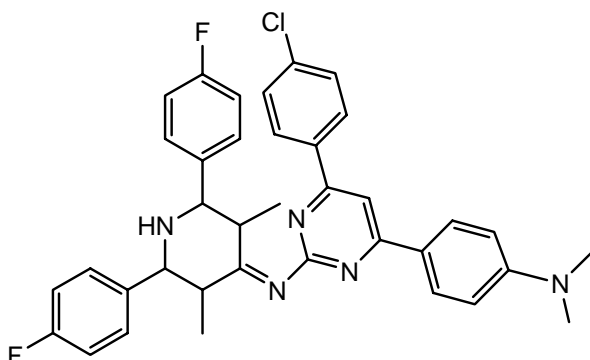
Molecular formula : C₃₈H₃₆F₂N₄O₃



Molecular weight : 635 **R_F Value** : 0.89
Melting point : 94-98 °C **Yield** : 74%.
Solubility : Soluble in chloroform, DMSO, Ethanol, DMF, Benzene
Elemental Analysis : C-71.65(71.91); H- 5.69(5.72); N-8.82(8.83); O-7.45(7.56)
F-5.89(5.99).
IUPAC Name : 4 - (2 - (2, 6-bis (4-flouorophenyl)-3-isopropyl piperidin-4-ylidene
amino)-6-(3, 4-dimethoxyphenyl) pyrimidin -4-yl) phenol

COMPOUND CODE NO: 19A

Molecular formula : C₃₇H₃₄ClF₂N₅

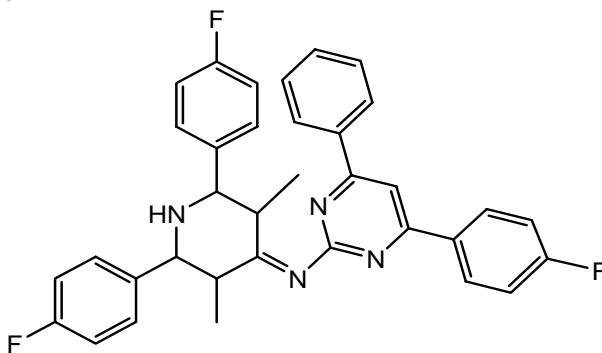


Molecular weight : 622 **R_F Value** : 0.99
Melting point : 110-114 °C **Yield** : 68%.
Solubility : Soluble in chloroform, DMSO, Ethanol, DMF, Benzene
Elemental Analysis : C-71.52(71.43); H- 5.49(5.51); N-11.86(11.26); F-6.43(6.11)
Cl - 5.69(5.70).

IUPAC Name : N-(2, 6-bis (4-fluorophenyl)-3, 5-dimethylpiperidine-4-ylidene)-4-(4-chloro phenyl)-6-(4-(dimethyl amino phenyl) pyrimidine-2-amine

COMPOUND NO: 20A

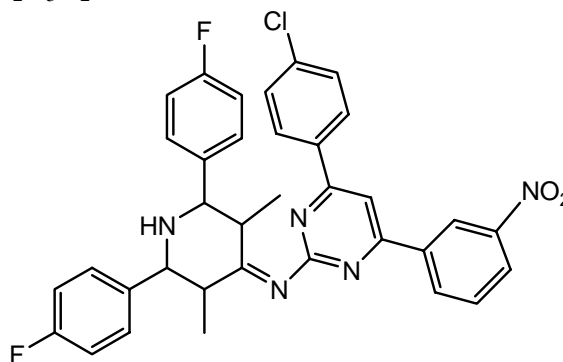
Molecular formula : C₃₅H₂₉F₃N₄



Molecular weight : 563 **R_F Value** : 0.88
Melting point : 144-148 °C **Yield** : 67%.
Solubility : Soluble in chloroform, DMSO, Ethanol, DMF, Benzene
Elemental Analysis : C-72.41(74.72); H- 5.75(5.20); N-9.85(9.96); F -10.43(10.13).
IUPAC Name : N-(2, 6-bis (4-fluorophenyl)-3, 5-dimethylpiperidine-4-ylidene)-4-(4-fluorophenyl)-6 phenyl) pyrimidine-2-amine.

COMPOUND NO: 21A

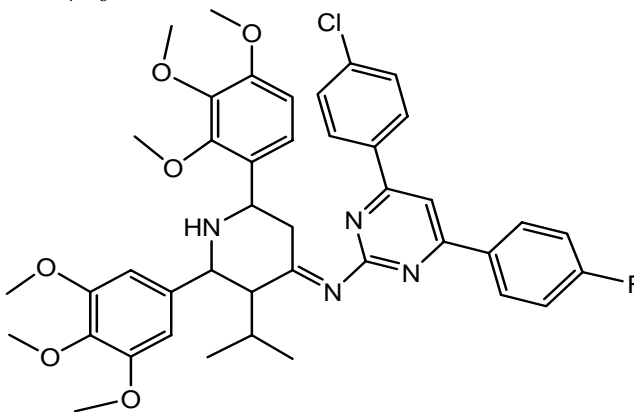
Molecular formula : C₃₅H₂₈ClF₂N₅O₂



Molecular weight : 624 **R_F Value** : 0.92
Melting point : 86-90 °C **Yield** : 64%.
Solubility : Soluble in chloroform, DMSO, Ethanol, DMF, Benzene
Elemental Analysis : C-66.98(67.36); H- 4.87(4.52); N-11.54(11.22); O-5.43(5.13)
F- 6.11(6.09); Cl-5.57(5.68).
IUPAC Name : N-(2, 6-bis (4-fluorophenyl)-3, 5-dimethylpiperidine-4-ylidene)-
4-(4-chlorophenyl)-6-(3-nitrophenyl) pyrimidine-2-amine

COMPOUND NO: 22A

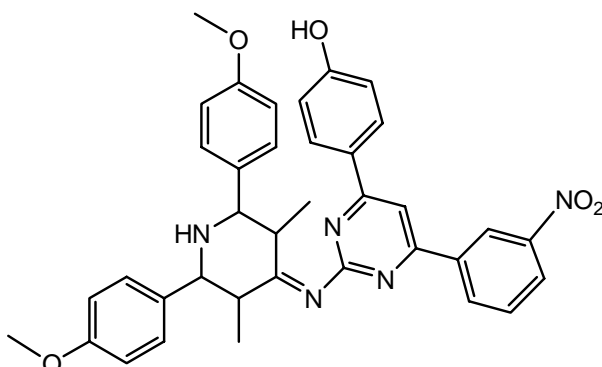
Molecular formula : C₄₂H₄₄ClFN₄O₆



Molecular weight : 755 **R_F Value** : 0.96
Melting point : 80-84 °C **Yield** : 64%.
Solubility : Soluble in chloroform, DMSO, Ethanol, DMF, Benzene
Elemental Analysis : C-65.16(66.79); H- 5.05(5.87); N-7.23(7.42); O-12.62(12.71)
Cl -4.77(4.69); F-2.58(2.52)
IUPAC Name : 4-(4-chlorophenyl)-6-(4-fluorophenyl)-N-(3-isopropyl-6-(2,3,4-
trimethoxyphenyl)-2-(3,4,5-trimethoxyphenyl)piperidine-4-ylidene pyrimidine-2-amine

COMPOUND NO: 23A

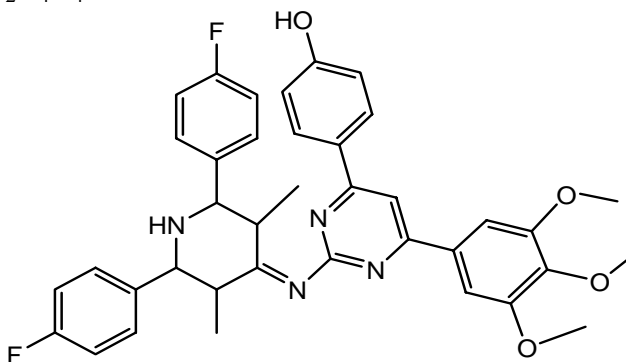
Molecular formula : C₃₇H₃₅N₅O₅



Molecular weight : 630 **R_F Value** : 0.94
Melting point : 152-158 °C **Yield** : 59%.
Solubility : Soluble in chloroform, DMSO, Ethanol, DMF, Benzene
Elemental Analysis : C-70.45(70.57); H- 5.48(5.60); N-11.35(11.12); O-12.68(12.70).
IUPAC Name : 4 – (2 - (2, 6-bis (4-methoxyphenyl)-3,5dimethyl piperidin-4-ylidene amino)-6-(3-nitrophenyl) pyrimidin -4-yl) phenol

COMPOUND NO: 24A

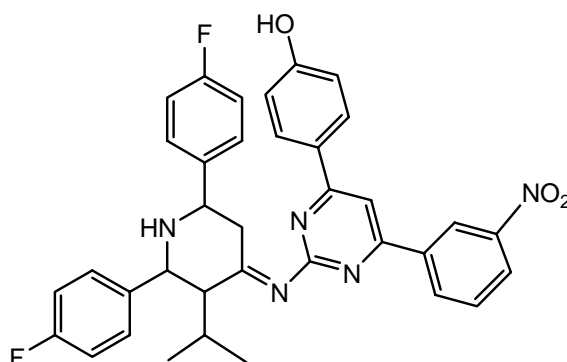
Molecular formula : C₃₈H₃₆F₂N₄O₄



Molecular weight : 651 **R_F Value** : 0.98
Melting point : 140-146 °C **Yield** : 64%.
Solubility : Soluble in chloroform, DMSO, Ethanol, DMF, Benzene
Elemental Analysis : C-70.41(70.14); H- 5.89(5.58); N-8.72(8.61); O-9.65(9.83)
F-5.86 (5.84)
IUPAC Name : 4 – (2 - (2, 6-bis (4-fluorophenyl)-3,5dimethyl piperidin-4-ylidene amino)-6-(3,4,5-trimethoxyphenyl) pyrimidin -4-yl) phenol

COMPOUND NO: 25A

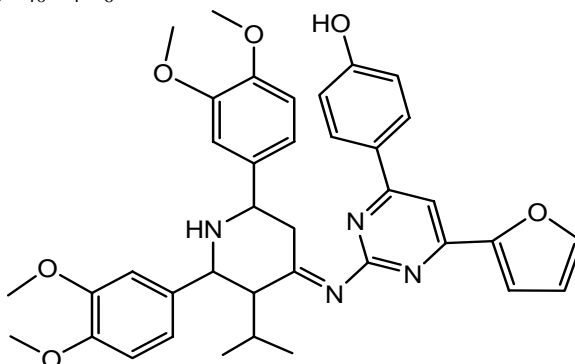
Molecular formula : C₃₆H₃₁F₂N₅O₃



Molecular weight : 620 **R_F Value** : 0.89
Melting point : 72-76 °C **Yield** : 67%.
Solubility : Soluble in chloroform, DMSO, Ethanol, DMF, Benzene
Elemental Analysis : C-69.54(69.78); H- 5.50(5.04); N-11.24(11.30); O-7.43(7.75)
F-6.18 (6.13).
IUPAC Name : 4 – (2 - (2, 6-bis (4-fluorophenyl)-3 isopropyl piperidin-4-ylidene amino)-6-(3-nitrophenyl) pyrimidin -4-yl) phenol

COMPOUND NO: 26A

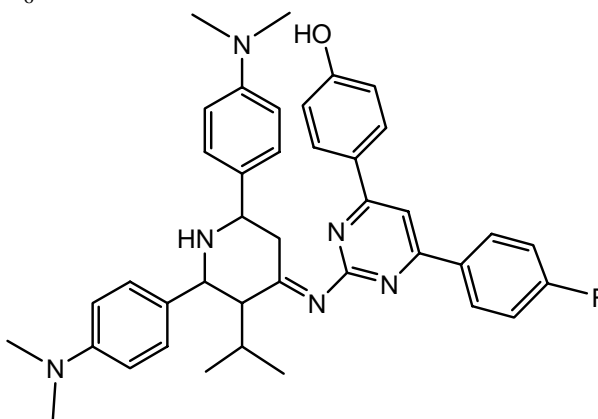
Molecular formula : C₃₈H₄₀N₄O₆



Molecular weight : 649 **R_FValue** : 0.89
Melting point : 116-120 °C **Yield** : 59%.
Solubility : Soluble in chloroform, DMSO, Ethanol, DMF , Benzene
Elemental Analysis : C-70.42(70.35); H- 6.32(6.21); N-8.56(8.64); O-14.87(14.80).
IUPAC Name : 4-2-(3-isopropyl-2, 6-bis (3, 4-dimethoxyphenyl) piperidine-4-ylideneamino)-6-(furan-2-yl) pyrimidine-4-yl) phenol

COMPOUND NO: 27A

Molecular formula : C₄₀H₄₃FN₆O



Molecular weight : 643 **R_F Value** : 0.99

Melting point : 112-116 °c **Yield** : 68%.

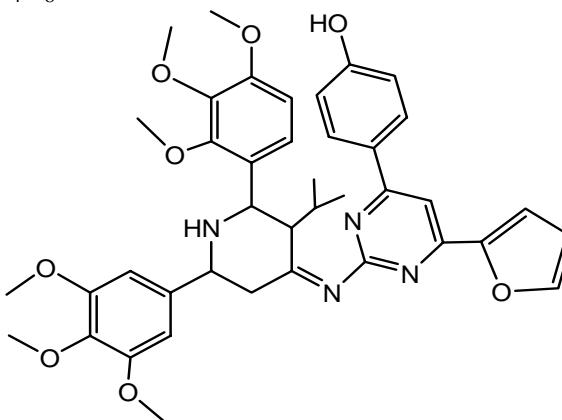
Solubility : Soluble in chloroform, DMSO, Ethanol, DMF, Benzene

Elemental Analysis : C-74.14(74.74); H- 6.66(6.74); F-2.88(2.96); N-13.56(13.07)
O-2.59(2.49)

IUPAC Name : 4 - (2 - (2, 6-bis (4-(dimethyl amino)phenyl)-3- isopropyl piperidin-4-ylidene amino)-6-(4-fluorophenyl) pyrimidin -4-yl) phenol

COMPOUND NO: 28A

Molecular formula : C₄₀H₄₄N₄O₈



Molecular weight : 690 **R_FValue** : 0.96

Melting point : 128-134 °c **Yield** : 54%.

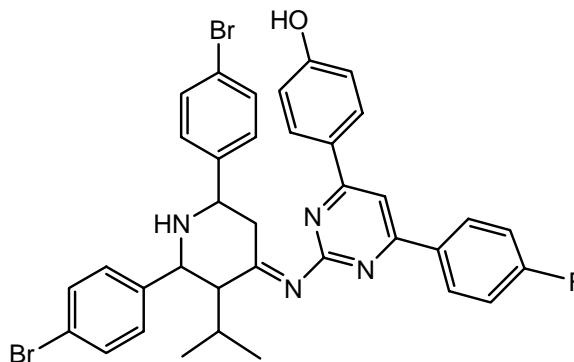
Solubility : Soluble in chloroform, DMSO, Ethanol, DMF, Benzene

Elemental Analysis : C-67.64(67.91); H- 6.45(6.26); N-7.87(7.90); O-18.43(18.06).

IUPAC Name : 4 - (2 - (3-isopropyl-2, 6-bis (3,4,5-trimethoxyphenyl)- piperidin-4-ylidene amino)-6-(furan-2-yl) pyrimidin -4-yl) phenol

COMPOUND NO: 29A

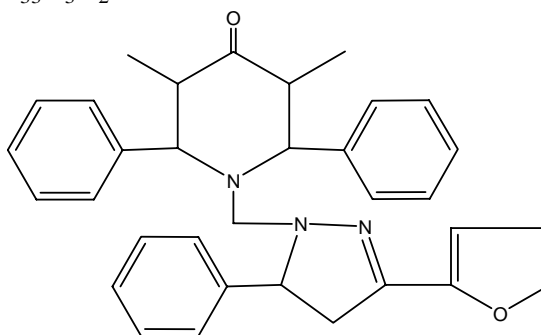
Molecular formula : C₃₆H₃₁Br₂FN₄O



Molecular weight : 714 **R_F Value** : 0.96
Melting point : 118-122 °C **Yield** : 64%.
Solubility : Soluble in chloroform, DMSO, Ethanol, DMF, Benzene
Elemental Analysis : C-60.44(60.52); H- 4.75(4.37); N-22.61(22.37); O-2.23(2.24)
Br-22.42(22.37); F-2.54(2.66).
IUPAC Name : 4-(2-(2, 6-bis (4-bromophenyl)-3- isopropyl piperidin- 4- ylidene amino)-6-(4-fluorophenyl) pyrimidin -4-yl) phenol

COMPOUND CODE NO: P 1

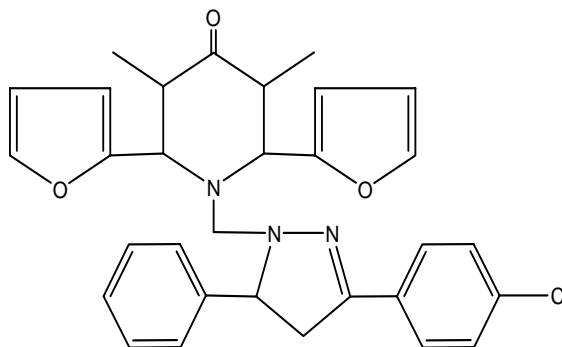
Molecular formula : C₃₃H₃₃N₃O₂



Molecular weight : 503 **R_FValue** : 0.78
Melting point : 280-284 °C **Yield** : 54%.
Solubility : Soluble in chloroform, DMF, Acetone, Glacial acetic acid, Benzene
Elemental Analysis : C-78.16(78.80); H- 6.78(6.60); N-8.56(8.34); O-6.67(6.35).
IUPAC Name : 1-(3-(furan-2-yl)-4, 5-dihydro-5-phenylpyrazol-1-yl)-3,5-dimethyl-2,6-diphenylpiperidin-4-one

COMPOUND NO: P 2

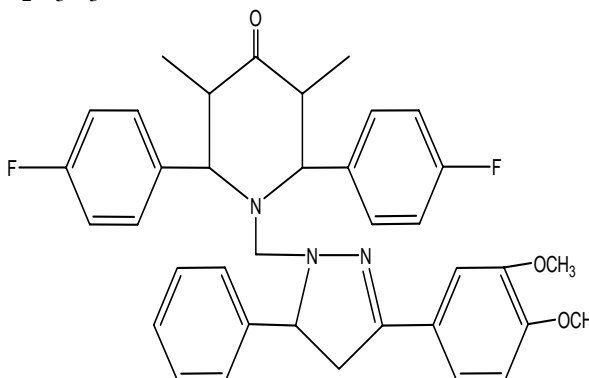
Molecular formula : C₃₁H₃₀ClN₃O₃



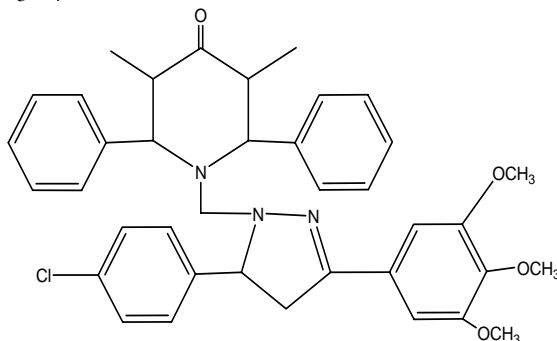
Molecular weight : 528 **R_F Value** : 0.80
Melting point : 248-254 °C **Yield** : 54%.
Solubility : Soluble in chloroform, DMF, Acetone, Glacial acetic acid, Benzene
Elemental Analysis : C-70.62(70.51); H- 5.75(5.73); N-6.54(6.71); O-10.55(10.28).
IUPAC Name : 1-(3-(4-chlorophenyl)-4,5-dihydro-5-phenylpyrazol-1-yl)methyl-2,6-di(furan-2-yl)-3,5-dimethylpiperidin-4-one

COMPOUND NO: P 3

Molecular formula : C₃₇H₃₇F₂N₃O₃



Molecular weight : 609 **R_F Value** : 0.86
Melting point : 256-262 °C **Yield** : 45%.
Solubility : Soluble in chloroform, DMF, Acetone, Glacial acetic acid, Benzene
Elemental Analysis : C-72.41(72.89); H- 6.45(6.12); N-6.81(6.89); O-7.43(7.87)
F-6.56(6.23)
IUPAC Name : 2,6-bis(4-fluorophenyl)-1-(4,5-dihydro-3-(3,4-dimethoxyphenyl)-5-phenylpyrazol-1-yl)methyl-3,5-dimethylpiperidin-4-one

COMPOUND NO: P 4**Molecular formula** : C₃₈H₄₀ClN₃O₄

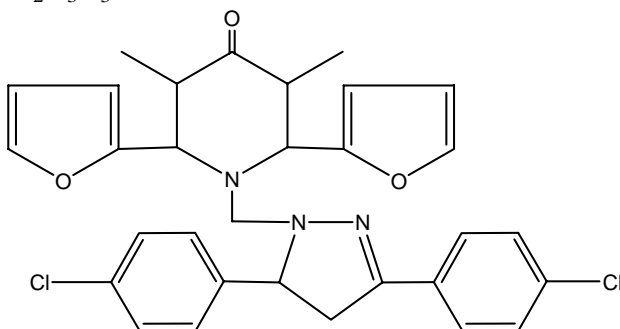
Molecular weight : 638 **R_F Value** : 0.98

Melting point : 248-254 °C **Yield** : 64%.

Solubility : Soluble in chloroform, DMF, Acetone, Glacial acetic acid, Benzene

Elemental Analysis : C-71.45(71.52); H- 6.56(6.32); N-6.44(6.58); O-10.65(10.03)
Cl- 5.67(5.56).

IUPAC Name : 1- (5-(4-chloro phenyl)-4, 5-dihydro-3- (3,4,5-trimethoxyphenyl) pyrazol-1-yl) methyl)-3,5-dimethyl-2,6-diphenylpiperidin-4-one

COMPOUND NO: P 5**Molecular formula** : C₃₁H₂₉Cl₂N₃O₃

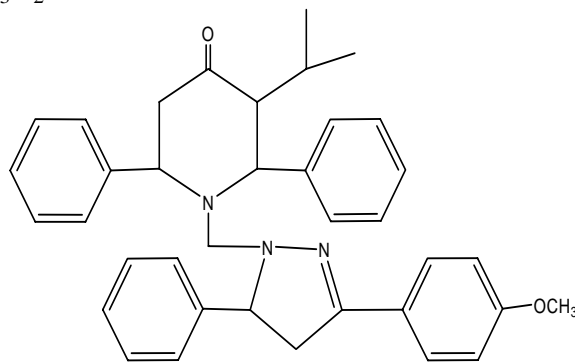
Molecular weight : 562 **R_F Value** : 0.88

Melting point : 278-284 °C **Yield** : 53%.

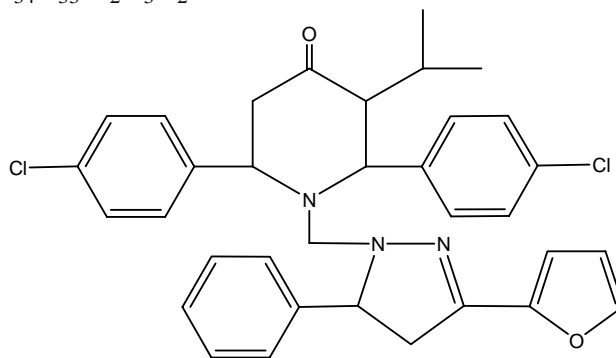
Solubility : Soluble in chloroform, DMF, Acetone, Glacial acetic acid, Benzene

Elemental Analysis : C-72.41(66.19); H- 5.75(5.20); N-11.41(7.47); O-10.43(10.03)
Cl-12.78 (12.61)

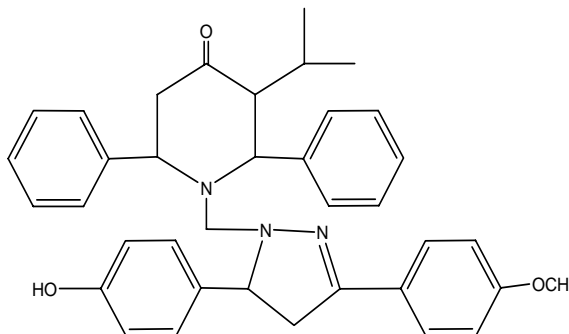
IUPAC Name : 1- (3,5-bis(4-chloro phenyl)-4, 5-dihydropyrazol-1-yl) methyl)-2,6-di(furan-2-yl)-3,5-dimethylphenylpiperidin-4-one

COMPOUND NO: P 6**Molecular formula** : C₃₇H₃₉N₃O₂

Molecular weight : 557 **R_F Value** : 0.86
Melting point : 262-268 °C **Yield** : 52%.
Solubility : Soluble in chloroform, DMF, Acetone, Glacial acetic acid, Benzene
Elemental Analysis : C-79.54(79.68); H- 7.24(7.05); N-7.78(7.53); O-5.65(5.74).
IUPAC Name : 1-(4,5-dihydro-3-(4-methoxy phenyl)-5-phenylpyrazol-1-yl) methyl)-3-isopropyl-2,6-diphenylpiperidin-4-one

COMPOUND NO: P 7**Molecular formula** : C₃₄H₃₃Cl₂N₃O₂

Molecular weight : 587 **R_F Value** : 0.95
Melting point : 245-251 °C **Yield** : 54%.
Solubility : Soluble in chloroform, DMF, Acetone, Glacial acetic acid, Benzene
Elemental Analysis : C-69.38(69.62); H- 5.45(5.67); N-7.14(7.16); O-5.34(5.46)
 Cl-12.23(12.09)
IUPAC Name : 2, 6-bis (4-chlorophenyl)-1-((3-(furan-2-yl)-4,5-di hydro phenyl-pyrazol-1-yl) methyl)-3-isopropylpiperidin-4-one

COMPOUND NO: P 8**Molecular formula** : C₃₇H₃₉N₃O₃

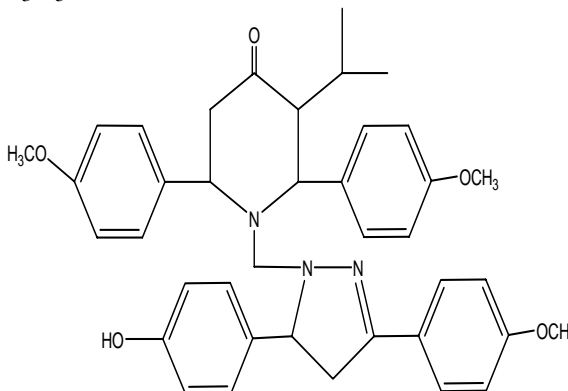
Molecular weight : 574 **R_F Value** : 0.86

Melting point : 234-240 °C **Yield** : 56%.

Solubility : Soluble in chloroform, DMF, Acetone, Glacial acetic acid, Benzene

Elemental Analysis : C-77.54(77.46); H- 6.76(6.85); N-7.45(7.32); O-8.56(8.37).

IUPAC Name : 1-(4,5-dihydro-5-(4-hydroxyphenyl)-3-(4-methoxyphenyl)pyrazol-1-yl)methyl-3-isopropyl-2,6-diphenylpiperidin-4-one

COMPOUND NO: P 9**Molecular formula** : C₃₉H₄₃N₃O₅

Molecular weight : 633 **R_F Value** : 0.81

Melting point : 263-269 °C **Yield** : 65%.

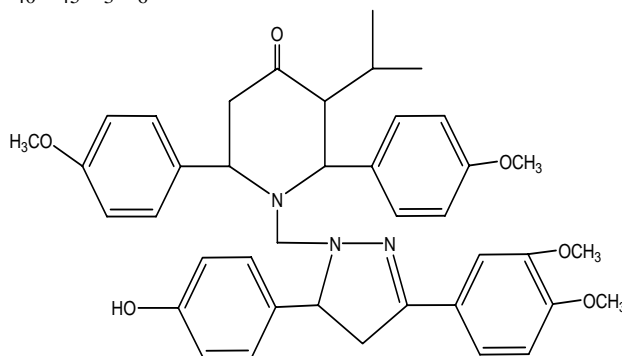
Solubility : Soluble in chloroform, DMF, Acetone, Glacial acetic acid, Benzene

Elemental Analysis : C-73.27(73.91); H- 6.79(6.84); N-6.75(6.63); O-12.56(12.62).

IUPAC Name : 1-(4,5-dihydro-5-(4-hydroxyphenyl)-3-(4-methoxyphenyl)pyrazol-1-yl)methyl-3-isopropyl-2,6-bis(4-methoxyphenyl)piperidin-4-one

COMPOUND NO: P 10

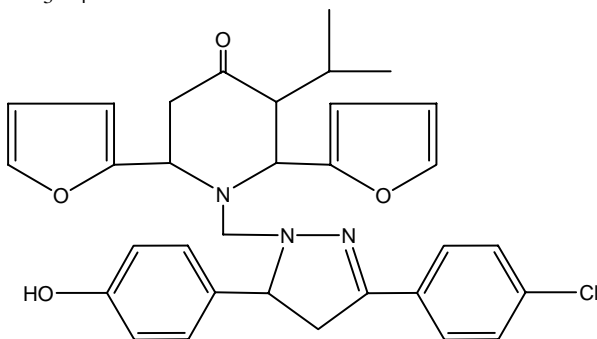
Molecular formula : C₄₀H₄₅N₃O₆



Molecular weight : 663 **R_F Value** : 0.72
Melting point : 234-240 °C **Yield** : 56%.
Solubility : Soluble in chloroform, DMF, Acetone, Glacial acetic acid, Benzene
Elemental Analysis : C-72.78(72.38); H- 6.65(6.83); N-6.75(6.33); O-14.45(14.46).
IUPAC Name : 1-(4,5-dihydro-5-(4-hydroxyphenyl)-3-(3,4-dimethoxyphenyl)pyrazol-1-yl)methyl-3-isopropyl-2,6-bis(4-methoxyphenyl)piperidin-4-one

COMPOUND NO: P 11

Molecular formula : C₃₂H₃₂ClN₃O₄



Molecular weight : 558 **R_F Value** : 0.95
Melting point : 245-261 °C **Yield** : 58%.
Solubility : Soluble in chloroform, DMF, Acetone, Glacial acetic acid, Benzene
Elemental Analysis : C-68.79(68.87); H- 5.75(5.78); N-7.55(7.53); O-11.45(11.47)
Cl-6.43(6.35)
IUPAC Name : 1-(3-(4-(4-chloro phenyl)-4,5-dihydro-5-(4-hydroxy phenyl)pyrazol-1-yl)methyl)-2,6-di(furan-2-yl)-3, isopropylpiperidin-4-one

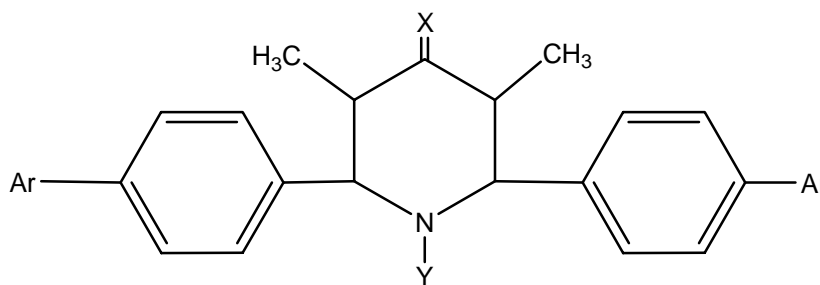
11.2 SPECTRAL STUDIES-DISCUSSION

A number of 2, 6-diaryl piperidine-4-ones have been synthesized by the Mannich condensation of various aliphatic ketones, substituted aldehydes and ammonium acetate in 1:2:1 ratio using ethanol as solvent. The synthesis of several simple piperidine-4-ones by the condensation of aliphatic ketones with aromatic aldehydes and ammonia has been reported by Baliah, et al ¹⁹⁶.

A two step synthetic route furnished various substituted Aminopyrimidines and Pyrazolines. The ketone of piperidine-4-ones react with primary amino group of the Aminopyrimidines to form Schiff bases(1A-29A). The N-H group of the piperidones undergo condensation with the 2-pyrazoline to give the Mannich bases(P1-P11).

All the synthesized 4-piperidones were characterized through Infra red, Nuclear Magnetic Resonance and Mass spectral Data.

INFRARED SPECTROSCOPY



X= 2-Aminopyrimidines, C=O

Y= 2-pyrazolines, H

The preferred conformation of all the piperidone precursors with alkyl groups at C3 and C5 has been shown to be chair and the phenyl and the alkyl groups occupying equatorial positions ^{371,372}. The crystal structure of 2,6-diphenyl-4-piperidone was solved by Singh et al. ³⁷³. The two phenyl groups attached to the piperidone ring are found to be oriented cis to each other with respect to the piperidone ring.

The IR spectral data of the synthesized compounds is presented in Table 11.1.

Two reviews on the Infrared spectra of heterocyclics by Katritzky et al. ^{374, 375} was the main source of information and guidance in the identification and analysis of the spectra.

Heterocyclic compounds containing nitrogen may exhibit three kinds of group frequencies, those including C-H or N-H vibrations, those involving the motion of the ring and those due to the group frequencies of the substituents on the ring³⁷⁶.

The carbonyl stretching band usually observed at 1720 cm⁻¹ region³⁷⁷ in piperidine-4-ones is not found in the IR spectra of the Aminopyrimidine derivatives of piperidones (1A-29A) confirming the formation of the Schiff bases. C=N and C-N bands³⁷⁸ which appear in the appropriate regions further confirms the presence of Schiff bases.

Absence of strong N-H stretching in the region of 3300cm⁻¹ proves the formation of the N-Mannich bases in the 2-pyrazoline substituted piperidones (P1-P11).C=N and C-N stretching vibrations of pyrazolines were found in the expected regions. The strong band at 1700cm⁻¹ region is due to the carbonyl stretching³⁷⁷.All these vibrations prove the formation of N-Mannich bases.

In compounds 1A-29A, the strong absorption bands observed at 3300 cm⁻¹ range is assigned to the N-H stretching²¹³ mode of the secondary amines. The medium intensity band at 3100 cm⁻¹ region in all these compounds is the characteristic band of C-H absorption in aliphatic saturated³⁷⁹ heterocyclic group.

Bands at 1602cm⁻¹ and 1500 cm⁻¹ are assigned to stretching mode of C=C and C-C of the phenyl rings respectively. A group of four bands appearing between 1650 cm⁻¹ and 1450 cm⁻¹ is characteristic of the skeletal stretching modes of the unsaturated C-C bonds. According to Bellany³⁸⁰ out of these four bands,the bands near1600 cm⁻¹ and 1500 cm⁻¹ are highly characteristic of the phenyl ring itself and is taken in conjunction with the C-H stretching band at 3033 cm⁻¹ range.

The C-H vibrations of the CH₃ group are classified into two asymmetric and one symmetric stretching vibration by Katritzky et al³⁸¹.The asymmetric vibrations occur in the region of 2900 cm⁻¹ and the symmetric stretching vibrations occur in 2800 cm⁻¹ region.

The N-H wagging appears as a band at 920 cm⁻¹NH o/p bending and i/p bending are found in the region of 1140 cm⁻¹ and 1250 cm⁻¹ respectively.

Ring out of plane bending absorption occurs at 720 cm⁻¹ region. The ring breathing (cyclic) appears as a strong band at 1020 cm⁻¹.

Presence of pyrimidine skeletal in the Aminopyrimidine derivatives of piperidin-4-ones (1A-29A) was shown by the vibrations in the range of 1500-1600 cm^{-1} .

Ring oxygen stretching vibration³⁸² was observed in the region of 1313-1240 cm^{-1} . C-Cl, C-Br and C-F stretching modes appeared in the range of 550-800 cm^{-1} and 1220 cm^{-1} respectively³⁸³.

The CH_2 asymmetric and symmetric stretching vibrations appear at 2980 cm^{-1} and 2830 cm^{-1} respectively. The i/p deformation of the C-H in methylene group leads to a band at 1420 cm^{-1} region. The CH_2 rocking modes appear in the region of 950 cm^{-1} . The methylene deformation occurs at 1415 cm^{-1} region.

¹H NUCLEAR MAGNETIC RESONANCE

Sivasubramania et al.³⁸⁴ studied the PMR spectra of cis-2, 6-diphenyl piperidin-4-ones and their derivatives. They furnished the following assignment for 3-methyl-2, 6-diphenyl -4-piperidones.

C2, C6 H	C3, C5 H	N-H	Aromatic protons
δ 3.96	δ 2.5	δ 1.95	δ 7.25

Pandiarajan et al.³⁸⁵ investigated the PMR spectra for about fourteen 2, 6-diaryl piperidine-4-ones with and without alkyl groups at N, C-3 and C-5. They suggest that these compounds exist predominantly in chair form with aryl and alkyl substituents in the equatorial positions. The values assigned by him were found to be from δ 3.63-3.72 for 2a, δ 2.69-2.74 for 5a δ 2.61-2.83 for 5eq and δ 3.63-4.1 for 6 axial protons. The aromatic protons were reported to be in the range of δ 7.29-7.39.

The PMR spectral data of the piperidine-4-ones synthesized in the present work are furnished in Table 11.2

The PMR spectrum of the synthesized compounds with CH_3 at 3,5 positions of the piperidine-4-ones has A_3BX and A_3BX spin systems for heterocyclic ring protons³⁸³. The CH_3 , H-3, H-2 and CH_3 , H-5, H-6 of the A_3BX spin systems afford each one doublet in the region of δ 0.68 and δ 0.70 for methyl protons and two doublets for H-3, H-2 around δ 2.82 and δ 3.60 and two doublets around δ 2.84, δ 3.69 for H-5 and H-6 respectively^{385, 378}. The aromatic protons of the two phenyl rings provide a multiplet

around δ 6.9- δ 7.9. The NH proton was assigned δ value in the region of 2.07. H-5 of the Aminopyrimidine appears in the range of δ 7.52³⁸³.

The ¹H NMR spectrum of compounds with isopropyl group at R has ABX and AX spin systems³⁸⁶ for heterocyclic ring protons. The H-2, H-3a and H-3eq of the ABX spin systems offered three doublets of doublets about δ 3.85, 2.20 and δ 2.90 respectively. The protons H-5 and H-6 of the AX spin system gave doublets at 2.10 and 3.90ppm indicating that these two protons are diaxially oriented. The isopropyl CH proton signal was found at 2.20ppm and the methyl protons were observed at δ 0.8 and δ 1.00. The methoxy protons were found in the region of δ 3.73-3.78. The N-H proton shows the signal at 2.00ppm. The H-5 of the Aminopyrimidine appears at δ 7.57³⁸⁷.

The PMR spectrum of P5 has A₃BX and A₃BX spin systems for heterocyclic ring protons. The CH₃, H-3, H-2 and CH₃, H-5, H-6 of the A₃BX spin system offered each one doublet in the region of 1.16 ppm for methyl protons and the two doublets for H-3, H-2 at δ 3.12, 4.35 and two doublets at δ 3.14 and 4.33 for H-5 and H-6 respectively³⁷⁸. The aromatic protons gave multiplets in the region 7.06-8.0 ppm. The furyl protons were found to appear at 6.06, 6.24 and 7.28 ppm. The H-4ax, H-5ax, and H-5 eq. protons of pyrazoline appeared at δ 3.90, 4.30, and δ 4.60 respectively²³². The strong deshielding of the C-5 protons compared with the C-4 protons of the pyrazoline ring may be due to the structure of the compound. The CH₂ protons due to the N-CH₂ appeared at δ 3.62³⁸⁸. The disappearance of N-H peak at 2.1 ppm confirms the formation of the Mannich bases.

Due to the substitution in the aromatic ketone in the 4th position of the piperidone there is interaction between the substituted >C=N and the equatorial hydrogen at C5 (α) of the piperidone. So the equatorial α (C-H) bond gets polarized. As a result of this polarization the equatorial hydrogen acquires a slight +ve charge and the carbon acquires a slight -ve charge. This is again confirmed by the greater shielding of the α -carbon(C-5) in ¹³C NMR spectrum. The -ve charge on the α - carbon (C-5) is transmitted to α -axial hydrogen (H-5)ax and β -carbon(C6) to some extent and so the axial hydrogen at C-5 is shielded (up field resonance) where as equatorial hydrogen at C-5 is deshielded (downfield resonance)³⁷⁸.

¹³C NUCLEAR MAGNETIC RESONANCE

The signals in the ¹³C NMR spectrum were assigned based on their positions, integrals, multiplicities and on comparison with the corresponding signals observed in the closely related 3,5 dimethyl 2,6 diphenyl piperidin-4-ones³⁸⁵. Manimekalai et al. synthesized and carried out the spectral studies of some heteroaryl piperidine-4-ones and their derivatives. They furnished the following assignment for 3,5 dimethyl 2,6 difuryl piperidin-4-ones.

C2, C6	C3, C5	C4	alkyl carbon
59.54, 58.39	39.05, 35.50	162.55	20.32, 16.25

The ¹³C Spectra of compound 5A and P1 are presented along with the ¹H NMR spectra. The ¹³C NMR spectral data of the piperidin-4-ones synthesized in the present work are tabulated in table 11.3

The ¹³C NMR of the piperidine derivatives with substituted Aminopyrimidines gave the δ_c at 55.29 to 61.70 for C-2 and δ_c 52.05-61.82 for C-6. The signals for C-3 and C-5 were found to be between 38.6-50.92 and 29.64-35.50 ppm respectively. The C=N gave the δ_c value at 154.72-162.91. The aromatic carbons gave multiplets in the range of δ_c 127.8-150.6. The alkyl carbons appeared in the range of 21.0-21.6. The O-Me carbons gave the signals at 54.7-56.2 ppm. The other carbons also appeared in the appropriate regions.

The conversion of the C=O group into C=N shields all heterocyclic ring carbons except C-2. The >C=N group in the compounds is less polar compared to >C=O group. It has been previously reported that³⁸⁹ decrease in electro negativity is expected to shield α carbon but deshield β and γ carbons. Thus, the shielding magnitude observed on C-3 and C-5 carbons (α) and deshielding observed on C-2 and C-6 carbons (β) in 1A-29A are in accordance with the lower electro negativity of >C=N group compared to >C=O group. The shielding magnitude observed on C-5 due to C=N linkage is considerably greater than those on C-3. This can be explained on the following basis. There is severe interaction between C=N and equatorial α (C-H) bond. Due to these interactions the equatorial bond is polarized. As a result of this polarization, the equatorial hydrogen

acquires a slight positive charge and the 5 α -carbon acquires a slight negative charge. Because of the negative charge on the α -carbons they are shielded to a greater extent than β -carbons. In isopropyl substituted compounds the C-5 has a equatorial hydrogen and so the α -carbon acquires a negative charge which leads to the shielding of C-5 than C-3. The methyl carbons at C-3 and C-5 resonate considerably at downfield (20.0-21.6) compared to other alkyl group due to conversion of ketone to $>C=N$. This causes the deshielding of the methyl carbons. All these observations support the boat conformation of the 3, 5 dimethyl 2, 6 diaryl N-substituted piperidin-4-ones.

The other pyrimidinyl carbons C-2, C-4 and C-6²⁴⁰ give the signals at the range of δ_c 160 due to $C=N$ and C-5 CH resonates at up field in the range of δ_c 114.1-113.43 because of the decreased electro negativity (shielding) of $C=C$ when compared to $C=N$.

In pyrazoline substituted piperidin-4-ones there is not much shielding of the heterocyclic ring carbons because there is no substitution in the ketone group. Thus C-2, C-3, C-4, C-5 and C-6 resonate at the expected frequencies. The alkyl groups were found at δ_c 8.1-10.5. The isopropyl carbon gave signals at 20.1-22.1 ppm. O-methoxyl carbons were found to be at 55.9-56.4 ppm. The furyl³⁸³ carbons C-2 and C-5 appeared in δ_c 141.5-45.2 region, the C-3, C-4 gave the peaks at 109.2-110.1 ppm. The C-3 and C-4 of pyrazoline showed two signals at δ_c 38.2-49.2 ppm. The signal of the C-5 carbon (azomethine linkage) appeared in 151.5-155.6 ppm. Aromatic carbons showed signals in the expected region.

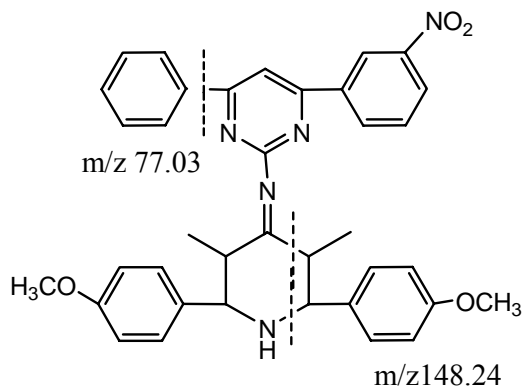
MASS SPECTRUM

Quin et al³¹⁰ studied the mass spectra of 1-methyl -4- phosphorinone and 1-methyl-4-piperidone and correlated each other. They found that the fragments resulted from the cleavage of piperidin-4-ones resembled that of N-methyl piperidine³⁹¹ with initial cleavage occurring at 2, 3-bond and neither the cleavage of N-Me bond nor the 1, 2 cleavage to lose ethylene

For the 2,6-diaryl substituted-4-piperidones, the fragmentation patterns are found to resemble the N-methyl -4-piperidone to some extent starting with cleavage at 2,3 bond.

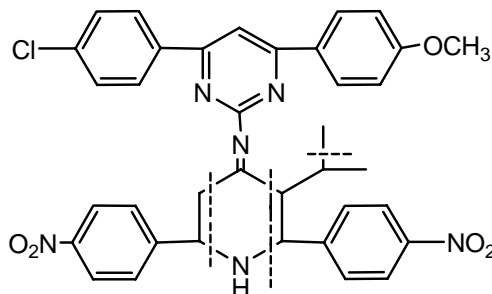
The compound, N-(2, 6-bis (4-methoxyphenyl)-3, 5-dimethylpiperidine 4-ylidene)-4-(3-nitrophenyl)-6-phenylpyrimidine -2-amine (1A) follows the given

fragmentation pattern. A number of fragments have been obtained in the mass spectrum of compound 1A. The molecular ion peak was observed as at m/z 614 (80%). A weak (M+1) peak was noted at m/z 615 (14%). The base peak at m/z 77 (100%) is due to the formation of phenyl radical.



A medium peak at m/z 148 is ascribed to the formation of methyl styrene.

The compound 4-(4-chlorophenyl)-N-(3-isopropyl-2,6-bis(4-nitrophenyl)piperidine-4-ylidene)-6-(4-methoxyphenyl)pyrimidine-2-amine (5A) gives the molecular ion peak at m/z 677 (55%). The (M+1) peak was observed at m/z 678 (17%). The loss of methyl radical from the isopropyl group explains the intense peak at m/z 354 (89%).



The formation of substituted styrene molecule explains the base peak at 177 (100%). The weak fragment appearing at m/z 149 (10%) explains the formation of styrene with substitution in the aromatic ring.

The compounds containing 2-pyrazoline as substituent also showed similar fragmentation pattern giving the M ion peak and M+1 peak. The base peak was observed either at styrene or phenyl radical peak. All the synthesized compounds provided the expected fragments in the Mass spectrum.

COSY NMR SPECTRUM

For compounds 5A {(4-(4-chlorophenyl)-N-(3isoprpyl-2,6-bis(4-nitrophenyl) piperidine -4-ylidene)-6-(4-methoxyphenyl) pyrimidine -2-amine} and P1 {(1-(3-(furan-2-yl)-4, 5-dihydro-5-phenylpyrazol-1-yl)-3,5-dimethyl-2,6-diphenylpiperidin-4-one} ¹H-cosy NMR spectrum was recorded to confirm the assignments. The Cosy spectrum of 5A reveals that the downfield doublet at 3.29ppm which is unambiguously assigned to H-5 shows cross peak with the doublet at 3.42ppm. Therefore, the doublet at 3.42 ppm is obviously due to H-6 only. The up field doublet at 2.55ppm H-3 shows cross peak with the doublet at 3.30ppm and this confirms the assignment of the signal at 3.30ppm for H-2.

The Cosy spectrum of P1 reveals that the downfield doublet at 2.88 ppm which is unambiguously assigned to H-5 shows cross peak with the doublet at 4.12 ppm. Therefore, the doublet at 4.12 ppm is obviously due to H-6 only. The up field doublet at 2.87 ppm H-3 shows cross peak with the doublet at 3.80 ppm and this confirms the assignment of the signal at 3.80 ppm for H-2.

TABLE 11.1 IR SPECTRAL DATA OF THE AMINOPYRIMIDINE SUBSTITUTED PIPERIDINE-4-ONES

VIBRATIONAL ASSIGNMENT	1A	2A	3A	4A	5A	6A	7A	8A
N-H stretching	3387.52(s)	3311(m)	3312.97(w)	3313.41(s)	3328.59(m)	3318.2(s)	3332.97(w)	3328.59(w)
C-H Str Hetero	2970.9(m)	3197.34(w)	3168.41(w)	3172.51(w)	3107.04(m)	3108.3(w)	3107.71(w)	3066.40(w)
C-H Str Phenyl	2930.97(m)	3007.79(m)	2967.91(m)	2983.93(w)	3068.19(w)	3007.79(w)	3008.02(w)	3008.02(w)
CH3 asymmetric	2970.9(m) 2836.14(m)	2935.19(m) 2963.81(m)	2927.8(m) 2862.74(w)	2972.47(w) 2935.3(w)	2997.99(w) 2849.87(m)	2987.55(w) 2852.56(w)	2947.85(w) 2973.84(w)	2935.94(w) 2867.87(w)
CH3 symmetric	2880.24(w)	2880.8(w)	2836.0(m)	2869.48(w)	2880.90(w)	2878.60(w)	2837.79(w)	2836.15(w)
C=C Str phenyl	1680.94(m)	1638.0(w)	1613.79(m)	1606.97(s)	1656.58(s)	1657.74(m)	1605.9(s)	1651.48(m)
C-C Str Phenyl	1519.25(s)	1515.27(s)	1518.44(s)	1518.19(s)	1511.31(s)	1512.48(m)	1460.86(m)	1519.98(s)
Sym.CH3Deformation	1348.5(s)	1366.55(w)	1383.39(m)	1372.49(m)	1381.8(w)	1345.22(m)	1346.61(m)	1377.56(m)
N-H i/p bending	1304.07(m)	1322.39(m)	1303.39(s)	1303.79(w)	1304.82(m)	1323.6(m)	1327.17(m)	1347.6(m)
C-H i/p bending	1270.82(m)	1262.4(m)	1255.19(m)	1285.6(m)	1259.45(m)	1263.3(m)	1285.91(s)	1265.64(m)
NH o/p bending	1134.57(m)	1144.02(m)	1134.65(s)	1149.64(w)	1171.46(m)	1168.93(w)	1152.45(m)	1143.84(m)
CH o/p Bending	743.92(m)	764.56(m)	754.98(m)	765.18(m)	677.73(m)	739.21(m)	677.30(m)	770.47(m)
Ring o/p bending	710.79(m)	725.82(w)	724.51(w)	738.45(w)	739.41(s)	722.00(m)	739.19(w)	727.88(w)
Ring Breathing	1034.75(s)	1023.66(s)	1034.19(s)	1035.36(s)	1035.36(s)	1017.68(m)	1033.93(s)	1024.61(s)
N-H wagging	922.03(w)	943.35(m)	911.33(w)	911.33(m)	959.24(w)	984.68(m)	976.55(m)	949.89(m)
C=N Stretching	1613.6(m)	1594.93(m)	1604.07(m)	1590.07(m)	1540.95(m)	1576.80(w)	1550.28(w)	1606.92(w)
C-N Stretching	1183.2(m)	1160.09(m)	1183.29(m)	1177.41(m)	1197.18(m)	1197.26(m)	1198.35(w)	1166.05(m)
Pyrimidine skeletal	1568.12(m)	1581.35(w)	1586.87(m)	1566.84(m)	1594.25(m)	1576.80(w)	1584.52(m)	1593.84(w)

TABLE 11.1 IR SPECTRAL DATA OF THE AMINOPYRIMIDINE SUBSTITUTED PIPERIDINE-4-ONES –CONTINUED

VIBRATIONAL ASSIGNMENT	9A	10A	11A	12A	13A	14A	15A	16A
N-H stretching	3314.25(s)	3308.72(s)	3314.32(s)	3314.33(m)	3307.18(s)	3309.63(s)	3313.02(w)	3307.00(w)
C-H Str Hetero	3082.62(w)	3098.52(w)	3117.22(w)	2975.47(m)	3085.03(w)	3051.04(w)	3084.53(w)	3080.51(w)
C-H Str Phenyl	2965.00(w)	2992.68(w)	2977.37(w)	2936.54(w)	3027.76(w)	2999.4(w)	2997.07(w)	3010.21(w)
CH3 asymmetric	2942.95(w) 2875.28(w)	2961.01(w) 2935.3(w)	2936.39(w) 2883.22(w)	2883.98(w) 2840.83(w)	2967.38(w) 2930.93(w)	2932.33(w) 2905.93(w)	2971.08(w) 2931.74(w)	2969.1(w) 2936.75(w)
CH3 symmetric	2809.10(w)	2838.03(w)	2818.7(w)	2820.71(w)	2866.54(w)	2873.08(w)	2870.95(w)	2838.42(w)
C=C Str phenyl	1595.20(m)	1648.24(m)	1605.42(m)	1593.92(s)	1602.05(s)	1605.07(s)	1614.67(s)	1602.37(w)
C-C Str Phenyl	1509.12(s)	1508.14(s)	1509.16(s)	1509.77(s)	1508.66(s)	1509.89(s)	1518.84(s)	1510.28(s)
Sym.CH3Deformation	1378.22(m)	1379.91(m)	1379.72(s)	1379.31(m)	1377.8(s)	1380.4(m)	1371.87(m)	1354.42(w)
N-H i/p bending	1318.56(w)	1301.42(m)	1339.58(s)	1305.35(w)	1301.84(s)	1309.11(m)	1304.29(s)	1336.47(w)
C-H i/p bending	1257.42(w)	1260.09(m)	1285.64(s)	1258.93(w)	1281.59(w)	1282.41(w)	1271.12(w)	1265.05(m)
NH o/p bending	1142.57(m)	1130.6(w)	1143.49(w)	1144.32(w)	1129.16(m)	1125.84(m)	1134.12(m)	1139.65(w)
CH o/p Bending	758.72(m)	751.62(m)	766.45(s)	767.76(m)	766.86(s)	762.62(m)	755.27(m)	758.75(m)
Ring o/p bending	725.72(w)	714.74(m)	734.58(w)	704.17(m)	714.73(m)	736.17(m)	727.84(w)	722.04(w)
Ring Breathing	1012.7(s)	1011.28(s)	1043.78(s)	1010.1(s)	1028.85(s)	1015.81(s)	1034.89(s)	1025.22(s)
N-H wagging	925.64(w)	924.67(m)	924.49(w)	924.99(w)	932.56(w)	934.32(w)	910.12(w)	916.81(w)
C=N Stretching	1548.25(m)	1595.99(s)	1591.77(w)	1657.28(m)	1541.59(w)	1541.72(w)	1588.21(s)	1588.02(w)
C-N Stretching	1158.72(m)	1166.06(w)	1156.98(w)	1171.6(w)	1129.16(m)	1158.78(m)	1183.71(s)	1158.84(w)
Pyrimidine skeletal	1570.25(w)	1553.41(w)	1566.74(m)	1567.64(w)	1558.89(w)	1560.14(w)	1559.84(w)	1558.15(w)

TABLE 11.1 IR SPECTRAL DATA OF THE AMINOPYRIMIDINE SUBSTITUTED PIPERIDINE-4-ONES -CONTINUED

VIBRATIONAL ASSIGNMENT	17A	18A	19A	20A	21A	22A	23A	24A
N-H stretching	3309.56(s)	3309.3(s)	3315.26(s)	3314.3(m)	3314.53(m)	3309.68(m)	3300.00(s)	3314..7(m)
C-H Str Hetero	3071.16(w)	3002.8(w)	3080.51(w)	3168.52(w)	3172.51(w)	3058.27(w)	2996.92(w)	3124.8(w)
C-H Str Phenyl	3051.42(w)	2965.96(w)	2969.00(w)	3059.19(m)	3062.41(w)	3015.37(w)	2982.9(w)	3075.6(w)
CH3 asymmetric	2966.6(w) 2932.46(w)	2934.48(w) 2906.75(w)	2933.94(w) 2876.48(w)	2973.57(w) 2935.01(w)	2972.32(w) 2935.96(w)	2975.26(w) 2943.82(w)	2971.25(w) 2931.89(w)	2969.01(m) 2934.42(m)
CH3 symmetric	2873.72(w)	2824.43(w)	2808.08(w)	2875.09(w)	2876.05(w)	2895.19(w)	2870.92(w)	2881.4(m)
C=C Str phenyl	1605.14(m)	1602.18(s)	1592.18(m)	1597.86(w)	1603.87(w)	1604.07(w)	1614.68(s)	1605.41(s)
C-C Str Phenyl	1510.7(s)	1509.52(s)	1509.09(s)	1509.13(s)	1509.04(s)	1508.46(s)	1454.03(s)	1491.65(m)
Sym.CH3Deformation	1380.46(m)	1380.48(m)	1378.22(m)	1377.89(m)	1378.03(m)	1394.7(m)	1372.22(m)	1378.3(m)
N-H i/p bending	1310.09(m)	1308.93(w)	1308.76(w)	1339.92(m)	1347.43(w)	1330.82(m)	1304.47(m)	1327.61(m)
C-H i/p bending	1267.7(w)	1265.23(m)	1267.39(w)	1296.12(w)	1283.99(w)	1270.3(m)	1271.26(m)	1285.83(s)
NH o/p bending	1125.88(m)	1126.58(w)	1144.76(m)	1146.11(w)	1144.56(w)	1127.4(s)	1134.47(w)	1153.77(m)
CH o/p Bending	762.52(m)	761.57(m)	760.64(m)	762.92(m)	760.75(m)	760.99(w)	755.12(m)	767.39(m)
Ring o/p bending	736.05(m)	736.14(w)	727.68(w)	735.18(s)	726.40(w)	727.35(m)	724.36(m)	722.41(w)
Ring Breathing	1016.14(s)	1025.18(s)	1013.8(s)	1014.78(s)	1014.38(s)	1012.44(m)	1034.93(s)	1014.04(m)
N-H wagging	934.19(w)	932.71(w)	924.67(w)	922.50(m)	922.85(m)	932.83(w)	910.22(w)	924.96(m)
C=N Stretching	1659.26(m)	1638.09(w)	1575.45(w)	1578.85(w)	1558.98(w)	1558.98(w)	1518.90(s)	1509.03(m)
C-N Stretching	1158.65(m)	1158.25(m)	1157.64(w)	1158.57(w)	1160.18(w)	1158.14(w)	1150.51(w)	1129.53(w)
Pyrimidine skeletal	1593.8(w)	1551.19(w)	1528.45(w)	1558.95(w)	1593.62(w)	1589.05(w)	1587.98(s)	1569.81(w)

TABLE 11.1 IR SPECTRAL DATA OF THE AMINOPYRIMIDINE SUBSTITUTED PIPERIDINE-4-ONES –CONTINUED

VIBRATIONAL ASSIGNMENT	25A	26A	27A	28 A	29A
N-H stretching	3309.73(s)	3307.07(w)	3332.27(w)	3309.35(s)	3314.26(s)
C-H Str Hetero	3046.81(w)	3080.71(w)	3107.76(w)	3002.78(w)	3083.51(w)
C-H Str Phenyl	3006.85(w)	3010.25(w)	3008.32(w)	2965.46(w)	2969.07(w)
CH3 asymmetric	2966.49(m) 2932.54(m)	2969.18(w) 2936.85(w)	2947.65(w) 2973.88(w)	2934.72(w) 2906.35(w)	2937.94(w) 2876.67(w)
CH3 symmetric	2875.07(w)	2838.44(w)	2837.49(w)	2824.24(w)	2818.08(w)
C=C Str phenyl	1605.55(s)	1602.36(w)	1605.19(s)	1602.68(s)	1599.18(m)
C-C Str Phenyl	1470.75(w)	1510.20(s)	1460.46(m)	1509.67(s)	1509.79(s)
Sym.CH3Deformation	1380.37(m)	1354.56(w)	1346.51(m)	1380.88(m)	1376.22(m)
N-H i/p bending	1309.18(m)	1336.76(w)	1327.37(m)	1308.87(w)	1328.76(w)
C-H i/p bending	1283.95(w)	1265.65(m)	1285.96(s)	1265.43(m)	1265.39(w)
NH o/p bending	1125.85(s)	1139.94(w)	1152.15(m)	1126.57(w)	1134.76(m)
CH o/p Bending	762.46(m)	758.76(m)	677.20(m)	761.53(m)	764.64(m)
Ring o/p bending	720.01(w)	722.34(w)	739.89(w)	736.76(w)	737.68(w)
Ring Breathing	1015.65(s)	1025.28(s)	1033.90(s)	1025.12(s)	1015.8(s)
N-H wagging	933.70(w)	916.88(w)	976.35(m)	932.77(w)	934.67(w)
C=N Stretching	1509.7(s)	1588.82(w)	1550.24(w)	1638.59(w)	1585.45(w)
C-N Stretching	1158.43(m)	1158.86(w)	1198.55(w)	1158.22(m)	1177.64(w)
Pyrimidine skeletal	1568.02(w)	1558.65(w)	1584.56(m)	1551.79(w)	1558.45(w)

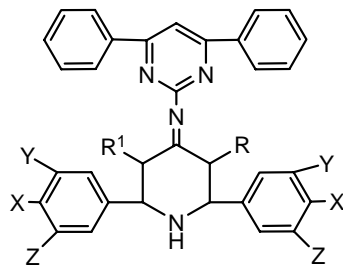
TABLE 11.1 IR SPECTRAL DATA OF THE 2-PYRAZOLINE SUBSTITUTED PIPERIDIN-4-ONES

VIBRATIONAL ASSIGNMENT	P1	P2	P3	P4	P5	P6	P7	P8
C=O stretching	1704.08(vs)	1704.16(vs)	1704.79(s)	1701.08(vs)	1702.42(s)	1700.77(vs)	1701.79(s)	1708.08(vs)
C-H Str Hetero	3063.86(w)	3063.65(w)	3080.16(w)	3086.21(w)	3084.15(w)	3058.27(w)	3084.16(w)	3085.21(w)
C-H Str Phenyl	3031.93(w)	3030.95(m)	3060.86(w)	3064.17(w)	3064.51(w)	3029.62(w)	3067.86(w)	3062.17(w)
CH3 asymmetric	2977.1(w) 2935.48(w)	2977.13(m) 2935.28(m)	2977.02(w) 2936.18(w)	3037.51(w) 2965.43(w)	2993.81(w) 2938.99(w)	3015.37(w) 2978.2(m)	2976.02(w) 2963.18(w)	3027.51(w) 2965.33(w)
CH3 symmetric	2886.53(w)	2886.53(m)	2883.93(w)	2967.53(w)	2949.45(w)	2935.3(w)	2893.93(w)	2967.33(w)
CH2 asymmetric	2872.27(w)	2814.98(w)	2832.66(w)	2934.95(w)	2830.67(w)	2903.72(w)	2830.66(w)	2930.95(w)
CH2 symmetric	2829.37(w)	2824.18(w)	2671.66(w)	2844.45(w)	2875.73(w)	2809.25(w)	2871.40(w)	2824.45(w)
CH2 Stretching	2786.47(w)	2791.43(w)	2674.40(w)	2775.21(w)	2746.49(w)	2795.83(w)	2774.40(w)	2795.21(w)
CH2 Rocking	985.65(m)	985.52(m)	984.16(m)	986.85(w)	989.52(m)	984.83(s)	983.16(m)	976.85(w)
CH2 deformation	1436.72(w)	1436.36(w)	1419.66(m)	1436.11(w)	1431.26(w)	1418.91(m)	1429.66(m)	1437.11(w)
C=C Str phenyl	1600.68(w)	1599.04(w)	1604.31(m)	1610.34(m)	1609.09(s)	1599.74(vs)	1609.31(m)	1609.34(m)
C-C Str Phenyl	1449.07(s)	1456.06(s)	1455.33(m)	1458.65(w)	1454.29(s)	1458.28(m)	1458.33(m)	1456.65(w)
Sym.CH3Deformation	1377.76(m)	1377.65(m)	1378.17(m)	1375.64(m)	1370.28(m)	1380.22(m)	1376.17(m)	1377.64(m)
C-H i/p bending	1269.19(m)	1269.01(m)	1263.56(w)	1270.64(w)	1268.78(s)	1263.62(s)	1273.56(w)	1280.64(w)
CH o/p Bending	751.03(m)	751.05(m)	761.88(m)	765.82(s)	756.30(w)	779.04(m)	765.88(m)	766.82(s)
Ring o/p bending	733.67(m)	733.55(w)	693.00(m)	713.69(m)	713.54 (w)	721.83(m)	698.00(m)	714.69(m)
Ring Breathing	1028.45(m)	1028.39(s)	1025.47(m)	1028.02(m)	1030.66(s)	1015.86(s)	1028.47(m)	1029.02(m)
C=N Stretching	1555.24(w)	1506.09(w)	1509.12(s)	1502.91(w)	1502.64(s)	1511.5(s)	1509.12(s)	1512.91(w)
C-N Stretching	1206.51(w)	1181.47(w)	1156.61(w)	1152.7(m)	1169.86(s)	1171.68(s)	1156.81(w)	1172.7(m)

IR SPECTRAL DATA OF THE 2-PYRAZOLINE SUBSTITUTED PIPERIDIN-4-ONES-CONTINUED

VIBRATIONAL ASSIGNMENT	P9	P10	P11
C=O stretching	1704.28(s)	1704.42(s)	1701.16(vs)
C-H Str Hetero	3063.75(w)	3082.15(w)	3067.65(w)
C-H Str Phenyl	3030.82(w)	3064.21(w)	3060.95(m)
CH3 asymmetric	2961.01(w) 2935.3(w)	2963.81(w) 2938.09(w)	2997.13(m) 2965.28(m)
CH3 symmetric	2835.95(w)	2909.45(w)	2896.53(m)
CH2 asymmetric	2872.98(w)	2835.67(w)	2824.98(w)
CH2 symmetric	2824.14(w)	2815.73(w)	2854.18(w)
CH2 Stretching	2745.54(w)	2756.49(w)	2741.43(w)
CH2 Rocking	974.24(w)	969.52(m)	983.52(m)
CH2 deformation	1440.43(w)	1441.26(w)	1437.36(w)
C=C Str phenyl	1608.48(s)	1608.09(s)	1594.04(w)
C-C Str Phenyl	1458.81(m)	1453.29(s)	1452.06(s)
Sym.CH3 Deformation	1360.05(m)	1360.28(m)	1370.65(m)
C-H i/p bending	1248.56(s)	1248.78(s)	1268.01(m)
CH o/p Bending	752.40(w)	750.30(w)	759.05(m)
Ring o/p bending	703.02(w)	730.54(w)	723.55(w)
Ring Breathing	1031.91(s)	1031.66(s)	1028.29(s)
C=N Stretching	1512.02(m)	1512.64(s)	1506.29(w)
C-N Stretching	1169.8(s)	1169.8(s)	1181.27(w)

TABLE-11.2 - ¹H NMR DATA OF AMINOPYRIMIDINE SUBSTITUTED PIPERIDINE- 4-ONES



COMPOUNDS	X	Y	Z	R	R ¹	H 2a	H 3a	H		H 6a	Aromatic protons	NH	Other Protons
								5ax	5eq				
1A	OCH ₃ 3.70	H	H	CH ₃ 0.68	CH ₃ 0.70	3.69	2.84	2.82	-	3.60	6.9-7.9	2.07	7.52 (H-5)
2A	OCH ₃ 3.89	OCH ₃ 3.87	H	CH ₃ 0.80	CH ₃ 0.82	3.97	2.74	2.72	-	3.55	7.10-7.49	1.73	7.48 (H-5)
3A	OCH ₃ 3.71	H	H	CH ₃ 0.8	CH ₃ 1.20	3.85	2.55	2.55	-	3.84	7.00-7.52	2.16	7.57 (H-5)
4A	OCH ₃ 3.60	H	H	CH ₃ 0.80	CH ₃ 1.2	3.85	2.90	2.50	-	3.81	7.20-7.50	2.12	4.25 (Ar-OH) 7.63 (H-5)
5A	NO ₂	H	H	2.16 1.08 1.12	-	3.30	2.55	2.20	3.29	3.42	6.90-7.9	1.62	3.64 (OCH ₃) 7.60 (H-5)
6A	NO ₂	H	H	2.17 1.81 1.00	-	3.62	2.82	2.20	3.30	3.49	6.9-7.62	1.66	3.74 (OCH ₃) 7.60 (H-5)
7A	NO ₂	H	H	2.17 1.10 1.23	-	3.92	2.55	2.96	3.21	3.90	6.85-7.22	1.61	3.83-3.88 (OCH ₃) 3.95 (Ar-OH) 7.20 (H-5)
8A	OCH ₃ 3.86	OCH ₃ 3.86	H	CH ₃ 0.83	CH ₃ 0.85	3.49	2.88	2.52	-	3.56	6.81-7.26	2.17	3.90(Ar-OH) 7.60(H-5)

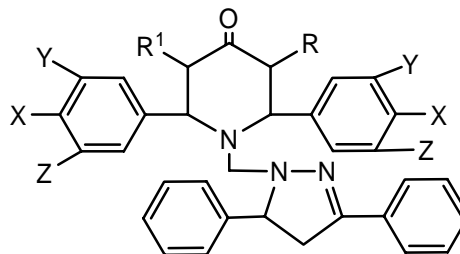
TABLE-11.2 - ¹H NMR DATA OF AMINOPYRIMIDINE SUBSTITUTED PIPERIDINE- 4-ONES-CONT'D

COMPOUNDS	X	Y	Z	R	R ¹	H 2a	H 3a	H		H 6a	Aromatic protons	NH	Other Protons
								5ax	5eq				
9A	NO ₂	H	H		-	3.85	2.49	2.79	3.37	3.83	7.02-7.81	2.10	3.80-3.90(OCH ₃) 7.63 (H-5)
10A	H	NO ₂	H	CH ₃ 0.83	CH ₃ 1.6	3.64	2.87	2.86	-	3.63	6.7 1-7.50	2.07	7.50(H-5), Furan - 7.24(H5), 6.66(H4), 6.65(H3).
11A	F	H	H	CH ₃ 0.67	CH ₃ 0.67	3.57	2.49	2.49	-	3.54	6.88 -7.90	2.48	7.48 (H-5) 3.80(O Me)
12A	F	H	H	CH ₃ 0.67	CH ₃ 0.67	3.81	2.49	2.49	-	3.56	7.00 -7.86	2.48	7.60 (H-5) 4.51-(Ar-OH)
13A	H	H	H		-	3.98	2.49	2.45	3.25	3.78	7.24 -7.53	2.48	4.02 (Ar-OH) 7.53 (H-5)
14A	F	H	H		-	3.98	2.84	2.49	3.60	3.78	7.12 -7.57	2.44	4.02 (Ar-OH) 7.57 (H-5)
15A	OCH ₃ 3.76	H	H	CH ₃ 0.80	CH ₃ 0.80	3.81	3.3	2.48	-	3.65	6.97 -7.94	2.49	7.57 (H-5)
16A	H	H	H		-	3.66	2.84	2.49	2.95	3.61	7.00 -7.83	2.29	3.70-3.72 (OCH ₃) 4.01 (Ar-OH) 7.58 (H-5)
17A	F	H	H		-	3.85	2.50	2.49	2.95	3.55	7.01 -7.82	2.30	3.62-3.65(O Me) 7.61(H-5)
18A	F	H	H		-	3.85	2.50	2.49	-	3.67	6.90 -7.82	2.30	3.78-3.80(OCH ₃) 4.40 (Ar-OH) 7.60 (H-5)
19A	F	H	H	CH ₃ 0.8	CH ₃ 1.00	3.95	2.30	2.30	-	3.90	6.92 -7.33	2.00	7.72 (H-5),2.85, 2.85 (Ar-N Me) ₂

TABLE-11.2 - ¹H NMR DATA OF AMINOPYRIMIDINE SUBSTITUTED PIPERIDINE- 4-ONES-CONT'D

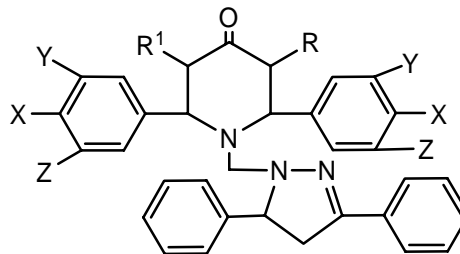
COMPOUNDS	X	Y	Z	R	R ¹	H 2a	H 3a	H		H 6a	Aromatic protons	NH	Other Protons
								5ax	5eq				
20A	F	H	H	CH ₃	CH ₃	3.80	2.54	2.52	-	3.85	6.92-7.48	2.10	7.70 (H-5)
21A	F	H	H	CH ₃ 0.67	CH ₃ 0.67	3.90	2.52	2.50	-	3.92	6.9-7.33	2.18	7.36(H-5)
22A	OCH ₃ 3.73	OCH ₃ 3.75	OCH ₃ 3.78	2.20 0.8 1.00	-	3.90	2.10	2.20	3.12	3.85	6.08 -7.33	2.00	7.57 (H-5)
23A	OCH ₃ 3.75	H	H	CH ₃ 0.80	CH ₃ 0.80	3.89	2.50	2.48	-	3.90	6.72-7.31	2.20	7.62 (H-5)
24A	F	H	H	CH ₃ 0.68	CH ₃ 0.70	3.92	2.30	2.30	-	3.78	6.92 -6.79	2.00	7.65 (H-5), 4.92 (Ar-OH),3.72, 3.76,3.78.(O Me)
25A	F	H	H	2.12 0.80 1.00	-	3.90	2.52	2.50	3.18	3.69	6.92 -7.31	2.26	7 .62 (H-5), 4 .92 (Ar-OH)
26A	OCH ₃ 3.71	OCH ₃ 3.71	H	2.20 1.00 1.20	-	3.92	2.10	2.20	3.14	3.84	6.61 -7.31	2.10	7.60 (H-5), 4.48 (Ar-OH), Furan – 7.4 (H5), .6.3 (H4), 6.3 (H3).
27A	N(Me ₂) 2.85	H	H	2.26 0.80 1.00	-	3.84	2.64	2.50	3.33	3.80	6.54 -7.31	2.20	7 .70 (H-5), 4 .50 (Ar-OH)
28A	OCH ₃ 3.72	OCH ₃ 3.73	OCH ₃ 3.74	2.12 1.00 1.20	-	3.80	2.40	2.54	3.39	3.82	6.08-7.31	2.10	7 .62 (H-5), 4 .48 (Ar-OH) Furan – 7.4 (H5), 6.3 (H4), 6.3 (H3).
29A	Br	H	H	2.20 0.80 1.00	-	3.90	2.52	2.22	3.21	3.62	7.01-7.38	2.20	7 .68 (H-5), 4 .80 (Ar-OH)

TABLE-11.2 ¹H NMR DATA OF 2-PYRAZOLINE SUBSTITUTED PIPERIDINE- 4-ONES



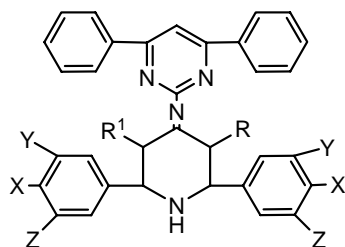
COMPOUNDS	X	Y	Z	R	R ¹	H 2a	H 3a	H		H 6a	CH ₂	Aromatic protons	Other Protons
								5ax	5eq				
P1	H	H	H	CH ₃ 1.16	CH ₃ 1.16	3.80	2.87	2.88	-	4.12	3.64	7.08 -7.21	Pyrazoline (1.9,1.6)-H-4, (3.9)-H-5 Furan – 7.4 (H5), 6.3 (H4), 6.3 (H3).
P2	Furyl			CH ₃ 1.14	CH ₃ 1.14	3.92	2.70	2.86	-	4.37	3.62	7.0 8 -7.61	Pyrazoline (1.91,1.65)-H-4, (3.90)-H-5 Furan – 7.42 (H5), 6.3 (H4), 6.31 (H3).
P3	F	H	H	CH ₃ 1.18	CH ₃ 1.16	4.20	2.94	2.96	-	4.31	3.81	6.92 -7.21	Pyrazoline (1.95,1.63)-H-4, (3.89)-H-5. (3.73,3.73)-OMe
P4	H	H	H	CH ₃ 1.10	CH ₃ 1.09	3.75	2.76	2.82	-	4.14	3.60	7.08 -7.22	Pyrazoline (1.90,1.62)-H-4, (3.92)-H-5,(3.73)- OMe
P5	Furyl			CH ₃ 0.99	CH ₃ 0.98	3.95	2.72	2.68	-	4.07	3.59	7.06 -7.60	Pyrazoline (1.94,1.65)-H-4, (3.90)-H-5 Furan –6.03 (H4), 6.30 (H3), 7.28(H5),
P6	H	H	H	1.85 0.90 1.05	-	4.12	2.92	2.98	2.88	4.12	3.70	6.80 -7.52	Pyrazoline (1.91,1.63)-H-4, (3.96)-H-5 (3.76)-OMe

TABLE-11.2 -¹H NMR DATA OF 2-PYRAZOLINE SUBSTITUTED PIPERIDINE- 4-ONES-CONT'D



COMPOUNDS	X	Y	Z	R	R ¹	H 2a	H 3a	H		H 6a	CH ₂	Aromatic protons	Other Protons
								5ax	5eq				
P7	Cl	H	H		-	3.98	2.85	2.90	2.84	3.99	3.62	7.07-7.21	Pyrazoline (1.92,1.68)-H-4, (3.97)-H-5 Furan – 7.14 (H5), 6.23 (H4), 6.03 (H3).
P8	H	H	H		-	3.92	2.76	2.82	2.87	4.17	3.68	6.8-7.5	Pyrazoline (1.95,1.63)-H-4, (3.89)-H-5. (3.62,3.65)-OMe (5.23) Ar-OH
P9	OMe 3.72	H	H		-	3.86	2.92	2.88	2.95	3.96	3.60	6.72 -7.5	Pyrazoline (1.91,1.63)-H-4, (3.92)-H-5 (3.65)-OMe, (5.03) Ar-OH
P10	OMe 3.73	H	H		-	3.85	2.85	2.69	2.79	4.10	3.71	6.72 -7.10	Pyrazoline (1.97,1.68)-H-4, (3.88)-H-5 (3.67)-OMe, (5.08) Ar-OH
P11	Furyl				-	3.95	2.94	2.98	2.84	4.02	3.54	6.68 -7.60	Pyrazoline (1.95,1.64-H-4, (3.99)-H-5. (3.62,3.62)-OMe (5.25) Ar-OH

TABLE- 11.3 ¹³C NMR DATA OF AMINOPYRIDINE SUBSTITUTED PIPERIDINE-4-ONES



COMPOUNDS	X	Y	Z	R	R ¹	C2	C3	C4	C5	C6	Aromatic carbons	Other carbons
1A	OCH ₃ 54.9	H	H	CH ₃ 212	CH ₃ 21.0	58.82	41.65	159.45	29.78	56.82	127.0 - 139.7	162.60(C2),160.50(C4), 112.80(C5),160.80(C6)
2A	OCH ₃ 54.7	OCH ₃ 54.9	H	CH ₃ 20.8	CH ₃ 21.0	61.11	47.67	157.68	29.65	60.78	126.6 - 139.5	164.2(C2),162.10(C4), 109.80(C5),162.50(C6)
3A	OCH ₃ 55.0	H	H	CH ₃ 212	CH ₃ 21.1	59.71	49.86	162.55	30.32	59.68	126.8 - 139.9	161.50(C2),158.80(C4) 111.20(C5),158.20(C6)
4A	OCH ₃ 54.6	H	H	CH ₃ 21	CH ₃ 20.8	60.62	50.92	154.72	32.15	61.11	126.3 - 139.5	163.80(C2),162.40(C4), 108.20(C5),162.90(C6)
5A	NO ₂	H	H	26.9/21.1 21.1	-	55.29	38.60	169.81	30.65	54.84	126.4 - 145.35	161.71(C2),158.26(C4), 113.43(C5),158.16(C6), 55.01 (OMe)
6A	NO ₂	H	H	27.9/19.97 18.05	-	56.64	47.50	159.45	30.87	53.15	126.4 - 145.35	162.71(C2),158.43(C4), 113.45(C5),158.67(C6), 54.7(OMe)
7A	NO ₂	H	H	20.4 26.0/1.23	-	56.64	47.50	159.45	30.87	55.42	126.6 - 138.4	164.2(C2),162.10(C4), 109.80(C5), 162.50(C6) 54.7,54.9,55.2-(OMe)

TABLE-11. 3 ¹³C NMR DATA OF AMINOPYRIDINE SUBSTITUTED PIPERIDINE-4-ONES-CONTINUED

COMPOUNDS	X	Y	Z	R	R ¹	C2	C3	C4	C5	C6	Aromatic carbons	Other carbons
8A	OCH ₃ 56.2	OCH ₃ 56.2	H	CH ₃ 214	CH ₃ 21.6	61.6	39.5	161.2	35.5	54.28	113.2 - 149.9	163.6(C2),162.60(C4), 104.10(C5),162.60(C6) 54.7,54.9 -(OMe)
9A	NO ₂	H	H	27.95 20.05 20.10	-	61.70	44.65	157.45	29.64	55.25	127.0 - 139.2	161.50(C2),160.40(C4)112.50 (C5),161.30(C6)54.7,54.9 -(OMe)
10A	H	NO ₂	H	CH ₃ 21.1	CH ₃ 21.2	60.62	39.60	157.68	35.50	61.11	126.3 - 138.6	164.50(C2),163.40(C),111.40(C 5),161.46(C6)Furyl-153.46C(2), 110.11C(3),107.51C(4), 141.99C(5).
11A	F	H	H	CH ₃ 21.0	CH ₃ 20.8	59.51	32.69	162.55	29.78	62.15	126.6 - 138.4	163.4(C2),162.50(C4),110.7(C5) 162.40(C6),56.2-(OMe)
12A	F	H	H	CH ₃ 21.2	CH ₃ 21.2	59.54	31.65	162.57	29.78	62.15	126.6 - 138.8	162.6(C2),160.50(C4),110.80 (C5), 160.80(C6)
13A	H	H	H	26.01 20.05 19.34	-	56.10	47.67	157.45	30.87	54.11	127.0 - 139.7	163.6(C2),162.54(C4), 104.60(C5), 162.89(C6)
14A	F	H	H	27.05 20.05 20.10	-	56.20	50.92	157.68	29.65	52.05	126.3 - 138.6	161.50(C2),158.20(C4), 108.10(C5), 158.68(C6)
15A	OCH ₃ 54.9	H	H	CH ₃ 21.0	CH ₃ 21.2	61.64	39.86	161.34	33.00	53.97	126.5 - 137.9	163.8(C2),162.40(C4), 108.2(C5), 162.90(C6)
16A	H	H	H	201 26.9 20.00	-	56.35	49.51	162.55	32.88	53.15	127.0 - 138.9	163.4(C2),162.70(C4), 108.5(C5), 162.50(C6)

TABLE-11. 3 ¹³C NMR DATA OF AMINOPYRIDINE SUBSTITUTED PIPERIDINE-4-ONES-CONTINUED

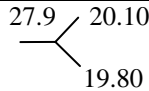
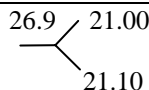
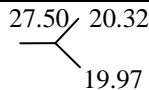
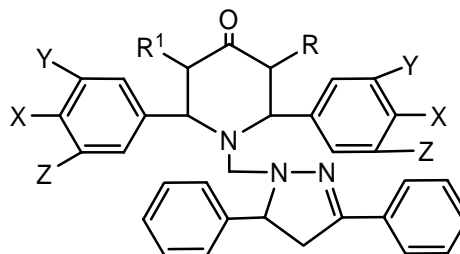
COMPOUNDS	X	Y	Z	R	R ¹	C2	C3	C4	C5	C6	Aromatic carbons	Other carbons
27A	N(Me ₂) 20.54, 20.6	H	H		-	56.10	43.29	162.55	30.32	60.72	127.8 - 140.4	161.71(C2),158.26(C4), 108.2(C5), 159.41(C6)
28A	OCH ₃ 56.2	OCH ₃ 56.2	OCH ₃ 56.2		-	60.6	40.1	158.3	29.78	61.6	105.5 - 150.6	163.60(C2),162.60(C4), 104.10(C5), 166.5(C6) Furyl-157.7C(2),107.21 C(3),105.51C(4),142.9(5).
29A	Br	H	H		-	56.66	43.21	162.91	30.87	59.80	126.4 - 138.4	163.6(C2),162.7(C4), 109.2(C5), 162.8(C6)

TABLE-11. 3 ¹³C NMR DATA OF 2-PYRAZOLINE SUBSTITUTED PIPERIDINE- 4-ONES



COMPOUNDS	X	Y	Z	R	R ¹	C-2	C-3	C-4	C-5	C-6	CH ₂	Aromatic carbons	Other carbons
P1	H	H	H	CH ₃ 10.5	CH ₃ 10.5	71.0	49.5	212.5	49.5	71.0	67.6	126.9 - 139.9	Pyrazoline -46.6- C3, 38.3-C4, 155.6-C5. Furyl- 143 C(2),109.5 C(3),109.9C(4), 143.9 C(5).
P2	Furyl			CH ₃ 8.1	CH ₃ 8.1	59.3	47.1	212.5	47.1	54.3	63.4	127.1 - 138.3	Furyl141.5C(2),110 C(3),105.9C(4), 151.1 C(5). Pyrazoline -49- C3, 40.1-C4, 151.8-C5
P3	F	H	H	CH ₃ 10.5	CH ₃ 10.5	71.0	49.5	212.5	49.5	71.0	68.2	129.8 - 149.9	Pyrazoline-49.1- C3, 40.1-C4, 151.8C5.56.2(O Me)
P4	H	H	H	CH ₃ 8.9	CH ₃ 8.9	69.0	47.8	210.6	50.1	71.0	65.2	126.7 - 139.9	Pyrazoline -49.2- C3, 41.2-C4, 151.8-C5. OMe- 56.2,56.4,56.0

COMPOUNDS	X	Y	Z	R	R ¹	C-2	C-3	C-4	C-5	C-6	CH ₂	Aromatic carbons	Other carbons
P5	Furyl			CH ₃ 10.3	CH ₃ 10.3	66.4	49.3	212.0	48.0	66.6	66.6	127.5 - 138.4	Pyrazoline -48.8- C3, 38.5-C4, 153.2-C5. Furyl- 142.2 C(2),109.3 C(3),110.1C(4), 145.2 C(5).
P6	H	H	H	20.2 20.6 20.6	-	67.2	50.4	209.4	51.6	68.0	67.5	126.4 - 138.4	Pyrazoline -49.0- C3, 39.5-C4, 151.5-C5,OMe- 56.2
P7	Cl	H	H	20.1 20.5 20.5	-	69.4	47.8	211.5	48.0	68.6	63.2	127.3 - 141.2	Pyrazoline -48.6- C3, 41.2-C4, 151.8-C5. Furyl- 141.5 C(2),110.0 C(3),104.9C(4), 152.0 C(5).
P8	H	H	H	20.5 20.6 20.5	-	60.5	47.9	211.5	39.0	65.7	67.9	127.3 - 140.5	Pyrazoline -49.6- C3, 38.5-C4, 150.8-C5,OMe- 55.9
P9	OMe 3.72	H	H	1.92 0.80 1.00	-	67.5	50.4	212.2	51.0	67.0	68.4	127.1 - 138.5	Pyrazoline -49.0- C3, 39.5-C4, 155.6-C5,OMe- 56.2,56.4
P10	OMe 3.73	H	H	1.79 0.08 1.00	-	67.2	49.5	212.8	50.5	66.8	67.8	129.8 - 147.3	Pyrazoline -49.6- C3, 38.8-C4, 152.8-C5,OMe- 55.9,56.0
P11	Furyl			1.97 0.08 3.95	2.94	61.70	47.67	211.60	49.2	60.40	68.2	127.6 - 138.9	Pyrazoline -46.6- C3, 38.2-C4, 154.6-C5. Furyl- 143-C2,109.2-C3, 109.5-C4,143.8-C5

MASS SPECTRAL DATA OF THE SYNTHESIZED COMPOUNDS

Compound 1A

m/z values (%)

614.28(80%), 615.14(14%), 290.54(14%), 323.26(10%), 77.03(100%), 122.45(52%), 92.02(69%), 148.24(60%).

Compound 2A

m/z values (%)

697.64(68%), 698.91(13%), 313.14(12%), 383.42(10%), 111.06(68%), 92.16(72%), 178.09(100%).

Compound 3A

m/z values (%)

682.16(65%), 683.24(16%), 356.18(10%), 323.18(8%), 154.98(60%), 92.05(80%), 148.08(100%)

Compound 4A

m/z values (%)

584.68(70%), 585.72(20%), 261.28(20.5%), 92.25(45%), 148.08(68%), 323.42(16.5%), 77.52(100%), 93.06(62%).

Compound 5A

m/z values (%)

677.02(55%), 678.14(17%), 309.18(12%), 367.28(14%), 107.05(44%), 111.42(30%), 92.25(38%), 354.16(89%), 177.07(100%).

Compound 6A

m/z values (%)

642.71(76%), 643.72(15%), 275.11(13%), 367.27(18%), 77.18(100%), 107.65(20%), 92.85(40%), 354.16(73%), 177.47(65%).

Compound 7A

m/z values (%)

718.95(80%), 719.84(15%), 351.16(14%), 367.27(17%), 167.60(35%), 93.24(28%), 92.41(32%), 354.16(65%), 177.45(100%).

Compound 8A

m/z values (%)

689.84(75%), 690.58(14%), 306.16(24%), 383.58(19%), 122.02(38%), 93.52(30%), 92.56(22%), 178.69(100%).

Compound 9A**m/z values (%)**

672.64(78%),673.52(16%),305.11(15%),367.15(17%),137.26(19%),77.08(100%),92.12(34%),354.26(85%),177.81(64%)..

Compound 10A**m/z values (%)**

623.13(80%),624.25(16%),269.56(14%),353.14(27%),67.42(20%),111.42(16%),92.38(42%),163.46(100%).

Compound 11A

609.41(77%),610.24(20%),309.26(18%),299.17(20%),107.24(36%),111.32(24%),92.04(40%),136.26(100%).

Compound 12A**m/z values (%)**

560.82(80%),561.64(19%),261.19(16%),299.27(13%),77.41(100%),93.14(76%),92.42(38%),136.52(58%).

Compound 13A**m/z values (%)**

556.72(62%),557.84(24%),279.82(21%),277.18(14%),95.12(45%),93.12(60%), 92.38(35%),264.71(70%),132.09(60%),77.24(100%).

Compound 14A**m/z values (%)**

592.56(70%),593.87(20%),279.18(18%),313.17(26%),95.45(48%),93.63(24%),92.48(26%),300.26(80%),150.08(100%).

Compound 15A**m/z values (%)**

621.24(71%),622.13(19%),297.04(15%),323.18(24%),95.62(30%),111.24(22%),92.52(34%),148.08(100%)

Compound 16A**m/z values (%)**

598.67(80%),599.74(16%),321.11(13%),277.28(21%),137.46(25%),93.72(60%),92.58(45%),264.17(80%),132.48(100%)

Compound 17A**m/z values (%)**

653.28(50%),654.15(19%),339.17(20%),313.16(14%),137.07(30%),111.48(42%),
92.62(30%),300.15(67%),150.10(100%).

Compound 18A**m/z values (%)**

634.85(69%),635.92(27%),321.11(22%),313.15(17%),137.58(14%),93.42(18%),92.62(38%),300.1
8(65%)

Compound 19A**m/z values (%)**

622.28(78%),623.41(25%),322.19(18%),299.14(12%),120.08(20%),111.41(30%),92.54(32%),136.
16(100%)

Compound 20A**m/z values (%)**

562.75(72%),563.64(17%),263.08(25%),299.14(13%),95.02(24%),77.43(100%),92.52(68%),136.6
6(85%).

Compound 21A**m/z values (%)**

624.19(90%), 625.25(27%),324.04(14%),299.25(18%),122.42(35%),111.34(40%),92.45(42%),
136.42(100%).

Compound 22A**m/z values (%)**

755.42(82%),756.13(27%),297.48(18%),457.45(20%),95.12(35%),111.45(46%),92.45(40%),444.4
5(685),222.14(100%).

Compound 23A

629.83(84%),630.91(18%),306.17(28%),323.19(14%),122.12(48%),93.42(56%),
92.14(42%),148.18(100%).

Compound 24A**m/z values (%)**

650.65(74%),651.72(25%),351.14(16%),299.18(21%),167.47(37%),93.03(70%),
92.16(39%),136.26(100%).

Compound 25A**m/z values (%)**

619.87(71%),620.68(28%),306.47(18%),313.25(22%),122.12(42%),93.43(62%),
92.23(43%),300.17(43%),150.18(100%).

Compound 26A**m/z values (%)**

648.66(65%),649.57(19%),251.26(19%),397.22(25%),67.41(38%),93.12(78%),
92.41(55%),384.42(52%),192.11(100%).

Compound 27A**m/z values (%)**

642.84(54%), 643.75(22%), 279.08(18%),363.26(21%),95.02(32%),93.05(40%),
92.04(64%), 350.17(42%), 175.13(100%).

Compound 28A**m/z values (%)**

708.81(65%),709.72(20%),251.16(22%),457.24(52%),67.11(28%),93.42(85%),92.45(58%),
444.25(25%),222.13(100%).

Compound 29A**m/z values (%)**

714.37(64%),715.28(24%),279.57(21%),433.00(14%),95.13(32%),93.15(28%), 92.13(42%),
419.29(32%),210.01(100%).

Compound P1**m/z values (%)**

503.66(73%), 504.78(24%), 278.17(20%), 25.14(14%),118.01(75%),67.61(60%),77.03(100%),
83.06(70%), 69.94(64%).

Compound P2**m/z values (%)**

528.25(52%),529.46(10%),258.11(16%),269.08(54%),108.25(67%),111.05(35%),77.51(100%),
69.53(55%)

Compound P3**m/z values (%)**

608.82(61%),610.71(19%),314.15(17%),295.16(13%),136.08(58%),137.061(40%),77.46(100%),83.
52(60%),69.04(80%)

Compound P4**m/z values (%)**

638.10(70%),639.46(21%),278.15(18%),359.12(24%),118.42(73%),167.08(28%),111.24(14%),
83.16(40%),69.07(34%)77.42(100%),

Compound P5**m/z values (%)**

528.25(42%),529.46(24%),258.11(16%),269.08(54%),108.25(67%),111.05(35%),77.51(100%),
69.53(55%)

Compound P6**m/z values (%)**

557.76(78%), 558.64(12%), 292.14(15%), 265.13(24%),277.15(45%),132.09(24%),107.05(64%)
77.55 (100%), 83.16(55%), 69.64(80%).

Compound P7**m/z values (%)**

586.64(55%), 587.72(22%), 360.19(20%), 225.11(11%), 345.16(64%),166.05(90%),67.81(35
%),77.43 (100%), 83.42(45%), 69.15(80%).

Compound P8**m/z values (%)**

573.75(63%), 574.62(25%), 212.08(15%), 281.13(8%), 278.13(84%), 107.05(80%), 93.41
(60%),77.41 (100%), 83.16(70%).

Compound P9**m/z values (%)**

633.74(56%), 634.76(23%), 352.19(16%), 281.13(18%), 337.17(54%), 162.10(100%),107.26
(42%),93.42 (38%), 83.06(32%), 69.14(60%).

Compound P10**m/z values (%)**

663.81(74%), 664.72(22%), 352.19(15%), 311.16(20%), 337.16(24%), 162.10(100%),93.14
(32%), 83.06 (60%), 69.14(90%).

Compound P11**m/z values (%)**

558.10(60%), 559.21(22%), 272.13(16%), 285.07(13%), 257.10(30%),122.07(100%),111.41
(34%),93.03 (90%), 83.60(59%), 69.50(24%).

12. *IN VITRO* ANTI-CANCER ACTIVITY

Today, the Greek term carcinoma is the medical term for a malignant tumor derived from epithelial cells. It is Celsus who translated *carcinus* into the Latin *cancer*, also meaning crab. Galen used "*oncos*" to describe *all* tumours, the root for the modern word oncology.

Hippocrates described several kinds of cancers. He called benign tumours as *omas*, which means swelling, and malignant tumours as *carcinus*, meaning crab or crayfish in Greek. This name probably comes from the appearance of the cut surface of a solid malignant tumour, with a roundish hard center surrounded by pointy projections, vaguely resembling the shape of a crab. He later added the suffix *-oma*, meaning swelling in Greek, giving the name *carcinoma*. Since it was against Greek tradition to open the body, Hippocrates only described and made drawings of outwardly visible tumors on the skin, nose, and breasts. Treatment was based on the humor theory of four bodily fluids (black and yellow bile, blood, and phlegm). According to the patient's humor, treatment consisted of diet, blood-letting, and/or laxatives. Through the centuries it was discovered that cancer could occur anywhere in the body, but humor-theory based treatment remained popular until the 19th century with the discovery of cells.

The first known surgical treatment for cancer was described in the 1020s by Avicenna (Ibn Sina) in *The Canon of Medicine*. He stated that the excision should be radical and that all diseased tissue should be removed, which included the use of amputation or the removal of veins running in the direction of the tumor. He also recommended the use of cauterization for the area being treated if necessary.

In the 16th and 17th centuries, it became more acceptable for doctors to dissect bodies to discover the cause of death. The German professor Wilhelm Fabry believed that breast cancer was caused by a milk clot in a mammary duct. The Dutch professor Francois de la Boe Sylvius, a follower of Descartes, believed that all disease was the outcome of chemical processes, and that acidic lymph fluid was the cause of cancer. His contemporary Nicolaes Tulp believed that cancer was a poison that slowly spreads, and concluded that it was contagious.

With the widespread use of the microscope in the 18th century, it was discovered that the 'cancer poison' spread from the primary tumor through the lymph nodes to other sites ("metastasis"). This view of the disease was first formulated by the English surgeon Campbell De Morgan between 1871 and 1874. The use of surgery to treat cancer had poor results due to problems with hygiene. The renowned Scottish surgeon Alexander Monro saw only 2 breast tumor patients out of 60 surviving surgery for two years. In the 19th century, asepsis improved surgical hygiene and as the survival statistics went up, surgical removal of the tumor became the primary treatment for cancer. With the exception of William Coley who in the late 1800s felt that the rate of cure after surgery had been higher *before* asepsis (and who injected bacteria into tumors with mixed results), cancer treatment became dependent on the individual art of the surgeon at removing a tumor. During the same period, the idea that the body was made up of various tissues, that in turn were made up of millions of cells, laid rest the humor-theories about chemical imbalances in the body. The age of cellular pathology was born.

When Marie Curie and Pierre Curie discovered radiation at the end of the 19th century, they stumbled upon the first effective non-surgical cancer treatment. With radiation came also the first signs of multi-disciplinary approaches to cancer treatment. The surgeon was no longer operating in isolation, but worked together with hospital radiologists to help patients.

Cancer is large and complex family of malignancies manifested with uncontrolled and undifferentiated cellular growth that can affect virtually every organ in the body. Cancer begins in the body cells, which are constantly dividing and multiplying to replace old and damaged cells. Sometimes, cells begin to divide unnecessarily, forming excess tissue known as tumor.

CYTOTOXICITY STUDIES

Tissue culture has been used to screen many anticancer drugs since there is clear correlation between the *in vitro* and *in vivo* activities of potential chemotherapeutic agents. There is scientific justification for cytotoxicity^{392,393} testing in tissue culture, since animal models are in many ways inadequate for predicting the effects of chemicals

on humans since there are many metabolic differences between species. Cytotoxicity studies involve the analysis of morphological damage or inhibition of zone of outgrowth induced by the chemicals tested.

12.1 MATERIALS AND METHODS

MTT assay

Principle: Yellow MTT (3-(4,5-Dimethylthiazol-2-yl)-2,5-diphenyltetrazolium bromide, a tetrazole) is reduced to purple formazan in the mitochondria of living cells. The absorbance of this colored solution can be quantified by measuring at a certain wavelength (usually between 500 and 600 nm) by a spectrophotometer. The absorption max is dependent on the solvent employed. This reduction takes place only when mitochondrial reductase enzymes are active, and therefore conversion can be directly related to the number of viable (living) cells. When the amount of purple formazan produced by cells treated with an agent is compared with the amount of formazan produced by untreated control cells, the effectiveness of the agent in causing death of cells can be deduced, through the production of a dose-response curve. Solutions of MTT solubilized in tissue culture media or balanced salt solutions, without phenol red, are yellowish in color. Mitochondrial dehydrogenases of viable cells cleave the tetrazolium ring, yielding purple MTT formazan crystals which are insoluble in aqueous solutions. The crystals can be dissolved in acidified isopropanol. The resulting purple solution is spectrophotometrically measured. An increase in cell number results in an increase in the amount of MTT formazan formed and an increase in absorbance. The use of the MTT method does have limitations influenced by: (1) the physiological state of cells and (2) variance in mitochondrial dehydrogenase activity in different cell types.

The assay can be performed entirely in a microtiterplate (MTP). It is suitable for measuring cell proliferation, cell viability or cytotoxicity. This method involves culturing the cells in a 96-well microtiterplate, and then incubating them with MTT solution for approximately 2 hours. During incubation period, viable cells convert MTT to a water-insoluble formazan dye. The formazan dye in the MTP is solubilized and quantified with an ELISA plate reader. The absorbance directly correlates with the cell number. This is applicable for adherent cells cultured in MTP.

Materials for MTT assay

- RPMI-1640 media (Himedia, Mumbai, India)
Composition of RPMI; 9.54 g/lit, 10%FBS, 2000mg sodium bicarbonate, 250µl each of penicillin (60mg/ml), streptomycin (100mg/ml), Amphotericin (200mg/ml).
- Foetal bovine serum (Gibco's, USA)
- Penicillin-G (Himedia, Mumbai, India)
- RPMI-1640, (Himedia, Mumbai India)
- Streptomycin (Himedia, Mumbai, India)
- Amphotericin-B.
- Phosphate buffered saline (PBS) (Himedia, Mumbai, India)
- Trypsin 0.25% (Trypsin-EDTA [1x] in HBSS, Gibco's UK)
- Ethylenediamine tetra-acetic acid (EDTA) (Himedia, Mumbai, India)
- Dimethyl sulphoxide (DMSO) (Merck India Ltd, Mumbai, India)
- MTT (3-(4,5-dimethylthiazol-2yl)-2,5-diphenyltetrazolium bromide)-4mg/ml (Himedia, Mumbai, India)
- Lysis buffer (15% SLS in 1:1DMF and water).

Additional equipments required

- CO₂ incubator (WTC Binder, Germany)
- Laminar air flow cabin (Klenzaid, Chennai, India)
- Refrigerated centrifuge (Biofuge Fresco, by Heraeus, Germany)
- ELISA-reader (for MTP) (Anthos 2010, Germany)
- Deep freezer (Polar Angelantoni Industries, Italy)
- Ultrasonic bath (Transonic [460/H], by Elma®, Germany)
- Vacuum pump (Zenith [model: PDF-2-2.5], Mumbai, India)
- Pipettes (Eppendorf, Hamburg, Germany)
- Culture plates (Felcon, Germany)
- Centrifuge tubes (Felcon, Germany)
- Aerosol resistant tips (Tarsons, Mumbai, India)
- Flat-bottomed 96-well MTP, tissue culture grade (Tarsons, Mumbai, India)

Cell lines used

- HCT 15-colorectal cancer cells.

Experimental Procedure**Preparation of antibiotic solutions****Penicillin-G**

- 0.61 g (one vial) of penicillin-G was weighed and dissolved in 1 ml of sterile phosphate buffered saline (PBS).
- Contents were stirred for 5 minutes.
- The contents were sterilized with syringe by passing through 0.22-micron filter aliquot of 5 ml fractions in 15 ml storage vials and stored at -20° C until use.

Streptomycin sulfate

- 10 mg (one vial) of streptomycin sulfate was weighed and dissolved in 10ml of sterile PBS.

Amphotericin-B

- 250 mg of Amphotericin-B was weighed and dissolved in 10 ml of sterile PBS.

Preparation of Dulbecco's PBS

- 9.6 g (one vial) of D-PBS was suspended in 800 ml triple distilled water and mixed until dissolved.
- It was then autoclaved at 121° C (15 lbf) for 15 minutes.
- After cooling to room temperature aseptically, sterile 100ml calcium chloride (1mg/ml) solution and 100 ml Magnesium chloride (1mg/ml) solution were added and mixed.

Preparation of RPMI-1640 Medium

- 10.39 g (one vial) of RPMI-1640 was weighed in a sterile conical flask.
- The contents were dissolved in 900 ml of Milli-Q (triple distilled) water by stirring and the antibiotic solutions were added (100 U/ml Penicillin-G Sodium, 50 μ g/ml of streptomycin and 2 μ g/ml of Amphotericin-B)
- Once all constituents of the medium were completely added, the pH was adjusted to 7.2 to 7.5 with 0.1 N Hydrochloric acid.
- The volume was made up to one liter with triple distilled water.

- Contents were transferred to the Millipore filtration kettle (Duran, Germany) supported by 0.22 microns membrane filter, kept in laminar flow hood that was connected to the outlet by negative pressure pump and filtered.
- Pressure was adjusted such that the flow rate of medium from the filtration unit is 10-12 min/L i.e., 100 ml/min.
- 5 ml of the sample is taken in T₂₅ tissue culture flask; kept for 24 hours in CO₂ incubator at 37.0°C for sterility check.
- 100 ml of sterile Fetal Bovine Serum was added to 900 ml medium.
- Reconstituted medium was checked for sterility by transferring 5ml of medium into a T₂₅ tissue culture flask and incubating for 24 hours in CO₂ incubator 37.0°C.

Trypsinization

- The media was aspirated from each flask, removed and discarded.
- Monolayer was rinsed with 5-10 ml PBS to remove traces of serum and the rinsing solution was aspirated.
- 1 ml of 0.25 % trypsin-EDTA (Himedia) was added to each flask and spread evenly over cell monolayer and depending on cell type, the flask was either placed in hood or in incubator for 2-5 minutes.
- The flask was gently ‘tapped’ for dislodging the cells.
- Then the cells were re suspended in 8 ml of the medium containing serum to stop the action of the trypsin. Gentle pipetting was carried out up and down for breaking up the clumps.
- Cell suspension was transferred to a properly labeled 15 ml centrifuge tube.
- The tubes were centrifuged at 1000 rpm for 5 minutes.
- The pellet was re suspended in 5-10 ml of medium depending upon the size of the pellet or cell number.

Method

0.1ml of the cell suspension (containing 5×10^6 cells/100 μ l) and 0.1ml of the test solution (0.01 μ M - 100 μ M in 1% DMSO such that the final concentration of DMSO in media is less than 1%) were added to the 96 well plates and kept in 5% CO₂ incubator at 37⁰ C for 72 hours. Blank contains only cell suspension and control wells contain 1% DMSO and cell suspension

After 72 hours, 20µl of MTT was added and kept in carbon dioxide incubator for 2 hours followed by the addition of isopropanol (100 µl).Then 100µl of lysis buffer was added to all the wells. The plate was covered with aluminum foil to protect it from light. Then the 96 well plates are kept in rotary shaker for 10-20 minutes.

After 10-20 minutes, the 96 well plates were processed on ELISA reader for absorption at 562nm. The readings were averaged and viability of the test samples was compared with DMSO control. The standard drug used is doxorubicin the concentration of 500nM. The percentage growth inhibition was calculated using the following formula

$$\% \text{ Growth Inhibition} = 100 - \frac{\text{Mean Absorbance of Sample}}{\text{Mean Absorbance of Control}} \times 100$$

12.2 RESULTS AND DISCUSSION

All the synthesized compounds were tested *in vitro* against colorectal cell lines (HCT 15). The results are tabulated in table 12.1.

TABLE 12.1 PERCENTAGE GROWTH INHIBITION OF SYNTHESIZED COMPOUNDS

COMPOUND NO	IC ₅₀ VALUES IN (μM)	% GROWTH INHIBITION AT DIFFERENT CONCENTRATIONS (μM)				
		0.01	0.1	1	10	100
1A	1	0.00	38.25	63.13	65.10	66.34
2A	1	0.00	44.15	54.76	59.37	60.56
3A	0.1	0.00	49.98	58.89	60.18	61.86
4A	5	0.00	25.56	42.14	63.57	62.20
5A	2	0.00	39.98	47.34	60.54	62.38
6A	10	0.00	32.54	39.56	50.76	54.10
7A	1	0.00	35.24	65.13	67.12	69.37
8A	1	0.00	34.64	54.33	62.13	68.74
9A	10	0.00	34.13	37.45	56.13	65.39
10A	0.1	0.00	49.19	52.46	63.41	65.60
11A	1	0.00	26.98	37.23	57.77	64.38
12A	5	0.00	34.96	45.13	69.10	69.68
13A	0.1	0.00	49.64	57.08	59.84	65.49
14A	1	0.00	0.00	49.91	58.23	63.59
15A	2	0.00	35.21	45.05	54.09	63.17
16A	10	0.00	38.57	40.00	52.83	65.06
17A	5	0.00	29.32	42.04	60.62	62.53
18A	5	0.00	38.24	44.41	58.68	60.08
19A	1	0.00	0.00	50.21	58.43	62.78
20A	1	0.00	0.00	49.90	52.17	57.86
21A	0.01	62.82	60.94	68.35	68.61	68.68
22A	2	0.00	24.2	38.1	63.2	65.5
23A	1	0.00	32.5	59.9	62.8	55.3
24A	1	39.39	41.16	50.75	50.84	59.29

COMPOUND NO	IC ₅₀ VALUES IN (µM)	% GROWTH INHIBITION AT DIFFERENT CONCENTRATIONS (µM)				
		0.01	0.1	1	10	100
25A	0.01	80.51	49.25	58.63	74.58	75.62
26A	0.1	0.00	53.14	57.23	61.03	63.61
27A	1	0.00	38.21	56.07	59.00	62.23
28A	1	0.00	40.54	52.13	57.52	59.06
29A	1	0.00	37.51	50.76	55.04	56.69

Compounds which show a % growth inhibition of about 68% is considered to be *in vitro* active. From the data provided in the table 12.1 it can be seen, that the compounds 21A and 25A show the least IC₅₀ values 0.01 and 0.01 respectively. The compound 21A maintains the same level of activity through out the working range (0.01-100 µM). There is no concentration related gradation in the activity profile. In the case of compound 25A, the peak activity is noted in the minimum concentration of 0.01 µM itself. Even though there is a decrease in the activity with increase in the concentration, the activity profile remained well above the required level.

The other compounds showing significant activity are 3A, 10A, 13A and 26A. The compounds 6A, 9A and 16A show less activity with IC₅₀ values in the range of 10 µM. All the other compounds showed moderate activity with IC₅₀ values in the range of 1-5 µM.

The pyrimidine Schiff bases are a class of compounds that hydrolyse readily under mild acidic conditions, such compounds could be hydrolysed selectively by the tumour cells as it is known that majority of the tumours contain cells with lower pH than the cells in the normal tissue. Hydrolysis of these compounds *in vivo* may liberate the active aldehyde to act as alkylating agent and at the same time the pyrimidine is freed to act as an antimetabolite. Besides, the azomethine linkage may be operative by a postulated chelation mechanism.

By studying the SAR of the molecules 21A and 25A, it is understood that may be the presence of the electronegative substructures like F, Cl and OH influences the anticancer activity along with the already specified reasons. The presence of m-NO₂ toxicophore may be an added feature for the activity against the cancer cell lines. The

toxic effect on the normal cell lines can be counteracted by incorporating detoxifying substructures.

It is already seen that compounds showing a PASS Pa values between 0.5-0.7, show activity in the experiment, they can serve as new leads that is New chemical Entities. (NCE). Thus the molecules 21A and 25A can serve as NCE and further refining of these molecules can make them as new drug candidates. The graphical representation of the % inhibition of the compounds are given in Figures 12.1-12.4.

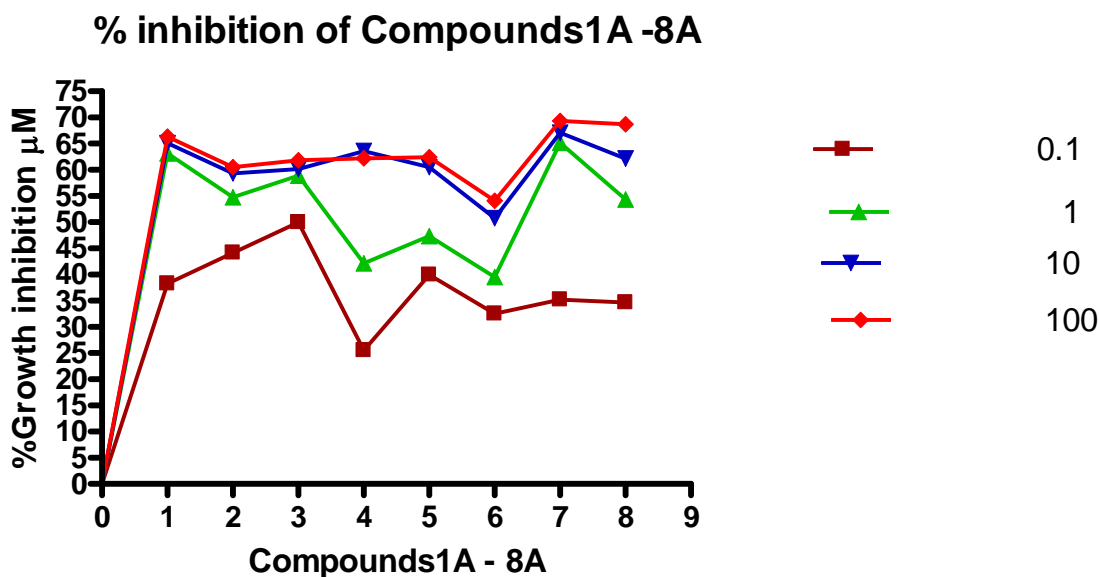


FIGURE 12.1 % INHIBITION OF COMPOUNDS 1A-8A

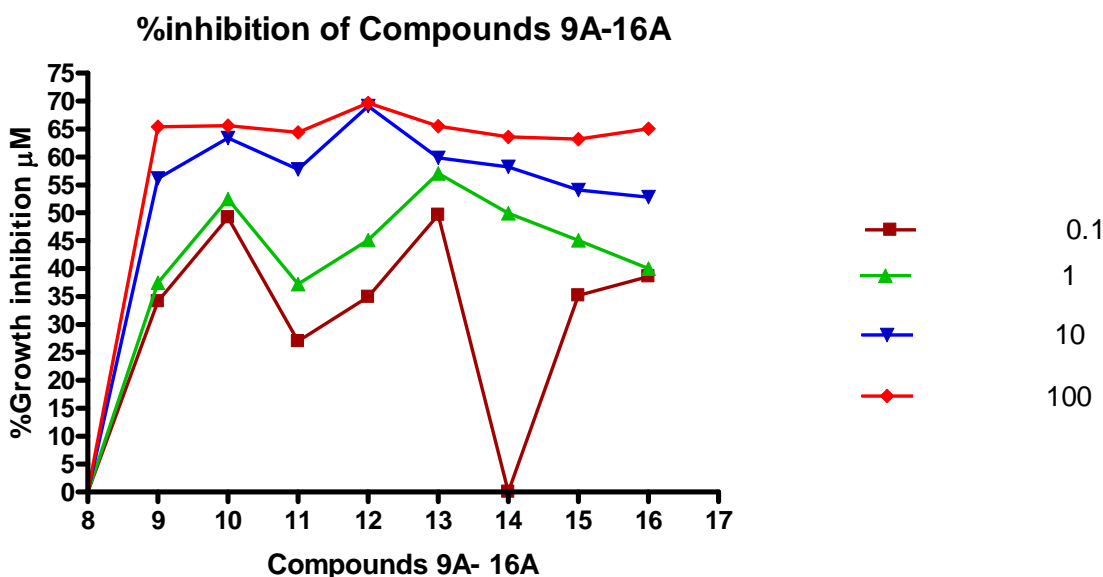


FIGURE 12.2 % INHIBITION OF COMPOUNDS 9A-16A

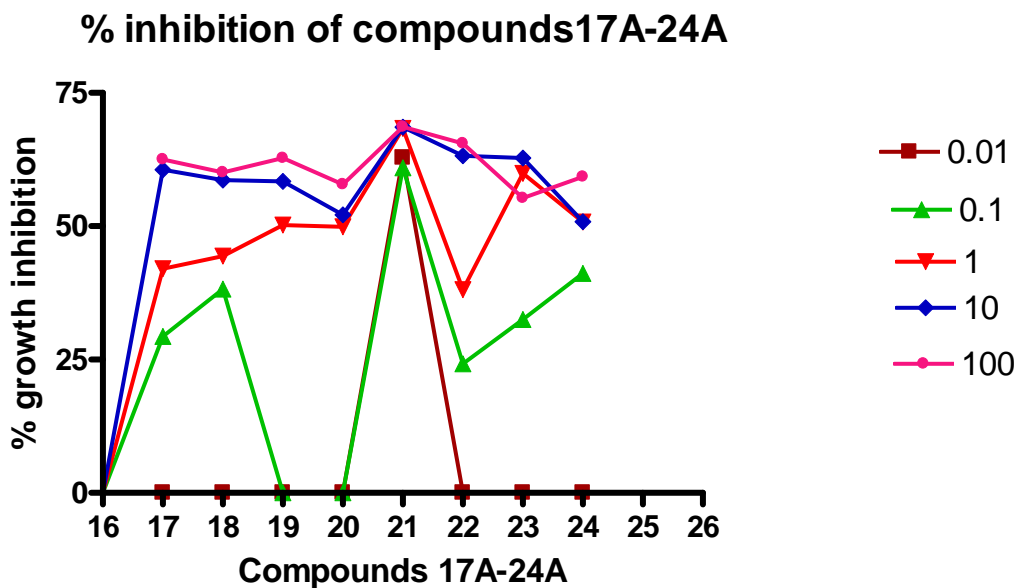


FIGURE 12.3 % INHIBITION OF COMPOUNDS 17A-24A

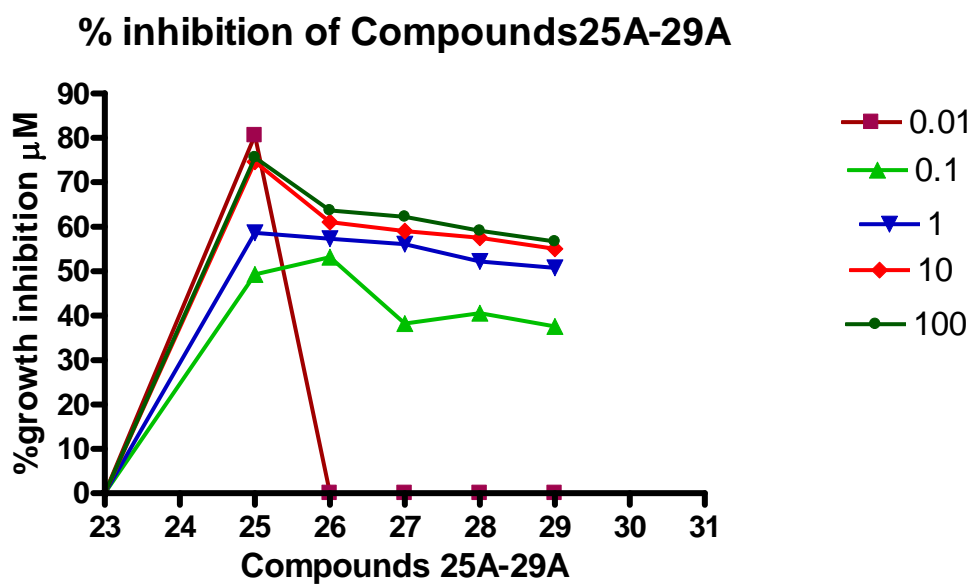


FIGURE 12.4 % INHIBITION OF COMPOUNDS 17A-24A

13. PHOSPHATASE INHIBITION ACTIVITY

13.1 MATERIALS AND METHODS

The phosphorylation-dephosphorylation of cellular proteins is a major regulatory mechanism for many eukaryotic signaling pathways. Aurora-A kinase (STK15) is necessary for centrosome maturation, for assembly and maintenance of a bipolar spindle, and for proper chromosome segregation during cell division. Aurora-A is an oncogene that is over expressed in multiple human cancers³⁹⁴. Regulation of kinase activity apparently depends on phosphorylation of Thr-288 in the T-loop. In addition, interactions with targeting protein for *Xenopus* kinesin-like protein 2 (TPX2) allosterically activate Aurora-A. The Thr-288 phosphorylation is reversed by type-1 protein phosphatase (PP1). Protein phosphatase-1 (PP1) is a protein serine/threonine phosphatase extraordinarily conserved among eukaryotes as an essential gene. Its critical function occurs in mitosis because various eukaryotic cells undergo metaphase arrest due to PP1 mutations or inhibition³⁹⁵⁻³⁹⁹.

Phosphorylation stimulates kinase activity. Three phosphorylation sites have been identified in *Xenopus* Aurora A by mass spectrometry. Phosphorylation of Thr295 (Thr288in human Aurora A) in the activation loop is essential for kinase activity⁴⁰⁰.

STK15 contains two functional binding sites for protein phosphatase type 1 (PP1), and the binding of these proteins is cell cycle-regulated peaking at mitosis. Activated STK15 at mitosis phosphorylates PP1 and inhibits PP1 activity *in vitro*. *In vivo*, PP1 activity co-immunoprecipitated with STK15 is also reduced. These data indicate that STK15 inhibits PP1 activity during mitosis. Also, PP1 is shown to dephosphorylate active STK15 and abolish its activity *in vitro*. These results suggest that a feedback regulation through phosphorylation/dephosphorylation events between STK15 kinase and PP1 phosphatase operates through the cell cycle. Deregulation of this balance may contribute to anomalous segregation of chromosomes during mitotic progression of cancer cells²⁹³.

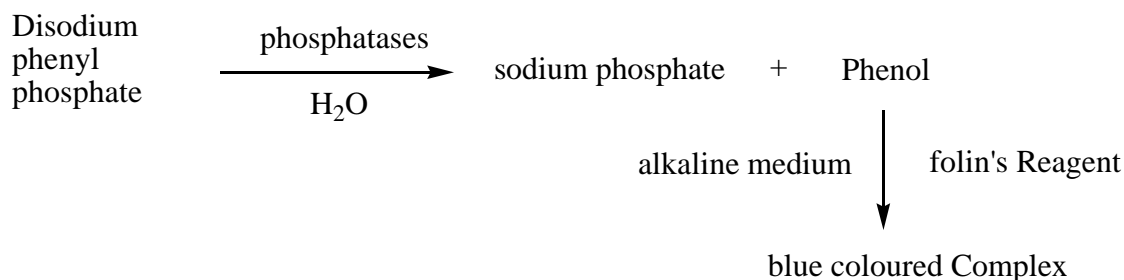
In contrast to *C.elegans*, recent studies in mammalian cells have highlighted a major role of serine/threonine protein phosphorylation in apoptosis⁴⁰¹.

Cells that have lost the protein phosphatase 1 (PP1)-like dis2/sds21 phosphatase activities prematurely enter mitosis and remain in a defective mitotic state with high

kinase activity and without sister chromatid disjunction. Over expression of PP1-like phosphatase, on the other hand, delays the entry into mitosis. Cells that have lost PP2A-like ppa2 phosphatase activity also prematurely enter mitosis with a reduction in cell size⁴⁰² leading to Apoptosis.

From all these observations it is very clear that phosphatase inhibition can lead to anticancer activity either by inhibiting the phosphorylation of Aurora A kinase or by entering the mitosis with defective cells thus leading to Apoptosis.

The most common method to assay phosphatases is by King and Armstrong method in which the substrate disodium phenyl phosphate is hydrolyzed to form sodium phosphate with the liberation of phenol. The liberated phenol reacts with the phosphomolybdic acid in folin's reagent alkaline medium to produce a blue colored complex which is read at 620 nm.



REAGENTS AND CHEMICALS:

Substrate - 0.1M Di sodium phenyl phosphate in distilled water.

Enzyme - Alkaline phosphatases from liver.

2g of the fresh liver is homogenized with 20ml of bicarbonate buffer whose pH is 10.4. The contents are mixed well and centrifuged at low speed and the supernatant is the enzyme used.

Activator - 0.1M Magnesium chloride in distilled water.

Inhibitor - The compounds P1-P11.

Folin's reagent - Mixed with water in the ratio of 1:2

Inhibitor - 15% sodium carbonate

Buffer - Bicarbonate buffer

Solution A: 0.2M anhydrous sodium carbonate (21.2g) in 1000 ml of distilled water.

Solution B: 0.2 M sodium bicarbonate (16.8g) in 1000 ml of distilled water.

38.5 ml of solution A and 11.5 ml of solution B are mixed and diluted to 100ml using distilled water and the pH is found to be 10.4.

PHOSPHATASE INHIBITION ASSAY

Preparation of Standard Curve

Serial dilutions of phenol containing concentrations in the range of 20-280 mcg/ml were prepared with water. All the test tubes were treated with 1ml of folin's reagent and 1.5 ml of bicarbonate buffer. The blue colour formed was measured by noting the absorbance at 620nm. The absorbances were then plotted against the concentrations of phenol to give the standard graph.

Test Solution Preparation

The assay is done in three concentration level for each compound. Stock solutions containing 2mg (2000 mcg) of compounds P1-P11 were prepared individually. From these solutions three different concentrations each containing 50 mcg (20 µl), 125 mcg (50 µl), and 250 mcg (100 µl) were used for the assay.

Experimental procedure

Standard solution preparation

1ml of substrate + 1.5ml of buffer + 2.5ml water + 0.1ml of magnesium chloride -----pre incubated at 37°C for 5 minutes.

Test solution preparation

1ml of substrate + 1.5ml of buffer + Test solution (20/50/100 µl) + 0.1ml of magnesium chloride -----pre incubated at 37°C for 5 minutes.

Blank preparation

1ml of substrate + 1.5ml of buffer + 2.5ml water + 0.1ml of magnesium chloride -----pre incubated at 37°C for 5 minutes.

After this 0.1(10mcg) ml of enzyme was added to all the test tubes except the blank and again incubated at 37°C for 15 minutes. After incubating 1ml of folin's reagent is added to all the test tubes. At this stage 2ml of 15% sodium carbonate is added to all the test tubes to stop the reaction. The final volume was made up to 10ml in all the tubes. The blue color developed in the test tubes were then measured by noting the absorbance at 620nm.

13.2 RESULTS AND DISCUSSIONS

Preparation of Standard Curve

The different absorbances obtained from the serial dilutions of the standard solutions (Phenol) are given in Table 13.1.

TABLE 13.1 STANDARD GRAPH DATA

CONCENTRATION(MCG)	ABSORBANCE(OD)
0	0
20	0.03
40	0.06
80	0.12
120	0.18
160	0.24
200	0.3
240	0.36
280	0.42
320	0.48
360	0.54
400	0.6
440	0.66
480	0.72
520	0.78
560	0.84

Standard solutions of phenol were assayed with the Folin's reagent and the absorbance was measured at 620nm. The phenol concentration curve obtained over a wide concentration range is illustrated in Figure 13.1. The assay was found to be linear up to

almost 300 mcg which represented an absorbance range of about 3 units. The linearity range is between 20-300mcg and the linear regression (R) for the data was 0.9997.

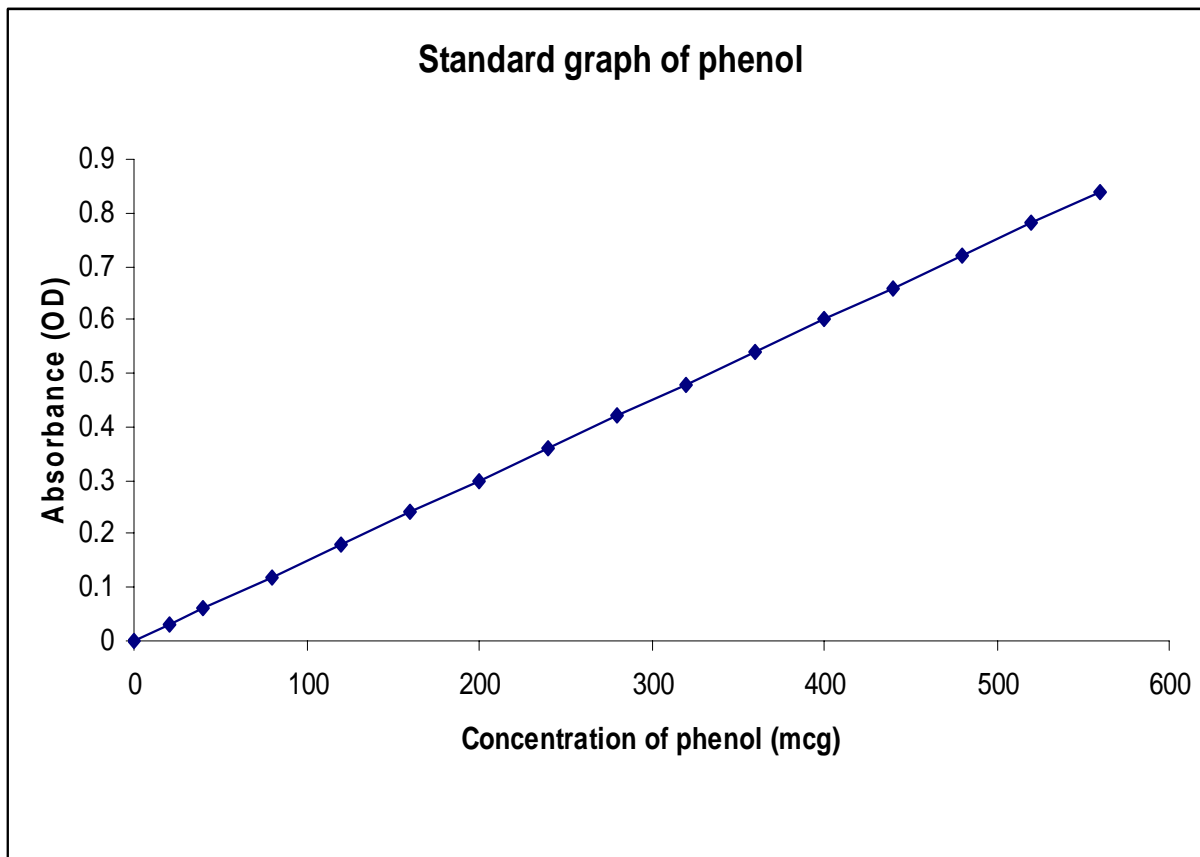


Figure 13.1 Standard Graph of Phenol

PHOSPHATASE INHIBITION ASSAY

The test and the blank solutions were assayed with Folin's reagent and the absorbances were measured at 620nm. The data are presented in table 13.2.

The principle of the assay relies on the ability of the alkaline and protein phosphatases to utilize Disodium phenyl phosphate as a substrate and their capability to cleave it into sodium phosphate and phenol. The product of the reaction, free phenol can then be detected colorimetrically with Folin's reagent. The amount of the phenol formed is directly proportional to the activity of enzyme.

In the standard solution 1ml of the substrate is treated with the enzyme. The absorbance of this solution reflects the amount of phenol released from 1ml of the substrate. The amount of phenol formed in the standard solution is taken as the standard

value. The reduction in the amount of phenol formed from this value shows the inhibitory action of the compounds.

The absorbance of this standard solution was found to be 0.760. The amount of phenol formed is read from the standard graph and it was found to be 506.66 mcg.

TABLE 13.2 PHOSPHATASE INHIBITION ACTIVITIES

COMPOUND NO	CONCENTRATION mcg	AMOUNT OF PHENOL mcg
P1	50	333 ± 2,00
	125	146 ± 2.34
	250	106 ± 2.89
P2	50	333 ± 1.99
	125	73 ± 2.07
	250	53 ± 2.67
P3	50	265 ± 2.54
	125	246 ± 2.31
	250	13 ± 2.67
P4	50	193 ± 2.04
	125	106 ± 2.00
	250	99 ± 1.98
P5	50	240 ± 2.53
	125	86 ± 2.32
	250	79 ± 2.56
P6	50	126 ± 2.65
	125	112 ± 2.43
	250	59 ± 2.31
P7	50	133 ± 2.43
	125	59 ± 2.16
	250	32 ± 2.11
P8	50	132 ± 2.05
	125	113 ± 2.00
	250	105 ± 2.19
P9	50	140 ± 2.34
	125	100 ± 2.56
	250	60 ± 2.76
P10	50	140 ± 2.49
	125	106 ± 2.90
	250	80 ± 2.43
P11	50	85 ± 2.56
	125	40 ± 2.65
	250	33 ± 2.02

Amount of phenol formed are mean ± SE of triplicate values

In the test solutions the compounds (test solutions) are included. Because these inhibitors inhibit the enzymatic activity of phosphatases, the enzyme activity is reduced which in turn leads to reduced amount of formation of phenol. So if there is a reduction in the concentration of phenol when compared with the standard, it can be concluded that the compounds possess phosphatase inhibition activity. The amount of phenol formed is inversely proportional to inhibitory activity.

The compounds P1-P11 were used in three concentration levels (50/125/250mcg). The absorbances of these solutions were measured at 620nm after carrying out the assay with Folin's reagent. The concentrations of the phenol formed in these solutions were obtained from the standard graph of phenol.

From the analysis of the data it can be seen that all the compounds P1-P11 are possessing phosphatase inhibition activity. In addition to that they also show a gradation in their dose response. All the compounds show less inhibition at 50 mcg, moderate inhibition at 125 mcg and a fairly good inhibition at 250 mcg.

The compounds P1-P11 have 2-pyrazoline moiety as a sub structure in common. The azomethine linkage in the pyrazoline is already shown to be active against various cancers

The compounds P1-P5 at 50 mcg concentration level shows very less inhibition. A concentration dependent increase in inhibitory activity was observed with P1, P2, P3, P4, and P5. That is better inhibitory activity was observed with higher concentrations (250 mcg).

The compounds P6-P11 showed better inhibition in all the three concentration levels. In all these compounds the C3 of piperidin-4-one ring contain isopropyl group which may contribute to the increase in inhibitory activity.

Of all compounds the compound P3 at the 250mcg concentration level shows best activity which is attributed to the high electro negativity of fluoro phenyl substructures. The compounds P7 and P11 show almost similar activities which are better than other compounds at 250 mcg concentration level. This may be due to the synergistic effect of isopropyl group and the electro negative substructures like p-Cl phenyl, P-OH phenyl and Furyl rings. The graphical representation of the phosphatase inhibitory activity of the compounds P1-P11 is given in Figure 13.2 and the diagrammatic

representation is given in Figure 13.3. The correlation between the PASS prediction values and the Phosphatase inhibitory activity is shown in Table13.3.

By observing the data given in Table13.3, it can be concluded that the activities predicted by PASS is comparable with the results obtained experimentally. This shows the accuracy of the PASS prediction.

TABLE13.3 CORRELATION BETWEEN PASS VALUES AND PHOPHATASE INHIBITORY ACTIVITY.

COMPOUND NO	PHOSPHATASE INHIBITION Pa VALUES(PASS)	PHOSPHATASE INHIBITION IN DIFFERENT CONCENTRATIONS		
		50mcg	125 mcg	250mcg
P1	0.723	333	146	106
P2	0.737	333	73	53
P3	0.738	265	246	13
P4	0.732	193	106	99
P5	0.713	240	86	79
P6	0.729	126	112	59
P7	0.711	133	59	32
P8	0.727	132	113	105
P9	0.731	140	100	60
P10	0.729	140	106	80
P11	0.765	85	40	33

Amount of phenol formed in three different concentrations

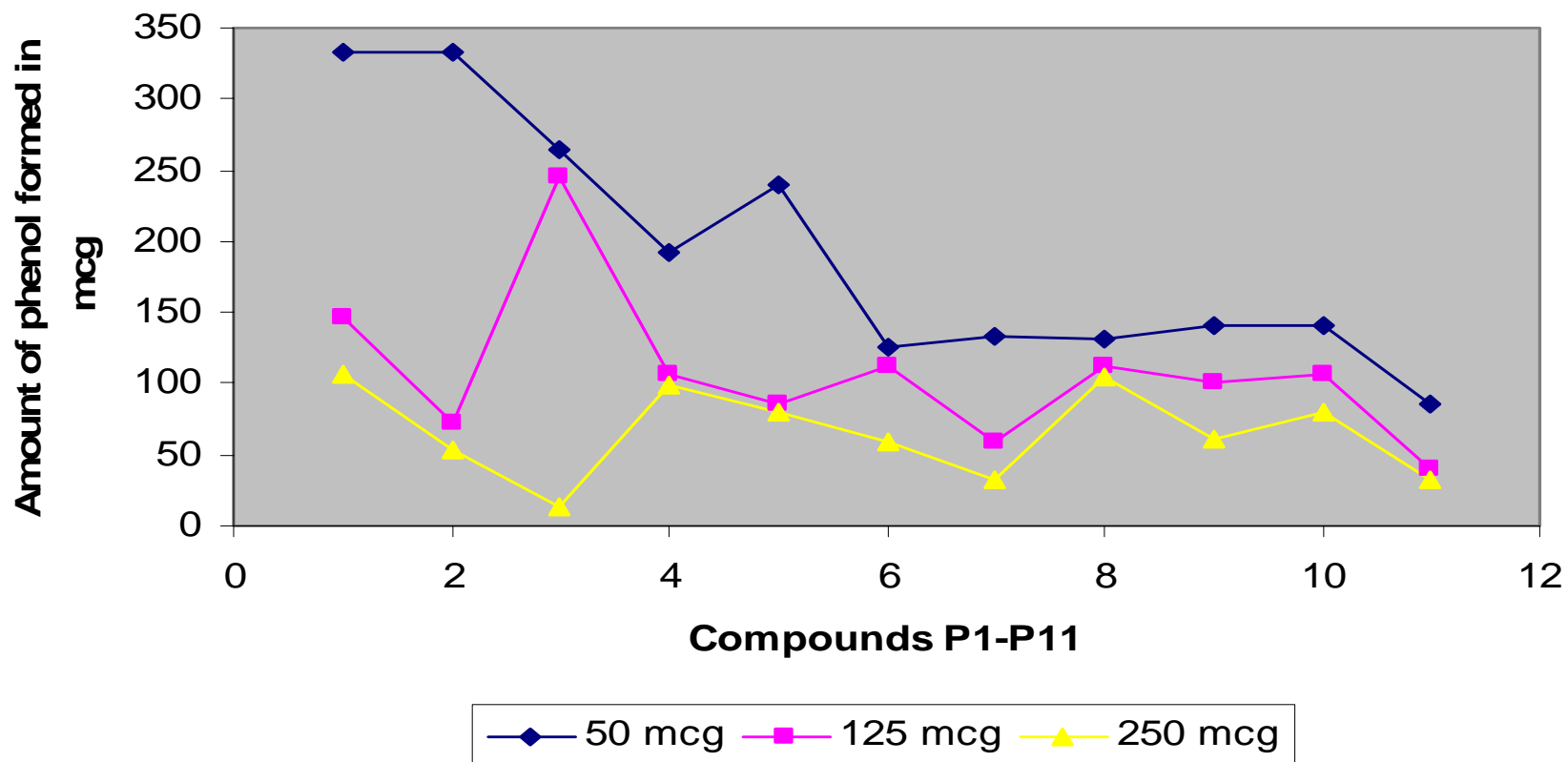


Figure 13.2 Phosphatase inhibitory activity of compounds P1-P11

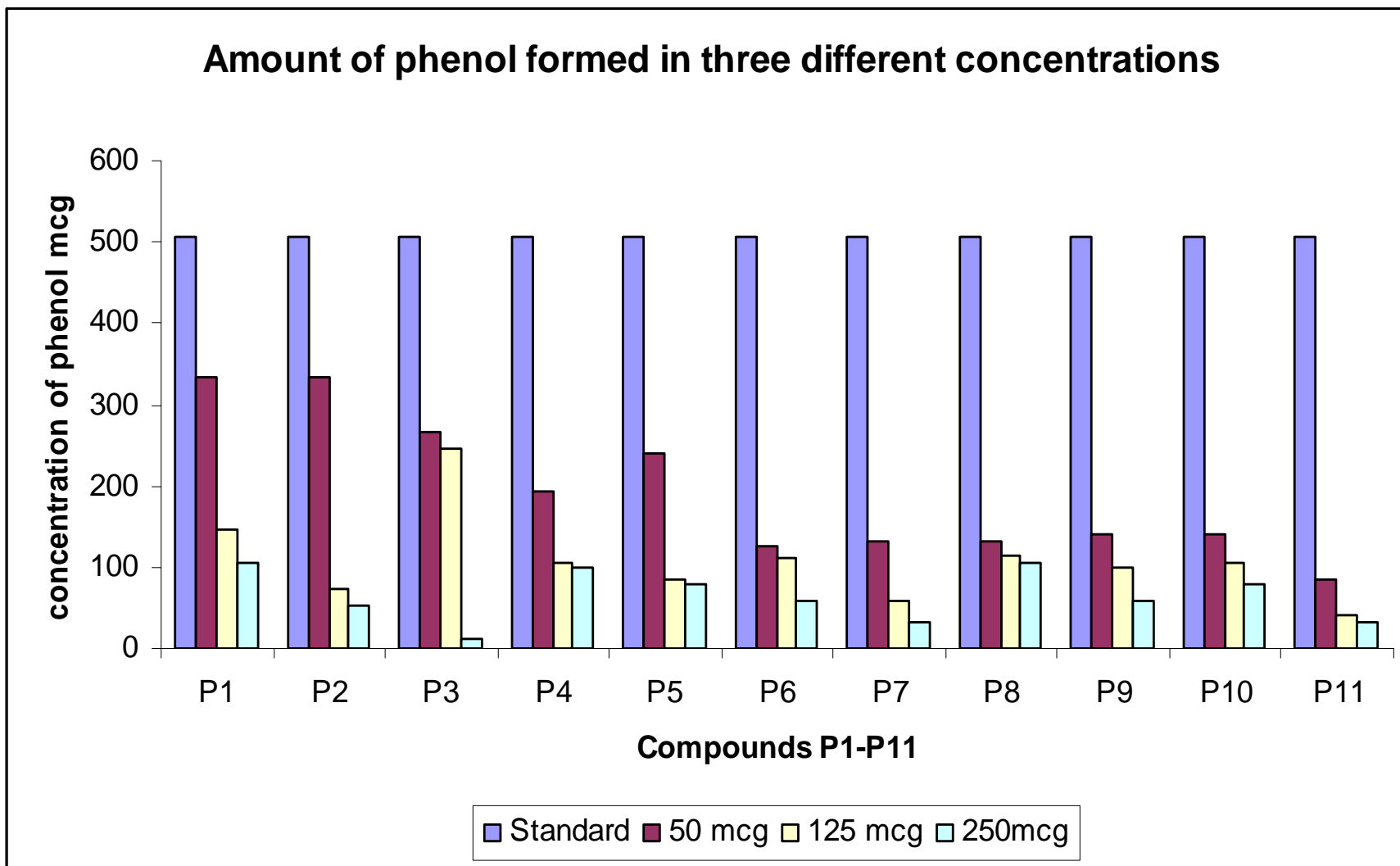


Figure 13.3 Phosphatase inhibitory activities of compounds P1-P11

14. SUMMARY AND CONCLUSION

The Aurora kinase family is a collection of highly related serine/threonine kinases that functions as a key regulator of mitosis. In mammalian cells, Aurora has evolved into three related kinases known as Aurora-A, Aurora-B, and Aurora-C. These kinases are over expressed in a number of human cancers, and transfection studies have established Aurora-A as a bone fide oncogene. Because Aurora over expression is associated with malignancy, these kinases have been targeted for cancer therapy.

So in the present study, it was decided to design some inhibitory lead compounds of Aurora kinase A as using computational tools like Catalyst (pharmacophore modeling) and GLIDE(structure based drug design/Docking).Then the designed compounds were synthesized and screened for anticancer studies.

Eighty two Aurora A kinase inhibitors from Medicinal Chemistry Journals were selected for modeling studies based on chemical and biological diversity. The selected molecules were then divided into 21 training set molecules and 61 test set molecules. Using the training set molecules pharmacophore models (hypothesis) were generated in Hypogen (Catalyst). The most active molecule in the training set fits very well with the top scoring pharmacophore hypothesis.

The best hypothesis consists of one hydrogen bond acceptor, one hydrophobic aliphatic and two ring aromatics. The best hypothesis Hypo-1 is characterized by the highest cost difference (58 bits), lowest RMS deviation (1.30) with a correlation of 0.94The best pharmacophore hypothesis was used to screen the 61 Aurora A Kinase inhibitors in the Aurora kinase inhibitor data base.

The model developed was shown to be a good model with 0.65 as Goodness of Hit score (GH) and a enrichment factor of 1.154.

GLIDE was the docking program used for the structure based drug design.

The 82 Aurora A inhibitors used for the pharmacophore studies were considered for docking study to develop comparative model. Out of the 82 inhibitors 21 were used in the training set. Crystal structure of Aurora A (PDB code: Imq4) was employed for the docking studies Structure based docking studies were carried out using Glide on Aurora A kinase inhibitors to the 3D structure of Aurora A kinase and generated 50 best docking

poses. The best poses were selected based on the scoring functions and poses orientation with the active site amino acids.

To get a better VS model, a MLR analysis was carried out using pharmacophore model and the docking scoring function. A combination of Pharmacophore model, GLIDE SP dock score gave a good model.

The VS model obtained was further used to search the virtual library consisting of 10,000 structurally diversified molecules generated using fragment and knowledge based design, which yielded 300 molecules as potent Hits.

The hits obtained were used for PASS prediction studies. A consensus was obtained between the docking scores and the PASS prediction values and finally 40 Hits were selected for synthesis and screening. The docking scores >-7 and prediction values above 0.6 were taken into consideration. PASS predicted some of the molecules to be active against colorectal cancer (1A-29A) and some other molecules to be inhibitors of phosphatase enzyme (P1-P11).

A Drug likeness screening was carried out for all the 40 Hits including Lipinski rule of five and Toxicity assessment. All most all the compounds exhibited 2 violations of the Lipinski rule which was found to be normal with anticancer drugs. It is proven that kinase inhibitors in general have high molecular weight and LogP values. So these violations were accepted in the present study.

In toxicity assessment all the compounds showed Green colour code except nine molecules having nitro and dimethyl amino substitution exhibiting mutagenicity and Tumorigenicity. But still these molecules were also included in the *in vitro* screening because so many active scaffolds have these substructures and their activities were also predicted to be good. These hits can be further refined to reduce the unwanted reactions by including detoxifying sub structures.

The designed molecules have piperidine-4-ones scaffold attached with 2-Aminopyrimidine (1A-29A) and 2-Pyrazoline (P1-P11) substructures.

The Schiff bases and Mannich bases of piperidine-4-ones were synthesized according to the synthetic scheme and characterized by IR, ^1H NMR, ^{13}C NMR, COSY NMR and Mass spectroscopy.

The compounds were subjected to *in vitro* anticancer studies in colorectal cell lines (1A-29A). The compounds 21A and 25A show the least IC₅₀ values 0.01 and 0.01 respectively. The compound 21A maintains the same level of activity through out the working range (0.01-100 μM). There is no concentration related gradation in the activity profile. In the case of compound 25A, the peak activity is noted in the minimum concentration of 0.01 μM itself. Even though there is a decrease in the activity with increase in the concentration, the activity profile remained well above the required level. The other compounds showing significant activity are 3A, 10A, 13A and 26A. The compounds 6A, 9A and 16A show less activity with IC₅₀ values in the range of 10 μM. All the other compounds showed moderate activity with IC₅₀ values in the range of 1-5 μM.

The compounds P1-P11 were subjected to phosphatase inhibition activity. The compounds P1-P11 were used in three concentration levels (50/125/250mcg). The absorbances of these solutions were measured at 620nm after carrying out the assay with Folin's reagent. The concentrations of the phenol formed in these solutions were obtained from the standard graph of phenol.

From the analysis of the data it can be seen that all the compounds P1-P11 are possessing phosphatase inhibition activity. In addition to that they also show a gradation in their dose response. All the compounds show less inhibition at 50 mcg, moderate inhibition at 125 mcg and a fairly good inhibition at 250 mcg.

The compounds P1-P11 have 2-pyrazoline moiety as a sub structure in common. The compounds P1-P5 at 50 mcg concentration level shows very less inhibition. A concentration dependent increase in inhibitory activity was observed with P1, P2, P3, P4, and P5. That is better inhibitory activity was observed with higher concentrations (250 mcg).

The compounds P6-P11 showed better inhibition in all the three concentration levels. In all these compounds the C3 of piperidin-4-one ring contain isopropyl group which may contribute to the increase in inhibitory activity.

Of all compounds, the compound P3 at the 250mcg concentration level shows best activity. Thus the compounds P3, P7 and P11 can be further developed to get effective phosphatase inhibitors.

By arriving at the leads 21A and 25A for anticancer activity, the aim of the work to develop leads for anticancer activity was fulfilled. These analogues can be novel templates for lead optimization purpose in cancer chemotherapy.

To conclude the anticancer leads obtained in this study can be refined further to get a potent anticancer molecules. Drugs targeting multiple kinases have proven to be effective against treatment of various diseases. The activities of serine/threonine protein phosphatases needs further study, but it is clear that these enzymes are potential targets for novel therapeutics with applications in many diseases, including cancer, inflammatory diseases and neuro degeneration.

Computational techniques have provided starting points for designing multiple inhibitors against individual targets using crystal structural information of kinases and pharmacophore of kinase inhibitors. So these techniques can be explored further to design new drug candidates for various diseases.

REFERENCES

1. Donald J. Abraham, editor. *Burger's Medicinal Chemistry and Drug Discovery*. Volume 1: Drug Discovery Sixth ed. New York: John Wiley and Sons Inc., Publication; 2003.
2. Povl krogsgaard-Larsen, Tommy Liljefors and ulf Madsen, editors *Text book of drug design and discovery*. Third ed. London: Taylor and Francis: 2004.
3. Cohen NC, Blaney JM, Humblet C, Gund P, and Barry DC. *Molecular Modeling Software and Methods for Medicinal chemistry*. *J. Med. Chem.* 1990, 33(3): 883-894.
4. Salzmann M, Permshin K, Wider G, Senn H and Wuthrich K. [¹³C]-constant-time[¹⁵N, ¹H]-TROSY-HNCA for sequential assignments of large proteins *J. Biomol. NMR*, 1999; 14:85-88.
5. Hajduk PJ, Meadows RP and Fesik SW. *NMR-based screening in drug discovery*, *Q. Rev. Biophys.* 1999; 32(3):211-240.
6. Hajduk PJ, Sheppard G, Nettesheim DG, Olejniczak ET, Shuker SB, Meadows RP. *Discovery of Potent Non peptide Inhibitors of Stromelysin Using SAR by NMR*. *J. Am. Chem. Soc.* 1997; 119(25):5818-5827.
7. McDowell LM. and Schaefer J. *High-resolution NMR of biological solids* *Curr. Opin. Struct. Biol.* 1996; 6(5): 624-629.
8. Ishima R, Torchia DA. *Protein dynamics from NMR*. *Nat. Struct. Biol.*, 2000; 7:740-743.
9. McDowell LM, McCarrick MA, Studelska DR, Guilford WJ, Arnaiz D, Dallas JL. *Conformations of Trypsin-Bound Amidine Inhibitors of Blood Coagulant Factor Xa by Double REDOR NMR and MD Simulations*. *J. Med. Chem.*, 1999; 42(19):3910- 4918.
10. Moore JM. *NMR techniques for characterization of ligand binding: Utility for lead generation and optimization in drug discovery* *Biopolymers*, 1999; 51(3):221-243.
11. Fejzo J, Lepre CA, Peng JW, Bemis GW, Ajay, Murcko MA, and Moore JM. *The SHAPES strategy: an NMR-based approach for lead generation in drug discovery* *Chem. Biol.* 1999; 6(10): 755-769.
12. Dinsmore CJ, Bogusky MJ, Culberson JC, Bergman JM, Homnick CF, Zartman CB, *et al.* *Conformational Restriction of Flexible Ligands Guided by the Transferred NOE Experiment: Potent Macrocyclic Inhibitors of Farnesyltransferase*. *J. Am. Chem. Soc.* 2001; 123(9), 2107-2108.

13. Hajdu J, Neutze R, Sjogren T, Edman K, Szoke A, Wilmouth R, and CM,Wilmot, Analyzing protein functions in four dimensions *Nat. Struct. Biol.*, 2000; 7(11):1006-1012.
14. Perrakis A, Morris R, and Lamzin VS. Automated protein model building combined with iterative structure refinement *Nat. Struct. Biol.*, 1999; 6(5):458-463.
15. Beddell CR, Ed. *The Design of Drugs to Macromolecular Targets*, New York;John Wiley & Sons: 1992.
16. Kuntz ID. Structure-Based Strategies for Drug Design and Discovery. *Science*, 1992; 257: 1078-1082.
17. Finn PW and Kavradi LE. Computational Approaches to Drug Design. *Algorithmica*, 1999; 25(2-3):347-371
18. Joseph-McCarthy D. Computational approaches to structure-based ligand design. *Pharmacol. Ther.* 1999; 84:179-191.
19. Mezey PG. Computer Aided Drug Design: Some Fundamental Aspects. *J. Mol. Model.* 2000; 6(2):150-157.
20. Meyer EF, Swanson SM, and Williams JA, Molecular modelling and drug design *Pharmacol. Ther.* 2000; 85 (3):113-121.
21. Schnecke V Kuhn LA. Virtual screening with solvation and ligand-induced complementarity. *Perspect. Drug Discov. Des.* 2000; 20(1): 171-190.
22. Oldenburg KR., Annual report in medicinal chemistry. Bristol JA, editor. London: Academic Press; 1998; Vol. 33: 301.
23. Kingston DG .The practice of Medicinal chemistry. Wermuth CG. Editor .London: Academic Press; 1996; Vol. 1:101.
24. Hobbs de Witt S. The practice of Medicinal chemistry. Wermuth CG. Editor. London: Academic Press; 1996; Vol. 1:117.
25. Arup K Ghose and John J. Wendoloski. Pharmacophore modelling: methods, experimental verification and applications. *Perspectives in Drug Discovery and Design.* 1998; Vol. 9/10/11(0): 253-271.
26. Ferguson AM, Patterson DE, Garr C and Underiner T. Designing Chemical Libraries for Lead Discovery. *J. Biomol. Screen.* 1996; 1(2): 65-73.
27. Young SS, Sheffield CF and Farnen M. Optimum Utilization of a Compound Collection or Chemical Library for Drug Discovery. *J.Chem.Inf.Comput.Sci.* 1997; 37(5) 892-899.

28. Potter, T. and Matter H. Random or Rational Design? Evaluation of Diverse Compound Subsets from Chemical Structure Databases. *J Med Chem* 1998; 41(4): 478-488.
29. Toney JH, Fitzgerald PM, Grover- Sharma N, Olson SH, May WJ, Sundelof JG et al. Antibiotic sensitization using biphenyl tetrazoles as potent inhibitors of *Bacteroides fragilis* metallo- β -lactamase. *Chem. Biol.*, 1998; 5(4), 185-196.
30. Grueneberg S, Wendt B and Klebe G. Sub nanomolar Inhibitors from Computer Screening: A Model Study Using Human Carbonic Anhydrase II. *Angew. Chem. Int. Ed. Engl.*, 2001; 40(2):389-393.
31. Boehm HJ,Boehringer M,Bur D,Gmuender H, Huber W, Klaus W,et al. Novel Inhibitors of DNA Gyrase: 3D Structure Based Biased Needle Screening, Hit Validation by Biophysical Methods, and 3D Guided Optimization. A Promising Alternative to Random Screening. *J. Med. Chem.*, 2000; 43(14): 2664-2674.
32. Burley SK An overview of structural genomics. *Nat.Struct.Biol.*2000;7(11):932-934.
33. Abagyan R and Totrov M. High-throughput docking for lead generation *Curr. Opin. Chem. Biol.* 2001; 5(4): 375-382.
34. Muegge I and Rarey M. *Reviews in Computational Chemistry*, Lipkowitz KB and. Boyd D B, Editors, Wiley-VCH, New York,2001;Vol. 17:1-60.
35. Smith GR and Sternberg MJ. Prediction of protein–protein interactions by docking methods *Curr.Opin. Struct. Biol.* 2002; 12(1):28-35
36. Camacho CJ and Vajda S, Protein–protein association kinetics and protein docking. *Curr. Opin. Struct. Biol.*, 2002; 12(1):36-40.
37. Adrian H, Elcock, Sept D, and. McCammon JA. Computer Simulation of Protein- Protein Interactions *J. Phys. Chem. B*, 2001;105:1504-1518.
38. Shoichet BK and Kuntz ID. Predicting the structure of protein complexes : a step in the right direction *Chem. Biol.*, 1996; 3(3):151-156.
39. Sternberg MJ, Gabb HA and. Jackson RM. Predictive docking of protein—protein and protein—DNA complexes *Curr. Opin. Struct. Biol.* 1998; 8(2):250-256.

40. Filikov AV, Mohan V, Vickers TA, Griffey RH., Cook PD, Abagyan RA. and James TL., Identification of ligands for RNA targets via structure-based virtual screening: HIV-1 TAR. *J. Computer Aided Mol. Des.* 2000; 14(6):593.
41. Clark DE, Murray CW, and Li J .Reviews in Computational Chemistry, Lipkowitz KB and Boyd DB. Editors. Wiley- VCH, New York: 1997; Vol. 11:67-125.
42. Petsko GA Not just your average structures. *Nature* 1996; 3: 565 – 566.
43. Blundell TL, Sibanda BL, Sternberg MJE ,Thornton JM. Knowledge-based prediction of protein structures and the design of novel molecule. *Nature*, March 1987;326:347 - 352.
44. Martin JL. Protein Crystallography and Examples of its Applications in Medicinal Chemistry. *Curr. Med. Chem.* 1996; 3(6): 419-436.
- 45.. Zuiderweg ERP, Van Doren, SR, Kurochkin AV, Neubig RR. and Majumdar A. Modern NMR spectroscopy of proteins and peptides in solution and its relevance to drug design Perspectives in Drug Discovery and Design 1993;1: 391-417.
46. Bernstein FC, Koetzle TF, Williams GJB, Meyer EF, Brice MD, Rodgers JR., The protein data bank:A computer-based archival file for macromolecular structures *J. Mol. Biol.* 1977; 112(3): 535.
47. Hans.-Joachim Bohm and Klebe G. What Can We Learn from Molecular Recognition in Protein-Ligand Complexes for the Design of New Drugs? *Angew. Chem., Int. Ed. Engl.* 1996; 35(22), 2588-2614
- 48 Chothia, C. One thousand families for the molecular biologist. *Nature* 1992, 357, 543.
49. Moult J, Hubbard T, Bryant SH, Fidelas K and Pedersen JT. Critical assessment of methods of protein structure prediction (CASP): Round II. *Proteins* 1997; 29(Supp.1):2-6.
50. Janin J. Elusive affinities. *Proteins Struct. Funct. Genet.* 1995; 21(1):30-39.
51. Marrone TJ, Briggs JM and McCammon JA. Structure-Based Drug Design: Computational Advances. *Annu. Rev. Pharmacol. Toxicol.* 1997; 37: 71-90.
52. Murcko MA. Reviews in Computational Chemistry. Lipkowitz KB and Boyd DB. Editors. Wiley-VCH: New York; 1997; Vol. 17: 1-66.
53. Traxler P, Green J, Mett H, Sequin U, and Furet P. Use of a Pharmacophore Model for the Design of EGFR Tyrosine Kinase Inhibitors: Isoflavones and 3-Phenyl-4(1H)-quinolones. *J. Med. Chem.* 1999; 42(6): 1018-1026.
54. Traxler P, Bold G, Buchdunger E, Caravatti G , Furet P , Manley P , et al. Tyrosine kinase inhibitors: From rational design to clinical trials. *Med. Res. Rev.* 2001; 21(6):499- 512.

55. Bureau R, Daveu C, Lancelot JC and Rault S. Molecular Design Based on 3D-Pharmacophore. Application to 5-HT Subtypes Receptors. *J.Chem. Inf. Comput. Sci.* 2002; 42(2): 429-436.
56. Appelt K, Bacquet RJ, Bartlett CA, Booth CLJ, Freer ST, Fuhry MAM, Design of enzyme inhibitors using iterative protein crystallographic analysis. *J. Med. Chem.*1991; 34(7): 1925-1934.
57. Kuntz ID, Meng EC, and Shoichet BK. Structure-Based Molecular Design. *Acc. Chem. Res.*1994; 27(5), 117-123.
58. Babine RE and Bender SL. Molecular Recognition of Protein–Ligand Complexes: Applications to Drug Design *Chem. Rev.* 1997, 97(5), 1359-1472.
59. Greer J, Erickson JW, Baldwin JJ, and Varney MD. Application of the Three-Dimensional Structures of Protein Target Molecules in Structure-Based Drug Design. *J.Med. Chem.* 1994; 37 (8):1035-1054.
60. Ooms F. Molecular Modeling and Computer Aided Drug Design. Examples of their Applications in Medicinal Chemistry. *Current Medicinal Chemistry*, 2000;7:141-158.
61. An introduction to Drug design by Pandeya SN and Dimmock JR. New age international publishers; First edition:1997;197-203.
62. Hansch C, and Fujita T. p - σ - π Analysis. A Method for the Correlation of Biological Activity and Chemical Structure. *J. Am. Chem. Soc.* 1964; 86(8): 1616-1626.
63. Topliss JG. Utilization of operational schemes for analog synthesis in drug design. *J. Med. Chem.* 1972; 15(10):1006-1011.
64. Craig PN. Interdependence between physical parameters and selection of substituent groups for correlation studies. *J. Med. Chem.* 1971; 14(8): 680-684.
65. Drews J. Drug Discovery: A historical perspective. *Science.* 2000;287:1960-1964.
66. Cushman DW, Cheung HS, Sabo EF, and Ondetti MA, Design of potent competitive inhibitors of angiotensin-converting enzyme. Carboxyalkanoyl and mercaptoalkanoyl amino acids. *Biochemistry.*1977; 16(25):5484-5491.
67. Ondetti MA, Rubin B, and Cushman DW. Design of specific inhibitors of angiotensin-converting enzyme: new class of orally active antihypertensive agents. *Science*, 1977; 196(4288):441-444.
68. Huff JR and Kahn J. Discovery and clinical development of HIV-1 protease inhibitors. *Adv. Protein Chem.*, 2001; 56: 213-251.

69. Wlodawer A, Vondrasek J. INHIBITORS OF HIV-1 PROTEASE: A Major Success of Structure-Assisted Drug Design. *Annu. Rev. Biophys. Biomol. Struct.* 1998; 27:249-284.
70. Meek TD. Inhibitors of HIV-1 protease. *J. Enzyme Inhibition.* 1992; 6: 65-98.
71. Wlodawer A. and Erickson JW. Structure-Based Inhibitors of HIV-1 Protease. *Annu. Rev. Biochem.*, 1993;62:543-585.
72. Copeland RA. *enzymes: A practical introduction to structure, Mechanism and Data analysis*, 2nd edition, New York: Wiley-VCH:2000.
73. Washtien WL, Increased levels of thymidylate synthetase in cells exposed to 5-fluorouracil. *Mol. Pharmacol.* 1984; 25(1):171-177.
74. Doris R. Seeger, Donna B. Cosulich, James M. Smith, Martin E. Hultquist. Analogs of Pteroylglutamic Acid. III. 4-Amino Derivatives. *J. Am. Chem. Soc.* 1949; 71(5):1753-1758.
75. Matthews DA, Alden RA, Bolin JT, Freer ST, Hamlin R, Xuong N, et al. Dihydrofolate reductase: x-ray structure of the binary complex with methotrexate. *Science*, 1977; 197 (4302), 452-455.
76. Stark GR and Bartlett PA. Design and use of potent, specific enzyme inhibitors. *Pharmacol. Ther.* 1983; 23(1):45-78.
77. Segel IH., *Enzyme Kinetics: Behavior and Analysis of Rapid Equilibrium and Steady-State Enzyme Systems*, Wiley-Inter science, New York, 1975.
78. Shaw E in *Chemical Modification by Active-Site Directed Reagents*, P. D. Boyer, Ed., Academic Press, New York, 1970, pp. 91-147.
79. Lundblad RL., *Chemical Reagents for Protein Modification*, 2nd ed., CRC Press, Boca Raton FL, 1991.
80. Hixson Jr HF and Nishikawa AH. *Arch. Biochem. Biophys.* Affinity chromatography: Purification of bovine trypsin and thrombin. 1973; 154(2):501-509.
81. Skorey KI, Johnson NA, Huyer G, and Gresser MJ. *Protein Express. Purifi.* A Two-Component Affinity Chromatography Purification of Helix pomatia Arylsulfatase by Tyrosine Vanadate. 1999; 15(2):178- 187.
82. Norris FA and Majerus PW, Hydrolysis of phosphatidylinositol 3,4-bisphosphate by inositol polyphosphate 4-phosphatase isolated by affinity elution chromatography. *J. Biol. Chem.*, 1994; 269(12):8716-8720.
83. Knockaert M, Gray N, Damiens E, Chang YT, Grellier P, Grant K, et al. Intracellular targets of cyclin-dependent kinase inhibitors: identification by affinity chromatography using immobilised inhibitors. *Chem. Biol.* 2000; 7(11):411-422.

84. Fowler JS, MacGregor RR, Wolf AsP, Arnett CD, Dewey SL, Schlyer D, et al., Mapping human brain monoamine oxidase A and B with ¹¹C-labeled suicide in activators and PET. *Science*, 1987; 235(4787):481-485.
85. Muscate A, Levinson CL, and Kenyon GL .Kirk-Othmer Encyclopedia of Chemical Technology, 4th. ed, Howe-Grant M, Ed., John Wiley & Sons, New York, 1994,644-671.
86. Berman HM, Westbrook J, Feng Z, Gilliland G, Bhat TN, Weissig H. The Protein Data Bank. *Nucleic Acids Res.* 2000; 28:235-242.
87. Dror O, Shulman-Peleg A, Nussinov R, Wolfson H J. Predicting molecular interactions in silico: I. A guide to pharmacophore identification and its applications to drug design. *Curr Med Chem.* 2004 Jan; 11(1):71-90.
88. Hindle SA, Rarey M, Buning C, Lengae T. Flexible docking under pharmacophore type constraints. *J Comput Aided Mol Des.* 2002 Feb; 16(2):129-49.
89. Dina Schneidman-Duhovny, Ruth Nussinov and Haim J. Wolfson. Predicting Molecular Interactions in silico: II. Protein-Protein and Protein- Drug Docking. *Current Medicinal Chemistry*, 2004; 11(1): 91-107.
90. Ehrlich P. Über den jetzigen Stand der Chemotherapie. *Dtsch. Chem.Ges.* 1909, 42:17-47.
91. Osman F. Guner, Douglas R. Henry. Metric for Analyzing Hit Lists and Pharmacophores. In *Pharmacophore Perception, Development, and Use in Drug Design*, Osman F. Guner., Ed.; International University Line: La Jolla, California, 2000; 193-210.
92. Bures MG, Black-Schaefer C and Gardner GJ. The discovery of novel auxin transport inhibitors by molecular modeling and three-dimensional pattern analysis. *Comput.-Aided Mol. Des*, 1991; 5, 323-334.
93. Thierry Langer and Rémy D. Hoffmann *Pharmacophores and Pharmacophore Searches* Raimund Mannhold, Hugo Kubinyi ,Gerd Folkers.Editors. Wiley-Interscience, New York. 2006.
94. Catalyst 4.11 User Guide, Accelrys Inc., San Diego, CA 92121, USA, 2005.
95. Debnath, AK. Pharmacophore mapping of a series of 2, 4-diamino-5- deazapteridine inhibitors of Mycobacterium avium complex dihydrofolate reductase. *J. Med.Chem.*2002; 45:41-53.
96. Kurogi Y,Güner OF. Pharmacophore modeling and three-dimensional database searching for drug design using catalyst. *Curr. Med. Chem.* 2001; 8: 1035–1055.

97. Morris GM, Olson AJ, Goodsell DS. Protein-ligand docking. *Methods. Princ. Med. Chem.* 2000; 8:31-48.
98. Mestres J, Knegtel RM. A. Similarity versus docking in 3D virtual screening. *Perspect. Drug Discovery Des.* 2000; 20: 191- 207.
99. Vieth M, Hirst JD, Dominy BN, Daigler H, Brooks CL. Assessing search strategies for flexible docking. *J. Comput. Chem.* 1998; 19: 1623-1631.
100. Gilson MK, Given JA, Bush BL, McCammon JA. The statistical-thermodynamic basis for computation of binding affinities: a critical review. *Biophys. J.* 1997; 72:1047-1069.
101. Monard G, Merz Jr. KM. Combined Quantum Mechanical/ Molecular Mechanical Methodologies Applied to Biomolecular Systems. *Acc. Chem. Res.* 1999;32:904-911.
102. Berman HM, Bhat TN, Bourne PE, Feng Z, Gilliland G, Weissig H et al. The Protein Data Bank and the challenge of structural genomics. *Nature.Struct.Biol.*2000;7: 957–959.
103. Westbrook, J.; Feng, Z.; Chen, L.; Yang, H.; Berman, H. M. The Protein Data Bank and structural genomics. *Nucleic Acid Res.* 2003; 31:489–491.
104. Blundell TL, Jhoti H., Abell C. High-throughput crystallography for lead discovery in drug design. *Nature Rev. Drug Discov.* 2002; 1: 45–54.
105. Chen H, Lyne PD, Giordanetto F, Lovell T, Li J. On evaluating molecular-docking methods for pose prediction and enrichment factors. *J.Chem.Inf.Model.* 2006; 46: 401-415.
106. Bissantz C, Folkers G, Rognan D. Protein-based virtual screening of chemical databases Evaluation of different docking/scoring combinations. *J.Med.Chem.*2000; 43:4759-4767.
107. Glen RC, Allen SC. Ligand-protein docking: cancer research at the interface between biology and chemistry. *Curr. Med. Chem.* 2003; 10:763-777.
108. Kitchen DB, Decornez H, Furr JR, Bajorath J. Docking and scoring in virtual screening for drug discovery: methods and applications. *Nat. Rev. Drug Discovery*, 2004; 3: 935-949.
109. Ingo Muegge, Istvan J. Enyedy. Virtual Screening of Kinase Targets. *Curr. Med. Chem.* 2004; 11: 693-707.
110. Gohlke H, Klebe G. Statistical potentials and scoring functions applied to protein-ligand binding. *Curr. Opin. Struct. Biol.* 2001; 11: 231–235.
111. Glide, version 3.5; Schrodinger, L.L.C., New York, 2006.
112. Friesner RA, Banks JL, Murphy RB, Halgren TA, Klicic JJ, Mainz DT, et al. Glide: a new approach for rapid, accurate docking and scoring. 1. Method and assessment of docking accuracy. *J. Med.Chem.* 2004; 47: 1739-1749.

113. Halgren TA, Murphy RB, Friesner RA, Beard HS, Frye LL, Pollard WT, Banks, JL. Glide: a new approach for rapid, accurate docking and scoring. 2. Enrichment factors in database screening. *J. Med. Chem.* 2004; 47: 1750-1759.
114. Philip M. Weintraub, Jeffrey S. Sabol, John M. Kane, David R. Borcharding. Recent advances in the synthesis of piperidones and piperidines. 2003 April; 59(17), 2947-3188.
115. Pelle Lidstrom, Jason Tierney, Bernard wathey and Jaco Westman. Microwave Assisted organic Synthesis – a Review. *Tetrahedron.* 2001; 57: 9225 – 9283.
116. Suresh C. Ameta and Sarika Mehta. Green Chemical pathways: a need of the day, *Journal of Indian Chem. Soc.*, 2004; 81:1127-1140.
117. Andrejus Korolkovas. *Essentials of medicinal chemistry*, 2nd edition, Wiley-Inter science, Newyork;1988;3.
118. Vogel AI, Tatchell AR, Furnis BS, Hannaford AJ Smith PWG. *Vogel's Textbook of practical organic chemistry*, 5th edition, Prentice Hall publishers; 1996; 798-800.
119. Brown DJ. *The chemistry of heterocyclic compounds. The pyrimidines.* Wiley interscience publishers, 1964;16:156.
120. Hanafi H Zoorob, Mohamed M. Abou. Elzabab, Momdouch Abdel-Mogib and MohamedA Ismail. Peculiar reaction behaviour of Barbituric acid derivatives towards aromatic amines, *Tetrahedron* 1996; 52:1047-1058
121. McCall JM, Kloosterman D and B.V.Kamdar, *Cyanoimine chemistry, New routes to pyrimidinones and carbonyl aminoimino propanamides.* *J.Org Chem.*1979;44: 1562-1563.
122. Babaev EV. *Molecular design of heterocycles(3). The last two component type of synthesis of pyridine ring by insertion of beta carbon atom.* *Hetero.Chem.*1993; 29: 818-824.
123. Prajapati Gohain D, Ashim J. Thakur. Regioselective one pot synthesis of pyrimido (4, 5-d) pyrimidine derivatives in the solid state under microwave irradiation. *Bioorg. And Med. Chem. Lett.* 2006; 16: 3537-3540.
124. Mohammad M, Matthew D. Hill, *Synthesis of pyrimidines by direct condensation of amides and nitriles.* *Nature Protocol.*2007; 2:2019.
125. Mehdi Adib, Mohammad hosein Sayahi, Mesiam Nosrati, Long-guan Zhu, *A Novel one pot synthesis of 4H-pyrido(1,2-a)pyrimidines.* *Tetrahedron letters.* 2007; 48: 4195-4198.

126. Maurilio Tramontini, Luigi Angiolini ,Further advances in the chemistry of Mannich bases. *Tetrahedron*, 1990; 46(6), 1791-2230.
127. Gerhard Klebe. Virtual ligand screening: Strategies perspectives and limitations. *Drug Discovery Today*, 2006 July; (11), Numbers 13/14:581-594.
128. Juswinder Singh, Zhan Deng, Gaurav Narale and Claudio Chuaqui. Structural Interaction Fingerprints: A New Approach to Organizing, Mining, Analyzing, and Designing Protein–Small Molecule Complexes. *Chem Biol Drug Des* 2006; 67: 5–12.
129. William L. Jorgensen. The Many Roles of Computation in Drug Discovery. *Science*, 2004 19 March; vol 303:1813-1818.
130. Giovanna Scapin. Structural Biology and Drug Discovery. *Current Pharmaceutical Design*, 2006; 12: 2087-2097.
131. Mitchell A. Miller. Chemical database techniques in drug discovery. *Nature reviews drug discovery* 2002 march; volume 1: 220-227.
132. Ricardo M. Biondi and Angel R. Nebreda. Signalling specificity of Ser/Thr protein kinases through docking-site-mediated interactions. *Biochem. J.* 2003; 372: 1–13.
133. Albert C. Pierce, Kathryn L. Sandretto, and Guy W. Bemis. Kinase Inhibitors and the Case for CH . . . O Hydrogen Bonds in Protein–Ligand Binding. *PROTEINS: Structure, Function, and Genetics.* 2002; 49:567–576.
134. Janet Dancey and Edward A. Sausville. Issues and progress with Protein kinase inhibitors for Cancer treatment. *Nature reviews drug discovery.*2003 April;2: 296-313.
135. Adrian Gill, Protein kinases in drug discovery and development. *Drug Discovery Today* 2004 January No1; Vol. 9: 16-17.
136. Dongyu Sun,Claudio Chuaqui, Zhan Deng, Scott Bowes, Donovan Chin, *et al.*A Kinase-focused Compound Collection: Compilation and Screening Strategy. *Chem Biol Drug Des* 2006; 67: 385–394
137. Gerhard Muller. Towards 3D Structures of G Protein-Coupled Receptors: A Multidisciplinary Approach. *Current Medicinal Chemistry*, 2000; 7: 861-888.
138. Martin EM. Noble, Jane A. Endicott, Louise N. Johnson. Protein Kinase Inhibitors: Insights into Drug Design from Structure. *Science.* March 2004; Vol 303:1800-1805.
139. Adeel Malik.Databases and QSAR for CancerResearch.*Cancer informatics.*2006;2:99-111.
140. Agnese V, Bazan V, Fiorentino FP, Fanale D, Badalamenti G, Colucci G, *et al.* The role of Aurora-A inhibitors in cancer therapy. *Annals of Oncology.* 2007; 18 (Supplement 6): vi47–vi52.

141. Cheetham GM, Knegtel RM, Coll JT, Renwick SB, Senson L, Weber P, *et al.* Crystal structure of aurora-2, an oncogenic serine-threonine kinase. *J. Biol Chem* 2002; 277:42419-42422
142. Lee EC, Frolov A, Li R, Ayala G, Greenberg NM. Targeting Aurora Kinases for the treatment of prostate cancer. *Cancer Res.* 2006; 66(10): 4996-5002.
143. Warner SL, Munoz RM, Stafford P, Koller E, Hurley LH, VonHoff DD, Han H. Comparing Aurora A and Aurora B as molecular targets for growth inhibition of pancreatic cancer cells. *Mol.cancer Ther.*2006; 5(10):2450-8.
144. Meraldi P, Honda R, Nigg EA. Aurora kinases link chromosome segregation and cell division to cancer susceptibility. *Curr Opin Genet Dev* 2004; 14:29-36
145. Mahadevan D, Bearss DJ, Vankayalapati H. Structure-based design of novel anticancer agents targeting aurora kinases. *Curr.Med.Chem. Anticancer agents*, 2003;3(1):25-34.
146. Nowakowski J, Cronin CN, Mcree DE, Knuth MW, Nelson CG, Pavletich NP, *et al.* Structures of the cancer related Aurora-A, FAK and EphA2 protein kinases from nano volume crystallography. *Structure* 2002; 10: 1659-1667.
147. Soncini C, Carpinelli P, Gianellini L, Fancelli D, Vianello P, Rusconi L, *et al.* PHA -680632, a novel Aurora kinase inhibitor with potent antitumoral activity. *Clin Cancer Res.* 2006 Jul 1; 12(13):4080-9.
148. Manfredi MG, Ecsedy JA, Meetze KA, Balani SK, Burenkova O, Chen W, *et al.* Antitumor activity of MLN8054, an orally active small molecule inhibitor of Aurora A Kinase. *Proc Natl Acad Sci. U S A.* 2007 Mar 6; 104(10): 4106-11.
149. Hari N. Pati, Umashankar Das, Swagatika Das, Brian Bandy, Erik De Clercq, Jan Balzarini, *et al.* The cytotoxic properties and preferential toxicity to tumour cells displayed by some 2,4-bis(benzylidene)-8-methyl-8-azabicyclo[3.2.1] octan-3-ones and 3,5-bis(benzylidene)-1-methyl-4-piperidones. *European Journal of Medicinal Chemistry* 2008; xx: 1-9, doi:10.1016/j.ejmech.2008.03.015.
150. Jonathan R. Dimmock, Amitabh Jha, Gordon A. Zello, J. Wilson Quail, Eliud O.Oloo, Kurt H. Nienaber, *et al.* Cytotoxic N-[4-(3-aryl-3-oxo-1-propenyl)phenylcarbonyl]-3,5-bis(phenylmethylene)-4-piperidones and related compounds. *European Journal of Medicinal Chemistry* 37 (2002) 961-972.
151. Vladimir Krystof, Petr Cankar, Iveta Frysova, Jan Slouka, George Kontopidis, Petr Dzubak, *et al.* 4-Arylazo-3, 5-diamino-1H-pyrazole CDK Inhibitors: SAR Study, Crystal Structure in Complex with CDK2, Selectivity, and Cellular Effects. *Journal of Medicinal Chemistry*, published on web 09/29/2006 page est.: 9.4
152. Nicholas Keen and Stephen Taylor. Aurora-Kinase inhibitors as anticancer agents. *Nature Reviews cancer.* Dec 2004; Vol 4:927-936.
- 153.. Fancelli D, Moll J, Varasi M, Bravo R, Artico R, Berta D. 4,5,6-tetrahydropyrrolo [3,4-c]pyrazoles: identification of a potent Aurora kinase inhibitor with a favorable antitumor kinase inhibition profile. *J.Med.Chem.*2006;49(24):7247-51.
154. Moriarty KJ, Koblisch HK, Garrabrant T, Maisuria J, Khalil E, Ali F, The synthesis and SAR of 2-amino-pyrrolo [2, 3-d] pyrimidines: a new class of Aurora-A kinase inhibitors. *Bioorg .Med. Chem. Lett.* 2006 Nov 15; 16(22):5778-83.
155. Fancelli.D, Moll.J, Varasi.M, Berta.D, Bindi.S, Cameron.A,etal. A.Potent and selective Aurora inhibitors identified by the expansion of a novel scaffold for protein kinase inhibition. *J.Med.Chem.*2005, 48(8), 3080-4.
- 156.. Harrington EA, Bebbington D, Moore J, Rasmussen RK, Ajose-Adeogun AO, Nakayama T, *et al.* VX-680, a potent and selective small-molecule inhibitor of the Aurora kinases, suppresses tumor growth in vivo. *Nat Med.* 2004 Mar; 10(3):262-7.

157. Pevarello P, Fancelli D, Vulpetti A, Amici R, Villa M, Pittalà V, 3-Amino-1,4,5,6-tetrahydropyrrolo[3,4-c]pyrazoles: a new class of CDK2 inhibitors. *Bio.org Med Chem. Lett.* 2006 Feb 15; 16(4):1084-90.
158. Heron NM, Anderson M, Blowers DP, Breed J, Eden JM, *et al.* SAR and inhibitor complex structure determination of a novel class of potent and specific Aurora kinase inhibitors. *Bioorg. Med. Chem. Lett.* 2006 Mar 1; 16(5):1320-3.
159. Carpinelli P, Ceruti R, Giorgini ML, Cappella P, Gianellini L, Croci V, *et al.* PHA-739358, a potent inhibitor of Aurora kinases with a selective target inhibition profile relevant to cancer. *Mol Cancer Ther.* 2007 Dec; 6(12 Pt 1):3158-68.
160. Coumar MS, Wu JS, Leou JS, Tan UK, Chang CY, Chang TY, Aurora kinase A inhibitors: identification, SAR exploration and molecular modeling of 6,7-dihydro-4H-pyrazolo-[1,5-a]pyrrolo[3,4-d]pyrimidine-5,8-dione scaffold. *Bioorg. Med Chem. Lett.* 2008 Mar 1; 18(5):1623-7.
161. Venkatraman Mohan, Alan C. Gibbs, Maxwell D. Cummings, Edward P. Jaeger and Renee L. DesJarlais. Docking: Successes and Challenges. *Current Pharmaceutical Design*, 2005; 11: 323-333.
162. Gareth Jones, Peter Willett and Robert C. Glen. Molecular recognition of receptor sites using a Genetic Algorithm with a Description of Desolvation. *J.Mol.Biol.* 1995; 245: 43-53.
163. Thomas Lengauer, Christian Lemmen, Matthias Rarey and Marc Zimmermann. Novel technologies for virtual screening. *Drug Discovery Today.* 2004 1 January; Vol. 9: 27-34.
164. Gregory L. Warren, Webster Andrews C, Anna-Maria Capelli, Brian Clarke, Judith LaLonde, Millard H. Lambert, *et al.* A Critical Assessment of Docking Programs and Scoring Functions. *J. Med. Chem.* 2006; 49: 5912-5931.
165. Richard A. Friesner, Robert B. Murphy, Matthew P. Repasky, Leah L. Frye, Jeremy R. Greenwood, Thomas A. Halgren, *et al.* Extra Precision Glide: Docking and Scoring Incorporating a Model of Hydrophobic Enclosure for Protein-Ligand Complexes. *Journal of Medicinal Chemistry.* 2006; 49 (21):6177–6196
166. Natasja Brooijmans and Irwin D. Kuntz. Molecular recognition and docking algorithms. *Annu. Rev. Biophys. Biomol. Struct.* 2003; 32:335–73.
167. Tanja Schulz-Gasch, Martin Stahl. Scoring functions for protein–ligand interactions: a critical perspective. *Drug discovery today: Technologies.* 2004; vol1, (3):231-239.
168. Hongming Chen, Paul D. Lyne, Fabrizio Giordanetto, Timothy Lovell, and Jin Li. On Evaluating Molecular-Docking Methods for Pose Prediction and Enrichment Factors. *J. Chem. Inf. Model.* 2006; 46: 401-415.
169. Maria Kontoyianni, Laura M. McClellan, and Glenn S. Sokol. Evaluation of Docking Performance: Comparative Data on Docking Algorithms. *J. Med. Chem.* 2004; 47:558-565.
170. Esther Kellenberger, Jordi Rodrigo, Pascal Muller, and Didier Rognan. Comparative Evaluation of Eight Docking Tools for Docking and Virtual Screening Accuracy. *PROTEINS: Structure, Function, and Bioinformatics.* 2004; 57:225–242.
171. Perola E, Walters WP, Charifson PS. A Detailed Comparison of Current Docking and Scoring Methods on Systems of Pharmaceutical Relevance. *Proteins* 2004; 56: 235-249.
172. Krovat EM., Steindl T, Langer T. Recent Advances in Docking and Scoring. *Curr. Comput.-Aided Drug Des.* 2005; 1: 93-102.
173. Camille G. Wermuth. Similarity in drugs: reflections on analogue design. *Drug Discovery Today*, 2006 April; Volume 11, Numbers 7/8: 348-354.

174. Gilbert M., Rishton. Reactive compounds and invitro false positives in HTS. Drug Discovery Today, 1997; 2, No9: 382-384.
175. Deng XQ, Wang HY, Zhao YL, Xiang ML, Jiang PD ,*et al.*. Pharmacophore modelling and virtual screening for identification of new Aurora-A kinase inhibitors. Chem Biol Drug Des. 2008 Jun; 71(6):533-9.
176. Roberto Di Santo, Maurizio Fermeglia, Marco Ferrone, Maria Silvia Paneni, Roberta Costi, Marino Artico, *et al.* Simple but Highly Effective Three-Dimensional Chemical-Feature-Based Pharmacophore Model for Di keto Acid Derivatives as Hepatitis C Virus RNA-Dependent RNA Polymerase Inhibitors. J. Med. Chem. 2005; 48: 6304-6314.
177. Maria L, Lopez-Rodríguez, Bellinda Benhamu, Tania de la Fuente, Arantxa Sanz, Leonardo Pardo, and Mercedes Campillo, A Three-Dimensional Pharmacophore Model for 5-Hydroxytryptamine₆ (5-HT₆) Receptor Antagonists. Journal of Medicinal Chemistry, 2005; 5:247-250.
178. Gisbert schneider and uli fechner. Computer based de novo design of drug like molecules. Nature reviews drug discovery .2005 August; volume 4:| 649-663.
179. Mark Rogers-Evans, Alexander I Alaninea, Konrad H. Bleichera, Dagmar Kubea, and Gisbert Schneidera B. Identification of novel cannabinoid receptor ligands via evolutionary de novo design and rapid parallel synthesis. QSAR Comb. Sci. 2004; 23:426-430.
180. Theodora Steindl and Thierry Langer. Docking Versus Pharmacophore Model Generation: A Comparison of High-Throughput Virtual Screening Strategies for the Search of Human Rhinovirus Coat Protein Inhibitors. QSAR Comb. Sci. 2005; 24:470-479.
181. Johannes Kirchmair, Gerhard Wolber, Christian Laggner, and Thierry Langer, Comparative Performance Assessment of the Conformational Model Generators Omega and Catalyst: A Large-Scale Survey on the Retrieval of Protein-Bound Ligand Conformations. J. Chem. Inf. Model. 2006; 46: 1848-1861.
182. Sukumar sakamuri, Istran J. Enyedy, Alan P. Kozikowski, Wahiduz A. Zaman, Kenneth M. Johnson and Shaomang weng. Pharmacophore-Based Discovery, Synthesis and Biological evaluation of 4-Phenyl 1-aryl alkyl piperidines as Dopamine Transporter inhibitors. Bioorganic and Medicinal Chemistry letters. 2001; 11:495-500.
183. Istvan J. Enyedy, a Sukumar Sakamuri, Wahiduz A. Zaman, Kenneth M. Johnsonb and Shaomeng Wang, Pharmacophore-Based Discovery of Substituted Pyridines as Novel Dopamine Transporter Inhibitors. Bioorganic & Medicinal Chemistry Letters. 2003; 13:513-517.
184. Min-Yong Li, Keng-Chang Tsai and Lin Xia. Pharmacophore identification of $\alpha 1A$ -adrenoceptor antagonists. Bioorganic & Medicinal Chemistry Letters. 2005; 15:657-664.
185. Istvan J. Enyedy, Wahiduz A. Zaman, Sukumar Sakamuri, Alan P. Kozikowski, Kenneth M. Johnson and Shaomeng Wang. Pharmacophore-Based Discovery of 3,4-Disubstituted Pyrrolidines as a Novel Class of Monoamine Transporter Inhibitors. Bioorganic & Medicinal Chemistry Letters. 2001; 11:113-1118.
186. Krisztina Boda and A. Peter Johnson. Molecular Complexity Analysis of de Novo Designed Ligands. J. Med. Chem. 2006; 49:5869-5879.
187. Theodora M. Steindl, Carolyn E. Crump, Frederick G. Hayden, and Thierry Langer. Pharmacophore Modeling, Docking, and Principal Component Analysis Based Clustering: Combined Computer-Assisted Approaches To Identify New Inhibitors of the Human Rhinovirus Coat Protein .J. Med. Chem. 2005; 48: 6250-6260.

188. Stepanchikova AV, Lagunin AA, Filimonov DA and Poroikov VV. Prediction of Biological Activity Spectra for Substances: Evaluation on the Diverse Sets of Drug-Like Structures. *Current Medicinal Chemistry*. 2003;10:225-233.
189. Poroikov VV and Filimonov DA. How to acquire new biological activities in old compounds by computer Prediction. *Journal of Computer-Aided Molecular Design*, 2002; 16: 819–824.
190. Vladimir V. Poroikov, Dmitrii A. Filimonov, Wolf-Dietrich Ihlenfeldt, Tatyana A. Glorizova, Alexey A. Lagunin, Yulia V. Borodina, Alla V. Stepanchikova, and Marc C. Nicklaus. PASS Biological Activity Spectrum Predictions in the Enhanced Open NCI Database Browser. *J. Chem. Inf. Comput. Sci.* 2003; 43: 228-236.
191. Alka Marwaha. Goel RK and Mohinder P. Mahajan. PASS-Predicted design, synthesis and biological evaluation of cyclic nitrones as nootropics. *Bioorganic & Medicinal Chemistry Letters*. 2007; 17: 5251-5255.
192. Athina Geronikaki, Eugeni Babaev, John Dearden, Wim Dehaen, Dmitrii Filimonov, Irina Galaeva *et al.* Design, synthesis, computational and biological evaluation of New anxiolytics. *Bioorganic and Medicinal Chemistry*. 2004;12:6559-6568.
193. Hugo Kubinyi. Drug research: myths, hype and reality. *Nature reviews Drug Discovery* volume .2003; august, 2:665-668.
194. Nouri Neamati and Joseph J. Barchi, Jr. New Paradigms in Drug Design and Discovery. *Current Topics in Medicinal Chemistry*. 2002; 2: 211-227.
195. Tobias Wunberg, Martin Hendrix, Alexander Hillisch, Mario Lobell, Heinrich Meier, Carsten Schmeck, *et al.* Improving the hit-to-lead process: data-driven assessment of drug-like and lead-like screening hits. *Drug Discovery Today*, 2006 February; Volume 11, Number 3/4:175-180.
196. Noller CR and Baliah V. The Preparation of Some Piperidine Derivatives by the Mannich Reaction. *J. Am. Chem. Soc.* 1948; 70:3853-3855.
197. Andreev .LVOT, Shashikina MN, StaniShevskit LS and Tischenko IG, *Mol. Biol.*, 1974;100-7. *Chem. Abstr.*, 85,87112q(1976).
198. Jerome Bagely. R and Kenneth Spencer. H., *Eur. pat.* 277, 794 (1988); *Chem. Abstr.*, 109, 230817v 1988.202
199. Baracu, Ilena, Dobre and Niculescu Duvaz. I., *J. Prakt. chem.* 1985; 327(4):667 *Chem. Abstr.*, 148699w(1986).
200. Balasubramanian M and Padma. N. *Tetrahedron*. Studies on conformation: Preparation and stereochemistry of some 4-piperidinols 1963; 19(12): 2135-2143
201. Ebersberg. J and Haller. Rolf. *Arch. Pharm. (Wainheim)*, 1969;302(4):248 *Chem. Abstr.* 71, 1294z(1969).
202. Ganapathy. K and Vijayan. B. *Indian. J. Chem. Soc.* 1983; Vol. LX:572-574,
203. Ganellin CR and spickett RGW. Compounds affecting the central nervous systems: 1, 4-piperidones and related compounds. *Journal of Medicinal Chemistry*, 1965; 8(5):619-625.
204. Dharmarajan sriram, perumal yogeswari and kasinathan Madhu., *Bioorganic and Medicinal chemistry letters*. 2005; 15: 4502-4505.
205. Kabilan. S, Aridoss G, .Balasubramanian S, Parthiban P. *European Journal of medicinal chemistry*. Synthesis, stereochemistry and antimicrobial evaluation of some *N*-morpholinoacetyl-2,6-diaryl piperidin-4-ones .2007; 42:851-860.
206. Dharmarajan Sriram, Perumal Yogeewari, Prathiba Dhakla, Palaniappan Senthil kumar and Debjani Banerjee., *Bioorganic & Medicinal Chemistry Letters* 2007; 17:1888-1891.
207. Mobio IG, Soldatenkov AT, Federov VO. Ageev EA, Sergeeva. ND. *KhimFarm. Zh.*, 1989;23(4):4214. *Chem. Abstr*, 112,7331y(1990).

208. Achille Barco, Nikla Baricordi, Simonetta Benetti, Gisella Biondini, Carmela De Risi and Gian Piero Pollini. Diastereoselective synthesis of 2-substituted Piperidine-4-ones as convenient precursors for an asymmetric approach to carbacephams. *Tetrahedron*, 2003 October; 59(42): 8439-8444.
209. Hassan MMA and CasyA.F. PMR studies of N-substituted 2,5-dimethyl-4-Piperidones. *Organic Magnetic Resonance*, 1970 April; 2(2):197-208.
210. Scherer T, Hielkema.W, Krijnen.B, Hermant R.M, Eijckelhoff C, Kerkhof F, *et al.* Synthesis and exploratory photophysical investigation of donor-bridge-acceptor systems derived from N-substituted 4-piperidones. *Recl.Trav.Chim.Pays-Bas*. 1993; 112/10:535-548.
211. Rolf W. Hartmann, Martin Reichert. New Nonsteroidal Steroid 5 α -Reductase inhibitors. Syntheses and Structure-Activity Studies on Carboxamide Phenylalkyl-Substituted Pyridones and Piperidones. *Archiv der Pharmazie*. May2000; Volume 333(5), 145-153.
212. Philip M.Weintraub, Jeffrey S.Sabol, John M.Kane and David R.Borcherding. Recent advances in the synthesis of piperidones and piperidines. *Tetrahedron*. 2003; 59(17):2953-2989.
213. Sampathkumar R , Sabesan R and Krishnan S. Infrared characterization of 2,6-diaryl-4-piperidones. *Journal of Molecular Liquids*.2006; 126:130-134.
214. Venkatesan J, Pandeya. Synthesis and Biological evaluation of 4, 6–diaryl substituted –4, 5 –dihydro- pyrimidiyl –2- ureas, *Indian Drugs* 2005; 42 (7):447– 452.
215. El-Hashash MA, Mahmoud MR, Madboli. SA. 'A Facile one – pot conversion of chalcones to pyrimidine derivatives', *Indian. J. Chem.* 1993; 32 B: 449 – 452.
216. Guanglin Luo, Ling Chen, Graham S Poindexter. Microwave assisted synthesis of amino pyrimidines *Tetrahedron letters*, August 2002; Vol 43 Issue 33: 5739-5742.
217. Anjani Solankee and Jayesh Patel. 'Synthesis of chalcones, pyrazolines, amino-pyrimidine, pyrimidines -thiones' *Indian Journal of Chemistry* July 2004; Vol.43B: 1580 – 1584.
218. Amol Bhendkar AG, Doshi AW Raut. Synthesis and antimicrobial activity of 2 Amino – 4 (2' – furyl) –6- (Substituted phenyl) Pyrimidine derivatives. *Oriental. J. Chem.* 2003; 19(3):731 – 732.
219. Patel HS, Patel VK and. Dixit BC . Synthesis and antimicrobial activity of novel 2-amino-4- naphthyl-6-substituted phenyl pyrimidines, *Oriental. J. of Chem.* 2001; 17(3): 411– 414.
220. Kiran. S. Nimaral, K.H. Popat, S.L. Vasoya.. Synthesis of some new pyrimidine derivatives, *Indian. J. of Heterocyclic Chemistry*. 2003; 12:217 – 220.
221. Pasha MA, Ramachandra Swamy N and Jayashankara VP. One pot synthesis of 3, 4 dihydro-pyrimidin 2(1H)-ones /-thiones catalyzed by zinc chloride. *Indian Journal of chemistry*. April 2005; Vol. 44B: 823-826.
222. Mandhare PN, Rindhe SS, Patil LR and. Mane RA. Synthesis of substituted amino-pyrimidine derivatives, *In. J. of Hetero. Cyclic. Chem.* 2003;12:209 – 212.
223. Raga Basavaraj, Ahmad Ali, Omkar khandre and S.S.Sangapure. Synthesis of some new pyrazolines, isoxazoles and pyrimidines as potential Antimicrobial agents. *Indian Journal of Heterocyclic chemistry*, 2007; vol 17; 11-14.

224. Hiroatsu Matsumoto, Kazuyoshi Ikeda, Nobuyuki Nagata, Hiroaki Takayanagi, Yoshihisa Mizuno, Motohiro Tanaka and Takuma Sasaki Synthesis of 2, 8-Disubstituted Imidazo[1,5-*a*]pyrimidines with Potent Antitumor Activity. *J. Med. Chem.*, 1999; 42 (9):1661–1666.
225. Olcay Bekircan , and Hakan Bektas . Synthesis of Schiff and Mannich Bases of Isatin Derivatives with 4-Amino-4, 5-Dihydro-1H-1, 2, 4-Triazole-5-Ones. *Molecules* 2008; 13: 2126-2135.
226. Krishna C Joshi, Anushu Dandia and Sunita Bhagat. Studies in spiro Heterocycles: Part XXV-Synthesis of new fluorine containing 3'-phenyl spiro[3H-indole-3,2'-thiazolidine]-2,4'(1H)-diones and novel(2,3-dihydro-2-oxo-3-phenylamino-1H-indol-3-ylthio) ethanoic acid as antibacterial agents. *Indian Journal of chemistry*, August1990; 29(B):766-770.
227. Chakraborti SK and Barun Kumar DE. Synthesis of pyrimidine Schiff bases as potential anticancer agents. *J. Indian Chem. Soc.* Feb1973; Vol L: 137-138.
228. Khalafallah AK, .Hassan ME and. Soleman HA .Synthesis and Biological studies on some spiro schiff base derivatives. *J. Indian Chem. Soc.* 1992; Vol 69:318-320.
229. Hemant panwar, Verma RS, Srivatsava VK and Ashok kumar. Synthesis of some substituted azetidinyll and thiazolidinonyl-1, 3, 4- thiadiazino{6,5-b}indoles as prospective antimicrobial agents. *Indian Journal of Chemistry*.2006 Sep; Vol 45B: 2099-2104.
230. Upadhyay TM and. Barot VM. Synthesis and biological evaluation of some new pyrazolines. *Indian Journal of Heterocyclic Chemistry*, 2006; Vol 15:393-394.
231. Palaska E, Erol D, Demirdamar R. Synthesis and antidepressant activities of some 1,3 R,5-triphenyl -2-pyrazolines. *Eur. J. Med. Chem*, 1996; 31:43-47.
232. Mohammad Abid, Abdul Roouf Bhat, Fareeda Athar, Amir Azam. Synthesis, spectral studies and anti amoebic activity of new 1-N-substituted thiocarbamoyl-3-phenyl-2-pyrazolines. *European Journal of Medicinal chemistry*.2007; xx: 1-9.
233. Amol H. Bhendkar, A.G.Doshi and A.W.Raut. Synthesis and antimicrobial activity of 1 -acetyl- 3- (2-Furyl) -5- (substituted phenyl) - pyrazolines. *Oriental journal of Chemistry*, 2003; Vol 19(3):721-722.
234. Vineet Malhotra, Seema pathak, Rajendra Nath, Devashis Mukerjee and Kirpa Shanker. Substituted pyrazolines and their cardiovascular activity. *Indian journal of chemistry*, 2002; 41(B):1310-1313.
235. Werner Seebacher, Gunther Michl, Ferdinanad Belaj, Reto Brun, Robert Saf and Robert Weis. One-pot syntheses of 2-pyrazoline derivatives. *Tetrahedron*, 2003; 59: 2811-2819.
236. Asha Budakoti, Abdul R. Bhat, Fareeda Athar, Amir Azam. Syntheses and evaluation of 3-(3-bromo phenyl)-5-phenyl-1-(thiazolo [4,5-b] quinoxaline-2-yl)-2-pyrazolinederivatives. *European Journal of Medicinal Chemistry*.2008; 43:1749-1757.
237. Aridoss G, Balasubramanian S, Parthiban P, .Kabilan S. Synthesis, Stereochemistry and antimicrobial evaluation of some N-morpholinoacetyl-2,6-diaryl piperidine-4-ones. *European Journal of Medicinal Chemistry*, 2007; 42:851-860.
238. Padmavathi V, Thriveni P, Sudhakar Reddy G, Deepti D. Synthesis and antimicrobial activity of novel sulfone-linked bis heterocycles. *European Journal of Medicinal Chemistry*. 2008; 43:917-924.
239. Pandeya SN, .Sriram D, Nath G, Clercq E.De. Synthesis, antibacterial, antifungal and anti-HIV activities of Schiff and Mannich bases derived from Isatin derivatives and

- N-[4-(4'-chlorophenyl) thiazol-2-yl] thiosemicarbazide. European Journal of pharmaceutical Sciences.1999; 9:25-31.
240. Dharmarajan Sriram, Tanushree Ratan Bal, PerumalYogeeswari. Aminopyrimidimino Isatin analogues: Design of novel non-nucleoside HIV-1 reverse transcriptase inhibitors with broad-spectrum chemotherapeutic properties. J.Pharm.Pharmaceut.Sci. 2005; 8(3): 565-577.
241. Alagarsamy V, Murugesan S, Dhanabal K. Murugan M and Clercq E DE..Anti HIV, Antibacterial and Antifungal activities of some Novel 2-Methyl-3-(substituted methyl amino)-(3H)-quinazolin-4-ones .Indian Journal of pharmaceutical Sciences, March-April 2007 ; 69(2): 304-306.
242. Nalan Terzioglu, Nilgun Karah, Aysel Gursoy, Christophe pannecouque, Pieter leysen, *et al.* Synthesis and primary antiviral activity evaluation of 3-hydrazono-5-nitro-2-indolinone derivatives.ARKIVOC,2006(i),109-118.
243. Werner Scheithaner, Mary P.Moyer, Gary M.clark and Daniel D.Von Hoff. Application of a new preclinical drug screening system for cancer of the large bowel. Cancer Chemother. Pharmacol.1998; 21:31-34.
244. Konstantinos Dimas, Sophia Hatziantoniou, Sophia Tseleni, Humaira Khan, Aristidis Georgopoulos, Konstantinos Alevizopoulos, *et al.* Sclareol induces apoptosis in human HCT116 colon cancer cells *in vitro* and suppression of HCT116 tumor growth in immunodeficient mice. Apoptosis, 2007; Volume12 (4): 685-694.
245. Mel C. Schroeder, James M. Hamby, Cleo J. C. Connolly, Patrick J. Grohar, R. Thomas Winters, Mark R. Barvian, *et al.* Soluble 2-Substituted Aminopyrido[2,3-d]pyrimidin-7-yl Ureas. Structure-Activity Relationships against Selected Tyrosine Kinases and Exploration of *in-Vitro* and *in-Vivo* Anticancer Activity. J. Med. Chem. 2001; 44(12):1915-1926.
246. Kyoung Soon Kim, David Kimball S , Raj N. Misra, David B. Rawlins, John T. Hunt, Hai-Yun Xiao, *et al.* Discovery of Aminothiazole Inhibitors of Cyclin-Dependent Kinase 2: Synthesis, X-ray Crystallographic Analysis, and Biological Activities. J. Med. Chem. 2002; 45:3905-3927.
247. Sylvester R. Klutchko, James M. Hamby, Diane H. Boschelli, Zhipei Wu, Alan J. Kraker, Aneesa M. Amar *et al.* 2-Substituted Aminopyrido[2,3-*d*]pyrimidin-7(8*H*)-ones. Structure-Activity Relationships against Selected Tyrosine Kinases and *in Vitro* and *in Vivo* Anticancer Activity. J. Med. Chem. 1998; 41:3276-3292.
248. Palwinder Singh and Kamaldeep Paul. Anti-cancer activities of 5-acyl-6-[2-hydroxy/benzyloxy-3-(amino)-propylamino]-1, 3-dialkyl-1*H*-pyrimidin-2, 4-diones. Bioorganic & Medicinal Chemistry. 2006; 14: 8622–8625.
249. Ohashi.S, Sakashita G, Ban R, Nagasawa.M, Matsuzaki.H, Murata.Y, et al.Phosphoregulation of human protein kinase Aurora-A: analysis using antiphosphor-thr-288monoclonal antibodies.Oncogene, 2006;25(59):7691-702.
250. Hangauer Jr, David G. El-Araby, Moustafa E. Milkiewicz, Karen L. US Patent 7005445 - Protein kinase and phosphatase inhibitors and methods for designing them. US Patent Issued on February 28, 2006.
251. Daly JW. The Alkaloids,Cordell GA editor. Sandiego,CA;Academic press:1998; 141-144.
252. El-subbagh HI, Abu-Zaid SM, Mahran MA, Badria FA, Al-obaid AM Synthesis and Biological Evaluation of Certain α , β -Unsaturated Ketones and Their Corresponding Fused Pyridines as Antiviral and Cytotoxic Agents. J.Med.Chem.2000; 43:2915-2921

253. Fleet G.WJ, Ramsden NG, Witty DR, A practical synthesis of deoxy mannojirimycin and of (2s,3R,4R,5R) - 3,4,5- tri hydroxy pipercolic acid from D-glucose. *Tetrahedron*, 1989; 45:327-336.
254. Lijinsky W, Taylor HW. Carcinogenicity of methylated nitrosopiperidines *Int.J.Cancer*. 1975; 16(2):318-322.
255. Prosakov NS, Galvoronskaya LA Six membered systems. *Russ.Chem.Res.* 1978; 11:197.
256. Nimavat KS, Popat KH, Joshi HS. Synthesis, Anticancer, Antitubercular and Antimicrobial Activity of 1-substituted 3-Aryl-5-(3'-Bromophenyl)-pyrazolines. *Indian J.Hetero.Chem.* 2003; 12:225-228.
257. Manning G et al. The protein kinase complement of the human genome. *Science* 2002; 298: 1912-1934.
258. Murcko M and Caron P. Transforming the genome to drug discovery. *Drug Discov.Today* 2002; 7: 583-584.
259. Johnson SA, Hunter T. Kinomics: methods for deciphering the kinome, *Nat Methods* 2005; 2:17-25.
260. Carmena M, Earnshaw WC, The cellular geography of aurora kinases. *Nature Rev Mol Cell Biol* 2003; 4:842-854.
261. Agnese V, Bazan V, Fiorentino FP, Fanale D, Badalamenti G, Colucci G, Adamo V, Santini D, Russo A. The role of Aurora-A inhibitors in cancer therapy. *Annals of Oncology* 18 2007; (Supplement 6): vi47-vi52.
262. Langauer C, Kinzler KW, Vogelstein B. Genetic instabilities in human cancers. *Nature* 1998; 396:643-649.
263. Bischoff JR et al. A homologue of Drosophila aurora kinase is oncogenic and amplified in human colorectal cancers. *EMBO J* 1998; 17:3052-3065.
264. Carvajal RD, Tse A, Schwartz GK. Aurora kinases: new targets for cancer therapy. *Clin Cancer Res* 2006; 12(23):6869-75.
265. Yijiang Shi, Tony Reiman, Weiqun Li, Christopher A, Maxwell, Subrata Sen, Linda Pilarski, Tracy R. Daniels. Targeting aurora kinases as therapy in multiple myeloma. *Blood*, 2007; 109(9): 3915-3921.
266. Fu J, Bian M, Jiang Q, Zhang C. Roles of Aurora kinases in mitosis and tumorigenesis *Mol Cancer Rev* 2007; 5(1):1-10.
267. Crane R. et al. "Aurora A, Meiosis and Mitosis". *Biology of the Cell* 2003; 96: 215-229.
268. Chunqi M. et al. "Biphasic Activation of Aurora A Kinase during the Meiosis I-Meiosis II Transition in *Xenopus Oocytes*". *Molecular and Cellular Biology*. 2003; 23(5): 1703-1706
269. Hirota T et al. Aurora-A and an interacting activator, the LIM protein Ajuba, are required for mitotic commitment in human cells. *Cell* 2003; 114: 585-598.
270. Anand S, Penrhynlowe S, Venkitaraman AR. Aurora-A amplification Overrides the mitotic spindle assembly checkpoint inducing resistance to Taxol. *Cancer Cell* 2003; 3: 51-62.
271. Meraldi P, Honda R, Nigg EA. Aurora-A over expression reveals tetraploidization as a major route to centrosome amplification in p53^{-/-} cells. *EMBO J* 2002; 21:483-492.

272. Hannak, E. et al. "Aurora-A kinase is required for centrosome maturation in *Caenorhabditis elegans*". The Journal of Cell Biology . 2001;155 (7): 1109–1115.
273. Sugimoto K et al. Molecular dynamics of aurora-A kinase in living mitotic cells simultaneously visualized with histone H3 and nuclear membrane protein importin α . Cell Struct Funct 2002;27:457-467.
274. Berdnik D, Knoblich JA. Drosophila Aurora-A is required for centrosome maturation and actin-dependent asymmetric protein localization during mitosis. Curr Biol 2002; 12:640-647.
275. Giet R et al. Drosophila Aurora-A kinase is required to localize D-TACC to centrosomes and to regulate astral microtubules, J Cell Biol 2002; 156: 437-451.
276. Kufer TA et al. Human TPX2 is required for targeting Aurora-A kinase to the spindle. J Cell Biol 2002; 158:617-623.
277. Marumoto, T. et al. "Aurora-A Kinase Maintains the Fidelity of Early and Late Mitotic Evens in HeLa Cells". The Journal of Biological Chemistry. 2003; 278 (51): 51786–51795.
278. Zhu J, Abbruzzese JL, Izzo J et al. AURKA amplification, chromosome instability, and centrosome abnormality in human pancreatic carcinoma cells. Cancer Genet Cytogenet 2005; 159: 10–17.
279. Tanaka E, Hashimoto Y, Ito T et al. The clinical significance of Aurora-A/STK15/BTAK expression in human esophageal squamous cell carcinoma. Clin Cancer Res 2005; 11(5): 1827–1834
280. Andrews PD, Knatko E, Moore WJ, Swedlow JR. Mitotic mechanics: the auroras come into view. Curr Opin Cell Biol 2003; 15: 672–683.
281. Giet R, Uzbekov R, Cubizolles F, Le Guellec K, Prigent C. The *Xenopus laevis* aurora-related protein kinase pEg2 associates with and phosphorylates the kinesin related Protein XI Eg5. J Biol Chem 1999; 274: 15005–15013.
282. Tsai MY et al. A Ran signalling pathway mediated by the mitotic kinase Aurora A in spindle assembly. Nature Cell Biol 2003; 5: 242–248.
283. Wilde A, Zheng Y. Stimulation of microtubule aster formation and spindle assembly by the small GTPase Ran. Science 1999; 284: 1359–1362.
284. Kalab P, Pu RT, Dasso M. The ran GTPase regulates mitotic spindle assembly. Curr Biol 1999; 9: 481–484.
285. Carazo-Salas RE *et al.* Generation of GTP-bound Ran by RCC1 is required for chromatin-induced mitotic spindle formation. Nature. 1999; 400: 178–181.
286. Mori D, Yano Y, Toyo-oka K, Yoshida N, Yamada M, Muramatsu M, *et al.* NDEL1 phosphorylation by Aurora-A kinase is essential for centrosomal maturation, separation, and TACC3 recruitment. Mol Cell Biol 2007; 27: 352-367.
287. Hachet V, Canard C and Gonczy P. Centrosomes promote timely mitotic entry in *C. elegans* embryos. Dev Cell 2007; 12: 531-541.
288. Portier N, Audhya A, Maddox PS, Green RA, Dammermann A, Desai A, Oegema, K. A microtubule-independent role for centrosomes and aurora A in nuclear envelope breakdown. Dev. Cell 2007; 12: 515-529.
289. Graham M. T. et al., Crystal Structure of Aurora-2, an Oncogenic Serine/Threonine Kinase J. Biol. Chem. 2002; 277:42419-42422.
290. Castro A, Arlot-Bonnemains Y, Vigneron S et al. APC/Fizzy-related targets Aurora-A kinase for proteolysis. EMBO Rep 2002; 3: 457–462.
291. Littlepage LE, Ruderman JV. Identification of a new APC/C recognition domain, the A box, which is required for the Cdh1-dependent destruction of the kinase Aurora-A during mitotic exit. Genes Dev 2002; 16: 2274–2285.

292. Littlepage LE, Wu H, Andresson T et al. Identification of phosphorylated residues that affect the activity of the mitotic kinase aurora-A. *Proc Natl Acad Sci U S A* 2002; 99: 15440–15445.
293. Katayama H, Zhou H, Li Q et al. Interaction and feedback regulation between STK15/BTAK/aurora-A kinase and protein phosphatase 1 through mitotic cell division cycle. *J Biol Chem* 2001; 276: 46219–46224.
294. Emanuel S, Rugg CA, Gruninger RH et al. The in vitro and in vivo effects of JNJ-7706621: a dual inhibitor of cyclin-dependent kinases and aurora kinases. *Cancer Res* 2005; 65(19): 9038–9046.
295. Nigg E.A. Mitotic kinases as regulators of cell division and its checkpoints *Nat. Rev. Mol. Cell Biol.* 2001; 2: 21-32.
296. Goto H, Yasui Y, Nigg EA, Inagaki M. Aurora-B phosphorylates Histone H3 at serine28 with regard to the mitotic chromosome condensation. *Genes Cells*, 2002; 7: 11-17.
297. Karine Monier, Sandrine Mouradian, and Kevin F. Sullivan DNA methylation promotes Aurora-B-driven phosphorylation of histone H3 in chromosomal subdomain *J. Cell Sci.*, 2007; 120:101-114.
298. Edmund Chun Yu Lee et al., Targeting Aurora Kinases for the Treatment of Prostate Cancer. *Cancer Res.* 2006; 66: 4996-5002.
299. Hua Yang et al., Aurora-A Kinase Regulates Telomerase Activity through c-Myc in Human Ovarian and Breast Epithelial Cells *Cancer Res.* 2004; 64:463-467.
300. Jingyan Fu, Minglei Bian, Qing Jiang, and Chuanmao Zhang. Roles of Aurora Kinases in Mitosis and Tumorigenesis *Mol. Cancer Res.* 2007; 5:1-10.
301. Bedrick B. Gadea and Joan V. Ruderman. Aurora Kinase Inhibitor ZM447439 Blocks Chromosome-induced Spindle Assembly, the Completion of Chromosome Condensation, and the Establishment of the Spindle Integrity Checkpoint in *Xenopus* Egg Extracts *Mol. Biol. Cell.* 2005; 16:1305-1318.
302. Hauf, S. et al. The small molecule Hesperadin reveals a role for Aurora B in correcting kinetochore-microtubule attachment and in maintaining the spindle assembly checkpoint. *J. Cell Biol.* 2003; 161, 281–294.
303. Shiho Sakita-Suto et al., Aurora-B Regulates RNA Methyl transferase NSUN2 *Mol. Biol. Cell*, 2007; 18:1107-1117.
304. Harrington, E. A. et al. VX-680, a potent and selective small molecule inhibitor of the Aurora kinases, suppresses tumor growth in vivo. *Nature Med.* 2004; 10:262–267.
305. Rees DC, Congreve M., Murray CW. Carr R. Fragment-based lead discovery. *Nat. Rev. Drug Disc.* 2004; 3: 660-672.
306. Erlanson DA., McDowell RS, O'Brien T. Fragment-based drug discovery. *J. Med. Chem.* 2004; 47: 1-20.
307. Zartler, ER.; Shapiro, M. J. Fragonomics: Fragment-based drug discovery. *Curr. Opin. Chem. Biol.* 2005; 9: 366-370.
308. Philip JH. Fragment-Based Drug Design: How Big Is Too Big? *J. Med. Chem.* 2006; 49: 6972-6976.
309. Oprea, T. I. Current trends in lead discovery: are we looking for the appropriate properties? *J. Comput. Aided Mol. Des.* 2002; 6: 325-334.
310. Gill, A.; Cleasby, A.; Jhoti, H. The discovery of novel protein kinase inhibitors by using fragment-based high-throughput x-ray crystallography. *Chem. Bio Chem.* 2005; 6: 506-512.
311. Bohm, H. J.; Flohr, A.; Stahl, M. Scaffold hopping. *Drug Discov. Today. Technol.* 2004; 1: 217-224.
312. Zhao, H. Scaffold selection and scaffold hopping in lead generation: a medicinal chemistry perspective. *Drug Discov. Today.* 2007; 12: 149-155.

313. Ertl P, Jelfs S, Muhlbacher J, Schuffenhauer A, Selzer P. Quest for the rings. In silico exploration of ring universe to identify novel bioactive heteroaromatic scaffolds. *J. Med. Chem.* 2006; 49: 4568-4573.
314. Catalyst, version 4.11; Accelrys Inc: San Diego, CA 92121, USA, 2007.
315. Maestro version 1.0.9113; Schrodinger, L.L.C., New York, 2006.
316. Cerius2, version 4.11; Accelrys Inc: San Diego, CA 92121, USA, 2007.
317. Fragments descriptors, GVK Biosciences Pvt. Ltd.S-1, Phase-1, Technocrats Industrial Estate, Balanagar. Hyderabad, India. 2006.
318. Charifson PS, Corkery JJ, Murcko MA, Walters WP. Consensus scoring: A method for obtaining improved hit rates from docking databases of three-dimensional structures into proteins. *J. Med. Chem.* 1999; 42: 5100-5109.
319. Aparna V, Rambabu G, Panigrahi SK, Sarma JARP, Desiraju GR. Virtual screening of 4-anilinoquinazoline analogues as EGFR kinase inhibitors: importance of hydrogen bonds in the evaluation of poses and scoring functions. *J. Chem. Inf. Model.* 2005; 45: 725-738.
320. Howard BB, Ian AW. Selection of heterocycles for drug design. *J. Mol. Graph. Model.* 2005; 23: 51-58.
321. Hartshorn MJ, Murray CW, Cleasby A, Frederickson M, Tickle IJ, Jhoti H. Fragment-based lead discovery using X-ray crystallography. *J. Med. Chem.* 2005; 48: 403-413.
322. Poroikov V, Filimonov D. Computer-aided prediction of biological activity spectra. Application for finding and optimization of new leads. Holtje HD, Sippl W, editors. *Rational Approaches to Drug Design*. Barcelona: Prous Science, 2001.
323. Avidon VV. The criteria of chemical structures similarity and the principles for design of description language for chemical information processing of biologically active compounds. *Chem. Pharm. J. (Rus)* 1974; 8:22-25.
324. Piruzyan LA, Avidon VV, Rozenblit AB, et al. Statistical analysis of the information file on biologically active compounds. I. Data base on the structure and activity of biologically active compounds. *Chem Pharm J. (Rus)* 1977; 11:35-40.
325. Golender VE, Rozenblit AB. Logical structural approach to computer assisted drug design. *Drug Design*. Vol. 9.: Academic Press: New York ;1980.
326. Rozenblit AB, Golender VE. *Logical Combinatorial Methods in Drug Design*. Riga: Zinatne, 1983.
327. Burov YuV, Poroikov VV, Korolchenko LV. National system for registration and biological testing of chemical compounds: facilities for new drugs search. *Bull Natl Cent for Biol Active Comp (Rus)* 1990; 1:4-25.
328. PASS: Prediction of Biological Activity Spectra for Substances Vladimir Poroikov And Dmitri Filimonov, 2397-X Helma Ch13 R1 100104.
329. MDL Information Systems, (ONLINE)2002;(Nov 22, 2008) Inc., San Leandro, CA; Available from URL:<http://www.mdli.com>.
330. PASS: Prediction of Activity Spectra for Biologically Active Substances{ONLINE} 1995; {cited2008 May-2008}; Available from URL:<http://www.ibmh.msk.su/PASS>.
331. Lagunin A, Stepanchikova A, Filimonov D, Poroikov V. PASS: Prediction of Activity Spectra for Biologically Active Substances. *Bioinformatics*. 2000; 16:747-748.
332. Hiroshi katayama, Takahide Ota, fumiko Jisaki, yoshimichi Ueda, Takuji Tanaka, Shizuo Odashima, *et al.* Mitotic Kinase Expression and Colorectal cancer progression. *Journal of the National Cancer Institute*. 1999; 91(13):1160-1162.
333. Katayama H *et al.* Phosphorylation by aurora kinase A induces Mdm2-mediated destabilization and inhibition of p53. *Nature Genet* 2004; 36: 55-62.
334. De Groot AS, Rothman FG. In silico predictions; in vivo veritas. *Nat. Biotechnol.* 1999; 17: 533-534.

335. Terstappen GC, Reggiani A. In silico research in drug discovery. Trends Pharmacol. Sci. 2001, 22, 23-26.
336. Ajay A, Walters WP, Murcko MA. Can we learn to distinguish between "drug-like" and "nondrug-like" molecules? J. Med. Chem. 1998, 41, 3314-3324.
337. Gillet VJ, Willett P, Bradshaw J. Identification of biological activity profiles using substructural analysis and genetic algorithms. J.Chem.Inf.Comput.Sci. 1998; 38,165-179.
338. Wagener M, vanGeerestein VJ. Potential drugs and nondrugs: prediction and identification of important structural features. J. Chem. Inf. Comput. Sci. 2000; 40.
339. Xu J, Stevenson J. Drug-like index: a new approach to measure drug-like compounds and their diversity. J. Chem. Inf. Comput. Sci. 2000; 40: 1177-1187.
340. Brown RD, Hassan M, Waldman M. Combinatorial library design for diversity, cost efficiency, and druglike character. J. Mol. Graph Model 2000; 18: 427-437.
341. Mannhold R, van de Waterbeemd H. Substructure and whole molecule approaches for calculating log P. J. Comput. Aided Mol. Des. 2001; 15: 337-354.
342. Ghuloum AM, Sage CR, Jain AN. Molecular hashkeys: a novel method for molecular characterization and its application for predicting important pharmaceutical properties of molecules. J. Med. Chem. 1999; 42: 1739-1748.
343. Navia MA, Chaturvedi PR. Design principles for orally bioavailable drugs. Drug Discovery Today 1996; 1: 179-189.
344. Chan OH, Stewart BH. Physicochemical and drug delivery considerations for oral drug bioavailability. Drug Discovery Today 1996; 1: 461-473.
345. Mestres J. Virtual screening: a real screening complement to high throughput screening. Biochem. Soc. Trans. 2002; 30: 797-799
346. Hou T and Xu X. Recent development and application of virtual screening in drug discovery: an overview. Curr. Pharm. Des. 2004; 10:1011-1033.
347. Lipinski CA. *et al* Experimental and computational approaches to estimate solubility and permeability in drug discovery and development settings. Adv. Drug Deliv. Rev. 1997; 23: 3-25.
348. Congreve M. *et al*. A 'Rule of Three' for fragment-based lead discovery? Drug Discov. Today. 2003; 8, 876-877
349. Fattori D. Molecular recognition: The fragment approach in lead generation. Drug Discov. Today 2004; 9: 229-238.
350. Molinspiration Home page. Slovak Republic: Free online cheminformatics Services available from: www.molinspiration.com
351. Lipinski CA, Lombardo F, Dominy BW and Feeney PJ. Experimental and computational approaches to estimate solubility and permeability in drug discovery and development settings. Adv. Drug Deliv. Rev. 2001; 46: 3.
352. Michal Vieth, Jeffrey J. Sutherland, Daniel H. Robertson and Robert M. Campbell. Kinomics: Characterizing the therapeutically validated kinase space. Drug discovery Today. 2005; 10(12): 839-846.
353. Wenlock MC *et al*. A comparison of physicochemical property profiles of development and marketed oral drugs. J. Med. Chem. 2003; 46: 1250-1256.
354. David G. Lloyd, Georgia Golfis, Andrew JS, Knox, Darren Fayne, Mary J. Meegan, *et al*. Discovery Today. Feb. 2006; Volume 11: Number 3/4, 149-159.
355. Hann MM. and Oprea TI. Pursuing the leadlikeness concept in pharmaceutical research. Curr. Opin. Chem. Biol. 2004; 8, 255-263.
356. Walters WP and Murcko MA. Prediction of "drug-likeness". Adv. Drug Deliv. Rev. 2002; 54: 255-271.

357. Lipinski CA. Drug-like properties and the cause of poor solubility and poor permeability. *J. Pharmacol. Toxicol. Methods.* 2000; 44: 235–249.
358. Wang, R. *et al.* A new atom-additive method for calculating partition coefficients. *J. Chem. Inf. Comput. Sci.* 1997; 37: 615–621.
359. Leach AR. and Hann MM. The *in silico* world of virtual libraries. *Drug Discov. Today.* 2000; 5:326–336
360. Shuttleworth SJ. *et al.* Design and synthesis of protein super family targeted chemical libraries for lead identification and optimization. *Curr. Med.Chem.* 2005;12, 1239–1281.
361. Olah MM.*et al.* Strategies for compound selection. *Curr. Drug Disc. Tech.* 2004;1: 211–220.
362. Chen G,*et al.* Focused combinatorial library design based on structural diversity, druglikeness and binding affinity score. *J. Comb. Chem.* 2005; 7: 398–406.
363. Julian Blagg. Structure-Activity Relationships for *in vitro* and *in vivo* toxicity. Annual Reports in medicinal chemistry, 41: DOI 10.1016/S0065-7743(06)41024-1.
364. International conference on Harmonisation: Guidance on specific aspects of regulatory genotoxicity tests for pharmaceuticals. *Fed. Regist.* 1996; 61(80): 18197-18202.
365. Kedderis GL and Miwa GT, *Drug. Met. Rev.* 1988; 19(1):33.
366. Fishbein L. Potential Industrial Carcinogens and mutagens: Elsevier Scientific Publishing company: Amsterdam, The Netherlands, 1979.
367. Jeroen Kazius, ROSS McGuire and Roberta Bursi. Derivation and validation of toxicophores for mutagenicity prediction. *J. Med. Chem.* 2005; 48, 312-320.
368. Glende C, Schmitt H, Erdinger E, Engelhardt V, Boche G. Transformation of mutagenic aromatic amines into non mutagenic by alkyl substituents. Part I. Alkylation ortho to the amino function. *Mutat. Res.* 2001; 498: 19-37.
369. K. Mogilaiah & B. Sakram. Synthesis and antimicrobial screening of 2,4-diaryl-6-[2*ϕ*H-[1*ϕ*]-4*ϕ*-hydroxy-2*ϕ*-oxo-benzopyran-3*ϕ*-yl]pyridines and 2,6-diaryl-4-[2*ϕ*H-[1*ϕ*]-4*ϕ*-hydroxy-2*ϕ*-oxo-benzopyran-3*ϕ*-yl]pyridines. *Indian Journal of Chemistry*, Vol. 43b, Dec 2004, 2724-2726.
370. Hiremath SP, Rudresh K, Saundane AR. Synthesis and biological activities of new 5-hydrazino-10-substituted-7*H*-indolo[2,3-*c*]iso-quinolines and 1-(10-substituted-7*H*-indolo[2,3-*c*]isoquinolin-5-yl)-3,5-disubstituted pyrazoles, -3-methylpyrazol-5-ones and 3,5-disubstituted pyrazolines. *Indian Journal of Chemistry*, 2002; 41B: 394-399.
371. Hanack, M., “Conformations theory”, Translated by H.C. Neumann, Academic Press, New York, 1965.
372. Hirsch JA, Concepts in theoretical Organic Chemistry, Allyn and Bacon Inc., Boston, 1974.
373. Lambert JB, Bailey DS, Michel BF. Steric manipulation of the lone pair in piperidine. *Tetrahedron Lett.* 1970; 11 691-694.
374. Katritzky AR, Amble AP. Physical Methods of Heterocyclic Chemistry, Vol II, Academic Press, New York, 1963.
375. Katritzky AR, Taylor, Physical Methods of Heterocyclic Chemistry, Vol. IV, Academic Press, New York, 1971.
376. Silverstein RM, Clayton Bassler G, Morrill TC, Spectrometric Identification of Organic Compounds, Fourth edition John Wiley and Sons, New York, 1981.
377. Lyle RE and Lyle G, Resolution of 2,6-Diphenyl-1-methyl-4-piperidone Oxime, a Novel Example of Molecular Isomerism. *J. Org. Chem.* 1959; 24: 1682.
378. Manimekalai A, Jayabharathi J, Porselvi VM and Prabha N. Synthesis and spectral studies of some hetero aryl piperidin-4-ones and their derivatives. *Indian Journal of Chemistry.* 2007 April; 46(B): 681-689.

379. Young CW, Pletcher DE, Wright N. On olfaction and infrared radiation Theories. *Science* 1948 Oct 15; 108(2807):411-412.
380. Bellamy LJ, *The Infrared Spectra of Complex Molecules*, vol. I, Chapman and Hall, London, 1975, 79.
381. Katritzky AR, Infrared intensities. *J. Chem. Soc.* (1958) 4162.
382. Katritzky and Coats. *J. Chem. Soc.* 1959; 2062-2066.
383. Beckett AH and Stenlake JB. Editors. Text book of Practical Pharmaceutical Chemistry. Fourth edition-part two. CBS Publishers & Distributors; New Delhi: 379-408.
384. Sivasubramania S, Sundaravadivelu M, Arumugam N. *Indian J. Chem.* 1981; 20(B): 878-879.
385. Pandiarajan K, Shekar R, Anantharaman and Ramalingam V. *Indian J. Chem.* 1991; 30(B): 490-493.
386. Murugesan srinivasan, subbu perumal and sangavanaicker selvaraj. Synthesis, stereo and antimicrobial activity of 2,6-diaryl-3-(aryltio) piperidin-4-ones. *Chem. pharm. Bull.* 2006; 54(6): 795-801.
387. Laszlo Varga, Tamas Nagy, Istvan Kovesdi, Jordi Benet Buchholz, Gyorgy Dorman Laszlo urge et al. Solution-phase parallel synthesis of 4,6-diaryl pyrimidines-2ylamines and 2-amino-5,5-disubstituted -3,5-dihydro-imidazol-4-ones via a rearrangement. *Tetrahedron.* 2003; 59: 655-662.
388. Ali A Khalaf, Reda a Kabli, zimaity MT, Khalil AM, kaddah AM, Al-Rifaie HA. N-derivatisation of some 3-(2-furyl) and 3-(2-thienyl)-5-aryl-2-pyrazolines. *Indian Journal of Chemistry.* 1993; 32(B): 1125-1129.
389. Lambert JB, Netzel DA, Sun HN and Lilianstrom KK. Carbon-13 chemical shifts of the penta methylene heterocycles. *J. Am. Chem. Soc.* 1976; 98: 3778-3783.
390. Louis d. Quin and Tterror P. Touka. *J. Chem. Soc.* 1980; B5: 832-834.
391. Dugfield AM, Budzikiewicz H, Williams DH and Djerassi C. Mass Spectrometry in Structural and Stereochemical Problems. LXIV.¹ A Study of the Fragmentation Processes of Some Cyclic Amines. *J. Am. Chem. Soc.* 1965; 87: 810.
392. Michael C. Alley, Dominic A. Scudiero, Anne Monks, Miriam L. Hursey, Maciej J. Czerwinski, Donald L. Fine, et al. Feasibility of Drug Screening with Panels of Human Tumor Cell Lines Using a Microculture Tetrazolium Assay., *Cancer Res.* 1988; 48: 589-601.
393. Dominic A. Scudiero, Robert H. Shoemaker, Kenneth D. Paull, Anne Monks, Siobhan Tierney, Thomas H. Nofziger, et al. Evaluation of a Soluble Tetrazolium/Formazan Assay for Cell Growth and Drug Sensitivity in Culture Using Human and Other Tumor Cell Lines. *Cancer Res.*, 1988; 48: 4827-4833.
394. David L. Satinover, Craig A. Leach, P. Todd Stukenberg and David L. Brautigan. Activation of Aurora-A kinase by protein phosphatase inhibitor-2, a bifunctional signaling protein. *Proc. Natl. Acad. Sci. USA* 2004 101, 8625-8630.
395. Booher R. and Beach D. Involvement of a type 1 protein phosphatase encoded by *bws1+* in fission yeast mitotic control. *Cell*, 1989, 57, 1009-1016.
396. Doonan JH, MacKintosh C, Osmani S, Cohen P, Bai G, Lee EY and Morris NR. A cDNA encoding rabbit muscle protein phosphatase 1_α complements the *Aspergillus* cell cycle mutation, *bimG11*. *J. Biol. Chem.* 1991. 266, 18889-18894.
397. Doonan JH. and Morris NR. The *bimG* gene of *Aspergillus nidulans*, which is required for completion of anaphase, encodes a homologue of mammalian phosphoprotein phosphatase. *Cell*, 1989; 57: 987-996.
398. Fernandez A, Brautigan DL. and Lamb NJ. Protein phosphatase type 1 in mammalian cell mitosis: chromosomal localization and involvement in mitotic exit. *J. Cell Biol* 1992; 116: 1421-1430.

399. Ohkura H, Kinoshita N, Miyatani S, Toda T, and Yanagida M. The fission yeast *dis2+* gene required for chromosome disjoining encodes one of two putative type 1 protein phosphatases. *Cell*. 1989; 57, 997–1007.
400. Walter AO, Seghezzi W, Korver W, Sheung J. & Lees E. The mitotic serine/threonine kinase Aurora2/AIK is regulated by phosphorylation and degradation. *Oncogene* **19**, 4906–4916 (2000).
401. Garcia A, Cayla X, Guernon J, Dessauge F, Hospital V, Rebollo MP, Fleischer A, Rebollo A. Serine/threonine protein phosphatases PP1 and PP2A are key players in apoptosis. *Biochimie*. 2003 Aug; 85(8):721-6.
402. Yanagida M, Kinoshita N, Stone EM, Yamano H. Protein phosphatases and cell division cycle control. *Ciba Found Symp*. 1992; 170:130-40; discussion 140-6.